THE ROLE OF SKELETAL MUSCLE IN THE INITIATION AND PROGRESSION OF KNEE OSTEOARTHRITIS

Daniel Paul Tonge, BSc (Hons)

Thesis submitted to the University of Nottingham for the degree of Doctor of Philosophy, 2010

Division of Nutritional Science

School of Biosciences

University of Nottingham

Hindsight is an exact science.

J Potter

- Abstract -

It is established that patients with knee osteoarthritis (OA) exhibit marked muscle weakness, one of the most frequent and earliest reported symptoms associated with knee OA. Weakness primarily affects the quadriceps muscle with little evidence of hamstring involvement. Traditionally, muscle weakness has been considered a secondary effect in knee OA, resulting from disuse of the affected joint due to the presence of pain and/or inflammation, and therefore has received little attention with regards to its involvement in the initiation or progression of OA. However, there is clinical evidence which suggests that quadriceps weakness may precede the onset of radiographic evidence of OA and subsequent pain, and therefore may be directly involved in its pathogenesis. Furthermore, targeted exercise regimes aimed at improving quadriceps function indicate therapeutic benefits with regards to both the initiation and progression of knee OA. Quadriceps muscle dysfunction in knee OA is currently poorly understood and represents an unmet clinical need.

Consequently, the main aims of this work were to characterise quadriceps muscle dysfunction in the rodent meniscectomy-induced (MNX) and spontaneous guinea pig model of OA at the molecular level determining changes in muscle fibre type, metabolic potential, and muscle atrophy signalling. Furthermore, the effects of clenbuterol-induced quadriceps hypertrophy, prior to the induction of OA, on disease severity were considered in the rat MNX model. Thus far, the cDNA sequences encoding each member of the myosin heavy chain (MHC) gene family have yet to be determined in the guinea pig. Therefore, a further aim of this work was to generate novel cDNA sequence pertaining to the skeletal muscle-associated isoforms of MHC in the guinea pig, and to develop specific oligonucleotide primers to determine the abundance of each specific mRNA.

The development of MNX-induced and spontaneous OA was associated with changes in MHC I expression indicative of an increase in slow, type I muscle fibres. The assessment of muscle atrophy-associated genes revealed that neither model was

associated with overt quadriceps muscle atrophy, or increased muscle atrophy signalling. Combined, these data suggest that OA associated quadriceps dysfunction may result predominantly from altered contractile properties, as evidenced by altered MHC expression, rather than from reduced quadriceps mass *per se*. The administration of clenbuterol for 14 days induced marked increases in quadriceps mass relative to bodyweight. However, clenbuterol induced hypertrophy was unable to favourably modulate OA severity in the MNX-induced model in this experimental setting.

In conclusion this work has shown that OA is associated with altered quadriceps muscle properties, suggestive of a switch towards a slow-twitch muscle fibre type, in two independent animal models. Such data have important implications for the development of targeted pharmaceuticals and in the prescription of rehabilitation regimes aimed at improving OA severity or reducing disease progression. Moreover, the relationship of increased MHC I expression to joint stability and muscle function warrants further investigation in the OA setting.

- Acknowledgements –

It takes a great deal of time and effort to complete a PhD thesis, none of which would have been possible without the help and support of numerous colleagues and friends with whom I shared this exciting journey.

Firstly, I wish to thank my numerous PhD supervisors Drs Tim Parr, Simon Jones, Ronald Bardsley, Mike Doherty and Rose Maciewicz: Tim provided plentiful scientific advice, and had the willingness to allow me to find my own way – a trait that greatly enhanced what I have gained from this PhD. Simon supplied unparalleled advice on osteoarthritis, served as a sounding board for my ideas, and provided a link between the pharmaceutical industry and academia. He believed in me from the offset, and was instrumental in me presenting my work in some exotic (Quebec) and not so exotic (Loughborough, M1 Jct 23) places! On a personal level, he is a genuine person and a good friend – it has been a real privilege to work with him and I am grateful for all he has done. Ron provided infinite wisdom, scientific knowledge and support – he served as the voice of all reason and ensured my ideas stayed on track. Rose supplied scientific advice, infinite resources, and an honest opinion on matters – she also provided an endless stream of contacts in high-places and great career advice (accompanied by a fantastic Biryani!). I am also grateful to Mike Doherty for his clinical input and for ensuring the relevance of this project.

I wish to thank my wife Laura (who is also completing her PhD) for her endless support and for sharing this exciting journey with me. She has provided love and support throughout, and tolerated conversations of the molecular kind at the most unearthly hours. Without her backing, and the sacrifices we have made as a couple, this thesis would not have been possible.

My parents, Stella and Paul, have been continuously supportive throughout my studies and never once questioned my choice of career. I am eternally grateful for all they have done, and hope to repay them with some grandchildren in the near future!

I wish to thank Kate and Simon for providing rent-free lodgings at the start of this PhD, and Steve and Kathy for numerous wonderful trips to their house in France. In fact, it was during our regular visits to Descartes that most of my project planning and data interpretation took place.

Finally I wish to thank the bean-picking staff at Nespresso. Without the dark, bitter fruits of their labour, this process would have taken twice as long.

- Publications –

Some of the data presented in this thesis have been previously published as indicated below:

Original Publications:

Tonge, D. P., S. W. Jones, et al. (2009). "060 β2-Adrenergic agonist-induced hypertrophy of the quadriceps skeletal muscle does not modulate disease progression in the rodent meniscectomy model of osteoarthritis." Osteoarthritis and Cartilage **17**(Supplement 1): S41-S41.

Tonge, D. P., S. W. Jones, et al. (2009). "β2-Adrenergic agonist-induced hypertrophy of the quadriceps skeletal muscle does not modulate disease severity in the rodent meniscectomy model of osteoarthritis." Osteoarthritis and Cartilage **18**(4): 555-562.

Tonge, D. P., S. W. Jones, et al. (2010). "Characterisation of the Sarcomeric Myosin Heavy Chain Multigene Family in the Laboratory Guinea Pig." BMC Molecular Biology **11**:52

Original GenBank submissions:

Tonge, D. P., S. W. Jones, et al. (2009)

Cavia porcellus MyH1 5'UTR + cds GU288593

Cavia porcellus MyH2 5'UTR + cds GU288594

Cavia porcellus MyH4 5'UTR + cds GU288595

Cavia porcellus MyH1 3'UTR + cds GU288596

Cavia porcellus MyH2 3'UTR + cds GU288597

Cavia porcellus MyH4 3'UTR + cds GU288598

- Table of contents –

- LIST OF FIGURES -

- LIST OF TABLES -

CHAPTER 1 – GENERAL INTRODUCTION

1.1 – Osteoarthritis

1.1.1 – Background and definition

Osteoarthritis (OA), the most common joint disorder worldwide, is an active disease process involving cartilage destruction, subchondral bone thickening, and new bone formation (Peat, McCarney et al. 2001). OA comprises a heterogeneous group of disorders that affect all joint tissues, although articular cartilage and the adjacent subchondral bone show the most marked changes (Herrero-Beaumont, Roman-Blas et al. 2009). OA may be defined by the symptoms which it elicits, by radiographic evidence of structural pathology, or by a combination of the two. With reference to OA of the knee, the primary symptoms include quadriceps muscle weakness, joint stiffness, crepitus (grinding on joint motion) and pain.

1.1.2 – Prevalence

In the western world, OA is one of the primary causes of pain, functional loss and disability within the adult population. By 65 years of age, the majority of people have radiographic evidence of OA. On reaching 75 years of age, 80% of the population present with positive radiology. OA affects the knee, hip, hand and spine, and less commonly, the wrists and ankles (Arden and Nevitt 2006). Knee OA represents one of the most prevalent forms of osteoarthritis, with population-based studies estimating severe radiographic disease amongst 1% of 25-34 year olds, and 30% in those aged 75 and above (Arden and Nevitt 2006).

1.1.3 – Diagnostic criteria and current therapy

In the clinical setting, OA is routinely graded using standard radiographic films. The radiographic features associated with OA include joint space narrowing (JSN), bone contour abnormalities, subchondral sclerosis, osteophytosis and cyst formation (Arden and Nevitt 2006) and are graded using a system first described by Kellgren and Lawrence in 1957 (Kellgren and Lawrence 1957) (**TABLE 1.1**). This system assigns one of five grades to osteoarthritic lesions at various sites in comparison to a radiographic atlas.

TABLE 1.1 – Kellgren and Lawrence radiographic scoring system

Grade	OA	Description
Grade 0	None	No features of OA
Grade 1	Doubtful	Minute osteophyte, doubtful significance
Grade 2	Minimal	Definite osteophyte, unimpaired joint space
Grade 3	Moderate	Moderate diminution of joint space
Grade 4	Severe	Joint space greatly impaired / sclerosis of subchondral bone

The most widely utilised criteria for reaching a positive OA diagnosis were developed by the American College of Rheumatology (Altman, Alarcon et al. 1991). The criteria combine clinical features with the radiographic grading system of Kellgren and Lawrence, identifying only patients with knee-pain for most days of the prior month (**TABLE 1.2**). Knee OA is confirmed if knee pain is experienced for most days of the prior month in addition to; osteophytes, synovial fluid changes, morning stiffness and crepitus, or morning stiffness and creptius alone in patients over the age of 40 years.

TABLE 1.2 – American College of Rheumatology scoring criteria

Grade	Clinical and Radiographic feature	OA if present
1	Knee pain for most days of the prior month	1, 2 or 1, 3, 5, 6 or 1, 4, 5, 6
2	Osteophytes at joint margins (radiograph)	
3	Synovial fluid typical of OA (laboratory)	
4	Age > 40 years	
5	Morning stiffness > 30 minutes	
6	Crepitus on active joint motion	

Although routine histological diagnosis is rarely performed for the diagnosis of human OA, the microscopic features of OA include loss of chondrocytes and proteoglycan from the cartilage surface, cartilaginous ulceration and erosion, subchondral degeneration and osteophytosis (Bendele 2001). Histological diagnosis is useful for the assessment of OA in laboratory animals and other smaller species and has been described in detail by Bendele, 2001 (Bendele 2001), and specific animal scoring criteria developed by Huebner and Kraus, 2006 (Huebner 2006).

Recommendations for the treatment of OA underwent a NICE review in 2008, to include a more holistic approach to disease management. Following diagnosis, patient education and counselling are recommended in combination with monthly consultation by telephone. Aerobic exercise and local muscle strengthening are indicated in addition to weight loss in over-weight patients. Pain management recommendations suggest the administration of paracetamol and topical non-steroidal anti-inflammatory drugs (NSAIDS) in the first instance. Oral NSAIDS (including COX-II inhibitors) are only indicated if other analgesics are insufficient, and should be prescribed with caution due to potential gastrointestinal and cardiovascular side-effects. Surgery is only indicated in those patients were the severity of disease is having a substantial impact on their quality of life (NICE 2008). To date, no disease modifying drugs are available for the treatment of OA, which represents a great and unmet clinical need.

1.1.4 – Risk factors

Data from epidemiological studies have been used to elucidate several risk factors associated with the development and progression of OA. Such studies have provided an insight into those who are likely to develop the disease, which joint will be affected and moreover provided clues to its complex pathogenesis. A model for the pathogenesis of OA was developed by Dieppe in 1995 (Dieppe 1995) which separates risk factors into those systemic factors increasing the overall risk of disease, and mechanical risk factors which tend to be the primary determinant of which joint will likely be affected.

1.1.4.1 – Systemic risk factors

Systemic risk factors are thought to increase the overall susceptibility to degenerative joint changes and to decrease the effectiveness of the reparative response resulting in a predisposition to OA. The most compelling evidence links the incidence of OA with advancing age (Oliveria, Felson et al. 1995; Kirkwood 1997; Murphy and Lamb 2008). The age-related increase in OA prevalence is noted at all commonly affected sites, but is particularly notable in knee and hand OA (Arden and Nevitt 2006). This association is true of both radiographic and symptomatic disease in patients over the age of 65 years (Felson, Naimark et al. 1987).

Throughout reproductive life, both males and females share a comparable susceptibility to OA (Arden and Nevitt 2006). However, postmenopausal women experience an increased predisposition suggesting that differences in sex hormones may modulate the disease. Despite this, to date there is no definitive evidence linking oestrogen levels, or reproductive history with the incidence of OA (Samanta, Jones et al. 1993). Current hormone replacement therapy (HRT) *is* protective of osteophytosis and may protect against joint space narrowing however, this effect is lost when HRT has been discontinued for more than 12 months (Spector, Nandra et al. 1997). Moreover, post menopausal women taking oestrogen replacement therapy in various forms have been found to have larger tibial cartilage volumes than those who

have never taken HRT as assessed by magnetic resonance imaging, again strengthening the link with reduced OA severity (Wluka, Davis et al. 2001).

Obesity is amongst the most established and strongest risk factors for knee OA (Grotle, Hagen et al. 2008). Numerous longitudinal studies have identified a strong relationship between a body mass index (BMI) of >30 and the incidence of knee OA (Spector, Hart et al. 1994; Hochberg, Lethbridgecejku et al. 1995). However, increasing evidence notes a relationship between obesity and the incidence of hand OA (Carman, Sowers et al. 1994), suggesting that this involvement is not simply biomechanical and is therefore systemic in this capacity (Grotle, Hagen et al. 2008). Further studies have correlated both elevated serum cholesterol (Sturmer, Sun et al. 1998) and triglyceride (Cheras, Whitaker et al. 1997) concentration with OA, with serum cholesterol concentration reported as an independent risk factor for OA (Sturmer, Sun et al. 1998) in one large human clinical study.

Other systemic risk factors include high bone density (Hart, Cronin et al. 2002), genetics (Spector and MacGregor 2004) and nutritional status (McAlindon, Jacques et al. 1996). Please refer to Arden, 2006 for a comprehensive review of the systemic risk factors involved in the development of OA.

1.1.4.2 – Mechanical risk factors

Whereas systemic risk factors modulate the overall risk of developing OA, mechanical factors are more closely linked with determining which anatomical sites will be affected. Joint injury is widely accepted as a risk factor for knee OA (Davis, Ettinger et al. 1989; Felson 1990; Wilder, Hall et al. 2002). In addition to the direct effects of injury on the joint, disruption of joint biomechanics is suggested to further accentuate pathological damage, and contribute towards an increased risk of OA in later years (Arden and Nevitt 2006). The risk of knee OA is also elevated in patients who have gait abnormalities resulting in increased knee loading (Marks, Kumar et al. 1994), patients with anterior cruciate ligament insufficiencies (Longino, Frank et al.

2005) and most commonly, patients who have undergone partial meniscectomy surgery (Mills, Wang et al. 2008).

More recent studies have begun to describe a role of quadriceps muscle weakness in the pathogenesis of knee OA. Quadriceps involvement in the incidence and progression of knee OA will be reviewed in detail in **CHAPTER 1.3.8**.

1.1.5 – Summary

Osteoarthritis of the knee is a common disorder affecting cartilage, bone and skeletal muscle and causes significant morbidity. Current therapies for osteoarthritis offer only limited symptomatic relief. To date, no pharmaceuticals exist which are able to modulate the underlying disease process and therefore OA represents a great and unmet clinical need (Flannery 2010).

1.2 – Structure and Function of the Knee Joint

The knee joint is essentially composed of four main bones; the femur, tibia, fibula and patella. The knee joint comprises two different articulations between the femur and tibia, and between the femur and the patella forming the femorotibial and patellofemoral joints respectively. Each joint is held in the correct plane by a series of ligaments and muscles with associated tendons.

The knee is complemented with a selection of ligaments including the anterior and posterior cruciates, and the medial and lateral collateral ligaments. These serve to strengthen the knee structure as well as place restraints on the range of movements through which it can travel. Due to its location within the human skeleton, and the fact humans are bipeds, the knee joint is constantly exposed to varying forces which it must cushion and absorb to prevent the formation of pathological stresses. To cushion joint load, the articular surfaces are covered in cartilage, and the knee is equipped with the medial and lateral menisci which sit between the two articular surfaces of the femur and tibia. For a comprehensive review of the structure and biomechanics of the knee joint, see Bendjaballah, 1995 (Bendjaballah, Shirazi-Adl et al. 1995) (**FIGURE 1.1**).

Many muscles have insertions around the knee joint. Although some of these do not necessarily take part in gross knee movement, they play a crucial role in dynamic knee stability. The quadriceps muscle group sits above the patella and comprises the rectus femoris, vastus lateralis, intermedius and medialis. The quadriceps muscle group interacts with the patella via the patella ligament to extend the knee and maintain dynamic knee stability (**FIGURE 1.2**).

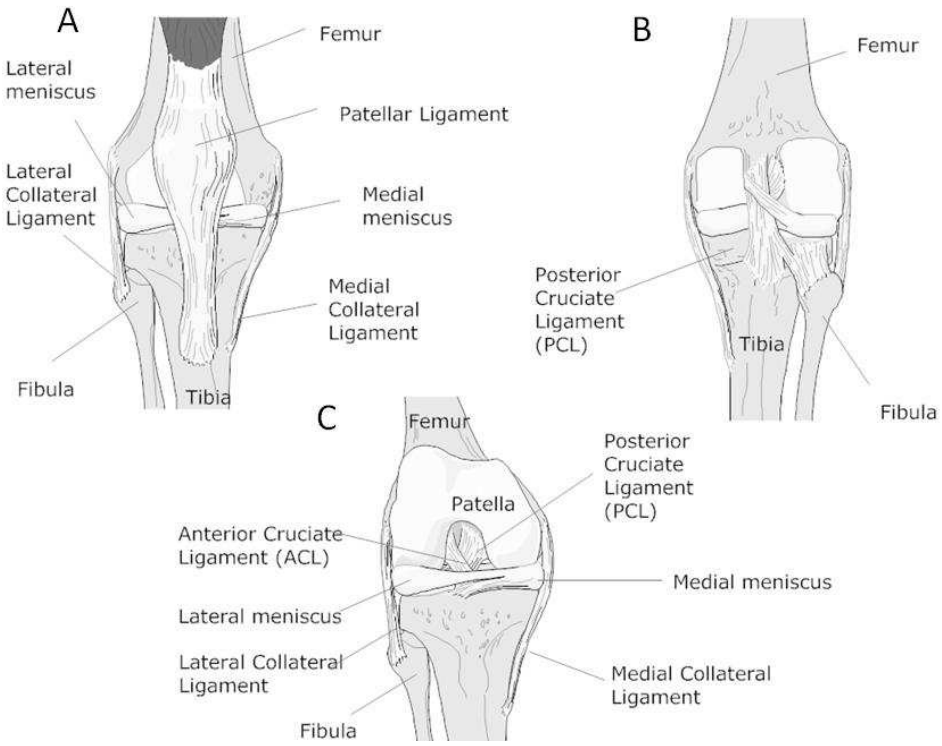

FIGURE 1.1 – Anatomical features of the human knee joint. (A) anterior extended, (B) posterior extended, (C) anterior at moderate flexion.

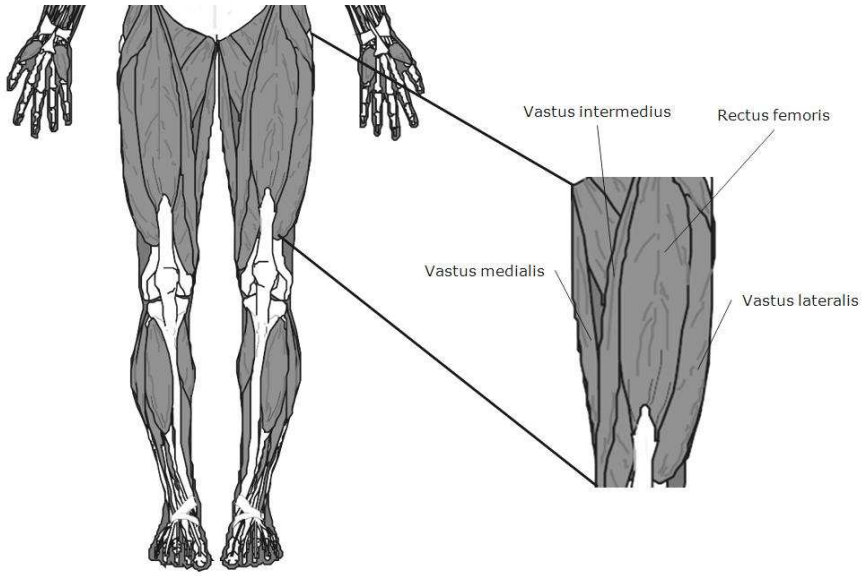

FIGURE 1.2 – Musculature of the human lower limb. The quadriceps muscle group comprising the vastus medialis, intermedius, lateralis and rectus femoris is highlighted.

1.3 – Skeletal Muscle

Skeletal muscle is one of the most highly organised structures in the biological world, and is primarily involved in the execution of voluntary movement (McNally, Lapidos et al. 2006). Skeletal muscle is composed of a number of muscle fibre types that differ with respect to their contractile, metabolic and molecular properties (Pette and Staron 2001). The characteristics of a skeletal muscle are a function of the contractile and metabolic properties of the muscle fibres from which it is composed.

1.3.1 – Structure

Skeletal muscle is composed of many individual muscle fibres (Dubowitz 2007). Each fibre is covered in endomycium and beneath this, resides the cell membrane or sarcolemma. Structurally, each muscle fibre is composed of many protein bundles called myofibrils, which in turn comprise alternate dark and light staining filaments (Dubowitz 2007). The sarcomere is composed of the thin (mostly actin) filaments, the thick (mostly myosin) filaments, and the giant filamentous molecule titin. The thin filaments are anchored in the Z-line, where they are cross-linked by α-actinin. The thick filament is located centrally in the sarcomere and constitutes the sarcomeric A-band. The myosin heads, or cross-bridges, on the thick filament interact with actin during activation. Titin spans the half-sarcomeric distance from the Z-line to the M-line, thus forming a third sarcomeric filament. In the I-band region, titin is extensible and functions as a molecular spring that develops tension upon stretch. In the A-band titin is inextensible due to its strong interaction with the thick filament. The distance from one Z-line to the next is defined as one sarcomere, the smallest integral contractile unit (McNally, Lapidos et al. 2006) (**FIGURE 1.3**).

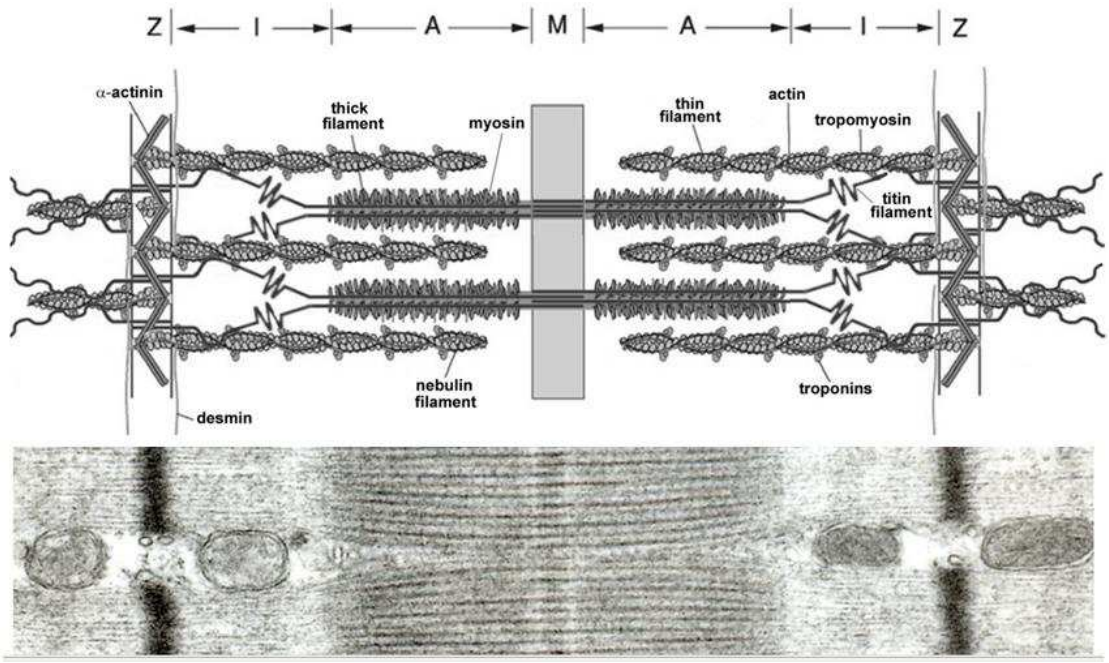

FIGURE 1.3 – Simplified model of two muscle sarcomeres in parallel. **Bottom**: electromicrograph showing the ultra-structural organisation of sarcomeres in parallel. Image reprinted from (Ottenheijm, Heunks et al. 2008)

1.3.2 – Skeletal muscle contraction

Muscle contraction consists of a cyclical interaction between myosin and actin driven by the concomitant hydrolysis of adenosine triphosphate (ATP) (Rayment, Holden et al. 1993). Myosin and actin, the components which respectively form the thick and thin filaments were amongst the first proteins to be purified with reference to muscle function (Block 1996). The hexametric protein myosin comprises two heavy chains (220 KDa) and four light chains (20-25 KDa), and forms the thick filaments. The terminus of myosin forms a globular head region required for the hydrolysis of ATP and binding of actin. The four light myosin chains are located between the globular head and the carboxy-terminal rod region (McNally, Lapidos et al. 2006). Thin muscle filaments are comprised of several proteins; however actin (43 KDa) is by far the most abundant constituent. Thick and thin regions of physical overlap form in which globular myosin heads project from the thick filaments to interact with thin actin filaments. ATP hydrolysis mediates a conformational change in the globular myosin

heavy chain head region, resulting in an interaction between the globular head and actin further along the filament and inducing a shortening of the muscle fibre.

Multiple isoforms of myosin heavy chain (MHC) exist, which comprise a family of molecular motors able to modulate the speed of skeletal muscle contraction (Rinaldi, Haddad et al. 2008). The contractile speed of a particular muscle fibre may therefore be determined, in part, by the isoform of MHC protein which it expresses. The sarcomeric MHC family consists of at least eight known isoforms, each encoded by a distinct gene located in two multigenic regions on two separate chromosomes (Weiss and Leinwand 1996). Six genes are encoded by a 300 – 600Kb segment on human and mouse chromosomes 17 and 11 respectively, in a cluster arrangement in the order MyH3/MyH2, MyH1/MyH 4, MyH 8/ MyH13 (5' – 3'). The MyH2, MyH1 and MyH4 genes encode the protein isoforms commonly termed MHC IIA, IIX and IIB. Of the eight sarcomeric isoform genes of MHC, four are known to be expressed in adult skeletal muscle: one "slow-twitch" (Type I) muscle associated MHC isoform is encoded by the MyH7β gene and three "fast-twitch" (Types IIA, IIX and IIB) muscle associated isoforms, associated with increasing contractile speed. A combination of the latter "fast-twitch" isoforms account for over 90% of MHC in adult skeletal muscle (Allen, Sartorius et al. 2001).

1.3.3 – Skeletal muscle metabolism

Muscle contraction is driven by the hydrolysis of adenosine triphosphate (ATP) (Rayment, Holden et al. 1993) which may be derived from the metabolism of fatty acids (β-oxidation) or carbohydrates (glycolysis). The β-oxidation of fatty acids takes place in the mitochondria of muscle fibres. Endothelial lipoprotein lipase (LPL) is involved in the transport of fatty acids from the circulatory system into the myocellular compartment (Fluck 2006). Hormone sensitive lipase (HSL) liberates free fatty acids from the intramyocellular lipid (IMCL) pool which are transported into the mitochondrion for β-oxidation by carnitine palmitoyltransferase 1 (CPT-1). The production of ATP via the β-oxidation of fatty acids is an oxygen-dependent process.

Carbohydrates reach the myofibre from the circulatory system and may be stored as glycogen, converted to triglycerides, or metabolised via glycolysis. In contrast to β-oxidation, the metabolism of carbohydrates via glycolysis is an oxygen independent process; however metabolism under these conditions leads to the production of lactate (Fluck 2006).

1.3.4 – Skeletal muscle fibre type classification - a historical overview

The characteristics of skeletal muscles are a function of the contractile and metabolic properties of the muscle fibres from which they are composed. Historically, the most basic form of skeletal muscle classification was based upon visual muscle pigmentation. Using this system, skeletal muscles were categorised as "red" or "white" (Dubowitz and Pearse 1960). For example, the soleus muscle was designated red, due to its appearance in contrast to the extensor digitorum longus (EDL) which was designated white. Physiological measurements of contractile speed (Brooke and Kaiser 1970) revealed that red fibres contracted slowly, whilst white fibres contracted more rapidly, enabling the delineation of type I (slow-twitch) and type II (fast-twitch) as the major skeletal muscle fibre types.

Early work using metabolic staining methods to measure oxidative and glycolytic activity noted that whereas type I fibres tended to be more oxidative, type II muscle fibres presented with varying degrees of glycolytic activity (Dubowitz and Pearse 1960). This resulted in the classification of slow oxidative fibres, and fast glycolytic fibres. Refined histochemical techniques later discriminated muscle fibres based upon their myosin ATPase activities and further subdivided type II fibres into IIA and IIB (Engel 1963; Guth and Samaha 1969; Brooke and Kaiser 1970). Further advances were also made with regards to the metabolic discrimination of fibre type and resulted in the classification slow-twitch oxidative (SO), fast-twitch oxidative (FO) and fast-twitch glycolytic (FG) (Peter 1972) fibres which were termed type I, IIA and IIB respectively.

More recent studies concentrated on the expression of muscle contractile elements, and reported that skeletal muscle fibres predominantly express a single isoform of myosin heavy chain (MHC) and that muscles could be classified by the predominant isoform of MHC expressed by their fibres (Gorza 1990). Moreover, Gorza and colleagues (Gorza 1990) reported a novel population of type II muscle fibres (subsequently named IIX), the contractile speed of which appeared to be intermediate between type IIA and type IIB. Because the muscle ATPase has been shown to reside within the heavy chain portion of myosin (Weiss and Leinwand 1996), it is unsurprising that histochemical differences in muscle fibre ATPase activity correlated well with the expression of specific isoforms of MHC. Within the last decade, advancing fibre typing methodologies have elucidated the existence of hybrid myofibres. Whereas “pure” myofibres express single isoforms of adult myosin (I, IIA, IIX and IIB); hybrid fibres express multiple, discrete isoforms of the MHC within a single fibre (Pette and Staron 2001). Hybrid fibres contain pairs of the major MHC isoforms and are classified according to their predominant isoform.

Based on these proposed systems, skeletal muscle fibres may be categorised into four different types; type I, IIA, IIX and IIB. Type I (slow oxidative) fibres are found in postural muscles were rapid movement is not essential. These fibres are particularly fatigue resistant and are therefore suited to prolonged periods of low-intensity contractile activity. Type IIA (fast oxidative, glycolytic) fibres display characteristics similar to both slow and fast fibres. They are relatively fatigue resistant, however have a faster contractile speed and are able to utilise both triglyceride and glycogen. Type IIX fibres are the fastest fibre found within human muscle (Harridge 2007) and have a rapid contractile speed and utilise glycogen for respiration. As such, they are particularly susceptible to fatigue and are only useful for short duration activities. Type IIB (fast glycolytic) fibres are found in many laboratory species. They have very rapid contractile speeds and utilise glycogen for respiration similarly to IIX fibres. Type IIB fibres are highly susceptible to fatigue and can sustain tetanus for less than one minute. **TABLE 1.3** contains a summary of the characteristics of current muscle fibre type nomenclature. Important inter-species differences include the absence of

IIB fibre expression in the locomotor muscles of the human (Harridge 2007), and evidence to suggest that rat type IIA muscle fibres are higher in oxidative activity than rat type I muscle fibres (Spangenburg and Booth 2003).

TABLE 1.3 – Characteristics of current muscle fibre type nomenclature.

Fibre Type	I	IIA	IIX	IIB
MHC Isoform	MHC I	MHC IIA	MHC IIX	MHC IIB
Colour	Red			White
Contractile Speed	Slow	Moderate	Fast	Very Fast
Fatigability	Low	Moderate	High	Highest
Metabolism	Oxidative	Oxidative / Glycolytic	Glycolytic	Glycolytic
Mitochondrial Content	High	High	Medium	Low

1.3.5 – Regulation of skeletal muscle fibre type

Skeletal muscle fibre type is determined by the differential expression of numerous genes which regulate contractile and metabolic processes. Muscle fibres are dynamic structures and are capable of modulating their phenotype in response to various conditions (Pette and Staron 2001). Phenotypic modulations affect all functional aspects of the muscle fibre including the expression of myofibrillar proteins, metabolic enzymes, glucose and fatty acid transporters and capillary density (Pette and Staron 2001). This section will consider the fibre type changes associated with innervation, exercise, mechanical load and hormone concentrations.

1.3.5.1 – Innervation

The importance of innervation in the specification of skeletal muscle fibre type has been reported in several studies (Pette and Staron 2001). Skeletal muscle is innervated by numerous motor neurones, each of which serves a small number of muscle fibres (McNally, Lapidos et al. 2006). Slow and fast muscle fibres are innervated by motor neurones which deliver slow and fast impulse patterns respectively (McNally, Lapidos et al. 2006). The importance of neuronal input in the specification of skeletal muscle fibre type has been derived from cross-innervation

studies which have reported reciprocal changes from fast to slow type muscle fibres when they are innervated with neurones of different impulse patterns (Eccles, Eccles et al. 1958; Buller, Eccles et al. 1960). Moreover, the importance of neuronal input in the maintenance of skeletal muscle fibre type has been demonstrated through studies which have shown that denervation leads to the loss of slow fibres in slow muscles and fast fibres in faster muscles respectively (d'Albis, Goubel et al. 1994; Huey and Bodine 1998). Although more recent studies suggest that the expression of neurotrophic factors may be implicated in the specification and maintenance of muscle fibre type (Boncompagni, Kern et al. 2007), studies replicating the effects of cross-innervation with electrical stimulation confirm that neuronal activity is central to this process (Pette, Smith et al. 1973).

1.3.5.2 – Exercise

Endurance training is associated with a conversion of muscle fibre type from type IIB (in rodents) towards type IIA (Wang, Zhang et al. 2004), an increase in oxidative metabolic enzymes and increased capillary density (Henriksson 1992). Similarly, strength training has also been associated with changes in muscle fibre type from IIB towards IIA (Staron, Malicky et al. 1990; Adams, Hather et al. 1993) however whether or not oxidative enzymes are also increased is less clear (Bishop, Jenkins et al. 1999).

1.3.5.3 – Loading and unloading

Both the induction of stretch-overload and mechanical loading result in the transition of muscle fibres from a fast to a slow phenotype (Pette and Staron 2001). Overloaded muscles have been reported to have increased type I muscle fibre abundance (Tsika, Wiedenman et al. 1996) and an associated elevation in MHC I mRNA and protein expression (Pette and Staron 2001). Conversely, muscle unloading is associated with the transition from slow to fast muscle fibre types. Unloaded rat soleus muscles have been reported to have reduced MHC I, increased MHC IIA expression and *de novo* synthesis of MHC IIB (Stevens, Gohlsch et al. 1999), a MHC isoform not normally found in the slow soleus muscle. Although muscle fibre

transitions are also evident in unloaded fast muscles, they tend to be less obvious and constitute more subtle fast to faster fibre-type switches (Adams, Haddad et al. 2000).

1.3.5.4 – Hormones

Of all hormones, thyroid hormone appears to have the greatest effect on skeletal muscle fibre type. Thyroid hormone is required for the decrease in neonatal MHC expression, and concomitant increase in type IIX (human) / IIB (rodents) muscle fibres occurring during development (Adams, Haddad et al. 2000). Hypothyroid rats show no impairment to type I muscle fibres however retain embryonic and neonatal MHC isoform expression in lieu of type II muscle fibre types (Adams, Haddad et al. 2000). Postnatally, a reduction of thyroid hormone is associated with fast to slow muscle fibre type transitions, whilst an increase in thyroid hormone concentration results in transitions from slow to fast (Adams, Haddad et al. 2000).

1.3.5.5 – Possible molecular control mechanisms

Changes in muscle fibre type require the coordinated expression of numerous functional gene groups including those encoding the contractile proteins, mitochondrial number, and fatty acid and glucose transport. As such it is appreciated that one single control mechanism is unlikely to be responsible for the diversity of fibre type (Spangenburg and Booth 2003). **FIGURE 1.4** contains a simplified overview of multiple possible fibre type gene regulatory pathways.

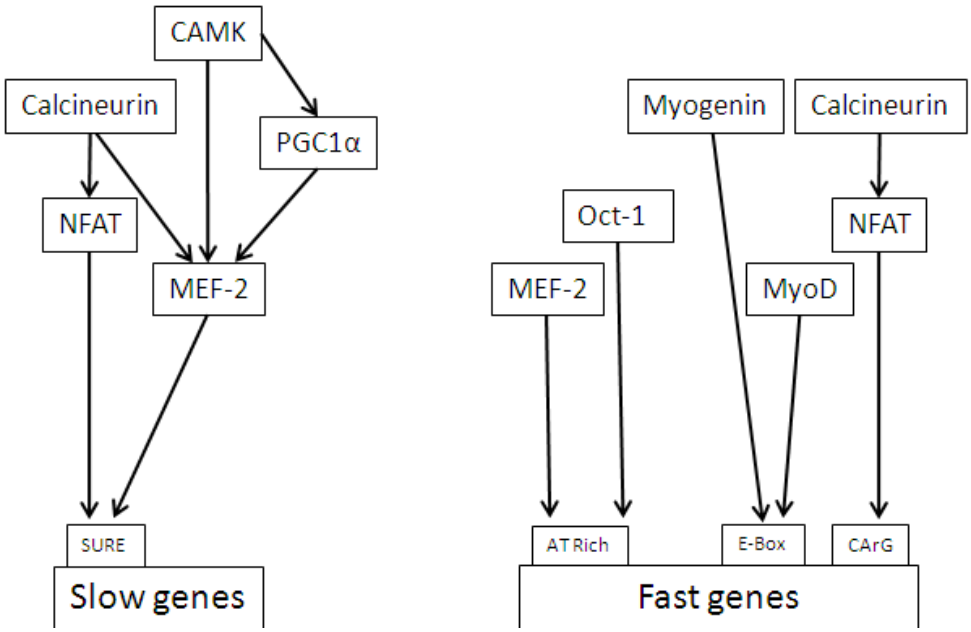

FIGURE 1.4: A simplified overview of multiple fibre type gene regulatory pathways. CAMK - calcium/calmodulin-dependent protein kinase II, PGC1α - peroxisome proliferator-activated receptor gamma coactivator-1 alpha, NFAT - Nuclear factor of activated T-cells, MEF-2 – myocyte enhancer factor-2, SURE – slow upstream element of troponin 1 promoter, MyoD – myogenic differentiation 1, AT rich – AT rich region of fast MHC promoter, CArG – fast MHC promoter element with NF1 and SRF binding capacity. Diagram adapted from (Spangenburg and Booth 2003).

1.3.6 – Regulation of skeletal muscle mass

In addition to fibre type plasticity, skeletal muscle is also subject to changes in mass, the maintenance of which is a fine balance between protein synthesis and protein degradation (Lang, Frost et al. 2007; Russell 2009). Skeletal muscle mass is increased when there is a net gain in protein synthesis. Increased skeletal muscle mass may result from hyperplasia, hypertrophy, or a combination of the two processes (Rehfeldt, Fiedler et al. 2000). Conversely, skeletal muscle mass is reduced when protein degradation occurs more rapidly than protein synthesis (Russell 2009), resulting in a decrease in the mass of existing muscle fibres (Chang 2007).

Postnatal growth is primarily a result of the enlargement and elongation of existing skeletal muscle fibres. The differentiation of skeletal muscle is therefore a prerequisite to the induction of skeletal muscle hypertrophy (Chang 2007). Skeletal muscle is derived from the specification of mesodermal pleuripotent stem cells to a myogenic lineage via the expression of myoblast determination factor (MyoD) and myf-5 (Johnston 2006). Myogenic precursor cells (myoblasts) undergo proliferation, associated with an increase in proliferating cell nuclear antigen (PCNA), to form myoblast pools (Rehfeldt, Fiedler et al. 2000). During differentiation, myoblasts are forced to exit the cell cycle and terminate proliferation. Cell cycle exit is associated with an increase in p21 expression (Johnston 2006) and is under the control of myogenin, MRF-4 and MEF-2 expression (Johnston 2006). On differentiation, myoblasts begin to express muscle-specific proteins and fuse to form multinucleated myotubes (Rehfeldt, Fiedler et al. 2000). During muscle development, muscle fibres develop from distinct myoblast populations (Miller, Everitt et al. 1993). Primary myofibres form first, and provide a framework for the subsequent formation of secondary myofibres (Miller, Everitt et al. 1993). A further pool of myoblasts, termed satellite cells, do not form muscle fibres but remain in close proximity to the myofibres where they retain their ability to proliferate and provide a source of new muscle tissue during postnatal growth (Amthor, Otto et al. 2009). In the adult, satellite cells are normally mitotically quiescence, and must therefore be activated in order to proliferate (Ono, Boldrin et al. 2010).

1.3.6.1 – Hypertrophy and Akt signalling

The IGF/PI3K/AKT axis is possibly one of the most well described pathways involved in the regulation of skeletal muscle mass (Glass 2005; Russell 2009). Insulin-like growth factor I (IGF-1) is sufficient for the induction of marked skeletal muscle hypertrophy (Rommel, Bodine et al. 2001). IGF-I stimulates the phosphatidylinositol-3-kinase (PI3K) pathway, resulting in the activation of downstream targets required for protein translation (Rommel, Bodine et al. 2001). Protein synthesis is controlled at the level of translational initiation by the inhibition of eukaryotic initiation factor

4e (eIF4E) by PHAS-1 (4EBP1) binding (Connolly, Braunstein et al. 2006) and the inhibition of eukaryotic initiation factor 2b (eIF2B) by glycogen synthase 3β (GSK3β) (Pap and Cooper 2002). The initial step in this pathway involves the phosphorylation, and inactivation of tuberous sclerosis complex 1 and 2 (Tsc1/2) known to inhibit mammalian target of rapamycin (mTOR) by PI3K activated Akt (Glass 2005). Activated mTOR hyperphosphorylates and inactivates PHAS-1 (4EBP1) thereby liberating eIF4E and enhancing protein synthesis (Connolly, Braunstein et al. 2006). Activated Akt is able to directly induce the inhibition of GSK3β by phosphorylation, and the activation of eukaryotic initiation factor 2b (eIF2B) (Glass 2005). Both exercise (McKoy, Ashley et al. 1999) and mechanical loading (Bamman, Shipp et al. 2001) are associated with hypertrophy and increased localised muscle expression of IGF-I. Over-expression studies in mice have also noted marked muscle hypertrophy in response to localised IGF-1 production (Musaro, McCullagh et al. 2001).

1.3.6.2 – Satellite cell proliferation

Skeletal muscle satellite cells are normally mitotically quiescent (Ono, Boldrin et al. 2010), although retain the ability to generate new muscle fibres or to provide new myonuclei (Rehfeldt, Fiedler et al. 2000; Amthor, Otto et al. 2009) following activation. β-catenin, downstream of GSK3β, has been implicated in the maintenance of the satellite cell population by promoting self-renewal (Perez-Ruiz, Ono et al. 2008). After muscle damage, satellite cells are activated and proliferate for muscle repair and regeneration (Kadi, Charifi et al. 2005). Satellite cell number is reported to increase following exercise, (Kadi, Schjerling et al. 2004) and steadily decrease in response to prolonged periods of detraining (Kadi, Schjerling et al. 2004). They are therefore considered imperative for the maintenance of skeletal muscle (Kurosaka and Naito 2009). The activation of satellite cells can be attributed to exercise, exercise-induced release of growth factors such as IGF-I, or the exercise-induced release of inflammatory substances (Kadi, Charifi et al. 2005). IGF-I has been shown to increase the proliferation of satellite cells via activation of the Raf-MEK-Erk pathway (Kadi, Schjerling et al. 2004).

1.3.6.3 – STARS signalling

In order for skeletal muscle to adapt to mechanical stresses, there is the requirement for a system capable of sensing such changes, and transducing these signals into an appropriate response. It has been proposed that the STARS (striated activator of Rho signalling) pathway provides such a system and links the transduction of external stress to the maintenance of skeletal muscle function via growth and remodelling (Russell 2009). The expression of STARS specific mRNA, and its downstream target serum response factor (SRF) have been found to increase during functional muscle overload (Mahadeva, Brooks et al. 2002). Moreover, STARS has been shown to be regulated by both MEF-2 and MyoD. Both of these transcription factors are activated by Akt (Xu and Wu 2000) and it has therefore been suggested that STARS and Akt may converge to form a complex pathway which regulates muscle growth and regeneration (Russell 2009).

1.3.6.4 – Atrophy and Akt signalling

Given that AKT signalling is associated with the induction of skeletal muscle hypertrophy, numerous studies have investigated the role of this signalling pathway in skeletal muscle atrophy (Russell 2009). Mechanical muscle unloading, dennervation, as well as numerous human muscle atrophy conditions are associated with reduced IGF-I production (Grounds 2002) and reduced AKT activation (Russell 2009). Moreover, molecular studies have reported reduced downstream activation of p70S6K, increased binding of 4EBP1 to eIF4E (Bodine, Stitt et al. 2001) and therefore reduced protein translation.

1.3.6.5 – Atrogene signalling

Although skeletal muscle atrophy may involve the calcium-dependent calpain system, the lysosomal protease system and the proteasome system (Jackman and Kandarian 2004), the majority of skeletal muscle proteolysis in many disease states may be attributed to an activation of the ubiquitin proteasome pathway (Jagoe and Goldberg 2001) as evidenced by numerous studies in humans and animal models of disease (Lecker, Jagoe et al. 2004). Degradation via the ubiquitin-proteasome pathway is a multistep process requiring ATP hydrolysis. The first stage involves the transfer of activated ubiquitin to the E2 ubiquitin-conjugating protein by E1 ubiquitin-activating enzyme. E2 ubiquitin-conjugating protein then transfers the ubiquitin to an E3 ubiquitin-ligase protein, which forms a complex with the protein destined for degradation. Following the addition of multiple ubiquitin molecules, the targeted protein is recognised by the 19S cap proteins of the 26S proteasome. The protein is then fed into the 20S core of the proteasome where it is degraded by active proteolytic enzymes (Orlowski and Dees 2003). Although several hundred different E3 ligases have been identified (Glass 2005), skeletal muscle atrophy has been consistently associated with significant increases in muscle ring-finger I (MuRF1) and muscle atrophy F-box (MAFBx) expression, which are often termed the "atrogenes". Both MuRF1 and MAFBx have been shown to have E3 ligase activity (Bodine, Latres et al. 2001). MuRF1/MAFBx expression is induced by dennervation (Lecker, Jagoe et al. 2004), chronic lipopolysaccharide-induced infection (Dehoux, van Beneden et al. 2003), as well as in 13 independent animal models of muscle atrophy (reviewed by Glass, 2005) confirming their pivotal role in skeletal muscle proteolysis. The expression of the E3 ligases is controlled via NFκβ signalling in the case of MuRF1, or the p38 MAPK cascade in the case of MAFBx. Tumour necrosis factor-like weak inducer of apoptosis (Tweak) activates NFκβ by phosphorylation and degradation of Iκβα (Dogra, Changotra et al. 2006) which in turn induces the expression of MuRF1 (Cai, Frantz et al. 2004). Similarly, NFκβ may be activated by tumour necrosis factor alpha (TNFα), also found to be elevated in several atrophy conditions (Hafer-Macko, Yu et al. 2005). NFκβ has been found to be elevated in

skeletal muscle atrophy due to disuse and sepsis (Glass 2005), and blockade of the NFκβ pathway can attenuate skeletal muscle atrophy (Li and Reid 2000). p38 MAPK activates MAFBx expression (Chen, Jin et al. 2007), the action of which is antagonised by dual specificity phosphatase 1 (Dusp1) via inhibition of p38 (Franklin and Kraft 1997). TNFα has been shown to induce MAFBx expression, an effect that is ameliorated by p38 inhibition (Li, Chen et al. 2005). Myosin heavy chain has been reported to be a specific target for proteosome degradation (Acharyya, Ladner et al. 2004).

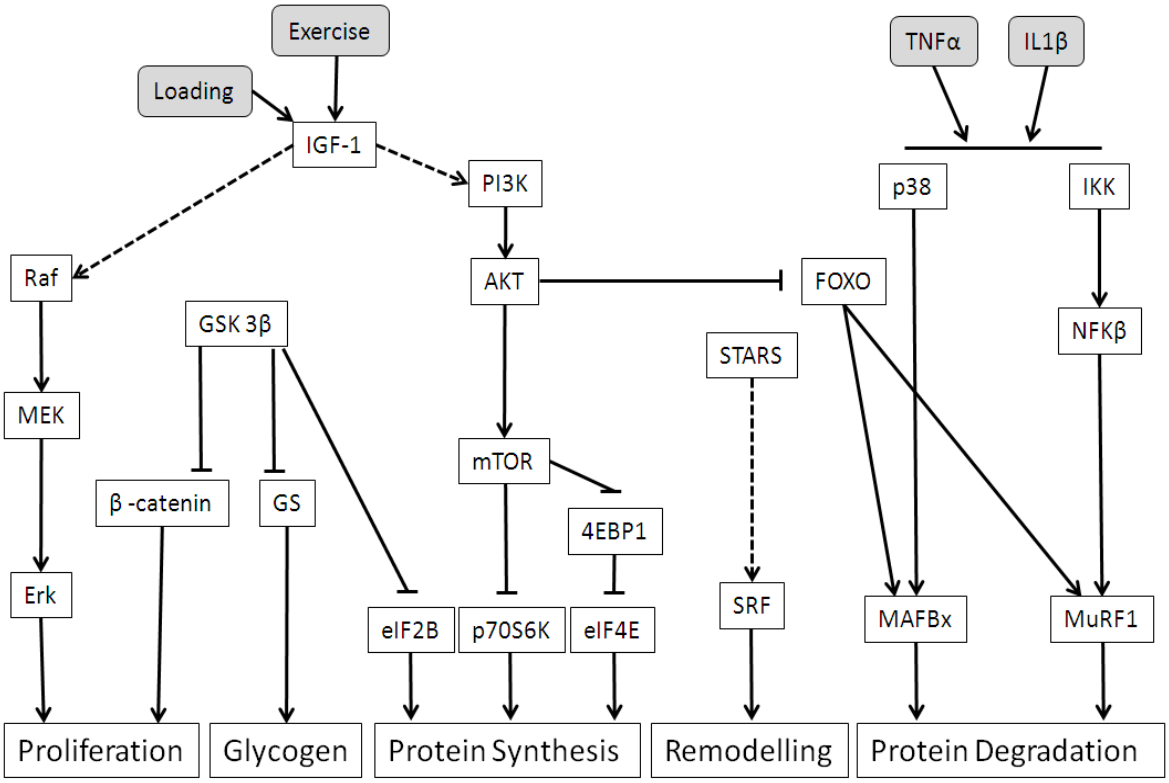

FIGURE 1.5: Summary of some of the signalling pathways involved in skeletal muscle proliferation, glycogen synthesis, protein synthesis, skeletal remodelling events and protein degradation. Raf – proto-oncogene c-raf , MEK – mitogen-activated protein, ERK – extracellular-signal-regulated kinase, GSK3β – glycogen synthase 3β, GS – glycogen synthase, eIF2B – eukaryotic translation initiation factor 2b, mTOR – mammalian target of rapamycin, p70S6K – ribosomal protein S6 kinase, 4EBP1 (PHAS-1) – eIF4E binding protein 1, STARS – striated activator of Rho signalling, SRF –

serum response factor, FOXO – forkhead box O, MAFBx – muscle atrophy F-box, MuRF1 – muscle ring finger protein 1, IKK – IK B kinase, NFKB – nuclear factor kappa-light-chain-enhancer of activated B cells, TNFα – tumour necrosis factor alpha, IL1β – interleukin 1β.

1.3.6.6 – Summary

The regulation of skeletal muscle may encompass both changes in muscle fibre type (contractile and metabolic), and changes in skeletal muscle mass. The regulation of skeletal muscle fibre type stems from several molecular pathways which result in the differential regulation of numerous gene groups which encode contractile, metabolic and transport-associated proteins. The regulation of skeletal muscle mass involves the complex interplay of protein synthesis and protein degradation. Increases in skeletal muscle mass are associated with both hypertrophic and hyperplastic responses which are mediated by numerous interconnecting molecular pathways. Decreases in skeletal muscle mass are associated with both increased protein degradation and decreased protein synthetic drive. The next section will consider changes in skeletal muscle fibre and mass in several pathological conditions.

1.3.7 – The effects of pathology on skeletal muscle fibre type and mass

Many human pathologies impact upon skeletal muscle function, both with respect to muscle fibre type, and the regulation of skeletal muscle mass. This section will give a brief overview of the effects of sarcopenia, cachexia, disuse and chronic obstructive pulmonary disease on parameters of muscle function. The effects of knee osteoarthritis will be considered separately in the next section.

Sarcopenia was originally described by Evans (Evans and Campbell 1993) and defined as an age-related decrease in lean body mass. Sarcopenia results in reduced strength, metabolic rate and aerobic capacity (Evans 2010). Sarcopenia is a multifactorial condition resulting from disuse, endocrine changes, inflammation and

insulin resistance (Lecker, Jagoe et al. 2004). The reduction of muscle bulk in sarcopenia has been attributed to the coordinate loss (Lexell, Taylor et al. 1988) and atrophy (Sato, Akatsuka et al. 1984) of muscle fibres. Although there is some contention with regards which fibre types are preferentially affected (Evans 2010), the general consensus indicates that type II muscle fibres are more susceptible to age-related atrophy than type I fibres (Bua, McKiernan et al. 2002).

Cachexia is the accelerated loss of skeletal muscle protein in the absence of reduced energy intake (Evans 2010) and may or may not include loss of adipose tissue (Lecker, Jagoe et al. 2004). Cachexia results in marked skeletal protein loss and contributes to nearly one-third of cancer related deaths (Acharyya, Ladner et al. 2004). As with many atrophy conditions, cachexia is thought to result from a coordinate increase in proteolysis and decrease in protein synthesis. Cachexia is moreover associated with inflammation and insulin resistance. Similarly to sarcopenia, cachexia results in the preferential atrophy of type II muscles fibres (Baracos, Devivo et al. 1995; Acharyya, Ladner et al. 2004), with type I fibres less affected. Despite many similarities with sarcopenia, cachexia is a distinct disease, and requires more careful management (Evans, Morley et al. 2008) given the high level of mortality associated with this condition.

Disuse atrophy has been well-described in patients following extended bed rest (Ohira, Yoshinaga et al. 1999) and in numerous animal models of un-loading (Giger, Bodell et al. 2009). More commonly, disuse atrophy is noted in patients undergoing orthopaedic surgery requiring joint casting (Reardon, Davis et al. 2001). Both human and animal studies have demonstrated a rapid decrease in protein synthesis and concomitant increase in proteolysis via the ubiquitin-proteasome pathway (Reardon, Davis et al. 2001). Unlike the majority of atrophy conditions that comprise type II fibre atrophy (Ohira, Yoshinaga et al. 1999; Giger, Bodell et al. 2009), disuse atrophy preferentially affects type I muscle fibres, with little evidence of type II fibre involvement. Type I fibres tend to accrue in slow, postural muscles such as the soleus

(Caiozzo, Haddad et al. 1996). Similar effects of slow type I muscles are also noted in rodents maintained in microgravity environments, with the exception that some studies report the de novo synthesis of MHC IIX fibres in space-flown rodents (Caiozzo, Haddad et al. 1996; Adams, Haddad et al. 2000), an observation that is not generally reported in disuse atrophy.

Chronic obstructive pulmonary disease is a generalised term used for chronic bronchitis, emphysema or both of these conditions. COPD results in breathlessness, increased incidence of chest infections and marked muscle weakness (Gosker, Engelen et al. 2002). Interestingly, COPD is associated with atrophy of the vastus lateralis, a component part of the quadriceps muscle group. The degree of atrophy is considered an independent predictor of mortality (Hansen, Gualano et al. 2006). There is no consensus with regards to which muscle fibres are preferentially affected. Whilst some studies report the preferential atrophy of MHC IIX fibres (and MHC IIA/IIX hybrid fibres) (Gosker, Engelen et al. 2002), others report type I / IIA fibre predominant atrophy (Jobin, Maltais et al. 1998; Whittom, Jobin et al. 1998).

1.3.8 – The effects of osteoarthritis on parameters of muscle function

It is established that patients with knee osteoarthritis (OA) exhibit marked muscle weakness (Slemenda, Heilman et al. 1998; Brandt, Heilman et al. 1999; Hurley 1999; Brandt, Heilman et al. 2000; Becker, Berth et al. 2004; Eyigor 2004; Ikeda, Tsumura et al. 2005; Mikesky, Mazzuca et al. 2006; Mohammadi, Taghizadeh et al. 2008; Nishimura, Hasegawa et al. 2010), which is one of the most frequent and earliest reported symptoms associated with knee OA (Longino, Frank et al. 2005). Weakness primarily affects the quadriceps muscle with little or no evidence of hamstring involvement (Brandt, Heilman et al. 1999), resulting in a reduced quadriceps to hamstring mass (Q/H) ratio (Hayes, Song et al. 2002).

Historically, muscle weakness has been considered a secondary effect in knee OA, resulting from disuse of the affected joint due to the presence of pain and/or

inflammation, and therefore has received little attention with regards to its involvement in the initiation or progression of OA. However, there is clinical evidence which suggests that quadriceps weakness may precede the onset of radiographic evidence of OA and subsequent pain (Hurley 1999), and therefore may be directly involved in its pathogenesis (Ikeda, Tsumura et al. 2005). Firstly, quadriceps weakness has been reported in patients with radiographic signs of knee OA in the absence of pain, suggesting that muscle weakness is unlikely to be due to disuse of a painful joint (Slemenda, Brandt et al. 1997). Secondly, quadriceps weakness was noted in a number of patient groups who are susceptible to developing knee OA, for example patients who have gait abnormalities resulting in increased knee loading (Marks, Kumar et al. 1994), patients with anterior cruciate ligament (ACL) insufficiencies (Longino, Frank et al. 2005) and most commonly patients who have undergone partial meniscectomy surgery as a treatment of medial meniscal tears (Mills, Wang et al. 2008). Initially, patients who have undergone meniscectomy have marked muscle weakness of the ipsilateral limb in the absence of manifest OA (Becker, Berth et al. 2004; Ericsson, Roos et al. 2006). However, at long-term follow-up, meniscectomised patients have an elevated incidence of OA (odds ratio = 10), compared to age and sex matched subjects with no history of meniscal injury (Lohmander, Englund et al. 2007). In these patient groups, quadriceps dysfunction was noted prior to any radiographic evidence of OA, again suggesting that the quadriceps dysfunction reported in knee OA was unlikely to be solely due to disuse atrophy.

Whether a strong quadriceps muscle can also be a protective factor in the initiation of OA is perhaps more debatable. A study examining the incidence of OA at a 5-year follow up in subjects with no radiographic evidence of OA at baseline, found that those subjects who developed OA had weaker quadriceps strength at baseline (Thorstensson, Petersson et al. 2004). Conversely, a recent longitudinal study conducted by Segal and colleagues 2009 found that although quadriceps strength was reduced with increasing Kellgren-Lawrence (KL) grade for tibiofemoral OA at

baseline, neither strength nor normal Q/H ratio was protective against the development of incident radiographic OA. However, of interest, increased quadriceps strength *was* protective against the development of incident symptomatic whole knee OA, albeit this was restricted to female participants once corrected for knee pain at baseline (Segal, Torner et al. 2009).

There is also contradictory evidence with regards quadriceps strength and disease progression in individuals with established knee OA. The assessment of patients with established knee OA showed that a strong quadriceps muscle was protective for cartilage loss at the lateral compartment of the patellofemoral joint (Amin, Baker et al. 2009) and joint space narrowing (Segal, Glass et al. 2010) over a 30 month period. Moreover an association between restricted quadriceps range-of-motion and increased progression (Nishimura, Hasegawa et al. 2010) has been reported. However, other studies have found this protective effect to be limited to females only (Slemenda, Heilman et al. 1998) and one study found a detrimental effect in malaligned and lax knees (Sharma, Dunlop et al. 2003).

Morphological studies suggest that the muscle dysfunction associated with knee OA is due, in part, to atrophy of quadriceps muscle fibres. A recent study noted that all patients assessed with knee OA presented with atrophy of type II fast-twitch muscle fibres, whilst less than one third of the patients presented with atrophy of type I slow-twitch muscle fibres (Fink, Egl et al. 2007) as assessed by histochemical staining. This suggests that quadriceps dysfunction in knee OA is most commonly associated with atrophy of fast-twitch type II muscle fibres, an observation supported by previous histochemical studies (Nakamura and Suzuki 1992), and reported in many other muscle atrophy associated conditions.

1.3.9 - Interventions for the amelioration of atrophy associated conditions

Atrophy is often a consequence of aging, cachexia, disuse, chronic obstructive pulmonary disease and osteoarthritis. Moreover, the effectiveness of glucocorticoid

treatments, such as dexamethasone, is limited due to muscle wasting which is a commonly reported side effect (Glass 2003). Currently, there are no safe and effective medicines available for the treatment of skeletal muscle atrophy (Glass 2003). Due to the clinical implications of skeletal muscle atrophy, amelioration of this debilitating condition has been considered in numerous studies.

1.3.9.1 – Exercise

The effects of various exercise paradigms have been shown to increase protein synthesis (Boirie 2009) and attenuate both age-related (Song, Kwak et al. 2006) and glucocorticoid-induced (Falduto, Czerwinski et al. 1990) muscle fibre atrophy. It is possible that exercise mediates the inhibition of atrophy via contractile input (Falduto, Czerwinski et al. 1990), via increased local IGF-I production (Chang 2007) and downstream increases in protein translation, or a combination of the two processes.

With reference to osteoarthritis, a number of studies have shown that exercises aimed at improving quadriceps function have beneficial symptomatic effects in knee OA patients (O'Reilly, Muir et al. 1999; Baker, Nelson et al. 2001; Thomas, Muir et al. 2002; Eyigor 2004; Keefe, Blumenthal et al. 2004; Rosemffet, Schneeberger et al. 2004; Diracoglu, Aydin et al. 2005; Mikesky, Mazzuca et al. 2006; Jan, Lin et al. 2008; Bezalel, Carmeli et al. 2010). For example, the impact of both high and low resistance training on subjects with knee OA was recently investigated, where it was reported that improved quadriceps function was associated with a reduction in knee pain and increased physical ability (Jan, Lin et al. 2008). Similarly, strength training and balance exercises were also shown to significantly reduce knee pain and improve physical ability (Diracoglu, Aydin et al. 2005). To date, only one randomised-controlled trial, evaluating the effects of strength training programs on the onset and progression of knee OA, has been conducted (Mikesky, Mazzuca et al. 2006). Patients with established knee OA undergoing 3 sessions of strength training (ST) per week had reduced joint space narrowing (JSN) at 30 month follow-up compared with those

patients undertaking range of motion (ROM) exercises for the same duration. However, patients undertaking ST who were radiographically normal at baseline exhibited a slightly elevated incidence of JSN than those undertaking ROM exercises.

1.3.9.2 – Molecular

Numerous studies have attempted to ameliorate atrophy by modulating components of molecular pathways known to be involved in the process (see **FIGURE 1.5**). At the molecular level, the inhibition of E3-ligases MuRF1 and MAFBx (Bodine, Latres et al. 2001), the constitutive activation of AKT (Bodine, Stitt et al. 2001) and the direct administration of IGF-I (Stitt, Drujan et al. 2004) have been shown to decrease (MuRF1/MAFBx) or even ablate (AKT/IGF-I) skeletal muscle atrophy. Such studies have provided new molecular drug targets against which novel pharmaceuticals may be directed in the hope of ameliorating muscle atrophy in a variety of clinical conditions (Glass 2005).

1.3.9.3 – Pharmacological

Testosterone is an important male steroid hormone, the effects of which increase muscle mass and reduce adipose tissue (Chang 2007). Anabolic steroids have been reported to increase skeletal muscle protein synthesis (Kadi, Eriksson et al. 1999; Sheffield-Moore 2000; Bhasin, Calof et al. 2006), decrease skeletal muscle proteolysis (Kutscher, Lund et al. 2002; Bhasin, Calof et al. 2006) and induce the activation of satellite cells (Kadi 2000; Bhasin, Calof et al. 2006). Testosterone administration has been associated with the hypertrophy of both type I and type II muscle fibres (Sinha-Hikim, Artaza et al. 2002; Bhasin, Calof et al. 2006), but has not been associated with relative changes in muscle fibre type composition (Sinha-Hikim, Roth et al. 2003). Testosterone administration has been reported to reverse atrophy induced by sarcopenia (Kovacheva, Sinha Hikim et al.), glucocorticoid administration (Bhasin, Calof et al. 2006) and human immune deficiency virus (HIV) infection (Bhasin, Calof et al. 2006). Conversely, testosterone administration has not been found to elicit any effects on atrophy induced by dennervation (Beehler, Sleph et al. 2006). Limited

information is available with respect to the potential signalling pathways via which testosterone elicits such hypertrophic effects, however the primary mechanism is thought to be via localised production of IGF-I (Chang 2007) and the subsequent activation AKT signalling (Stitt, Drujan et al. 2004).

The administration of β2-adrenergic agonists, such as clenbuterol, has been reported to induce skeletal muscle hypertrophy and decrease atrophy. Moreover, clenbuterol administration has been associated with slow to fast muscle fibre-type shifts, thereby demonstrating a potential to maintain the very fibre types lost to atrophy in numerous conditions (Baracos, Devivo et al. 1995; Whittom, Jobin et al. 1998; Bua, McKiernan et al. 2002; Gosker, Engelen et al. 2002; Acharyya, Ladner et al. 2004; Evans 2010). By virtue of their hypertrophic effects on skeletal muscle, the administration of β2-agonists has been examined in a number of atrophy associated conditions with a view to positively modulating disease outcomes.

The hypertrophic action of β2-agonist administration is thought to result from both increases in protein synthetic rate and decreased proteolysis. The binding of β2-agonists to β2-ARs leads to the activation of adenyl cyclase, an enzyme which catalyses the conversion of ATP to cAMP. cAMP binds to protein kinase A (PKA) and in doing so releases a catalytic subunit. The catalytic subunit phosphorylates a number of intracellular proteins including the cAMP response element binding protein (CREB). CREB is able to bind to the cAMP response element of various genes are thereby induce their transcription. β2-agonists have also been shown to activate the PI3K/Akt pathway leading to the activation of downstream signalling and subsequent increase in protein synthesis (Ryall and Lynch 2008). Kline and colleagues (Kline, Panaro et al. 2007) demonstrated that whilst clenbuterol-induced fast-fibre hypertrophy could be ablated by the use of rapamycin inhibitors (therefore blockading factors signalling downstream of mTOR), slow-fibre hypertrophy was unaffected suggesting the hypertrophy slow and fast fibres may be differentially regulated (Kline, Panaro et al. 2007). Moreover, β2-agonist administration has been

shown to have marked effects on skeletal muscle proteolytic systems. Although the precise mechanism of proteolytic inhibition remains unclear (Ryall and Lynch 2008), β2-agonists have been shown to reduce calcium dependent (calpain) mediated proteolysis by decreasing μ-calpain expression (Forsberg, Ilian et al. 1989), and increase expression of the endogenous inhibitor of calpain, calpastatin (PARR, BARDSLEY et al. 1992). β2-agonist administration has been further demonstrated to have potent effects on the ubiquitin-proteasome pathway. It has been proposed that the decreased proteolysis via this pathway is mediated by numerous β2-agonist induced changes including decreased ubiquitin availability (Costelli, GarcÃ-a-MartÃ-nez et al. 1995), decreased ubiquitination of target proteins (Busquets, Figueras et al. 2004), decreased E3 ligase expression (Kline, Panaro et al. 2007) and reduced proteasome activity (Busquets, Figueras et al. 2004).

β2-agonists have been implicated in the shift from slow to faster-twitch muscle fibre type (Ricart-Firinga, Stevens et al. 2000; Stevens, Firinga et al. 2000). Whether the increase in faster-fibre types is associated with an increase in glycolytic metabolic potential is perhaps less clear. Whilst Pellegrino and colleagues noted an increase in glycolytic metabolism (phosphofructokinase, PFK and lactate dehydrogenase, LDH) following clenbuterol administration in mice (Pellegrino, D'Antona et al. 2004), Mounier and colleagues, 2007 failed to replicate this finding in the rat (Mounier, Cavalié et al. 2007). Clenbuterol has been shown to have a greater hypertrophic effect on slow-twitch muscle when compared with faster-twitch muscles (Ricart-Firinga, Stevens et al. 2000; Stevens, Firinga et al. 2000; Herrera, Zimmerman et al. 2001), further suggesting a fibre type specific response.

Due to their hypertrophic and fibre modulating effects, β2-agonist use has recently been considered for the treatment of human pathologies which include a component of muscle weakness or atrophy including sarcopenia, cancer cachexia, disuse, microgravity and chronic obstructive pulmonary disorder. To date, β2-agonist

administration has not been considered with respect to ameliorating osteoarthritis associated skeletal muscle atrophy.

1.4 – Summary and Global Hypothesis

Osteoarthritis of the knee is associated with skeletal muscle dysfunction of the quadriceps muscle. Fibre typing studies have reported variable changes to the fibre-type composition of the quadriceps muscle group in response to osteoarthritis. Whilst the majority of evidence suggests that type II fibres are preferentially affected (Nakamura and Suzuki 1992), others report that up to one third of patients present with type I fibre atrophy (Fink, Egl et al. 2007). Furthermore, population-based studies have shown that a larger quadriceps mass may be protective of both the initiation of OA and disease progression in established disease. Central to this thesis is the hypothesis that muscle fibre type is altered in response to developing and progressing osteoarthritis of the knee.

The following specific hypotheses are addressed as follows;

Chapter 3 – Hypotheses

The development of meniscectomy-induced osteoarthritis will be associated with changes to the fibre-type composition of the quadriceps muscle group, potentially manifesting as a reduced type II fibre complement. Clenbuterol administration for 14 days will result in marked hypertrophy of the quadriceps muscle group, with an associated increase in the proportion of type II fast twitch muscle fibres. The induction of quadriceps hypertrophy and the potential modulation towards a faster-twitch muscle phenotype prior to the induction of OA will have a protective effect on the knee joint, assessed histologically 21 days post induction.

Chapter 4 – Hypotheses

The structure of the sarcomeric MHC family in the laboratory guinea pig will be clustered in a head-to-tail fashion, consistent with that of other species which have been previously described (chapter 1.3.3). Furthermore, enough sequence variability will exist between the various isoforms of MHC, at the mRNA level, as to allow the

design and validation of isoform-specific oligonucleotide primers for expression studies by quantitative PCR.

Chapter 5 – Hypotheses

Bilateral knee OA will present in the Dunkin Hartley guinea pig from around 3 months of age. Consistent with other literature, it is expected that the severity of OA will increase with advancing age and increasing body mass. Functional changes to the quadriceps muscle will occur coincident with the development of knee OA, and animals may present with changes to contractile (MHC) or metabolic muscle parameters.

Chapter 6 – Hypotheses

Rat-derived myotubes (L6.G8.C5) will express a range of MHC isoforms, indicative of the presence of multiple fibre types, and thus model the *in vivo* situation. Osteoarthritis has been associated with both elevated serum TNFα concentration and type II muscle fibre atrophy. Therefore it is hypothesised that the administration of recombinant rat TNFα to rat-derived myotubes will result in changes to their MHC composition, indicative of fibre type shifts. More specifically, it is hypothesised that TNFα will induce a reduction in the abundance of fast-type II fibre specific mRNAs (MHC IIX, MHC IIB).

The hypotheses are investigated within this thesis in four separate results chapters. Chapter 3 reports the effects of β2-adrenergic agonist administration on the severity of osteoarthritis in a rodent meniscectomy induced model. Chapter 4 comprises molecular tool development for the assessment of muscle MHC profile in the laboratory guinea pig, whilst Chapter 5 characterises muscle dysfunction in a spontaneous model of OA. Chapter 6 considers whether osteoarthritis-associated cytokines are able to induce skeletal muscle fibre-type changes in an isolated *in vitro* system.

CHAPTER 2 – ROUTINE MATERIALS AND METHODS

2.1 – Nucleic Acid Extractions and Procedures

2.1.1 – Extraction of total ribonucleic acids (RNA)

Prior to extraction, all plastic and glassware was autoclaved to ensure sterility. All solutions were prepared in RNase and DNase-free water (Molecular Biology grade water, Sigma). Total RNA was extracted from snap-frozen samples using TRIzol™ reagent (Invitrogen). Briefly, 1ml of TRIzol was added to a sterile 1.5ml tube containing 100mg of crushed sample. Samples were homogenised using a 10mm diameter Polytron™ probe for 2 cycles of 12 seconds; at all times the samples were kept on ice. Following centrifugation at 16,000g (Accuspin Micro, Fisher) for 10 minutes at 2^{o}C, the supernatant was transferred to a clean 1.5ml tube. The supernatant was incubated at room temperature for 5 minutes before the addition of 200µl chloroform per 1ml TRIzol. The tube was mixed vigorously by hand for 30 seconds and incubated at room temperature for 3 minutes. After centrifugation at 16,000g for 15 minutes at 2^{o}C, the upper aqueous phase was removed to a clean 1.5ml tube, avoiding the interphase. 500µl isopropanol and 250µl 0.8M sodium citrate / 1.2M sodium chloride was added per 1ml TRIzol. Samples were precipitated for 1 hour at -20^{o}C.

Following precipitation, samples were centrifuged at 16,000g for 10 minutes at 2^{o}C and the supernatant removed and discarded. The resulting RNA pellet was washed in 75% ethanol with DEPC treated water, and following centrifugation at 9,000g for 5 minutes at 2^{o}C, the supernatant discarded. The resultant RNA pellet was dissolved in 40µl of molecular biology grade water (Sigma) and stored at -80^{o}C until analysis.

2.1.2 – Removal of contaminating genomic deoxyribonucleic acid (DNA)

Prior to reverse transcription, all extracted total ribonucleic acids were treated with RQ1 DNase™ (Promega) to remove contaminating genomic DNA. Total RNA (40µl as previously resuspended) was incubated with 1U DNase in 5µl of buffer comprising 400mM Tris-HCl pH8.0, 100mM $MgSO_4$ and 10mM $CaCl_2$ for 30 minutes at 37^{o}C.

Following incubation, 150µl water and 200µl phenol/chloroform/isoamylalcohol (25:24:1) were added, vortexed briefly and the sample centrifuged at 16,000g for 5 minutes. The upper phase containing RNA was removed to a fresh tube containing 15µl 3M sodium acetate and 375µl ethanol and precipitated at -80^{o}C for 2 hours. Samples were centrifuged at 16,000g for 15 minutes and the supernatant discarded, washed in 75% (v/v) ethanol and then re-centrifuged at 16,000g for 5 minutes and resuspended in 40µl molecular biology grade water.

2.1.3 – RNA quality assessment and quantification

The concentration of RNA in molecular biology grade water was determined spectrophotometrically using the Nanodrop system (Thermo Scientific) blanked against a water standard. Measurements were taken at 260nm for nucleic acids, and 280nm for proteins. The ratio of these two measurements was calculated and a ratio of 1.8 – 2.0 (nucleic acid to protein) deemed acceptable.

RNA integrity was determined by 1.2% (w/v) agarose gel electrophoresis (**METHOD 2.1.4**). 5µl of RNA was combined with 1µl of loading buffer (Promega) and electrophoresed for 30 – 40 minutes at 70V - samples were stained and visualised in accordance with (**METHOD 2.1.4**). RNA samples with well-defined 18S and 28S ribosomal bands were deemed acceptable. Any samples with diffuse bands, indicative of RNA degradation were re-extracted from another 100mg tissue prior to first strand cDNA synthesis.

2.1.4 – Agarose gel electrophoresis

PCR amplicons and extracted RNAs were routinely resolved by horizontal non-denaturing agarose gel electrophoresis. The % concentration of agarose gel utilised was dependent on the size of the fragments to be resolved. 1.2% (w/v) agarose gels were used to resolve RNA extractions and larger PCR amplicons (> 1Kb). For PCR amplicons of 350 bp – 1 Kb, 1.5% (w/v) agarose gels were used, whilst smaller fragments (< 350 bp) were resolved on 1.8 – 2.0% (w/v) gels.

Agarose (Melford, UK) was prepared in TAE buffer (**APPENDIX A**), heated to boiling point in a standard microwave oven, and stirred to ensure that all agarose powder was dissolved. The solution was cooled to around 50^{o}C (hand hot) and poured into a gel former (Bio-Rad) with the corresponding gel comb (15-well). Gels were allowed to solidify initially at room temperature, before being set for 30 minutes at 4^{o}C.

Samples (generally 5µl) were combined with 1µl loading buffer (Promega) and loaded onto 1.2% (w/v) RNase and DNase-free agarose gel (Melford) prepared in TAE buffer (**APPENDIX A**). Samples were electrophoresed at 70V for 30 – 45 minutes, stained for 30 minutes in ethidium bromide (0.5µg/ml) and visualised under a UV light source. Images were captured (GelDoc 2000, Bio-Rad) and densitometry performed using software configured for ethidium bromide staining methodologies (Quantity-one, Bio-Rad). DNA markers (DNA ladder, Promega) were included in all runs to delineate the length (bp) of unknown resolved products.

2.1.5 – Generation of first-strand complimentary DNA (cDNA)

First strand complimentary DNA (cDNA) was obtained from total RNA by means of the reverse transcriptase reaction (Promega) using random primers. Reverse transcriptase, derived from Moloney Leukaemia Virus (MMLV) in this instance, transcribes RNA to DNA in a 5 – 3' direction from a single oligonucleotide primer using free nucleotides resulting in complementary DNA (cDNA) formation. 500ng total RNA (50ng/µl) was added to 0.5µg random hexamers (Promega) (unless otherwise stated) and 9µl of DNase/RNase free-water in thin-walled tubes (Alpha Laboratories). Samples were heated for exactly 5 minutes at 70^{o}C and then immediately placed on ice. 10 µl of master mix containing 5µl MMLV Reverse Transcriptase Buffer, 1.25µl 10mM dNTPs, 25U RNase inhibitor, 200U MMLV Reverse Transcriptase and 2.25µl molecular biology grade water was added to the RNA and left to incubate at room temperature for 10 minutes. Samples were heated to 42^{o}C for 1 hour to complete the elongation phase. The resulting cDNA was diluted 1 in 4 (v/v) with water, and stored at -20^{o}C prior to further analysis.

2.1.6 – Oligonucleotide primer design

Primers were designed from database sequences (details of which are included in the respective results chapter) in the case of rat studies, or conserved regions as determined from multi-species sequence alignment in the case of guinea pig expression studies. Sequence data was input into Primer3 in FASTA format, and primers designed using the default criteria (Primer size: 18 – 27bp, Melting Temperature: 55 – 62^{o}C, Amplicon size: 50 – 150bp) and sourced from MWG (Eurofins). All primers were high-purity salt free (HPSF) and synthesised at a concentration of 0.01μM. All oligonucleotide primer pairs were assessed by endpoint PCR, to ensure a single amplicon of the expected size was produced.

For quantitative PCR use, the efficiency of amplification by each primer set was assessed in a reaction using a series of known dilutions of pooled cDNA. The cDNA pool was produced, in general, by combining an equal aliquot of all samples from a particular study. To ensure the cDNA pool was as representative of the data set of possible, each sample was quantified independently by the primer pair in question, and any sample with a concentration > 2 standard deviations from the mean excluded from the pool. This step was introduced to reduce skewness of the data, and to identify samples which may be contaminated with potential PCR inhibitors and thus prevent them from affecting the total cDNA pool. The remaining samples, falling within 2 standard deviations of the mean were combined, diluted and amplified using the primer pair.

The efficiency of a PCR reaction is calculated by $10^{(-1/slope)}$, where the slope is determined by plotting $\log_{10}$ cDNA concentration against the crossing point (Cp). An efficiency of 2.0 represents the theoretical PCR reaction, with a doubling of amplicon abundance following each cycle. Efficiency was determined for all primer pairs, ensuring that the efficiency of amplification fell within the range 1.8 – 2.0 (90 – 100%).

2.1.7 – Polymerase chain reaction (PCR)

Polymerase chain reaction (PCR) is the amplification of a target sequence that is specific to a gene of interest. PCR can be used to obtain semi-quantitative (End-Point) or quantitative gene expression data dependent on the methodology used. Irrespective of technique, the basic principle of PCR is the same.

For the assessment of gene expression, total RNA was extracted, treated to remove contaminating genomic DNA and reverse transcribed as per (**METHODS 2.1.1 – 2.1.5**). For each PCR cycle, the cDNA strands were denatured at 94^{o}C, and the temperature reduced to the specific melting temperature of the oligonucleotide primer pair (55 – 65^{o}C) to allow annealing. The temperature was raised to 72^{o}C for 30 seconds, allowing the primers to extend and form the desired amplicon. PCR was allowed to proceed for a maximum of 35 cycles.

The cycle number at which the PCR is quantified is critical to how reflective the product abundance is of the amount of starting material. The initial phases of the PCR are characterised by exponential amplification, with each cycle resulting in a doubling in specific product. At this stage, quantification of the specific product abundance is reflective of the amount of starting material. As the amount of specific product increases, reaction constituents (primers, polymerase, and free nucleotides) become limited, and the relationship between the amount of specific product and amount of starting material declines. Therefore, quantification must be carried out in the exponential amplification phase (**FIGURE 2.1**).

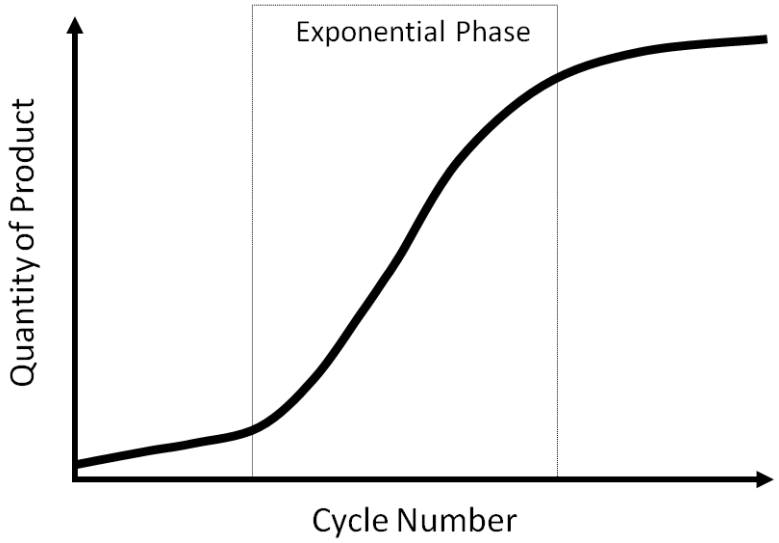

FIGURE 2.1 – Schematic of PCR Amplification Curve. The highlighted box shows the exponential phase of a theoretic PCR reaction from which expression data can be obtained. Following the exponential phase, the PCR reaction begins to plateau due to decreasing reaction constituent availability.

2.1.7.1 – End point PCR

End-point PCR reactions were utilised for confirming the presence or absence of a particular mRNA, and for confirming the size of the resulting amplicon were absolute quantification of mRNA abundance was not required.

End-point PCR reactions were performed on 5µl cDNA in AmpliTaq Gold PCR Buffer (ABI) with a final concentration of 1.5mM $MgCl_2$, 0.2mM dNTP mix (Promega), 0.3µM forward and reverse oligonucleotide primers (Eurofins) and 1.25U AmpliTaq (ABI) in a total reaction volume of 50µl in 200µl thin-walled tubes (Alpha Laboratories). Reactions were run on the DNA Engine (PTC200, MJ Research); cycling parameters were 94^{o}C for 10 minutes; 35 cycles of 94^{o}C for 30s, 55 - 60^{o}C***** for 30s, 72^{o}C for 30s followed by a final extension at 72^{o}C for 10 minutes. PCR products were resolved by 1.2% (w/v) agarose gel electrophoresis as per (**METHOD 2.1.4**).

*The initial annealing temperature for all reactions was determined by calculating the melting temperature of each primer ((4 x C + G) + (2 x A +T)) and subtracting 2^{o}C from the primer with the lowest melting temperature.

2.1.7.2 – Quantitative PCR

Quantitative PCR methodologies permit the rapid and relative quantification of specific DNA or RNA sequences from tissue samples, and thus provide a powerful means by which to assess gene expression. In contrast to end-point PCR where the amount of specific product is assessed at the end of a number of cycles (possibly outside of the exponential phase), quantitative PCR allows the assessment of specific product following each individual cycle. Quantitative PCR reactions were performed using the SYBR green system optimised for the LightCycler 480 (Roche). SYBR green technology utilises a sensitive dye that fluoresces only when bound with double stranded DNA (dsDNA). The fluorescence emitted from SYBR green is relative to the abundance of the target sequence, thereby enabling the quantification of PCR products in real-time. Quantitative PCR reactions were performed in triplicate on 5µl

cDNA in SYBR 1 Master mix (Roche), with a final concentration of 0.25µM forward and reverse primers in a total volume of 15µl. Cycling parameters were 95°C for 5 minutes prior to; 35 cycles of 10 seconds 95°C, 10 seconds 55°C and 30 seconds at 72°C. Single signal acquisition was set to read at 72°C for 1 second. All reactions were run on a 384-well white (Roche) microplate on a LightCycler LC480 (Roche) configured for SYBR green fluorescence determination as specified by the manufacturers. Quantitative data was generated by running all samples alongside a series of known serial dilutions of pooled cDNA. As SYBR green intercalates with any dsDNA, melt curve analysis was performed at the end of each completed analysis run to ensure only the specific product was amplified as indicated by a single melt peak, and therefore ensuring the SYBR green signal was derived only from the intended amplicon (**FIGURE 2.2**).

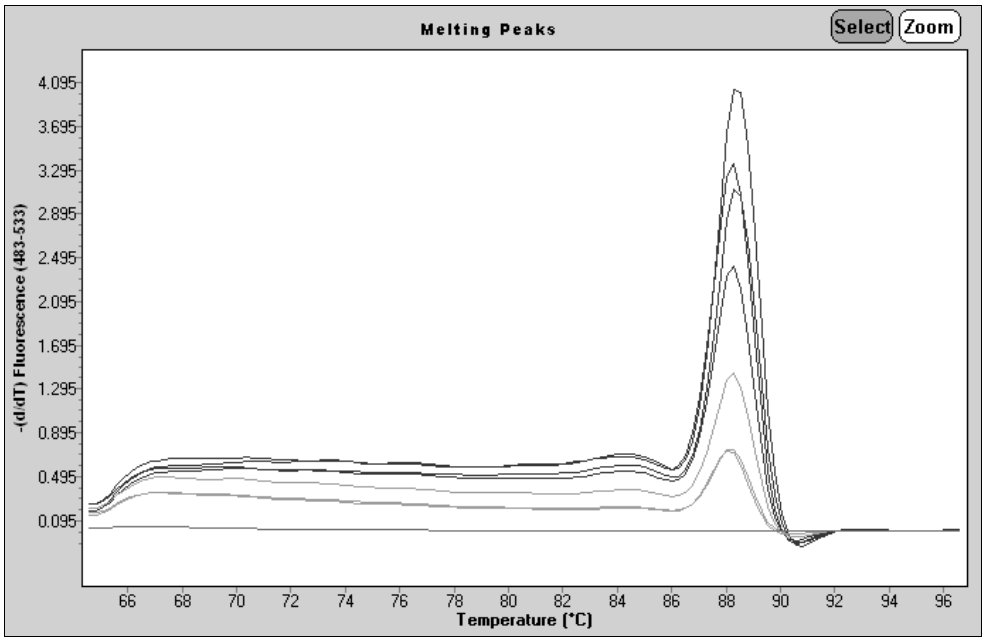

FIGURE 2.2 – Melting peak determined from the rate of change of the melt curve showing the presence of a single product size.

2.1.7.3 – Data normalisation

Quantitative PCR data was normalised by the use of internal reference genes or by the determination of cDNA concentration following reverse transcription. Detailed methodology of the chosen normalisation method is included within each chapter.

2.2 – Cloning of Polymerase Chain Reaction Amplicons

2.2.1 – PCR amplicon cleanup

Where indicated, PCR amplicons were purified from contaminating excess primers, nucleotides and salts using GenElute™ column-based technology (Sigma) prior to cloning. Briefly, fresh PCR amplicons were bound to the silica spin column, washed in 0.5ml of proprietary wash solution, and eluted in 50µl of molecular biology grade water. Products were either used immediately, or stored for up to 7 days at -20^{o}C.

2.2.2 – pGEMT Easy Vector cloning of PCR amplicons

Purified amplicons (as above) were cloned using the pGEM T-Easy vector system (Promega). 5µl Rapid Ligation Buffer, 1µl pGEM T-Easy vector, Xng PCR product and 3U of T4 Ligase were mixed well and incubated at 21^{o}C for 1 hour. The PCR amplicons were ligated at a molar ratio of 1:1 and 3:1 insert : vector to enhance the likely number of transformants. The amount of PCR product (X) to add was calculated as follows;

Insert (ng) = [Vector(ng) x Insert (Kb) / Vector (Kb)] x Insert/Vector molar ratio

Following ligation, the mixture (vector + insert) was transformed into competent *E.coli* JM109 (Promega). Briefly, 2µl of ligation reaction was added to a chilled, sterile 1.5ml tube and gently mixed with 50µl of thawed competent JM109 cells (10^{7} cfu/µg). The mixture was flicked gently to mix, and then left on ice for 20 minutes. The cells were heat shocked at exactly 42^{o}C for 50 seconds upon which the ligated

vector + insert were taken into the cells via the fenestrated cell wall. The cells were returned to ice for 2 minutes and a 950ul aliquot of LB media (**APPENDIX A**) added. The cultures were incubated at 37^{o}C aerobically with shaking for 1.5 hours. Following transformation, 100µl of the culture was plated onto 150mm diameter plates (Sarstedt) containing LB agar (**APPENDIX A**) supplemented with ampicillin (100µg/ml) under aseptic conditions, inverted, and incubated aerobically overnight at 37^{o}C.
Discrete colonies were harvested into 3ml of LB media containing 100µg/ml ampicillin, grown overnight at 37^{o}C with shaking at 170rpm (Lab Therm, Kuhner) purified and then identified by restriction endonuclease digest (**METHOD 2.2.5**).

2.2.3 – TOPO TA Vector cloning

Fresh PCR amplicons, without any additional preparation, were cloned using the TOPO TA™ vector system (Invitrogen). Two reaction concentrations including 0.5µl and 4µl of un-purified PCR amplicon per 6µl reaction were conducted to enhance the likely number of transformants. The PCR amplicon was incubated at 21^{o}C for 30 minutes in a sterile 1.5ml tube containing 1µl salt solution (1.2M NaCl, 0.06M $MgCl_2$), 1µl TOPO TA vector (10ng plasmid DNA, 50% v/v glycerol, 50mM Tris-HCl pH 7.4, 1mM EDTA, 1mM DTT, 0.1% v/v Triton X-100, 100µg/ml BSA) and RNase/DNase-free water to a total volume of 6µl. The reactions were placed on ice for 30 seconds, and then 2µl transferred to a thawed aliquot of TOPO 10 competent cells. Cells were incubated on ice for 30 minutes before being heat shocked at 42^{o}C for 30 seconds in a thermostatically control water bath. Cells were immediately placed on ice for 1 minute following heat shock to prevent irreversible damage. The cells were then incubated in 250µl of S.O.C media (**APPENDIX A**) for 60 minutes at 37^{o}C under aerobic conditions with shaking at 170 RPM (Lab Therm, Kuhner). Finally, 50µl of the resultant culture was plated- out onto on pre-warmed LB plates (150mm) containing 50µg/ml ampicillin and incubated overnight under the same conditions.

2.2.4 – Plasmid miniPrep

Plasmid mini-preparations were carried out using the GenElute plasmid miniprep kit (Sigma) which included all the required materials and reagents and was carried out according to the manufacturer's instructions. Briefly, 1.5ml of overnight culture was pelleted by centrifugation and resuspended in 200µl of proprietary re-suspension solution. The resulting solution was subjected to alkaline lysis and, following neutralization, the liberated plasmid DNA bound to a proprietary binding column. The bound plasmid DNA was washed using an ethanol containing wash solution, and eluted in 100µl of molecular biology grade water. All plasmid DNA was stored at -20^{O}C prior to use.

2.2.5 – Restriction endonuclease digest

All restriction endonuclease digest reactions were carried out in accordance with the manufacturer's recommendations (New England BioLabs, NEB). *EcoR1* digest was used to liberate cloned products from the multiple cloning site of pGEM-TEasy or TOPO TA plasmids. 5µl of purified plasmid DNA (250 – 500ng) was added to a reaction mixture containing 2µl proprietary buffer (NEB), 2µg bovine serum albumen (BSA), 10U EcoR1 and 12.3µl water. Reactions were incubated at 37^{O}C for 60 minutes.

*Bgl*1 digest was used to linearise the TOPO TA vector sequence for the production of linear clones with which to test the specificity of oligonucleotide primers. 10µl of purified plasmid DNA (500 – 1000ng) was added to a reaction mixture containing 5µl proprietary buffer (NEB), 2U *Bgl*1 and 34µl water. Reactions were incubated at 37^{O}C for 60 minutes. All reaction products were resolved on 1.2% (w/v) agarose gel (Melford), stained for 30 minutes in ethidium bromide (0.5µg/ml) and visualised under a UV light source (**METHOD 2.1.4**).

2.2.5 – DNA sequencing

Plasmid DNA was purified by plasmid mini-preparation (**METHOD 2.2.4**), its concentration determined spectrophotometrically (Nanodrop), diluted to 75ng/µl and submitted to MWG (Germany) for bi-directional sequencing using T7 and SP6 oligonucleotide primers targeting the vector sequence. This technique allowed sequencing across the cloning boundary, ensuring the full insert sequence was determined from insert sizes below 500-600bp.

2.3 – Protein Methodology

2.3.1 – General protein extraction

Samples of skeletal muscle (1g) were crushed to a powder under liquid nitrogen and homogenised using a 10mm diameter Polytron™ probe for 2 cycles of 12 seconds at speed setting 25 in 5ml of ice-cold protein extraction buffer (**APPENDIX A**). Prior to use, the protease inhibitors 4-(2-Aminoethyl) benzenesulfonyl fluoride hydrochloride (AEBSF), leupeptin and pepstatin were added to the extraction buffer at a concentration of 200µg/ml, 1 µg/ml and 1µg/ml respectively. 1ml of the resulting homogenate was removed to a separate 1.5ml tube containing 1ml of 2 X SDS PAGE loading buffer (**APPENDIX A**) and stored at -20^{o}C prior to analysis. The remaining homogenate was centrifuged at 16 000g for 10 minutes at 4^{o}C and the supernatant removed to a separate 1.5ml containing 1ml 2 X SDS PAGE loading buffer as previous. An independent 50µl aliquot of each fraction was added to 950µl 0.1M NaOH for protein concentration determination.

2.3.3 – Protein concentration determination

Protein concentration was determined according to the method of Bradford, 1976 (Bradford 1976) using sample aliquots diluted in 0.1M NaOH as above. BSA standards ranging from 0 - 60µg/ml were prepared from a stock solution of BSA (100µg/ml) and stored at -20^{o}C prior to use. 10µl of sample or BSA standard was added to a 96-well

microtitre plate (Sarstedt) in duplicate. 200µl of Bradford reagent (Bio-Rad) prepared according to the manufactures instructions was added to each well, mixed by pipetting and incubated at room temperature for 5 minutes. Absorbance was read at 520nm (Bio-Rad 680 XR), a calibration curve of A_{520} against the amount of protein in the BSA standards produced and the protein concentration of the unknown samples estimated.

2.3.4 – Sodium dodecyl sulphate polyacrylamide gel electrpohoresis (SDS PAGE)

SDS PAGE was carried out in accordance with the original method of Laemmli, 1970 (Laemmli 1970). Quadriceps muscle extracts prepared according to (**METHOD 2.3.1**) were diluted to 5µg/µl total protein in 1 x SDS PAGE loading buffer (**APPENDIX A**). Samples were boiled for 3 minutes to ensure complete denature of proteins and centrifuged at 16,000g at room temperature for 3 minutes to sediment any connective tissue.

Samples were applied to discontinuous 12% (w/v) polyacrylamide gels, of 1.5mm thickness cast using the Mini-Protean III system (Bio-Rad). The separating gel comprised 4ml 30% (w/v) acrylamide/0.8% (w/v) bis-acrylamide solution, 1.88ml 2M Tris-HCl pH 8.8, 0.1ml 10% (w/v) SDS and 3.93ml water. Polymerisation was induced by the addition of 80µl 10% (w/v) ammonium persulphate and 8µl N,N,N',N'-tetramethylethylenediamine (TEMED). The separating gel was poured into a gel former, and overlaid with a layer of water saturated butanol to ensure a level interface and prevent drying. Once set, the separating gel was washed in distilled water, and any excess water removed using filter paper (3M). The stack comprised 0.85ml 30% (w/v) acrylamide/0.8% (w/v) bis-acrylamide solution, 0.63ml 1M Tris-HCl pH 6.8, 50µl 10% (w/v) SDS and 3.40ml water. Polymerisation was induced by the addition of 80µl 10% (w/v) ammonium persulphate and 8µl TEMED as above and the stack poured directly on top of the separating gel. A gel-comb of corresponding thickness (1.5mm) with the desired number wells was placed in the stack and the whole gel set for 30 minutes at 4^0C.

For the detection of 4EBP1 protein (15 – 20 KDa), samples were diluted to 5µg/µl total protein, and 15µl loaded resulting in a total load of 75µg. Pre-stained protein markers (7 – 175KDa, BioRad) were included on each gel to delineate the size of any resultant proteins. Gels were run in SDS PAGE running buffer (**APPENDIX A**) at 200 V (constant voltage) for 40 minutes or until the samples had run around ¾ the length of the gel.

2.3.5 – Western blotting

Following electrophoresis, acrylamide gels were soaked in transfer buffer comprised of 0.4M glycine, 25mM Tris and 5% (v/v) propan-2-ol for 10 minutes at room temperature. One piece of 45µm pore size nitrocellulose and two pieces of filter paper (3M) per gel were cut to the size of the gel and soaked in the buffer alongside the gels. The nitrocellulose was placed on top of the pre-soaked gel and housed between two pieces of filter paper in a western blotting cassette (BioRad). The assembly was secured in a transfer tank (Mini-Protean III, BioRad) filled with transfer buffer, ensuring the gel-side of the assembly was orientated towards the cathode (and thus ensuring that proteins were transferred from the gel to the nitrocellulose membrane as the current passed through the apparatus). Gels were transferred at 0.2A for 2 hours (Power-Pac 300, Bio-Rad), with cool-water passed through the apparatus to prevent heating. A magnetic stir-bar was placed into the tank and the whole apparatus placed on a magnetic stirrer at moderate speed to prevent the precipitation of glycine from the transfer buffer. Precipitated glycine is known to adhere to the nitrocellulose membrane, increasing background signal following immunodetection (**FIGURE 2.3**).

Following transfer, the nitrocellulose was removed from the assembly and stored in TBS-T buffer (**APPENDIX A**) at 4^{o}C.

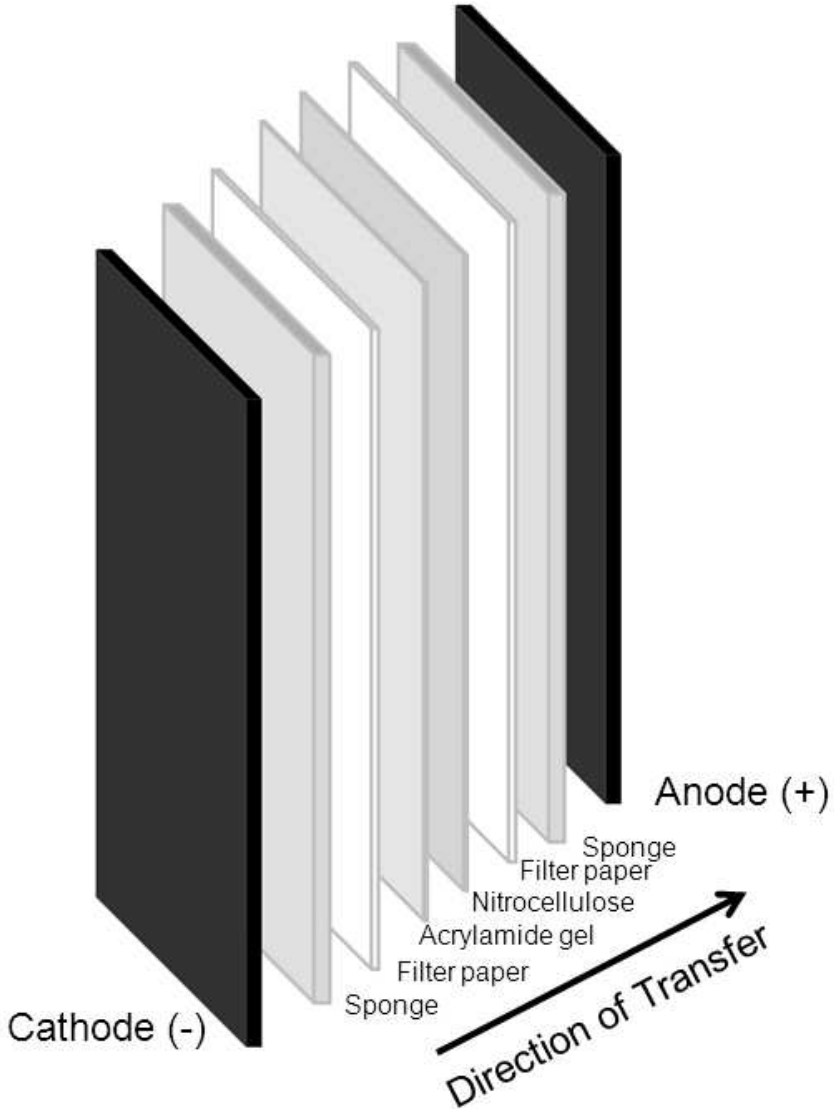

FIGURE 2.3 – Schematic showing Western blotting assembly. The arrangement of the sponges, filter paper, acrylamide gel and nitrocellulose membrane are shown in relation to the cathode and anode of the transfer apparatus.

2.3.6 – Ponceau staining

Prior to immunodetection, the nitrocellulose membrane was stained to ensure transfer of proteins (**METHOD 2.3.5**). The membrane was incubated in Ponceau S stain (**APPENDIX A**) with gentle agitation for 5 minutes. The membrane was de-stained in distilled water and viewed over a white light source. Successful transfer was confirmed by the presence of well-defined protein bands, of uniformed appearance across the length of the membrane. Membranes were completely de-stained prior to immunodetection in TBS-T buffer for 5 minutes with gentle agitation.

2.3.7 – Immunodetection

Electroblotted nitrocellulose membranes were immersed in 5% (w/v) non-fat milk powder in TBS-T buffer for 30 minutes at room temperature to prevent non-specific binding of antibodies to the surface of the membrane. For the detection of phosphorylated and total 4EBP1 protein, anti-4EBP1 and anti-phosphorylated 4EBP1 (thr37/46) (Cell Signalling Technology) rabbit anti-rat primary antibodies were sourced and each diluted 1:1000 in 5% (w/v) non-fat milk powder.

First, anti-phosphorylated 4EBP1 (thr37/46) was applied to the membrane for 1 hour at room temperature, shaking constantly throughout the incubation. The membrane was washed with 1% (w/v) non-fat milk powder for 30 minutes, changing the solution every 5 minutes. Following washing, the membrane was incubated in horseradish peroxidise conjugated anti-rabbit antibody diluted 1:5000 in TBS-T buffer for 1 hour. Following 30 minutes of washing as previous, immunodetection was carried out using enhanced chemiluminescence (ECL, GE Healthcare) according to the manufacturer's instructions. The membrane was exposed to photographic film (Hyperfilm, GE Healthcare) in a dark room for 1 – 3 minutes, developed in developing reagent (Kodak) for 2 minutes, rinsed in water and fixed (Kodak) for 2 minutes. Films were captured (Bio-Rad, FluorS) and analysed by densitometry (Quantity-One, V4.4.1, Bio-Rad) according to the manufacturer's instructions.

Following immunodetection with anti-phosphorylated 4EBP1 (thr37/46), the membrane was stripped of bound primary antibody by incubation in Restore solution (Pierce) with gentle agitation for 10 minutes at room temperature. To ensure all primary antibody-antigen complexes were removed, the membrane was washed in TBS-T buffer for 5 minutes, and then subjected to secondary antibody incubation, ECL treatment and exposure to photographic film as above. The lack of a signal following membrane exposure to photographic film for 5 minutes was considered indicative that all bound primary antibody had been successfully removed.

Total 4EBP1 protein was determined by repeating the procedure as above, treating the stripped membrane using the anti-4EBP1 antibody.

2.3.8 – Isocitrate dehydrogenase / lactate dehydrogenase enzyme activity

Isocitrate dehydrogenase (ICDH) and Lactate dehydrogenase (LDH) enzyme activities were respectively measured as an index of oxidative (aerobic) metabolism and glycolytic (anaerobic) metabolism. Both enzyme activities were measured in accordance with the original method of Brandstetter, 1998 (Brandstetter, Picard et al. 1998).

Whole quadriceps homogenates were prepared by combining frozen quadriceps tissue crushed under liquid nitrogen, with 40 volumes of homogenisation buffer comprising (250mM Sucrose, 2mM EDTA, 10mM Tris-HCl pH 8.0) and homogenising on high speed for 30 seconds on ice using a Polytron probe. Homogenates were cleared of any connective tissue by centrifugation at 9,000g for 15 minutes at 4^{o}C, and the resulting supernatants kept on ice.

For the determination of ICDH activity, 375.4mM isocitrate trisodium was prepared in ICDH reaction buffer comprising (38.9mM disodium phosphate, 0.5mM manganese chloride, 0.05% (v/v) Triton X100 and 0.36mM β-Nicotinamide adenine dinucleotide phosphate (β-NADP), pH 7.3). 7.5µl of supernatant (as above) was added to a transparent 96-well microtitre plate (Sarstedt) containing 270µl reaction

buffer per well. The plate was incubated at 28^{o}C for 15 minutes, and the absorbance at 340nm determined 6 times at intervals of 20 seconds.

For the determination of LDH activity, 2mM sodium pyruvate was prepared in a LDH reaction buffer comprising (50mM triethanolamine (TEA) and 5mM EDTA, pH 7.5). Quadriceps supernatants were diluted 1 in 10 in homogenisation buffer and 1µl added to a 96-well microtitre plate containing 290µl reaction buffer and 10µl 0.026mM NADH per well. The plate was incubated at 28^{o}C for 2.5 minutes, and the absorbance at 340nm determined 6 times at intervals of 20 seconds.

The rates of both enzymes were determined by measuring the absorbance change at 340nm (680XR plate reader, Bio-Rad) and expressed as mOD/min normalised to the total extractible protein of each sample (determined using the method of Bradford).

With reference to alternative histochemical techniques, it is suggested that the assessment of succinate dehydrogenase (SDH) and glycerophosphate could be performed on frozen skeletal muscle sections for the determination of oxidative and glycolytic metabolic potential respectively.

2.4 – Histopathology

2.4.1 – Fixation, processing and embedding

Knee joints were obtained for histopathological analysis by making a full thickness cut 2cm above and below the patella. Specimens were fixed in 10% neutral buffered formalin at 90^{o}C flexion for > 72 hours. To aid cutting, specimens of bone, removed of any extraneous tissue, were decalcified in 10% formic acid for 5 days – changing the solution every other day. Samples were dehydrated in ascending concentrations of ethanol, cleared in xylene and infiltrated with paraffin wax using a vacuum

assisted auto-processor (Leica TP 120 Carousel) following the following program (all concentrations are % v/v prepared in distilled water);

- 70% Ethanol – 1hr
- 70% Ethanol – 1hr
- 95% Ethanol – 1hr
- 95% Ethanol – 1hr
- 95% Ethanol – 1hr
- 100% Ethanol – 1hr
- 100% Ethanol – 1hr
- 100% Ethanol – 1hr
- 100% Xylene – 1hr
- 100% Xylene – 1hr
- Paraffin wax (61^{o}C) – 1hr
- Paraffin wax (61^{o}C) – 1hr

Following wax infiltration, samples were orientated into wax moulds with the anterior surface facing downwards. Samples were embedded in paraffin wax and allowed to harden on a cooled surface (4^{o}C). 4µm step-coronal sections were taken using a rotary microtome (RM 2245, Leica) at 300µm intervals resulting in approximately 10-sections per joint. Sections were adhered to charged slides (Superfrost) and dried at 50^{o}C overnight (**FIGURE 2.4**).

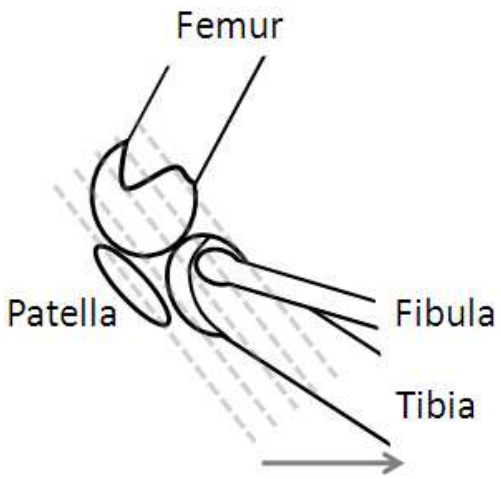

FIGURE 2.4 – Orientation of knee joints for microtomy. Dotted lines indicate angle of tissue sections, grey arrow indicates the direction of cutting.

Details of the comprehensive scoring criteria used to assess histological joint changes are included within CHAPTER 3.2.5 and CHAPTER 5.2.3 for the assessment of rat and guinea pig pathology respectively.

2.4.2 – Toluidine blue staining

Sections were de-waxed in xylene (10 minutes), rehydrated in descending concentrations of ethanol for 10 minutes at each concentration (100%, 90%, 70% v/v), and washed in running tap-water. Sections were incubated in 0.2% toluidine blue (w/v), 2% aluminium sulphate (w/v) in distilled water for 25 minutes at room temperature. Following staining, sections were dehydrated in ascending concentrations of ethanol (70%, 90%, and 100% v/v), cleared in xylene (10 minutes) and mounted using Di-n-butyl-phthalate-polystyrene-xylene (DPX, Thermo Scientific).

2.5 – Statistical Analysis

Details of the specific statistical tests used to assess statistical significance are included in each separate results chapter.

CHAPTER 3 - THE EFFECTS OF B2 ADRENERGIC AGONIST ADMINISTRATION ON THE SEVERITY OF OSTEOARTHRITIS IN A MENISCECTOMY-INDUCED RODENT MODEL

3.1 – Introduction and Rationale

Improving skeletal muscle strength and functional performance through intensive exercise regimes is often inappropriate or contraindicated for certain OA patients who are elderly, overweight, co-morbid and may be frail. β2-adrenergic agonists, such as clenbuterol, have potent anabolic effects on skeletal muscle, inducing increases in lean mass and contractile speed (Lynch, Schertzer et al. 2008) similar to those observed through targeted strength training protocols (as reviewed in chapter 1.3.4.3). Clenbuterol induces muscle hypertrophy via the stimulation of β_2-adrenoceptors and the subsequent activation of downstream signalling pathways (Lynch and Ryall 2008). In addition to marked increases in skeletal muscle mass in a number of animal models of muscle wasting (Maltin, Hay et al. 1989; Carbó, López-Soriano et al. 1997; Stevens, Firinga et al. 2000; Herrera, Zimmerman et al. 2001), clenbuterol has been shown to induce slow to fast muscle fibre-type transitions in certain muscle groups (Ricart-Firinga, Stevens et al. 2000; Stevens, Firinga et al. 2000).

Developing a pharmacological agent that is able to mimic intensive exercise regimes by improving muscle function in knee OA patients could provide a plausible route through which to modify the course of OA during both the initiation, and progression of this disorder (Hurley 1999; Pap, Machner et al. 2004; Mikesky, Mazzuca et al. 2006). The purpose of this study was to investigate whether clenbuterol induced hypertrophy of the quadriceps muscle, prior to disease induction, was able to modify the severity of joint disease, assessing joint pathology and behavioural pain in a meniscectomy-induced rodent model of OA.

3.1.1 – Hypotheses and aims

The development of meniscectomy-induced osteoarthritis will be associated with changes to the fibre-type composition of the quadriceps muscle group, potentially manifesting as a reduced type II fibre complement. Clenbuterol administration for 14 days will result in marked hypertrophy of the quadriceps muscle group, with an associated increase in the proportion of type II fast twitch muscle fibres. The induction of quadriceps hypertrophy and the potential modulation towards a faster-twitch muscle phenotype prior to the induction of OA will have a protective effect on the knee joint, assessed histologically 21 days post induction.

The following specific aims will be addressed utilising a rodent model of OA;

- Elucidate the effects of clenbuterol on quadriceps mass and function
- Investigate the effects of induced knee OA on quadriceps mass and function
- Determine whether a hypertrophic quadriceps can modulate OA severity

3.2 - Experimental Protocol

3.2.1 – Animals, housing and experimental outline

A total of 35 male Lewis rats (bodyweight = 280.4 + 1.7g) were group housed with free access to standard laboratory chow and water. Animals were subcutaneously administered with the potent β_2-adrenergic agonist clenbuterol HCl at a dosage of 1.5mg/kg/day bodyweight (n=15), or saline vehicle (n=20) for a total of 14 days. Animals were weighed daily, and the dosage of clenbuterol calculated based upon the most recent animal weight and administered immediately. Following pre-treatment (saline or clenbuterol), 5 animals from each group were sacrificed to assess the immediate effects of clenbuterol on muscle parameters. The remaining animals underwent either meniscectomy surgery (MNX) (clenbuterol pre-treated n=10; saline pre-treated n=10) or a sham control surgical procedure (saline pre-treated n=5).

Animal procedures were carried out by AstraZeneca pharmaceuticals, Alderley Edge, Macclesfield in accordance with the Home Office Animals (Scientific Procedures) Act 1986.

3.2.2 – Preparation of clenbuterol for subcutaneous administration

Clenbuterol hydrochloride ($C_{12}H_{18}Cl_2N_2O.HCl$ MW 277.2) was sourced from Alexis pharmaceuticals, UK. A 1.5mg/ml (w/v) solution was prepared in sterile physiological (0.9%) saline and 2ml aliquots stored at -20^{o}C. A fresh aliquot of compound was thawed for each day of dosing to minimise any degradation over the course of the study.

3.2.3 – Induction of OA via meniscectomy surgery

All surgery was carried out under 3.5% Isofluorane inhalational anaesthetics by an experienced surgeon (Mrs Ruth Webster, AstraZeneca, Macclesfield). The left leg of the rat was shaved and cleaned with pevidine antiseptic solution (National Vet

Supplies) prior to surgery in a separate designated preparation area. A small incision with iris scissors (Tungsten carbide iris scissors, Interfocus; 14558-11) was made longitudinally down the medial side of the knee and a cauteriser (Interfocus; 18000-00) used to work through both the connective tissue and muscle layers until the medial collateral ligament, anchoring the medial meniscus to the tibial plateau, was identified. Blood vessels along the line of the medial collateral ligament and the surrounding area were cauterised to maintain haemostasis. The ligament was grasped with fine tooth forceps (Bonn 1x2 teeth forceps, Interfocus; 11084-07) at the tibial end and cut with fine micro surgical scissors (Bonn extra fine iris scissors, Interfocus Ltd; 14084-08) until fully transected. The ligament was then transected again at the femoral end to remove the portion overlying the meniscus. This allowed direct access to the medial meniscus, and removed the possibility of the collateral ligament re-forming. The meniscus was freed from the fine connective tissue, allowing it to be held with fine forceps (Moria MC40 Straight Forceps, Interfocus; 11370-40) while a full thickness, medial transection was made. The knee was closed in two separate layers: the connective bilayer was sutured with 8-0 braided, absorbent suture material with a round bodied needle, using single interrupted stitches (Ethicon W9577) and the skin was closed with 5-0 braided, absorbent suture material with a spatula needle (Ethicon W9553), using a subcuticular running stitch, the terminal end of which is buried through the wound, towards the iliac crest. When necessary, a single support stitch was included as a precautionary measure using 8-0 suture material with a spatula needle (Ethicon W9560). The area was then cleaned with sterile physiological saline.

Following surgery, each animal was allowed to recover in a heated cage for up to 6 hours before being returned to their home cage. Wet diet (prepared by adding water to standard laboratory chow) was also provided for up to 12 hours post surgery. Cefalexin antibiotics were administered orally one hour prior to surgery and at 12, 24 and 36 hours post surgery (0.03ml/100g Ceporex oral drops; Schering-Plough Animal Health; granules dissolved in 6ml drinking water). Carprofen analgesics were

administered subcutaneously on induction of anaesthesia and 24 hours post surgery (0.01ml/100g Rimadyl; Pfizer).

Sham animals underwent the same surgical procedure with the omission of transection of the medial meniscus. All other treatment of these rats was identical to the other surgical group, including administration of antibacterial prophylaxis and post-operative analgesia.

3.2.4 – Incapacitance assessment

Weight bearing, as a surrogate of behavioural joint pain, was measured using an incapacitance meter (Linton Instrumentation, UK) on study days -2, 7, 14, 21, 28 and 35 as described previously (Ivanavicius, Ball et al. 2007). The operator was blinded to both the pre-treatment regime and any previous measurements. The difference in weight borne by the two hind limbs was measured by placing the rat in a Perspex tube so that each hind paw was resting on a separate transducer pad. The distribution of bodyweight on each paw over 3 seconds was recorded and the average of 3 separate measurements taken. Weight readings for the left and right limbs were taken and the difference between these calculated and plotted. Prior to inclusion in the study, rats were trained for one week to acclimatise them to the new apparatus.

3.2.5 – Termination and histopathology

Animals were terminated 21 days post surgery with a rising concentration of $C0_2$ and death confirmed by cervical dislocation. Knee joints were obtained for histopathological analysis by making a full thickness cut 2cm above and below the patella. The joints were formalin fixed and decalcified in 10% formic acid prior to processing by routine vacuum assisted wax infiltration (**CHAPTER 2.4**). Toluidine blue stained step-coronal sections were evaluated for proteoglycan loss, cartilage erosion and subchondral cartilage deposits. Sections were subjectively graded for the most severe changes in cartilage morphology assessing proteoglycan loss, erosion,

proliferation and fibrillation on any single section and given a score of between 0 and 4 as follows;

0 - Pathology not present

1 - Minimal change, small foci

2 - Mild change, up to 20% affected

3 - Moderate change, up to 50% affected

4 - Severe change, greater than 50% affected.

The maximum score for the tibial and femoral condyles was 12 respectively, giving a total obtainable knee score of 24. Proteoglycan loss was generally associated with a loss of chondrocytes and some chondrocyte clustering. Proliferation at the joint margin only referred to proliferation at the edge of the articular cartilage plateau and not proliferation down the lateral border resulting from the operative procedure. Erosion was regarded as the frank loss of cartilage matrix not just 'shrinkage' or 'thinning'. All histology was reported by an experienced board-certified pathologist (Dr Russell Westwood, AstraZeneca, Macclesfield) and second screened in house following appropriate training (AstraZeneca, Charnwood).

3.2.6 – Electrophoretic separation of MHC

Quadriceps muscle fibres were classified based upon their expression of myosin heavy chain protein. Quadriceps muscle samples (100mg) were crushed to a powder under liquid nitrogen and homogenised in 5ml of extraction buffer comprising 0.5M NaCl, 20mM pyrophosphate, 50mM Tris-HCl, 1mM EDTA, and 1mM DTT in distilled water, pH 8.0. Following centrifugation at 1000g for 10 minutes, 500µl aliquots of the resulting supernatant were added to an equal volume of 87% v/v glycerol (Fluka). Preparations were vortexed to ensure thorough mixing and stored at -20^{0}C until required. Following total protein determination (**METHOD 2.3.3**) 50ng protein was mixed with loading buffer 4% v/v 87% glycerol, 25mM 1M Tris-HCl pH 6.8, 8% w/v SDS and 20mg pyronin Y, with 10% v/v beta-mercaptoethanol added prior to use. The

myosin preparations were separated by sodium dodecyl sulphate polyacrylamide gel electrophoresis (SDS-PAGE) as described by Mizunoya, 2008 (Mizunoya, Wakamatsu et al. 2008). Separating gels consisted of 35% v/v glycerol, 8% w/v acrylamide bis-acrylamide 49:1 (Sigma), 0.2M Tris-HCl (pH 8.8), 0.1M glycine, 0.4% w/v SDS, 0.1% w/v ammonium persulphate, and 0.05% v/v N,N,N',N'-tetramethylethylenediamine (TEMED). The stacking gel consisted of 30% v/v glycerol, 4% w/v acrylamide bis-acrylamide 49:1, 70mM Tris-HCl (pH 6.7), 4mM EDTA, 0.4% w/v SDS, 0.1% w/v ammonium persulphate, and 0.05% v/v TEMED. Gels were prepared the day prior to running and stored at 4^0C. The lower running buffer consisted of 0.05M Tris HCl, 75mM glycine, and 0.05% w/v SDS. The upper running buffer was 6 x the concentration of the lower running buffer and beta-mercaptoethanol was added before use at a final concentration of 0.12% v/v. Electrophoretic separation was performed in two stages; sample entry into the stacking gel was run at 10mA for 40 minutes, whilst the remainder of the electrophoresis was carried out at 140V (constant voltage) for 21.3 hours. Throughout the electrophoresis, the apparatus was kept in a cold room at 4^0C.

Following electrophoresis, the different MHC isoforms were detected by silver staining (Talmadge and Roy 1993) using a silver staining kit (Plus One, GE Health Care) according to the manufactures instructions. Silver stained gels were imaged (Bio-Rad, FluorS) and densitometry performed (Quantity One, V4.0). The expression of each isoform of MHC was expressed as a percentage of the total MHC signal, allowing for subtle variations in sample load to be normalised.

Although traditional histochemical staining of frozen muscle sections provides data at the individual fibre level, the detection of MHC protein isoforms in quadriceps muscle homogenates allows the global assessment of MHC, and is therefore indicative of the contractile properties of the muscle as a whole.

3.2.7 – Low density microfluidic card array

In order to elucidate molecular changes in the transcriptome of the quadriceps skeletal muscle, a custom low-density array was designed comprising 48 targets of interest using the ABI Assay on Demand system, Applied Biosystems. The microfluidic card system utilises a one-step reverse-transcriptase (RT) polymerase chain reaction (PCR) based detection system arrayed onto a 384-well plate to determine relative mRNA expression changes.

Total RNA was prepared from 100mg of frozen quadriceps muscle using the TRIzol™ extraction method (**METHOD 2.1.1**). For each sample, a mastermix containing 53.1ul probes master (Qiagen, UK), 4U reverse transcriptase (Qiagen, UK), 47.8ul RNase/DNase-free water (Sigma, UK) and 212.5ng of total RNA was prepared on ice. The mixture was vortexed thoroughly, 100ul added to each sample well on the microfluidic card and centrifuged at 2000g, room temperature for 2 minutes in specifically designed buckets (Sorvall Legend and Heraeus). Centrifugation delivered 1µl of total RNA into each of the 384 wells on the card, significantly reducing the amount of bench time required to run multiple quantitative PCR analyses. Cards were run on the ABI Fast Cycler (7900HT) at 50^{o}C for 30 minutes for the reverse transcriptase reaction, 94.5^{o}C for 15 minutes to initiate the PCR reaction, and 40 cycles of 97^{o}C for 30 seconds and 59.7^{o}C for 1 minute.

Targets were selected to assess changes in protein synthesis, the negative regulation of skeletal protein synthesis, muscle atrophy, apoptotic potential, fatty acid metabolism, glucose metabolism, and the expression of proteins associated with metabolic status (**TABLE 3.1**).

TABLE 3.1 – Low-density array targets

Function	Symbol	Gene Name
Protein Synthesis	IRS1	Insulin receptor substrate
	Pik3cd	Phosphoinositide 3-kinase
	Akt	Akt
	Gsk3B	Glycogen synthase kinase 3β
	Frap1	Mammalian target of rapamycin
	Eif2b	Elongation factor 2B
	Eif4e	Elongation factor 4E
Negative Regulation and Degradation	Rela	NFκβ
	Tnfsf12	TNF like weak inducer of apoptosis
	Trim63	Muscle RING-finger protein 1
	Dusp1	Dual specificity protein phosphatase 1
	MAPK14	p38
	FBox32	MAFBx
	Psma5	Proteosome subunit 5
Muscle Atrophy	Gdf8	Myostatin
	Ctsl	Cathepsin L
	Capn1	Calpain I
	Capn2	Calpain II
	Capn3	Calpain III
Apoptosis	Bax	Bax
	Bcl2	Bcl2
	Casp3	Caspase III
	Casp12	Caspase XII
Fatty Acid Oxidation	Cpt1a	Carnitine palmitoyltransferase
	Lpin1	Lipin
	Adipor1	Adiponectin receptor 1
	Adipor2	Adiponectin receptor 2
	UCP3	Uncoupling protein 3
Glycolysis	Hk1	Hexokinase
Metabolic Regulators	Ppargc1a	PPAR gamma coactivator 1 alpha
	Ppargc1b	PPAR gamma coactivator 1 beta
	Ppara	Peroxisome proliferator activated receptor alpha
	Ppard	Peroxisome proliferator activated receptor delta
	Prkaa1	AMP Kinase 1
	Prkaa2	AMP Kinase 2

Of the 48 genes arrayed onto each card, 5 were designated as potential housekeeping genes and included 18S, TBP, ACTB, PPIA and HPRT (**TABLE 3.2**).

TABLE 3.2 – Low-density array potential housekeeping genes

Function	Symbol	Gene Name
Housekeeping	18S	18S ribosomal subunit
Genes	ActB	Beta Actin
	Hprt	Hypoxanthine phosphoribosyltransferase 1
	Ppia	Cyclophilin A
	TBP	TATA box binding protein

Relative expression data was derived using the comparative CP / dCT method (Schmittgen and Livak 2008). The raw crossing point (CP) value was taken for each sample and expressed relative to the first sample, defined as the calibrator (CP sample – CP calibrator). The calibrator could have been any sample from the data set, the first being selected for ease of analysis in Excel (Microsoft). Contrary to standard curve based methodologies (**METHOD 2.1.7.2**) whereby the amplification efficiency is calculated based up a standard curve of known dilutions of cDNA, the low-density array did not include space to accommodate a standard curve and therefore the amplification efficiency was set at 2 (or 100%) for all genes of interest. The relative CP value (relative to the control sample) was linearised by the formula;

$$2^{-(\text{CP Sample} - \text{CP Calibrator})}$$

In order to normalise the expression data effectively, the expression of all 5 housekeeping genes was analysed using validated normalisation software (GeNorm). The average stability of each housekeeping gene (termed *M*) was assessed independently according to the method of Vandesompele, 2002 (Vandesompele, De Preter et al. 2002). Taking the two most stable genes; the 3rd, 4rd and 5th gene was

sequentially added and the variance (*V*) calculated following each addition. The number of housekeeping genes employed was based on the lowest *V* value. A normalisation factor was derived based on the geometric means of the recommended number of housekeeping genes. All analysis was carried out automatically using GeNorm software version 3.5. Vandesompele, 2002 (Vandesompele, De Preter et al. 2002) includes a full explanation of the formulae used to calculate *M* and *V*.

Finally, the linearised expression value was normalised by dividing the dCT value (as calculated above) by the normalisation factor (also linear) based upon the geometric means of a number of housekeeping genes.

3.2.8 – Biospecimens

Whole bilateral quadriceps muscle samples, inclusive of the rectus femoris, were dissected, weighed and immediately snap frozen in isopentane cooled with liquid nitrogen. Care was taken to avoid inclusion of any adipose tissue or additional muscle, most importantly the tensor fasciae latae and sartorius which are located within the dissected area. Whole blood was drawn via cardiac puncture into clot-activator tubes (Sarstedt) and serum obtained by centrifugation. All serum was kept at -80^{o}C prior to analysis.

3.2.9 - Statistical analysis

All data are reported as means + standard error of the mean (S.E.M). Comparisons were performed using the independent samples t-test between two groups, or analysis of variance (ANOVA) between multiple groups. Where statistical significance of the ANOVA permitted, the Bonferroni test was used to test for significance, with significance accepted as $P < 0.05$. All statistical analyses were performed using SPSS 17.0. Symbols used to indicate statistical significance were; * $P < 0.05$; ** $P < 0.01$; *** $P < 0.001$. # $P = < 0.1$ was regarded as a trend (Tominaga, Ndu et al. 2006; Jung, Reichstein et al. 2010).

3.3 – Results

For enhanced clarity, the results are presented here in two parts. **3.3.1** Reports the effects of clenbuterol administration on weight parameters and quadriceps muscle function whilst **3.3.2** reports the effects of induced OA on quadriceps muscle function, and the modulatory effects of clenbuterol pre-treatment in this setting.

3.3.1 – Preliminary effects of clenbuterol administration

3.3.1.1 - Weight parameters

Subcutaneous administration of clenbuterol at a dosage of 1.5mg/kg/day resulted in an approximate 35% elevation in bodyweight gain (P = < 0.001) following 14 days of treatment compared to saline control treated animals. Clenbuterol-treated animals had visibly reduced adipose deposits, and larger more defined skeletal musculature, suggesting that increased animal weight was likely due to lean tissue deposition. In addition to bodyweight, quadriceps mass (wet weight) was also elevated (+ 40%) following clenbuterol treatment (6.52 + 0.21g) compared with saline treated controls (4.64 + 0.21g), (P = <0.001) (**FIGURE 3.1**). Statistical significance was maintained when quadriceps mass was normalised to total bodyweight (P = 0.020).

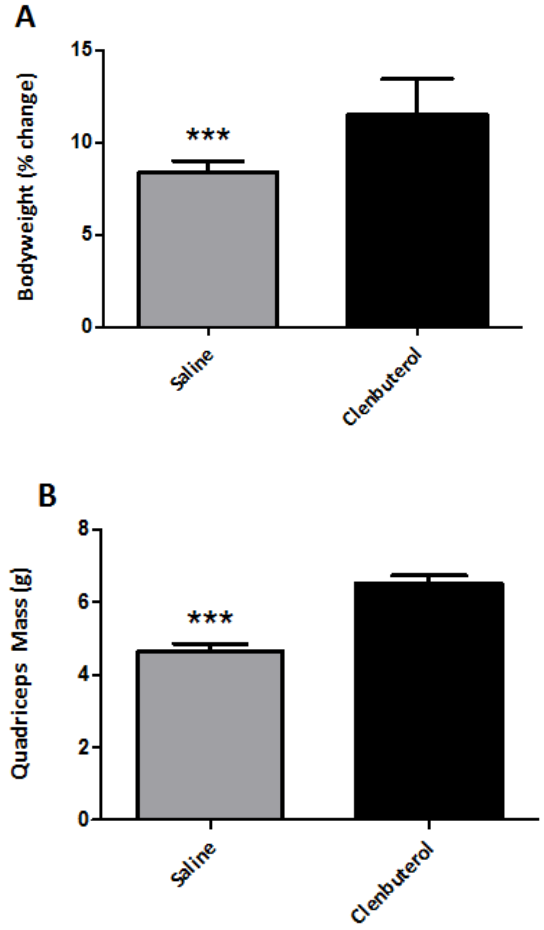

FIGURE 3.1 – The effects of 14 days administration of clenbuterol hydrochloride on % bodyweight change from the first day of pre-treatment (A) and quadriceps mass (B). Data are mean + S.E.M; n = 5.

3.3.1.2 - Contractile and metabolic potential of the quadriceps muscle

Quadriceps muscles were characterised with respect to their contractile and metabolic potential. Myosin Heavy Chain (MHC) composition of the quadriceps muscle was determined as an index of contractile capacity by high-resolution SDS PAGE. Control material from rat soleus (predominance of MHC I) and diaphragm (absence of MHC IIB) was included for reference. Electrophoretic separation revealed the rat quadriceps muscle to be composed predominantly of “fast twitch” MHC, with a composition of 4.85% type I, 7.25% type IIA, 22.34% type IIX and 66.55% type IIB. Clenbuterol administration did not induce any significant changes to the composition

of the quadriceps muscle following 14 days treatment (**FIGURE 3.2**). Representative photomicrographs, and associated control data are included in **APPENDIX B**.

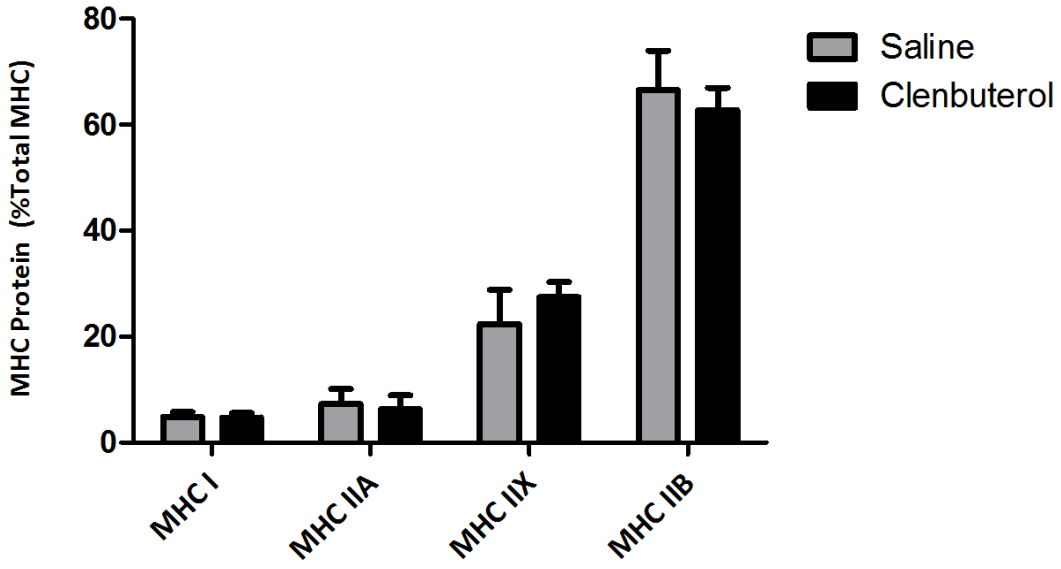

FIGURE 3.2 – The effects of 14 days administration of clenbuterol hydrochloride on MHC isoforms I, IIA, IIX and IIB. Data are mean densitometric value of each isoform expressed as a percentage of the total MHC signal + S.E.M; n = 5. Saline x Clenbuterol P = 0.988, 0.963, 0.631, 0.586 for MHC I, IIA, IIX and IIB respectively. Representative photomicrographs are included within **APPENDIX B**.

As an indication of oxidative metabolic potential, associated with slow-twitch muscle fibres, isocitrate dehydrogenase (ICDH) enzyme activity was determined. Similarly, glycolytic metabolic capacity, associated with faster-twitch fibres was assessed by the determination of lactate dehydrogenase (LDH) activity. Enzyme activities were normalised to extractable protein concentration and expressed as mOD/min/µg total protein. Clenbuterol administration had no effect on ICDH or LDH activity within the quadriceps muscle (**FIGURE 3.3**) following 14 days pre-treatment.

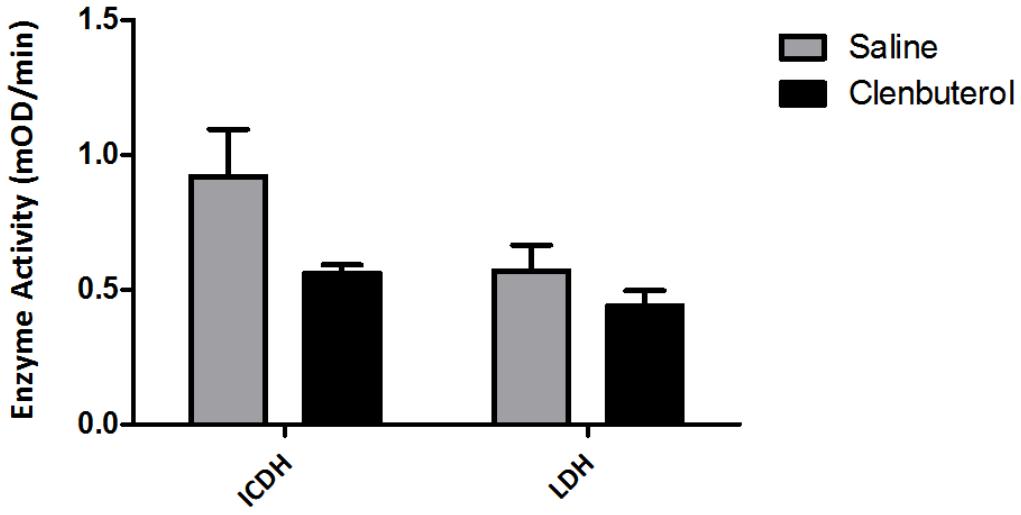

FIGURE 3.3 – The effects of 14 days administration of clenbuterol hydrochloride on ICDH and LDH activity in whole quadriceps homogenates. Data are mean mOD/min normalised to total extractable protein + S.E.M; n = 5. Saline x Clenbuterol P = 0.107 and 0.278 for ICDH and LDH activity respectively.

3.3.1.3 - Analysis of 4EBP1 expression in quadriceps muscle samples

As an index of protein synthetic potential, phosphorylated and total 4EBP1 protein was quantified by western blot. 4EBP1 is the elongation factor 4E (elF4E) binding protein that regulates mRNA translation by regulating the formation of the cap-initiation complex. When 4EBP1 is hyperphosphorylated by mTOR (mammalian target of rapamycin), its binding to elF4E is inhibited thereby enhancing protein synthesis (Connolly, Braunstein et al. 2006). Clenbuterol administration did not result in any significant changes to total, phosphorylated 4EBP1 or the ratio of phosphorylated to total 4EBP1 (P = 0.443, 0.171 and 0.683 respectively) (**FIGURE 3.4**).

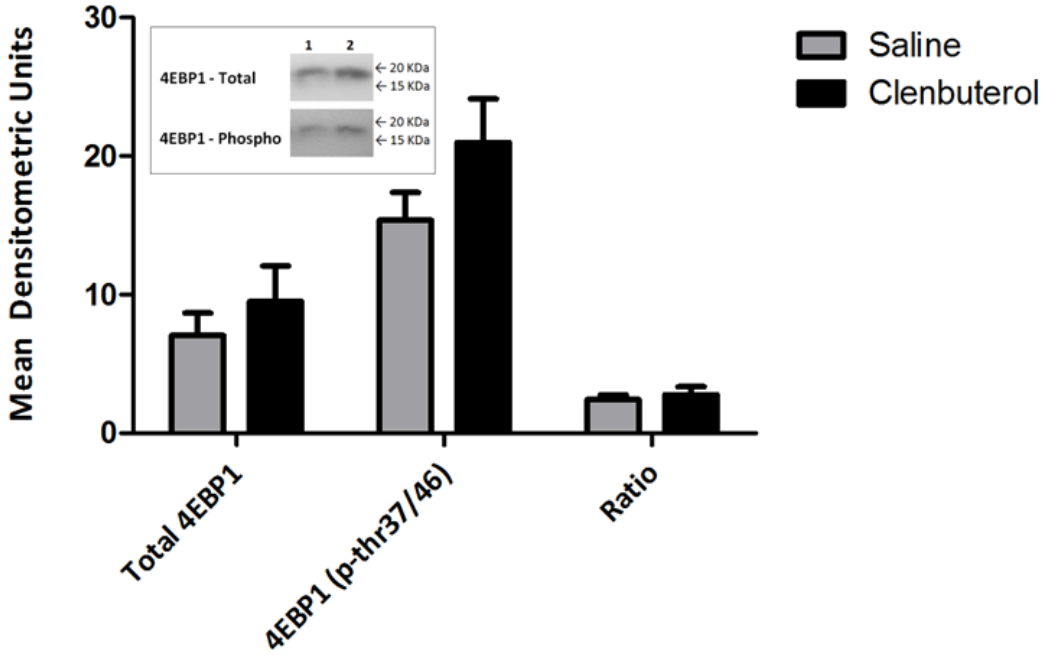

FIGURE 3.4 – The effects of 14 days administration of clenbuterol hydrochloride on the ratio of phosphorylated to total 4EBP1 protein. Data are mean densitometric units, normalised to total protein load + S.E.M; n = 5. Inset – Representative western blot - lanes 1 and 2 comprise animals from groups Saline 14d and Clenbuterol 14d respectively.

3.3.1.4 - Analysis of the quadriceps transcriptome

Transcriptome analysis of the treated quadriceps muscle specimens was conducted using custom low-density array as described in (**3.2.7**) and details of which can be found in **TABLE 3.1**. GeNorm software (v 3.5) was used to determine the most suitable housekeeping gene according to the method of Vandesompele, 2002 (Vandesompele, De Preter et al. 2002). Analysis revealed that beta-actin (ActB) and cyclophilin A (Ppia) were the most stable housekeeping genes in response to clenbuterol administration, and therefore most suitable for data normalisation. Both housekeeping genes displayed a stability index (*M*) of 0.229 which was considerably less than the suggested cut-off of *M* <1.5. Raw CP values were converted to relative expression values using the comparative CP method (Schmittgen and Livak 2008) and these values divided through by the normalisation factor determined from the geometric means of ActB and Ppia expression to derive normalised mRNA expression values.

As described in (**3.2.7**), targets were selected to assess changes in protein synthesis, negative regulation of skeletal protein, muscle atrophy, apoptotic potential, fatty acid metabolism, glucose metabolism, and the expression of nuclear receptors associated with metabolic status.

Markers of protein synthesis were generally unaffected by clenbuterol administration. Statistically, members of the PI3K / Akt family remained constant irrespective of treatment with the exception of mammalian target of rapamycin (mTOR) which displayed a trend towards increased mRNA in clenbuterol pre-treated quadriceps muscle (P = 0.058).

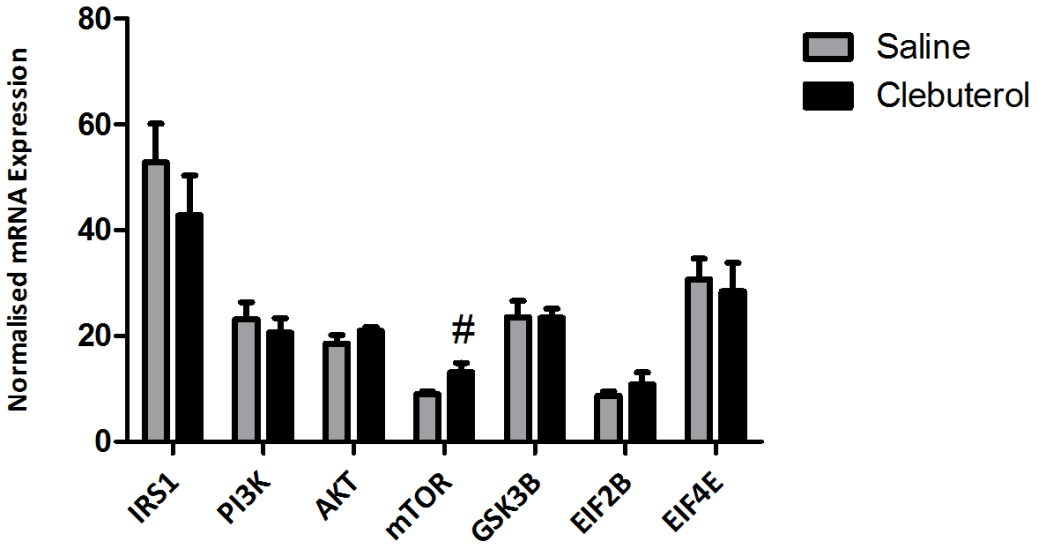

FIGURE 3.5 – The effects of clenbuterol administration on quadriceps muscle mRNA expression of markers of protein synthesis. Data are normalised expression values + S.E.M; n = 5.

Negative regulators of skeletal muscle protein were assessed by the determination of factors involved in proteosomal degradation. Analytes included the E3 ligases (MuRF1, MAFBx), the proteosome (subunit 5) in addition to upstream factors involved in the initiation of these (TWEAK, NFKB, DUSP1 and p38 MAPK). Clenbuterol administration decreased TWEAK mRNA (P = 0.059), increased DUSP1 mRNA expression (P = 0.013) and decreased MURF1 expression (P = 0.054).

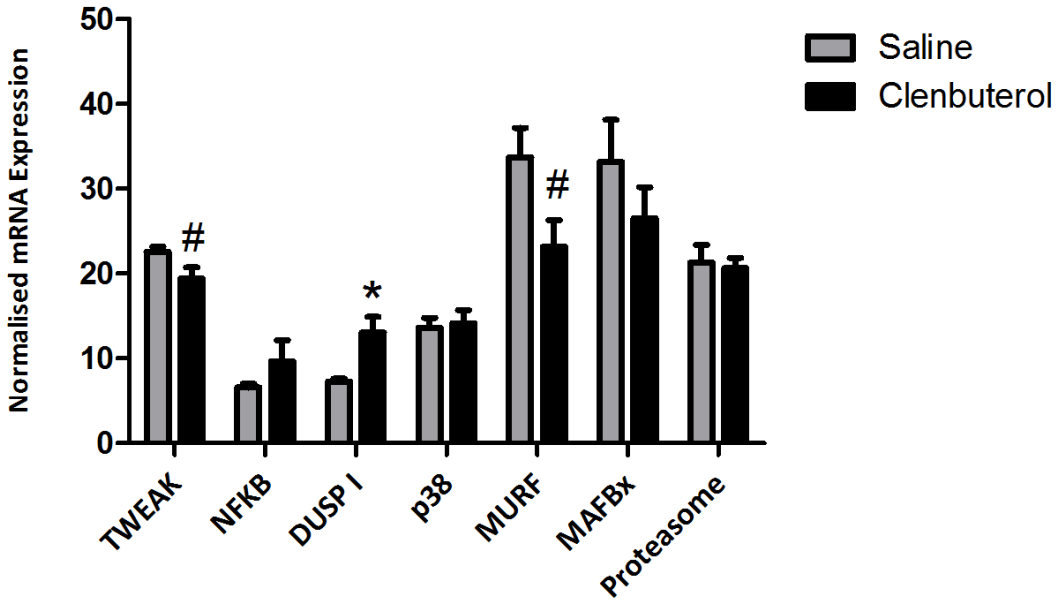

FIGURE 3.6 – The effects of clenbuterol administration on quadriceps muscle mRNA expression of negative regulators of protein synthesis. Data are normalised expression values + S.E.M; n = 5.

Factors implicated in muscle atrophying conditions were assessed and included myostatin, cathepsin L, and calpain members I – III. Both calpain I and muscle specific calpain III were up-regulated in clenbuterol pre-treated quadriceps specimens (P = 0.08 and 0.07 respectively). Clenbuterol administration had no effect on myostatin or cathepsin L mRNA expression.

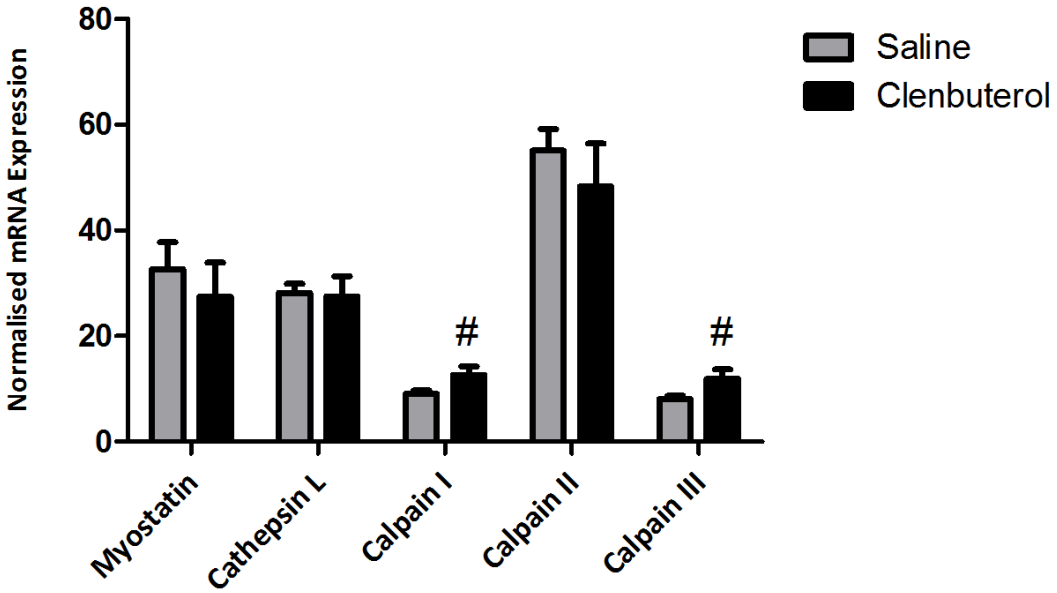

FIGURE 3.7 – The effects of clenbuterol administration on quadriceps muscle mRNA expression of atrophy associated factors. Data are normalised expression values + S.E.M; n = 5.

The apoptotic response potential was assessed by quantifying the mRNAs of pro-apoptotic Bax and anti-apoptotic Bcl2 in addition to the cysteine-dependent aspartate directed proteases III and XII (Caspases III, XII). Clenbuterol administration had no effect on the expression of apoptosis response related factors in quadriceps muscle specimens.

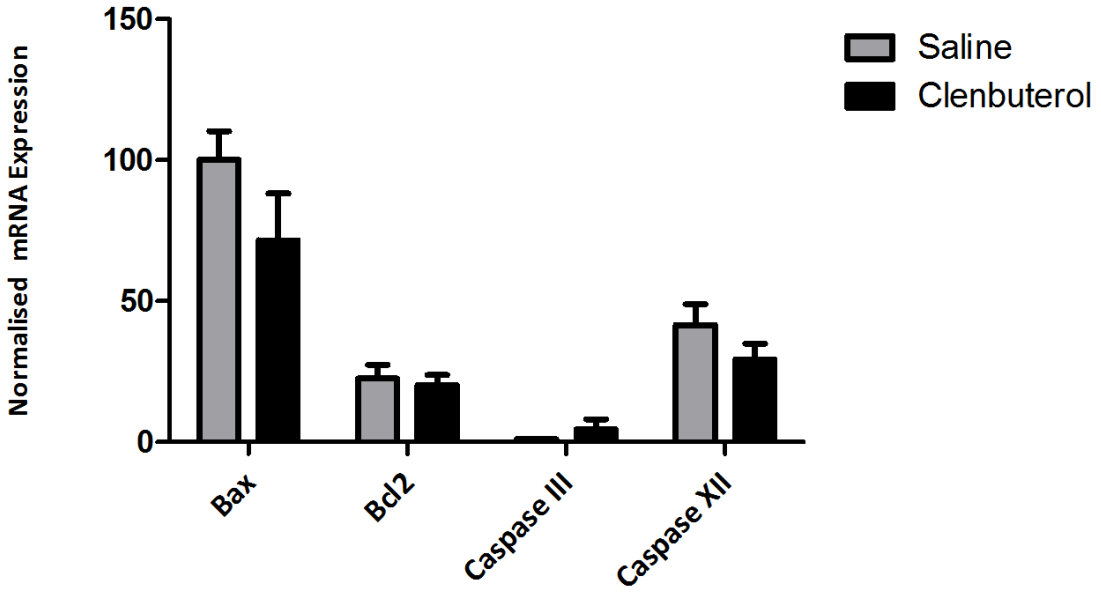

FIGURE 3.8 – The effects of clenbuterol administration on quadriceps muscle mRNA expression of apoptosis associated factors. Data are normalised expression values + S.E.M; n = 5.

Oxidative metabolic potential was assessed in quadriceps muscle specimens via the expression of mRNAs pertaining to Cpt1a, Lipin, Adiponectin receptor 1/2, and UCP3. Clenbuterol administration had no significant effects on the expression of any of these factors.

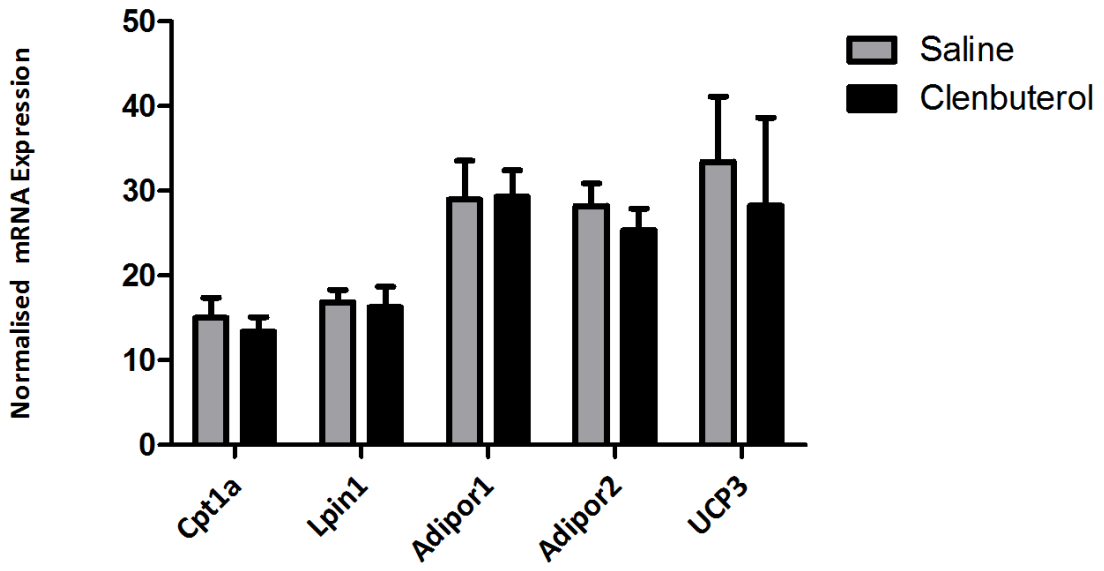

FIGURE 3.9 – The effects of clenbuterol administration on quadriceps muscle mRNA expression of factors associated with oxidative potential. Data are normalised expression values + S.E.M; n = 5.

Glycolytic potential was assessed by the sole expression of mRNA transcripts pertaining to hexokinase I – the enzyme responsible for catalysing the conversion of glucose to glucose-6-phosphate during the initial phase of glycolysis. Clenbuterol administration did not affect hexokinase I mRNA over the course of the study (P = 0.147).

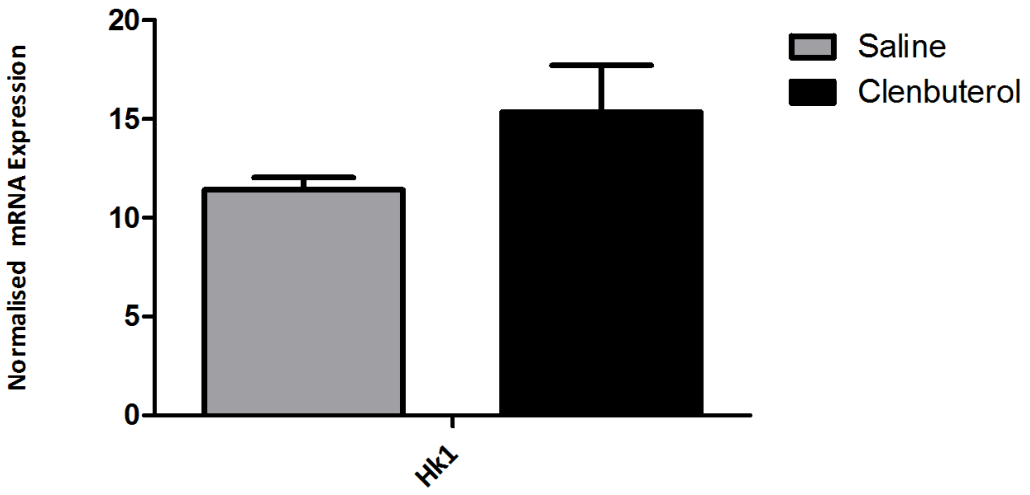

FIGURE 3.10 – The effects of clenbuterol administration on quadriceps muscle mRNA expression of hexokinase I. Data are normalised expression values + S.E.M; n = 5.

To detect potential changes in metabolite signalling, members from the PGC1, PPAR and AMP-activated protein kinase family were assessed with respect to clenbuterol treatment. None of the factors assessed were affected by clenbuterol pre-treatment.

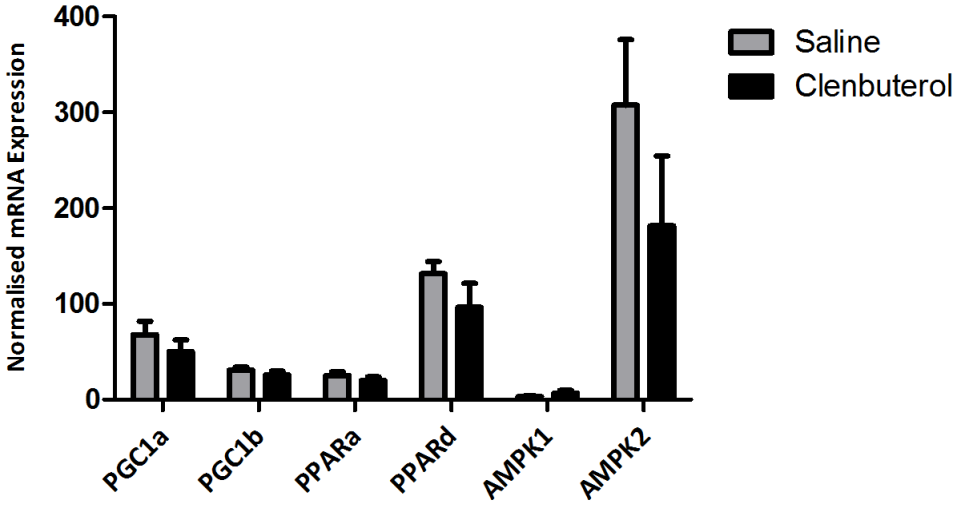

FIGURE 3.11 – The effects of clenbuterol administration on quadriceps muscle mRNA expression of metabolite signalling factors. Data are normalised expression values + S.E.M; n = 5.

TABLE 3.3 – Summary of Quadriceps mRNA expression changes following clenbuterol administration. Data are mean normalised expression + S.E.M; n = 5.

Function	Symbol	Saline	Clenbuterol	P =
Protein Synthesis	IRS1	52.822 ± 7.315	42.852 ± 7.500	0.369
	PI3K	23.132 ± 3.246	20.608 ± 2.744	0.569
	Akt	18.570 ± 1.575	20.938 ± 0.754	0.212
	Gsk3B	23.544 ± 3.089	23.410 ± 1.753	0.953
	mTOR	8.966 ± 0.546	13.120 ± 1.795	**0.058**
	EIF2B	8.720 ± 0.774	10.825 ± 2.30	0.467
	EIF4E	30.680 ± 3.927	28.455 ± 5.401	0.664
Negative Regulation and Degradation	NFκβ	6.580 ± 0.436	9.666 ± 4.463	0.304
	TWEAK	22.576 ± 0.620	19.454 ± 1.274	**0.059**
	MuRF	33.710 ± 3.459	23.200 ± 3.133	**0.054**
	Dusp1	7.250 ± 0.364	13.076 ± 1.799	**0.013**
	P38	13.620 ± 1.151	14.164 ± 1.521	0.783
	MAFBx	33.202 ± 4.932	26.520 ± 3.686	0.325
	Proteosome	21.296 ± 2.082	20.662 ± 1.202	0.799
Muscle Atrophy	Myostatin	32.628 ± 5.116	27.402 ± 6.489	0.525
	Cathepsin L	28.188 ± 1.689	27.526 ± 3.769	0.877
	Calpain I	9.066 ± 0.642	12.614 ± 1.647	**0.080**
	Calpain II	55.110 ± 4.060	48.282 ± 8.180	0.476
	Calpain III	8.024 ± 0.650	11.932 ± 1.751	**0.070**
Apoptosis	Bax	100.144 ± 10.142	71.550 ± 16.684	0.181
	Bcl2	22.564 ± 4.878	20.136 ± 3.736	0.703
	Caspase III	1.062 ± 0.088	4.540 ± 3.473	0.376
	Caspase XII	41.580 ± 7.362	29.266 ± 5.726	0.223
Fatty Acid Oxidation	Cpt1a	15.008 ± 2.385	13.396 ± 1.710	0.598
	Lipin	16.860 ± 1.433	16.256 ± 2.413	0.835
	Adipor1	28.972 ± 4.610	29.292 ± 3.133	0.956
	Adipor2	28.242 ± 2.667	25.368 ± 2.518	0.456
	UCP3	33.448 ± 7.678	28.282 ± 10.376	0.447
Glycolysis	Hk1	11.420 ± 0.616	15.358 ± 2.370	0.147
Metabolic Regulators	PGC1α	67.720 ± 14.140	50.248 ± 12.346	0.379
	PGC1β	30.743 ± 3.484	25.930 ± 3.852	0.439
	PPARα	25.168 ± 3.836	20.078 ± 3.793	0.431
	PPARδ	131.388 ± 12.893	96.485 ± 25.054	0.310

	AMPK1	3.312 ± 0.515	6.768 ± 2.957	0.241
	AMPK2	307.60 ± 68.300	181.450 ± 73.164	0.243

3.3.1.5 – Summary of the effects of clenbuterol on skeletal muscle characteristics

Clenbuterol administration over 14 days resulted in significant increases in bodyweight and quadriceps skeletal muscle mass. Assessment of the quadriceps skeletal muscle revealed that neither fibre-type nor metabolic potential were directly affected by Clenbuterol. Assessment of numerous mRNA transcripts associated with protein synthesis, degradation and metabolic signalling demonstrated a tendency towards decreased protein degradative signalling (MuRF / TWEAK) and increased calpain I and III activity indicative of skeletal muscle remodelling. Protein synthetic potential appeared unaltered.

3.3.2 – The effects of meniscectomy-induced OA and clenbuterol administration on parameters of quadriceps function

3.3.2.1 - Histopathological examination

Of those animals subjected to meniscectomy surgery, histopathological examination was performed as per **METHOD 3.2.5**. Microscopy of toluidine blue stained sections from the ipsilateral limbs revealed evidence of OA-like lesions, predominantly localised at the tibial condyle. Microscopically, meniscectomised tibias presented with proteoglycan and chondrocyte loss, erosion and ulceration of the articular surface, but limited evidence of subchondral degeneration. Femoral condyles showed evidence of proteoglycan loss; however this was less severe than that noted on the respective tibial condyles. No femoral erosion, ulceration or subchondral degeneration was noted within the experimental timeframe. Pre-treatment with clenbuterol prior to the surgical induction of OA had no effect on tibial or femoral pathology 21 days post surgery when compared with saline pre-treated animals. Microscopically, the severity of proteoglycan and chondrocyte loss, ulceration and subchondral degeneration remain unchanged irrespective of pre-treatment regime.
All sham operated control animals were free from OA at 21 days post surgery (**TABLE 3.4**) validating their use as a suitable surgical control.

TABLE 3.4 – The effects of meniscectomy-induced OA and clenbuterol administration on joint histopathology. Data are mean pathological scores + S.E.M; n = 10

Parameter	Sham	Saline MNX	Clen MNX	P =
Proteoglycan loss (TIB)	0	1.90 + 0.18	2.10 + 0.23	0.491
Erosion / ulceration (TIB)	0	1.10 + 0.35	1.30 + 0.34	0.663
Subchondral degeneration (TIB)	0	0.20 + 0.13	0.50 + 0.27	0.485
Proteoglycan loss (FEM)	0	0.40 + 0.22	0.80 + 0.25	0.202
Erosion / ulceration (FEM)	0	0 + 0	0 + 0	-
Subchondral degeneration (FEM)	0	0 + 0	0 + 0	-

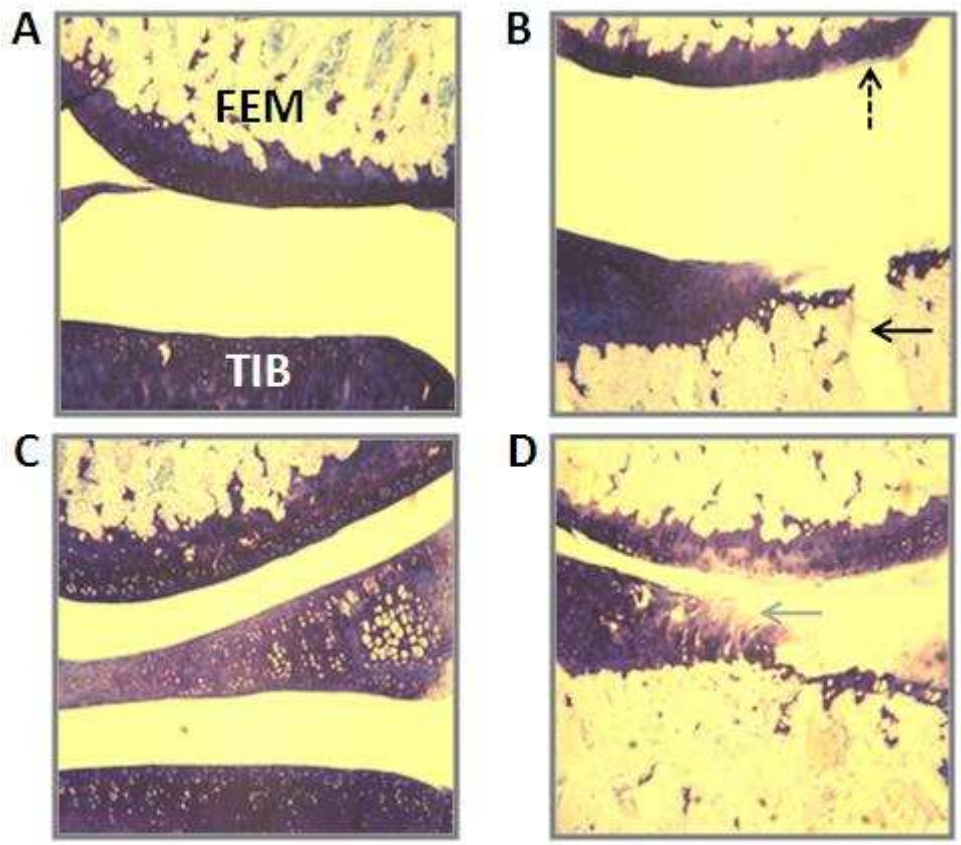

FIGURE 3.12 – Representative photomicrographs of tibiofemoral joints stained with toluidine blue and visualised at 4 x magnification. A – Saline MNX, lateral tibiofemoral joint; B – Saline MNX, medial tibiofemoral joint; C – Clen MNX, lateral tibiofemoral joint; D – Clen MNX, medial tibiofemoral joint. FEM – femoral condyle; TIB – tibial condyle.

Photomicrographs A + C show proteoglycan-rich lateral joint margins with no macroscopic defects. The articular joint surfaces are smooth and free from irregularities.

Photomicrographs B + D show pathological medial joint margins with proteoglycan loss (dashed arrow), joint fracture (black arrow), and fibrillation (grey arrow). Medial predominance is noted in this model due to transection of the medial meniscus whilst the lateral meniscus is left intact.

3.3.2.2 - Weight parameters

Daily weight records revealed that surgically-induced OA was associated with a reduction in bodyweight gain over the course of the study (d1 – d35) (16.92 + 1.12%) compared with those animals undergoing the sham control procedure (24.03 + 0.98%) P= 0.019. Clenbuterol pre-treatment suppressed the reduction in bodyweight gain post meniscectomy, leading to similar weight gain to those animals undergoing the sham control procedure (Clen MNX: 20.16% + 1.11, Sham: 24.03% + 0.98). The quadriceps from those animals with surgically induced OA (5.32 + 1.72g) were numerically smaller than animals undergoing the sham control procedure (5.91 + 1.19g) P = 0.089. However, when corrected for bodyweight, the reduction in quadriceps mass in response to OA induction was no longer evident (ANOVA P = 0.154) (**TABLE 3.5**). The previously noted hypertrophic effects of clenbuterol on quadriceps mass immediately following pre-treatment were no longer apparent at the study end point (d35), with clenbuterol pre-treated animals presenting with similar quadriceps mass relative to bodyweight to saline re-treatment animals.

TABLE 3.5 – The effects of meniscectomy-induced OA and clenbuterol administration on percentage bodyweight gain over the course of the study, quadriceps mass (g), and quadriceps relative to bodyweight mass (%). Data are mean + S.E.M; Sham n = 5, Saline/Clen MNX n = 10.

Parameter	Sham	Saline MNX	Clen MNX	P =
Bodyweight gain (%)	24.03 + 0.98[a]	16.92 + 1.12	20.16 + 1.11	**0.021**
Quadriceps mass (gram)	5.91 + 1.19	5.32 + 1.72	5.60 + 1.57	0.099
Quadriceps mass (%)	1.69 + 0.02	1.60 + 0.05	1.70 + 0.02	0.154

[a]Sham x Saline MNX (P = 0.019); Sham x Clen MNX (P = 0.236)

3.3.2.3 - Incapacitance assessment

With the aim of assessing behavioural joint pain in the operated animals, incapacitance assessment was performed throughout the study. Data revealed a 50:50 load distribution between the hind limbs prior to surgery (Grey Bar - **FIGURE 3.9**). Following meniscectomy surgery on study day 15, significantly less weight was placed on the ipsilateral limb (day 14 versus day 21, day 28, day 35; P = < 0.001). Weight distribution between the hind limbs of the meniscectomy treated animals resolved over a period of 14 days post surgery, although equal distribution was not achieved within the experimental timeframe. Pre-treatment with clenbuterol prior to the induction of OA had no effect of markers of behavioural joint pain (**FIGURE 3.13 grey line vs. black line**).

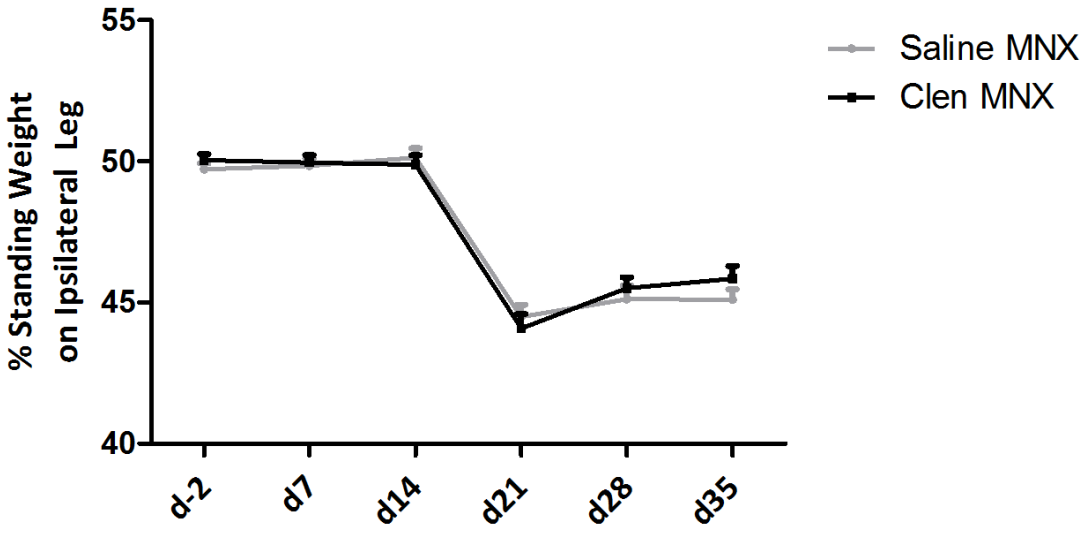

FIGURE 3.13 – The effects of MNX Surgery and pre-treatment regime on weight bearing. Data are percentage standing weight on the ipsilateral (operated) limb + S.E.M n = 10 for operated animals only. No significant effect of pre-treatment regime noted.

3.3.2.4 - Contractile and metabolic characteristics of the quadriceps muscle

Electrophoretic examination of the quadriceps muscles at 21 days post surgery was performed to examine changes in the MHC expression profile. Compared to the sham control animals, meniscectomy operated (saline pre-treated) animals exhibited a 115% increase in the protein expression of the slow twitch MHC I (P = 0.080), numerically *in lieu* of fast twitch MHC IIB. Pre-treatment with clenbuterol suppressed the OA associated increase in MHC I protein and numerically, maintained the MHC IIB complement.

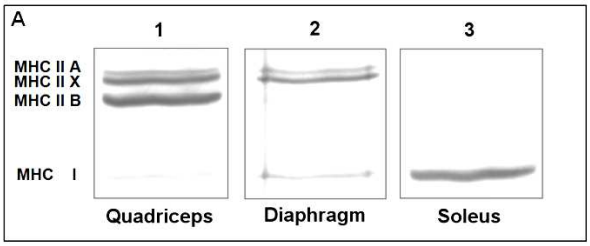

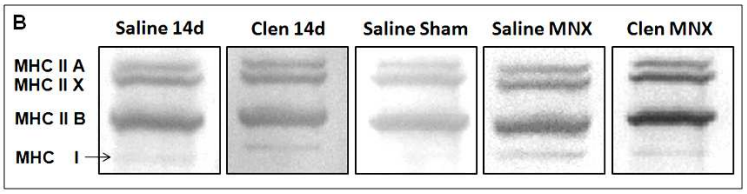

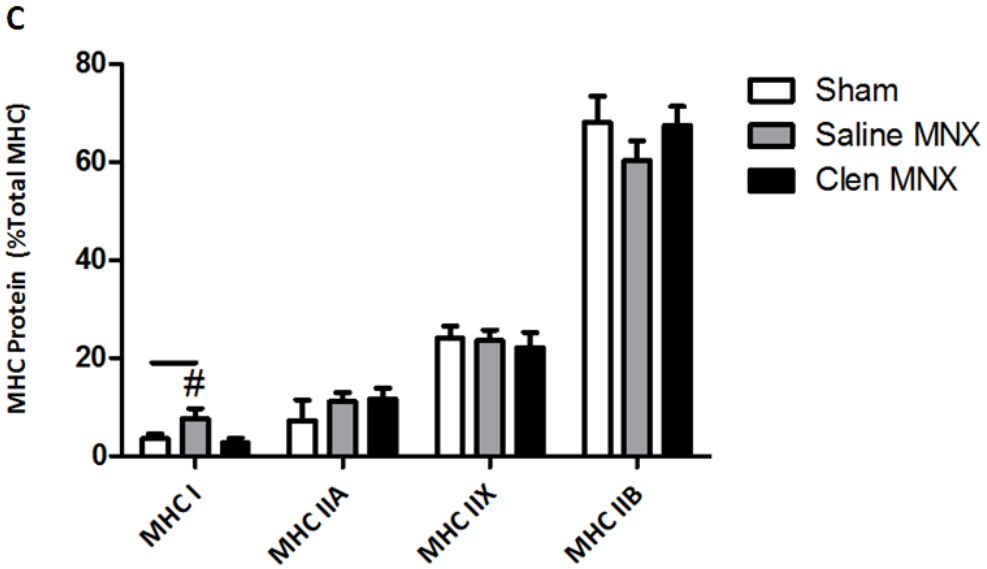

FIGURE 3.14 – The effects of meniscectomy-induced OA and clenbuterol administration on MHC isoforms I, IIA, IIX and IIB. (A) Silver stained electrophoretic MHC separation (50ng protein load) demonstrating the presence of four well-resolved bands in the rat quadriceps (Lane 1). Lanes 2 and 3 contain control material from rat diaphragm and soleus respectively with known MHC protein expression profiles. (B) Representative quadriceps muscle samples (50ng total protein) from each experimental group following termination. (C) Mean densitometry values of each isoform expressed as a percentage of the total MHC signal + S.E.M; Sham n = 5, Saline MNX / Clen MNX n = 10.

The metabolic potential of the quadriceps muscle samples was assessed by the quantification of ICDH and LDH enzyme activities in whole muscle homogenates. The surgical induction of OA had no effect on ICDH activity or LDH activity. Clenbuterol pre-treated animals undergoing MNX surgery had significantly elevated LDH activity (Sham x Clen MNX; P = 0.028), suggesting an interaction between the surgical induction of OA and clenbuterol pre-treatment.

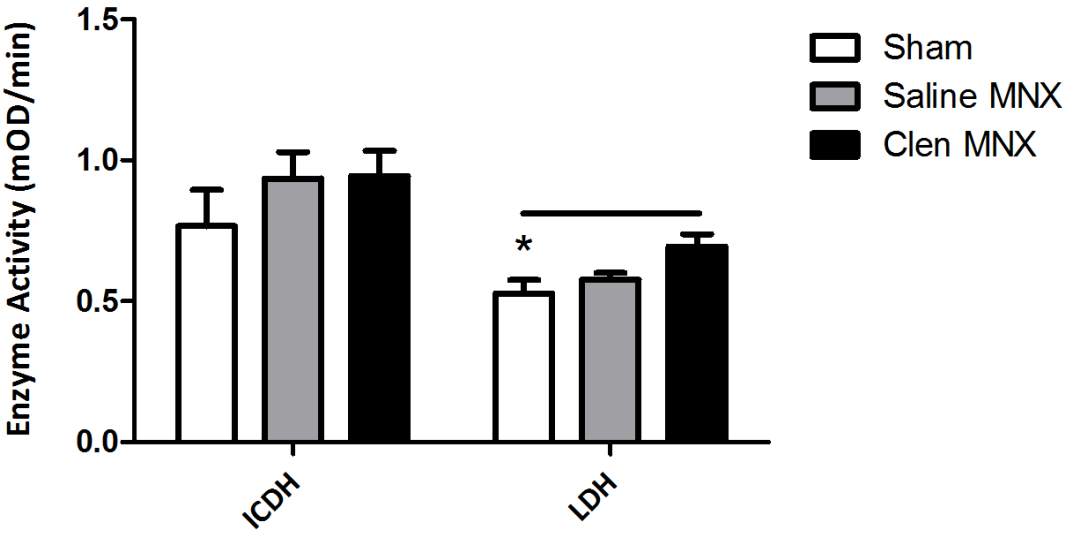

FIGURE 3.15 – The effects of meniscectomy-induced OA and clenbuterol administration on ICDH and LDH activity in whole quadriceps homogenates. Data are mean mOD/min normalised to extractable protein + S.E.M; Sham n = 5, Saline/Clen MNX n = 10. P = 0.495 and 0.018 for ICDH and LDH activity respectively; * indicates P = < 0.05.

3.3.2.5 - Analysis of 4EBP1 expression in quadriceps muscle samples

As an index of protein synthesis, phosphorylated and total 4EBP1 protein was quantified by western blot. Neither total nor phosphorylated 4EBP1 was affected by the induction of OA or clenbuterol pre-treatment. The ratio of phosphorylated to total 4EBP1 also remained constant (P = 0.287) (**FIGURE 3.16**).

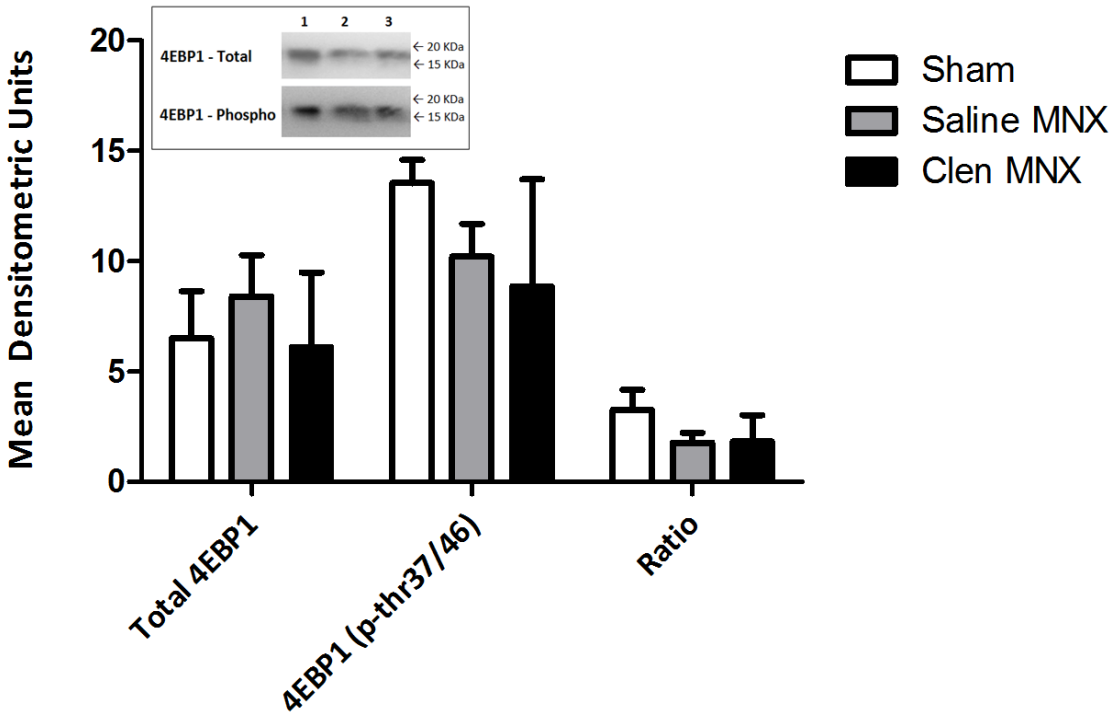

FIGURE 3.16 – The effects of meniscectomy-induced OA and clenbuterol administration on the ratio of phosphorylated to total 4EBP1 protein. Data are mean densitometric units, normalised to total protein load + S.E.M; Sham n = 5, Saline/Clen

MNX n = 10. Inset – Representative western blot - lanes 1, 2 and 3 comprise animals from groups Sham, Saline MNX and Clen MNX respectively.

3.3.2.6 - Analysis of the quadriceps transcriptome

As described in (**CHAPTER 3.2.7**), targets were selected to assess changes in protein synthesis, negative regulation of skeletal protein, muscle atrophy, apoptotic potential, fatty acid metabolism, glucose metabolism, and the expression of nuclear receptors associated with metabolic status in post-surgical quadriceps muscle specimens. GeNorm analysis revealed that HPRT and TATA binding protein (TBP) were most stable in response to the surgical induction of OA and clenbuterol pre-treatment and therefore the most suitable housekeeping genes for data normalisation. Both housekeeping genes displayed a stability index (*M*) of 0.273 which was considerably less than the suggested cut-off of *M* <1.5. Raw CP values were converted to relative expression values using the comparative CP method (Schmittgen and Livak 2008) as described previously (**CHAPTER 3.2.7**).

Markers of protein synthesis were generally unaffected by the surgical induction of OA or pre-treatment regime (**FIGURE 3.17**). IRS1 mRNA was unaffected by the induction of OA *per* se however, was reduced in animals pre-treated with clenbuterol prior to the induction of OA (P = 0.013 sham x Clen MNX).

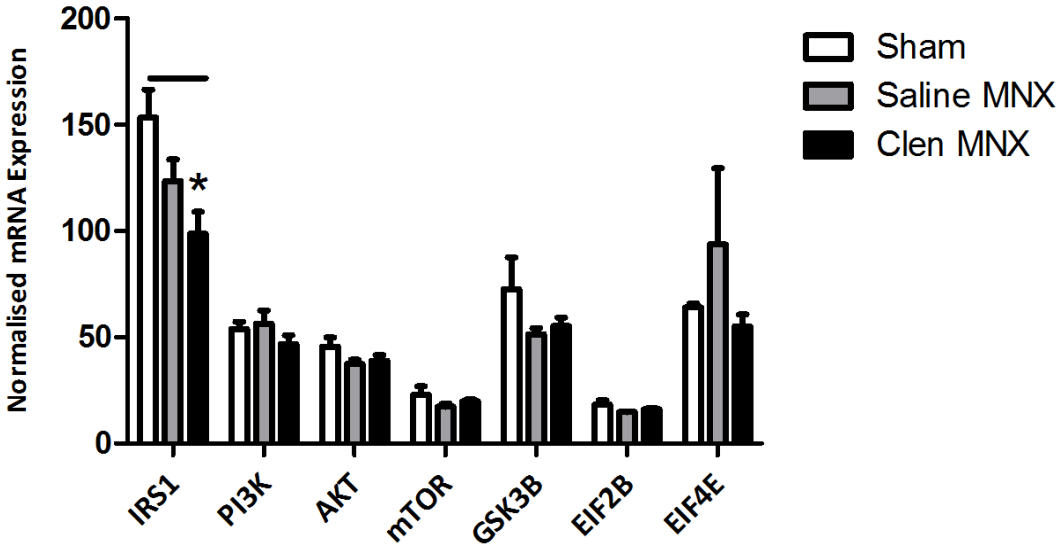

FIGURE 3.17 – The effects of meniscectomy-induced OA and clenbuterol administration on markers of protein synthetic potential. Data are normalised expression values + S.E.M; n = 5.

Negative regulators of skeletal muscle protein were assessed by the determination of factors involved in proteosomal degradation. None of the factors studied were modulated by in the surgical induction of OA, or pre-treatment with clenbuterol.

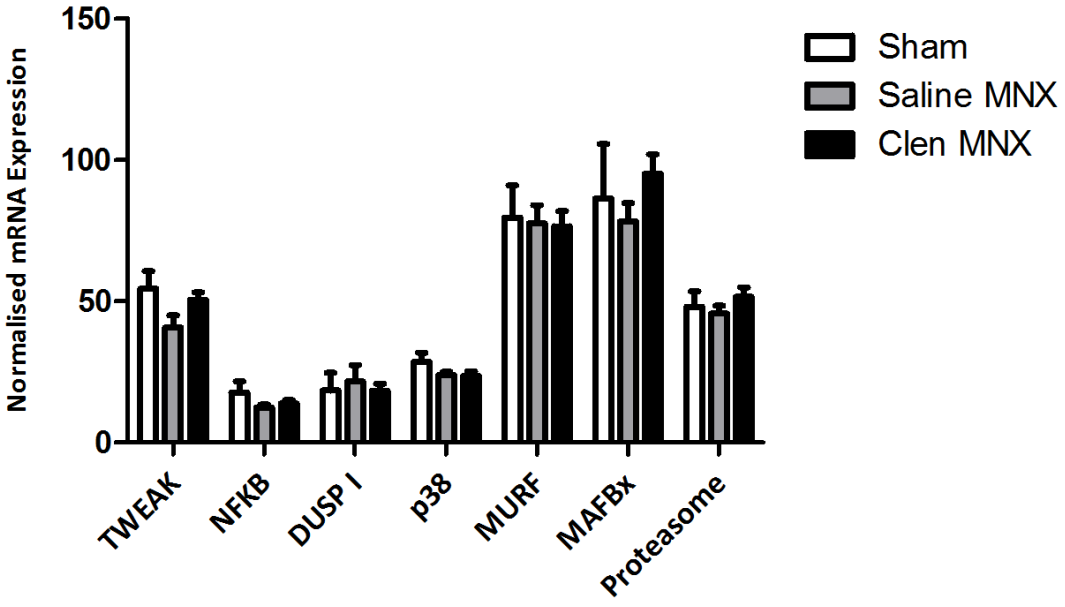

FIGURE 3.18 – The effects of meniscectomy-induced OA and clenbuterol administration on negative regulators of protein synthesis. Data are normalised expression values + S.E.M; n = 5.

Factors implicated in muscle atrophying conditions were assessed and included myostatin, cathepsin L, and calpain members I – III. None of the atrophy associated factors studies were modulated by the surgical induction of OA or clenbuterol pre-treatment.

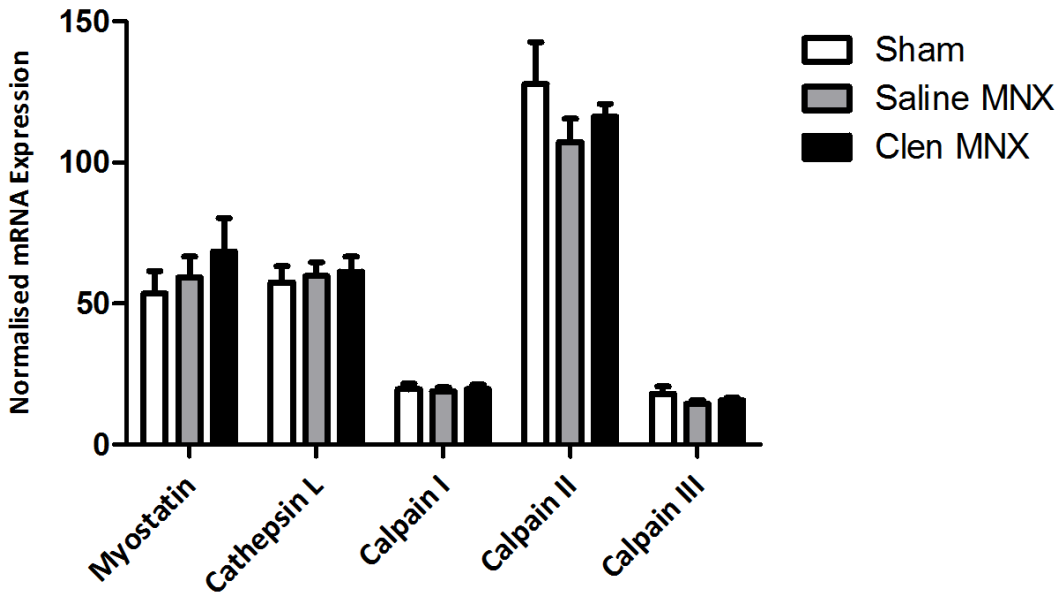

FIGURE 3.19 – The effects of meniscectomy-induced OA and clenbuterol administration on factors associated with muscle atrophying conditions. Data are normalised expression values + S.E.M; n = 5.

None of the apoptosis associated factors studies were modulated by the surgical induction of OA or clenbuterol pre-treatment.

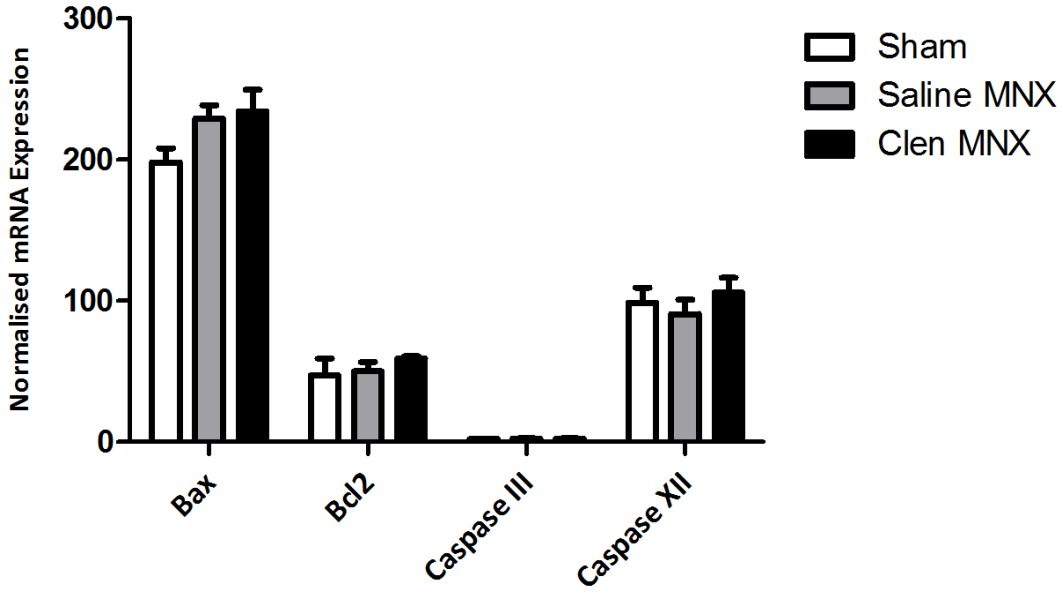

FIGURE 3.20 – The effects of meniscectomy-induced OA and clenbuterol administration on factors associated with the apoptotic response. Data are normalised expression values + S.E.M; n = 5.

Oxidative potential was assessed in quadriceps muscle specimens. Adiponectin receptor 2 (AdiporR2) was elevated in response to OA induction (P = 0.080). Pre-treatment with clenbuterol suppressed the OA associated increase in AdipoR2 with mRNA expression restored to that of sham control levels (P = 0.363). All other factors assessed were unaffected by surgery or pre-treatment regime.

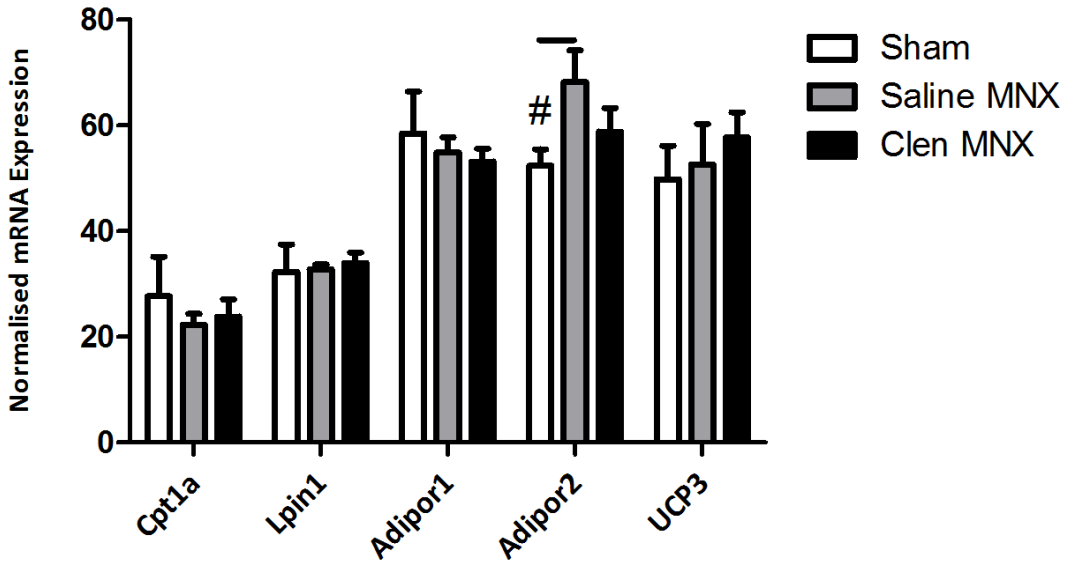

FIGURE 3.21 – The effects of meniscectomy-induced OA and clenbuterol administration on factors associated with fatty acid oxidation. Data are normalised expression values + S.E.M; n = 5.

Glycolytic potential was assessed by examining the expression of hexokinase I mRNA. Hexokinase I expression was unaffected by surgery or pre-treatment regime.

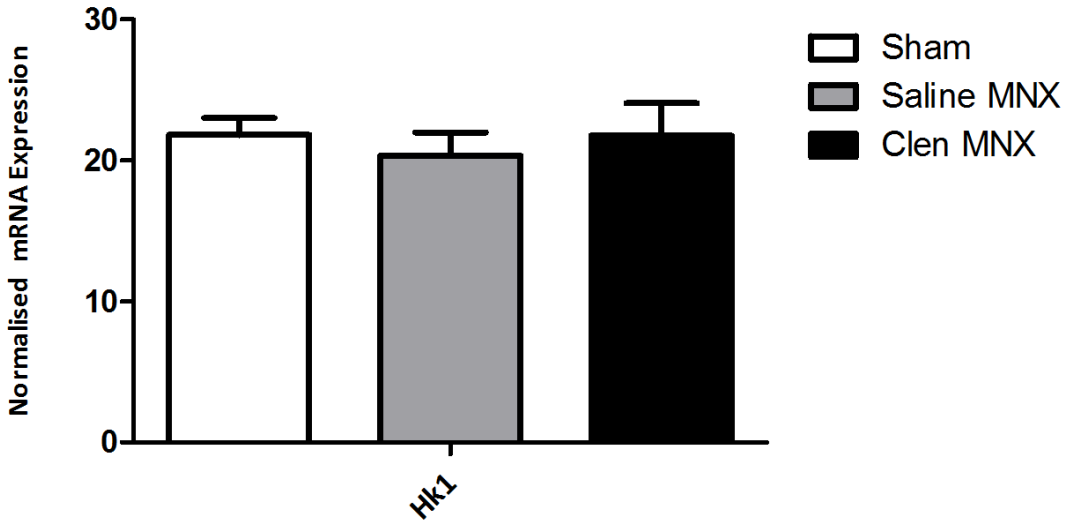

FIGURE 3.22 – The effects of meniscectomy-induced OA and clenbuterol administration on hexokinase I mRNA expression. Data are normalised expression values + S.E.M; n = 5.

When the expression of genes associated with metabolic signalling were assessed, PGC1α and β displayed similar expression profiles but were statistically unaffected by OA induction (Saline MNX) or pre-treatment (Clen MXN). Similarly, PPAR α and δ exhibited similar expression profiles however the expression of PPARα was reduced following the induction of OA (P = 0.096). AMP kinase I was unaffected by the induction of OA or pre-treatment regime whereas numerically, AMP kinase 2 was reduced following the induction of OA and rescued to sham levels with pre-treatment (P = 0.134). AMP Kinase I and 2 displayed differential responses to clenbuterol administration with mean AMP kinase I expression increased and AMP Kinase 2 reduced in response to treatment however these changes were not statistically significant.

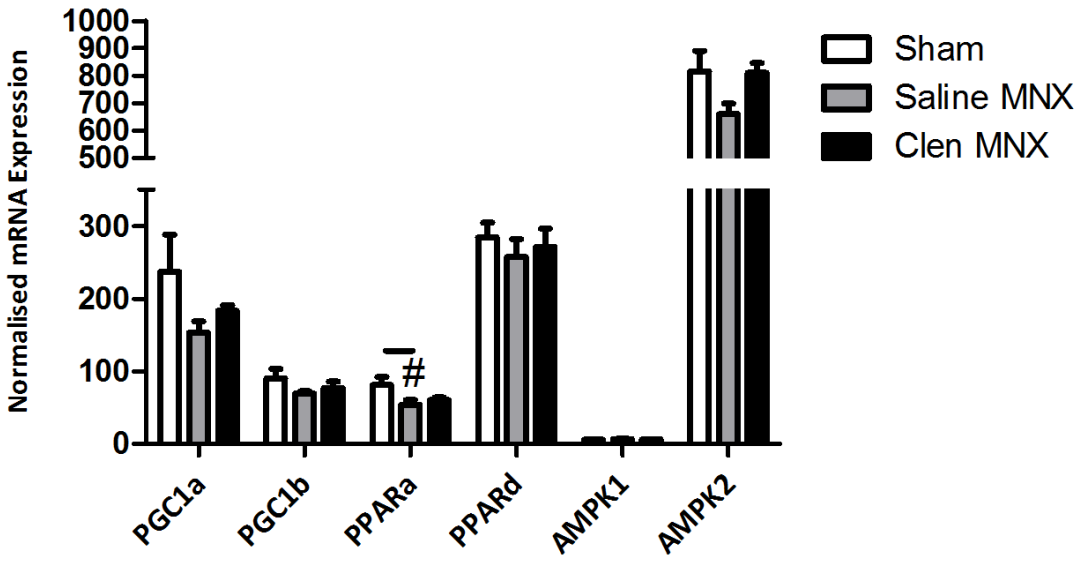

FIGURE 3.23 – The effects of meniscectomy-induced OA and clenbuterol administration on factors involved in metabolite signalling. Data are normalised expression values + S.E.M; n = 5.

TABLE 3.6 – Summary of Quadriceps mRNA expression changes following MNX and clenbuterol administration. Data are mean normalised expression + S.E.M; n = 5.

Gene	Sham	Saline MNX	Clen MNX	P =
IRS1	153.422 ± 13.171	123.546 ± 10.175	98.718 ± 10.404	**0.017**
PI3K	53.966 ± 3.305	56.364 ± 6.162	46.672 ± 4.187	0.346
Akt	45.560 ± 4.350	37.408 ± 2.078	36.848 ± 2.685	0.197
Gsk3B	72.548 ± 15.004	51.445 ± 2.871	66.314 ± 3.953	0.280
mTOR	22.866 ± 4.092	17.322 ± 1.439	19.728 ± 1.025	0.344
EIF2B	18.315 ± 2.111	14.670 ± 0.471	16.086 ± 0.603	0.223
EIF4E	64.095 ± 1.758	93.736 ± 35.742	55.042 ± 5.768	0.522
NFκβ	17.676 ± 3.968	12.480 ± 0.986	13.776 ± 1.316	0.318
TWEAK	54.470 ± 6.178	40.728 ± 4.293	50.538 ± 2.595	0.179
MuRF	79.732 ± 11.358	77.615 ± 6.483	76.572 ± 5.376	0.963
Dusp1	18.385 ± 6.291	21.733 ± 5.649	18.340 ± 2.468	0.878
P38	28.610 ± 3.247	23.890 ± 1.189	23.506 ± 1.710	0.237
MAFBx	86.384 ± 19.323	78.373 ± 6.480	95.190 ± 6.911	0.510
Proteosome	48.015 ± 5.524	45.635 ± 2.796	51.622 ± 3.284	0.610
Myostatin	53.576 ± 8.011	59.310 ± 7.385	68.402 ± 11.855	0.600
Cathepsin L	57.522 ± 5.837	59.815 ± 4.894	61.38 ± 5.352	0.883
Calpain I	19.730 ± 1.989	18.936 ± 1.400	19.650 ± 1.678	0.937
Calpain II	127.872 ± 14.846	107.288 ± 8.316	116.354 ± 4.481	0.386
Calpain III	18.010 ± 2.652	14.515 ± 1.277	15.800 ± 0.859	0.445
Bax	198.236 ± 9.852	226.244 ± 9.444	234.390 ± 15.217	0.104
Bcl2	47.040 ± 11.977	50.166 ± 6.532	59.200 ± 1.736	0.548
Caspase III	2.000 ± 0.347	2.478 ± 0.309	2.348 ± 0.412	0.626
Caspase XII	98.550 ± 10.700	90.513 ± 10.273	105.918 ± 10.566	0.634
Cpt1a	27.683 ± 7.500	22.296 ± 2.072	23.844 ± 3.274	0.731
Lipin	32.270 ± 5.252	32.758 ± 0.922	33.952 ± 2.039	0.934
Adipor1	58.508 ± 7.899	54.822 ± 2.897	53.182 ± 2.472	0.754
Adipor2	52.382 ± 3.106	68.240 ± 6.011	58.846 ± 4.470	**0.094**
UCP3	49.824 ± 6.371	52.602 ± 7.691	57.762 ± 4.719	0.581
Hk1	21.824 ± 1.194	20.342 ± 1.643	21.766 ± 2.296	0.802
PGC1α	237.053 ± 51.066	152.933 ± 15.560	183.482 ± 7.450	0.239
PGC1β	90.010 ± 13.180	69.353 ± 3.102	77.028 ± 8.553	0.389
PPARα	81.065 ± 10.965	53.493 ± 6.871	60.244 ± 3.643	**0.096**
PPARδ	284.215 ± 20.425	257.553 ± 24.292	271.034 ± 25.198	0.776

AMPK1	5.376 ± 0.672	6.720 ± 0.599	6.112 ± 0.575	0.313
AMPK2	815.622 ± 74.528	660.334 ± 38.018	810.230 ± 35.770	**0.099**

3.4 – Discussion

This is the first study to report the role of the quadriceps muscle and the effects of induced skeletal muscle hypertrophy on the severity of joint pathology in an animal model of osteoarthritis. Clenbuterol administration, for 14 days, resulted in marked skeletal muscle hypertrophy in the rat. Previous studies have reported that clenbuterol-induced hypertrophy is commonly associated with increased expression of the fast isoforms of MHC (Oishi, Imoto et al. 2002), and therefore an assessment of MHC composition following clenbuterol administration was undertaken. Clenbuterol did not induce any changes to the MHC protein composition of the quadriceps muscle in this study, suggesting that the contractile properties of this skeletal muscle were unaltered.

Clenbuterol administration was further associated with the expression of several key-modulators of muscle mass. Pro-synthetic mammalian target of rapamycin (mTOR) mRNA abundance was increased with clenbuterol treatment, inferring increased protein synthetic signalling. Conversely, the expression of the E3 ligase MuRF was decreased at the level of mRNA. An mTOR mediated decrease in MuRF and MAFBx expression may present one possible route via which clenbuterol may induce muscle hypertrophy (Kline, Panaro et al. 2007). Moreover, the mRNA of Dusp1, which antagonises the activation of MAFBx expression by p38 (Franklin and Kraft 1997), was increased by clenbuterol treatment. Additionally, tumour necrosis factor-like weak inducer of apoptosis (TWEAK) which activates MuRF1 expression via NFκβ (Cai, Frantz et al. 2004) was decreased following clenbuterol administration. By inference, the reduced expression of TWEAK may reason the decrease in MuRF1 expression noted in response to clenbuterol.

Clenbuterol administration was further associated with changes in calpain expression. Whilst calpain II remained unaltered by treatment, both calpain I and calpain III were modestly up-regulated. Previous studies have reported that exercise

induced hypertrophy is associated with the increased expression of calpain I (Higgins, Lasslett et al. 1988). Such data are consistent with the findings of this study, with the exception that hypertrophy was induced by clenbuterol rather than targeted exercise. Calpain II expression has been previously shown to be induced by both clenbuterol administration (Higgins, Lasslett et al. 1988) and exercise following immobilisation (Jones, Hill et al. 2004) however this finding was not replicated in this study, with clenbuterol treated animals presenting with similar calpain II expression to control animals. The function of calpain III is less clear with regards skeletal muscle atrophy and hypertrophy. Whilst mutations in the calpain III gene, leading to the loss of calpain III protein expression, have been found to be responsible for Limb Girdle Muscular Dystrophy type IIA (LGMDIIA), an autosomal recessive disorder characterised by progressive weakness and skeletal muscle atrophy (Jones, Hill et al. 2004), the stable over-expression of calpain III in mice had no effect on skeletal muscle morphology or function (Spencer, Guyon et al. 2002). Previous studies have however noted increased calpain III expression following the induction of skeletal muscle hypertrophy (Yang, Chen et al. 2007). As calpain III is intrinsically linked with sarcomeric remodelling (Kramerova, Kudryashova et al. 2005), it is one possibility that the increase in expression noted here was associated with the marked skeletal muscle hypertrophy noted in response to clenbuterol administration.

On balance, clenbuterol appeared to reduce skeletal muscle atrophy signalling and increase factors associated with skeletal muscle remodelling. That said, the effects of clenbuterol on protein synthetic signalling were less apparent than those on muscle atrophy signalling and limited to increased mTOR mRNA, with no overall effect on 4EBP1 activation.

The surgical induction of knee OA was associated with reduced weight gain, evidence of behavioural joint pain and the induction of MHC I protein in the quadriceps muscle. In this instance, the increase in MHC I protein was not associated with a concurrent increase in oxidative ICDH enzyme activity, which remained unaltered by

surgery. The induction of OA via MNX surgery was also associated with decreased PPARα and increased AdipoR2 expression. PPARα is reported to correlate positively with MHC type I fibres, and negatively with MHC type IIB fibres (Krämer, Ahlsén et al. 2006). In this instance however, PPARα expression appeared to correlate negatively with MHC I protein expression, the reason for which is unclear at this stage. Pre-treatment with clenbuterol prior to the initiation of OA countered the induction of MHC I protein, numerically maintained MHC IIB protein, and elevated glycolytic LDH enzyme activity ($P = 0.028$). However, clenbuterol pre-treatment was unable to modulate the severity of joint pathology or subsequent behavioural pain in this model.

The use of clenbuterol to induce skeletal muscle hypertrophy and promote lipolysis is well characterised across multiple species (Lynch and Ryall 2008). In this current study, following 2 weeks of clenbuterol treatment, a significant increase in the quadriceps muscle mass (+40%) was attained. However, at the study endpoint, the hypertrophic effect of clenbuterol was no longer apparent in the pre-treated animals, which presented with comparable quadriceps mass to bodyweight ratios. To determine the muscle fibre-type composition of the quadriceps, MHC protein expression was monitored. Of interest, it was found that although no changes to the MHC protein composition were noted in response to clenbuterol prior to surgery, subtle effects of clenbuterol on MHC protein expression and metabolic potential were observed in the period post surgery where clenbuterol suppressed the trend towards a meniscectomy surgery induced increase in MHC I and elevated LDH enzyme activity. Although only a trend association was noted between pre-treatment with clenbuterol and suppression of the increase in MHC I protein observed post surgery ($p = 0.081$), this is supported by several studies that report the slow to fast fibre inducing effects of clenbuterol in rodents (Lynch and Ryall 2008). The fact that these changes were not observed in the pre-treatment period may be due to the length of drug exposure and / or the muscle studied. The latter may be related to the natural distribution of MHC protein isoforms within the quadriceps muscle which is

comprised of over 85% fast MHC IIX / MHC IIB, and less than 15% slower MHC I / MHC IIA. Such a high baseline complement of fast MHC may reduce the impact of β-agonist administration with regards to its effect in inducing slow to fast fibre type transitions. Previous studies noting such changes were often conducted over a longer timeframe and tended to study the slow twitch soleus muscle, which is particularly susceptible to fibre type shifts. It is also possible however, that these changes were simply more evident in the predominantly slow soleus when compared with the predominantly fast quadriceps.

As previously noted, meniscectomy surgery was associated with a trend towards increased MHC I, indicative of a switch towards a slower more oxidative and fatigue resistant muscle type, more commonly associated with postural, anti-gravity muscles (Adams, Haddad et al. 1994). Such changes in muscle fibre type following meniscectomy may have important implications for rehabilitation, in particular the type of muscle strengthening program recommended. One possible reason for this change in MHC composition in response to meniscectomy surgery might be that it is a physiological attempt to increase the stability of the operated joint by increasing the complement of fatigue resistant, slow muscle fibres that surround it. A further possibility is that surgery-induced changes in weight bearing led to disuse atrophy of fast MHC IIB fibres, resulting in an increase in the relative proportion of slower MHC I fibres as noted previously (Gardiner, Favron et al. 1992). Noteworthy is that only mild changes to weight bearing were noted (approximately 4%) and it is unclear whether such modest perturbations are capable of inducing changes to the relative distribution of MHC.

A number of previous studies suggest that modulating muscle function through exercise may have an impact on the development and severity of OA in humans; therefore it must be considered why no effect was noted in this experimental model. The experimental approach chosen in the present study was to dose with clenbuterol for up to 2 weeks prior to surgical induction of OA, but to stop administration

immediately after surgery. This approach avoided any potential confounding factors of direct clenbuterol action at the joint or direct cardiovascular effects, and allowed the physiological impact of a hypertrophic quadriceps muscle on OA severity to be modelled. However, although clenbuterol resulted in marked increases in quadriceps mass during the pre-treatment period, this effect was not maintained throughout the time course of the study and may explain the lack of effect on OA severity reported. Another possibility might be the agent of choice used in this study to induce muscle hypertrophy. Although clenbuterol is effective in this regard, it also leads to an overall increase in animal bodyweight due to the induction of lean mass, a concurrent decline in fat mass and the relatively high mass of skeletal muscle compared to that of adipose tissue (Rothwell and Stock 1987). It is well known that weight is a risk factor for knee OA (Arden and Nevitt 2006). Moreover, bodyweight has been associated with the severity of OA in the Dunkin Hartley guinea pig where a 28% reduction in bodyweight led to a marked 40% decrease in OA severity (Bendele and Hulman 1991). By inference, it is therefore possible that this increased bodyweight in the clenbuterol treated animals compared to the control animals, at the time of induction, may have negated any potential beneficial effect of a strengthened quadriceps, and thus explains the lack of positive modulation noted during this study. A further possibility is that quadriceps muscle mass is not the sole determinant of the role of muscles in OA. Instead, it is likely that it is the coordinate modulation of several muscle parameters such as muscle fibre type composition and size of motor units recruited during exercise that together with mass, are key in eliciting an impact on OA pathology.

In addition it is also important to note that clenbuterol has greater hypertrophic effects on slow twitch muscles compared with faster twitch muscles (Stevens, Firinga et al. 2000; Herrera, Zimmerman et al. 2001). In the intact knee, agonist force is generated by the quadriceps muscle in tandem with antagonist force generation by the hamstrings producing joint stability (Hortobagyi, Westerkamp et al. 2005). If one considers the quadriceps / hamstrings balance (Q/H ratio) and that anabolic steroid

induced hypertrophy might elicit a greater strength increases in leg flexion over leg extension (Schroeder, Terk et al. 2003), it is possible that clenbuterol administration induced skeletal muscle hypertrophy disproportionately across the various muscles surrounding the knee joint, disrupting the fine balance of agonist and antagonist forces, leading to decreased joint stability. This could have a detrimental effect on the formation of joint pathology in a similar way to that observed in man with joint instability due to joint mal-alignments (Kalichman, Zhang et al. 2007). In this respect, β-agonist administration appears not to mimic strength training in which contractile movements impose work, and therefore hypertrophy, on both antagonistic muscles maintaining muscle synergy.

In summary, this study confirmed that the meniscectomy surgery protocol utilised resulted in the formation of consistent OA-like lesions in the rat which appeared morphologically similar to OA of the human knee. Moreover, the administration of clenbuterol was effective in the induction of marked skeletal muscle hypertrophy following administration for 14 days. Given the high baseline complement of fast-twitch muscle fibres in the quadriceps skeletal muscle, clenbuterol administration was not associated with changes to the fibre-type composition nor was it associated with changes indicative of an altered metabolic profile. Clenbuterol-induced skeletal muscle hypertrophy and a trend towards increased glycolytic potential, prior to the induction of OA, did not appear to modulate the severity of OA in this experimental model.

Although the MNX model of OA was beneficial in the assessment of OA and indispensible for the testing of muscle hypertrophy inducing agents, it was felt that the enhanced rate at which disease occurred may have precluded any beneficial effects of increased skeletal muscle mass. It was therefore proposed that animal models of OA that better mimic the human condition in terms of initiation and progression rates, may provide a more suitable platform on which to observe subtle

changes in disease progression brought about through modulating skeletal muscle function.

CHAPTER 4 – ELUCIDATING MYOSIN HEAVY CHAIN (MHC) SPECIFIC CDNA SEQUENCES IN THE DUNKIN HARTLEY GUINEA PIG

4.1 – Introduction and Rationale

In attempting to examine skeletal muscle in an animal model of knee-OA that better emulates the human condition, the spontaneous Dunkin Hartley guinea pig model was considered. However, quantifying skeletal muscle changes by the assessment of MHC in the guinea pig has proved problematic to date.

Several chronic conditions leading to skeletal muscle dysfunction are known to be associated with changes in muscle fibre-type (reviewed in **CHAPTER 1.3.7**) as determined by the expression of myosin heavy chain (MHC) isoforms at both the mRNA and protein level. Furthermore, many of these conditions are modelled, pre-clinically, in the guinea pig due to similar disease onset and progression to the human condition, and their generally well-characterised anatomy.

As described in **CHAPTER 1.3.2**, MHC composition is amenable to determination by protein and mRNA based methodologies, the latter quantifying the expression of MHC isoform-specific gene transcripts allowing the detection of earlier, and more subtle changes. As such, the MHC mRNAs, and associated specific oligonucleotide primers for PCR of all common laboratory species, such as the rat and mouse, have been available for some time. To date, it has not been possible to resolve guinea pig MHC isoforms using SDS PAGE. Moreover, due to incomplete genomic annotation, the assessment of guinea pig MHC mRNA expression has not been possible either, thus precluding full characterisation of the early changes in skeletal muscle in response to disease and disease modulation.

Therefore, the purpose of this study was to characterise the multigenic structure of the sarcomeric MHC family in the guinea pig, and to design and validate specific oligonucleotide primers to enable the assessment of MHC mRNA expression in relevant disease models. The molecular tools developed here were subsequently

utilised to assess changes in the quadriceps skeletal muscle in response to developing knee osteoarthritis in the laboratory guinea pig (**CHAPTER 5**).

4.1.1 – Hypotheses and aims

The structure of the sarcomeric MHC family in the laboratory guinea pig will be clustered in a head-to-tail fashion, consistent with that of other species which have been previously described (**CHAPTER 1.3.2**). Furthermore, enough sequence variability will exist between the various isoforms of MHC, at the mRNA level, as to allow the design and validation of isoform-specific oligonucleotide primers for expression studies by quantitative PCR.

The following specific aims will be addressed;

- Elucidate genes encoding for the various isoforms of MHC in the guinea pig
- Accurately determine the gene boundaries of each MHC isoform
- Derive novel partial coding sequence for each of the sarcomeric MHC isoforms
- Design and validate specific oligonucleotide primers for mRNA expression by quantitative PCR
- Perform promoter analysis in comparison to other well-characterised species

4.2 – Experimental Protocol

4.2.1 – Experimental approach

The experimental approach taken was to locate regions of cDNA sequence conserved between the "fast" isoforms of MHC in the rat and mouse by alignment. Primers were designed in the conserved regions, and used to amplify a region of novel sequence coding for MHC from guinea pig quadriceps cDNA. The resulting PCR products were cloned and sequenced bi-directionally. The novel guinea pig-derived sequence was subsequently used to query the partially annotated guinea pig genomic DNA database to locate the region of sequenced genome likely to encode the MHC gene family. Using the well-studied structure of the MHC family in numerous species as a reference, it was possible to advance along the guinea pig genomic sequence, and locate genes encoding each of the remaining MHC isoforms of interest.

Using 5 and 3' RACE methodology, the boundaries relating to the expressed regions of each of the MHC-associated genes were described, and specific oligonucleotide primers designed within areas of divergence. This approach was utilised to design isoform-specific primers for quantitative PCR, capable of determining the transcript abundance of each skeletal muscle-associated MHC with reference to muscle fibre-type.

4.2.2 – Biospecimens

Extensor digitorum longus, soleus and quadriceps femoris were dissected from 3 month old Dunkin Hartley strain guinea pigs (Harlan, UK) and immediately snap frozen in liquid nitrogen. Total RNA was extracted from 100mg of sample using TRIzol regent (Invitrogen). Contaminating genomic DNA was removed via DNase digestion (Promega), and the resulting RNA resuspended in DNase / RNase-free water. All RNA was stored at -80^{o}C prior to use. For standard PCR applications, complimentary DNA was generated by reverse transcription of 500ng total RNA using MMLV (Promega)

using a standard protocol and stored at -20^{o}C prior to analysis (**METHODS 2.1.1 – 2.1.5**) .

4.2.3 – cDNA sequence alignment and bioinformatics

All cDNA sequences were obtained from Ensemble Release 56 (Ensemble), and aligned using the ClustalW2 application (Larkin, Blackshields et al. 2007) configured for DNA analysis where indicated. Novel sequence data was compared to the partially annotated *Cavia porcellus* database using the BLAT utility (Kent 2002) available from Ensemble Release 56 (Ensemble).

4.2.4 – Rapid amplification of cDNA ends (RACE)

5' Rapid amplification of cDNA ends (5' RACE) was carried out using the GeneRacer™ system (Invitrogen). DNase digested total RNA (3000ng) was incubated with 10U calf intestinal phosphatase (CIP), 1µl CIP buffer (0.5M Tris-HCl pH 8.5, 1mM EDTA) and 40U RNaseOut (Invitrogen) at 50^{o}C for 60 minutes. 5' dephosphorylation specifically targets partial length, un-capped transcripts thus preventing their inclusion in this assay. RNA was precipitated by the addition of 90µl RNase/DNase-free water and 100µl phenol: chloroform (1:1) and vortexed vigorously for 30 seconds. Following centrifugation (Accuspin Micro, Fisher) at 16,000g for 5 minutes at room temperature, 100µl of the resulting aqueous phase was removed to a separate tube. To the resulting aqueous phase, 20µg mussel glycogen, 10µl 3M sodium acetate (pH 5.2) and 220µl 95% (v/v) ethanol were added and vortexed briefly. The precipitated RNA was centrifuged at 16,000g for 20 minutes (+4^{o}C), washed with 70% (v/v) ethanol and resuspended in 7µl RNase/DNase-free water. Following dephosphorylation, RNA was treated with tobacco acid pyrophosphatase (TAP) to remove the 5' cap structure and expose the terminal 5' phosphate in a reaction containing 0.5U TAP, 1µl buffer (0.5 M sodium acetate, pH 6.0, 10 mM EDTA, 1% v/v β-mercaptoethanol, 0.1% v/v Triton® X-100), 40U RNaseOut, and incubated at 37^{o}C for 60 minutes. The resulting dephosphorylated, de-capped RNA was precipitated as above. Finally, an RNA oligonucleotide was ligated to the exposed 5' phosphate using

T4 ligase in a reaction containing 5U T4 ligase, 1µl 10mM ATP, 40U RNaseOut in a buffer comprising (330 mM Tris-Acetate, pH 7.8, 660 mM potassium acetate, 100 mM magnesium acetate 5 mM DTT) at 37^{o}C for 60 minutes. Complimentary DNA was reverse transcribed from modified RNA using the GeneRacer modified Oligo dT primer (2pmole) and Superscript III (Invitrogen) according to the manufacturer's protocol. The resulting cDNA is subsequently referred to as "RACE ready cDNA".

4.3 – Results

4.3.1 – Identification of conserved regions

In order to generate a region of guinea pig cDNA encoding part the MHC multigenic family, all available MHC mRNAs were obtained from the mouse (*Mus musculus*) and rat (*Rattus norvegicus*) cDNA libraries, Ensemble release 56. Search terms comprised the official gene name as listed in **TABLE 4.1**. For the identification of conserved regions in which oligonucleotide primers for quantitative PCR could be designed, MyH1, MyH2 and MyH4 (MHC IIA, IIX and IIB respectively) cDNA sequences were aligned using ClustalW2 (EBI). Sequences were truncated at the 5' termini to exclude any sequence from the 5' untranslated region and include only sequence from the initiating "ATG" onwards. Sequence alignment revealed a conserved region, across both MHC isoform and species, between exons 5 and 10 (**FIGURE 4.1**) large enough to accommodate a pair of oligonucleotide primers. These primers were named GP_626bp after their theoretical amplicon size.

TABLE 4.1 – Gene names, cDNA sequence attributes and accession numbers

Species	Gene Name	MHC Isoform	Accession Number	Comments
Mus musculus	MyH1	IIX	NM_030679.1	Full Length cds
	MyH2	IIA	NM_001039545.2	Full Length cds
	MyH3	Embryonic	NM_001099635.1	Full Length cds
	MyH4	IIB	NM_010855.2	Full Length cds
	MyH8	Neonatal	NM_177369.3	Full Length cds
	MyH13	Extra-ocular	NM_001081250.1	Full Length cds
Rattus norvegicus	MyH1	IIX	NM_001135158.1	Full Length cds
	MyH2	IIA	NM_001135157.1	Full Length cds
	MyH3	Embryonic	NM_012604.1	Full Length cds
	MyH4	IIB	NM_019325.1	Full Length cds
	MyH8	Neonatal	XM_001080186.1	Full Length cds
	MyH13	Extra-ocular	XM_001078857.1	Full Length cds

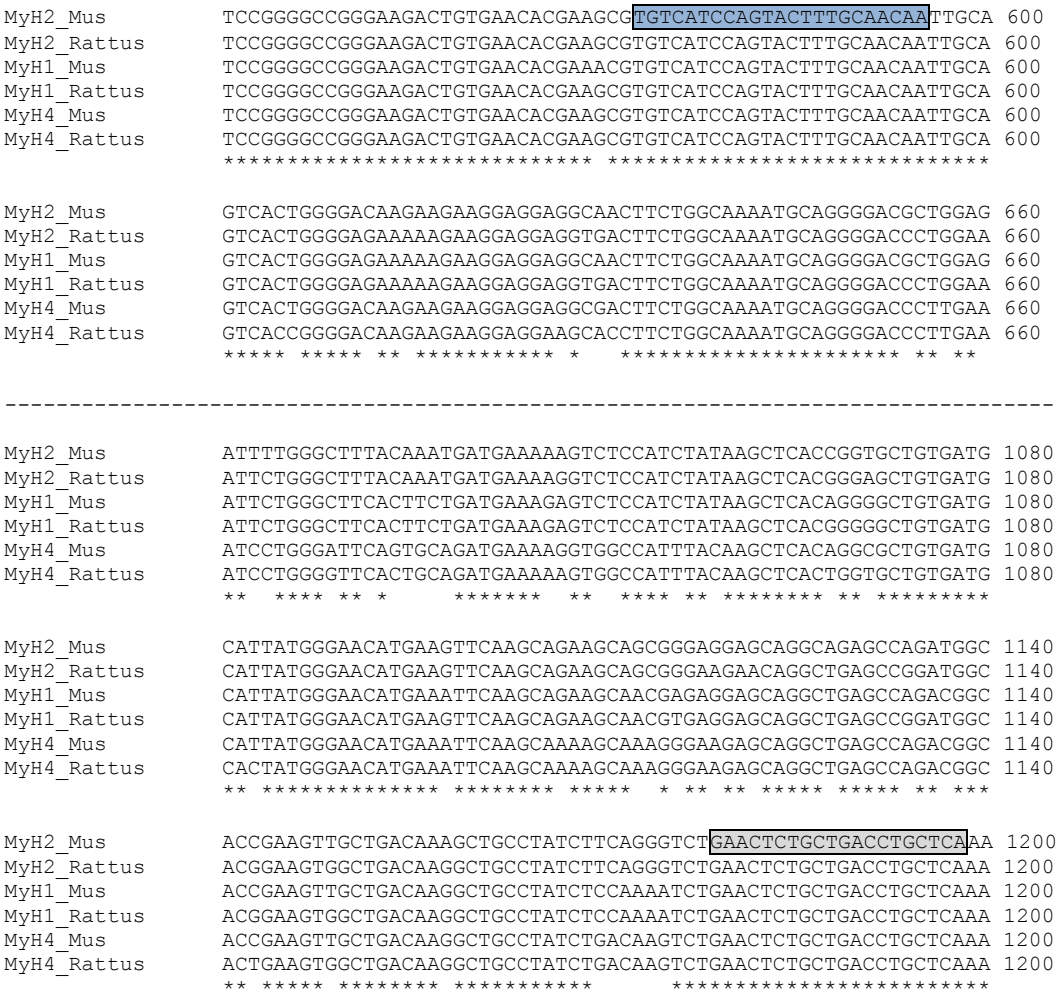

FIGURE 4.1 – cDNA sequence alignment of MHC (fast) mRNAs of mouse (Mus) and rat (Rattus) origin as indicated. Asterisks indicate nucleotides which are conserved across all 6 sequences. Primer pair GP_646bp are indicated in blue (forward) and grey (reverse) boxes.

4.3.2 – Generating a fragment of guinea pig sequence

In order to generate a region of guinea pig cDNA sequence encoding part the MHC multigenic family with which to query the gDNA database and locate the region in which it was encoded, quadriceps cDNA was subjected to endpoint PCR using primer pair GP_626bp (**METHOD 2.1.7**). PCR revealed the presence of an abundant transcript of the expected size (**FIGURE 4.2**).

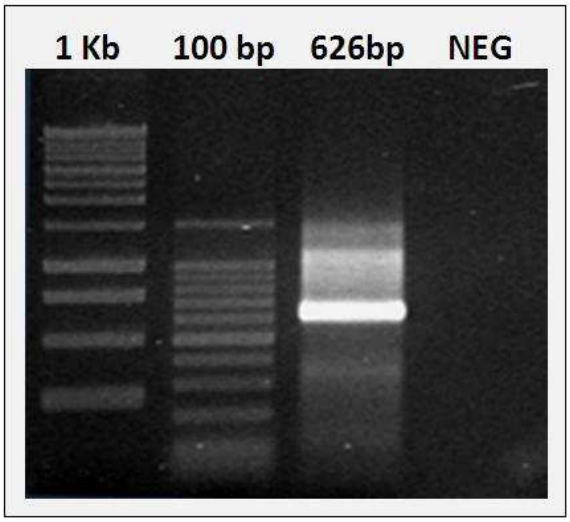

FIGURE 4.2 – Fragment of Guinea Pig sequence pertaining to MHC. 1Kb: 1Kb DNA ladder, 100bp: 100bp DNA ladder, 626bp: guinea pig quadriceps cDNA following PCR with GP_626bp primers; annealing temperature = 55^{o}C, NEG: no template control

In order to determine which MyH transcript the PCR amplicon was derived from, the resulting amplicon was cloned into the pGEM T-Easy vector system according to the manufacturer's instructions (Promega) (**METHOD 2.2.2**). Following transformation into JM109 competent cells (Promega), 5 clones were selected at random for DNA sequencing using M13 primers targeting the vector sequence to obtain full-length sequencing of the inserts. All 5 clones were identical; therefore the novel sequence was used to query the partially annotated *Cavia porcellus* gDNA database using BLAT

(Ensemble release 56) to include sequences from *Rattus norvegicus*, *Mus musculus and Cavia porcellus* with the intention of confirming the identity of the clone, and locating the genomic region in which it was encoded. BLAT analysis revealed the cloned sequence to be located towards the 5' termini of gene MyH2 in both *Rattus norvegicus* and *Mus musculus*. BLAT also revealed a sequence match in the un-annotated guinea pig gDNA database - this was assumed to correspond to MyH2 also.

4.3.3 – Determining the genomic location of other members of the MHC gene family

In all other species described, the MHC family of genes is located across two separate chromosomes. One chromosome encodes (in order) MyH3/MyH2, MyH1/MyH 4 and MyH8/MyH13 arranged in a head-to-tail fashion. The other chromosome encodes the cardiac (MyH7α) and slow skeletal muscle isoforms (MyH7β) (Weiss and Leinwand 1996). Using this knowledge, and the previously determined location of the guinea pig MyH2 gene as a starting point, it was possible to advance along the genomic sequence data (Ensemble release 56) in both the 5-3' and 3-5' direction, aligning individual exons from both *Rattus norvegicus* and *Mus musculus* MyH1, MyH2, MyH3, MyH4, MyH8 and MyH13 cDNAs (**TABLE 4.1**) to the guinea pig gDNA database, thus spatially mapping out the arrangement of genes in the guinea pig (**FIGURE 4.3**). During the course of this study, a full length cDNA pertaining to *Cavia porcellus* MyH7, known to encode the slow skeletal muscle isoform MHC I, was annotated in Ensemble release 56. MyH7 was therefore not analysed in any further detail, and the focus maintained on characterising the fast-twitch associated MHC genes (MyH1, MyH2 and MyH4).

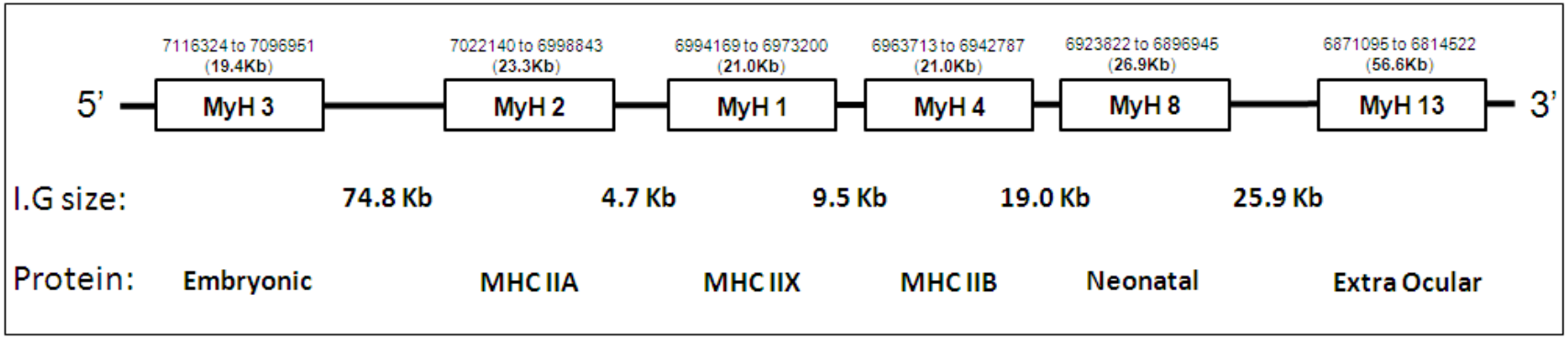

FIGURE 4.3 – Spatial arrangement of the multigenic myosin heavy chain (MHC) family in the laboratory guinea pig (*Cavia porcellus*) as determined through the retrieval of MHC isoform specific genes (MyH) from various species using multiple BLAT and subsequent alignment (ClustalW2). I.G – Intergenic region size (Kb); Protein – protein product of each gene.

4.3.4 – Determination of the gene boundaries of MyH1, 2 and 4 by 5’ and 3’ RACE

To accurately determine the transcriptome boundaries of each of the adult skeletal muscle associated MHC isoforms, the untranslated regions of each mRNA were extended using 5’ and 3’ RACE. The multiple exonic alignments (as previously described) from MyH1, MyH2 and MyH4 were obtained from the guinea pig genomic sequence, and the newly annotated putative cDNA sequence data (manually spliced from the genomic sequence) aligned using ClustalW2 (**FIGURE 4.4**).

Sequence homology across the coding sequence of the three guinea pig isoforms of MHC showed a particularly high level of conservation. As such, it was not possible to design isoform-specific RACE primers (to extend the untranslated regions), nor standard oligonucleotide PCR primers with which to conduct expression studies. The issue of extending the untranslated regions, and therefore demarcating the gene boundaries was overcome by designing 5’ and 3’ RACE primers to amplify all three isoforms of MHC as indicated in **FIGURE 4.4**. RNA derived from three different muscles was used in the 5’ and 3’ RACE protocol to enrich for the various MHC gene transcripts since extensor digitorum longus is known to predominantly express MyH1 and MyH4; soleus MyH2 and MyH7 whilst quadriceps is thought to express all four isoforms. With regards the design of PCR primers for analysis of expression, it was hypothesised that the sequence data from the un-translated region (derived through RACE) would likely be less well-conserved and therefore permit the design of gene-specific primers.

```
MyH1_Cavia      GTGACAGCCAAGACAGAAGGCGGAGCTACTGTAACAGTGAAGGATGACCAGGTGTTCCCC 237
MyH2_Cavia      GTAACTGTGAAAACCGAAGCGGGAGCGACCTTGACAGTGAAGGATGACCAGGTGTTCCCC 240
MyH4_Cavia      GTGACAGCCAAGACAGAAGGCGGAGCTACTGTCACAGTTAAGGAAGACCAAGTCTTTTCC 237
                ** ** *  ** ** ****  ***** **  * ***** ***** ***** ** **  **

MyH1_Cavia      ATGAACCCTCCCAAATACGACAAGATCGAGGACATGGCCATGATGACCCACCTGCACGAG 297
MyH2_Cavia      ATGAACCCTCCCAAATTTGACAAGATCGAGGACATGGCCATGATGACCCACCTGCACGAG 300
MyH4_Cavia      ATGAACCCTCCCAAATATGACAAGATCGAGGACATGGCCATGATGACCCACCTGCACGAG 297
                ****************  ****************************************

MyH1_Cavia      CCTGCGGTGCTGTACAACCTCAAAGAGCGTTACGCAGCCTGGATGATCTACACCTACTCG 357
MyH2_Cavia      CCTGCGGTGCTGTACAACCTCAAAGAGCGTTACGCAGCCTGGATGATCTACACCTACTCG 360
MyH4_Cavia      CCTGCCGTGCTGTACAACCTCAAAGAGCGTTACGCAGCCTGGATGATCTACACCTACTCG 357
                ***** ******************************************************

-------------------------------------------------------------------------------------------

MyH1_Cavia      AGAAGGCCAAGAAGGCCATCACTGATGCCGCCATGATGGCCGAGGAGCTGAAGAAGGAGC 5325
MyH2_Cavia      AGAAGGCCAAGAAGGCCATCACCGATGCCGCCATGATGGCCGAGGAGCTGAAGAAGGAGC 5335
MyH4_Cavia      AGAAGGCCAAGAAGGCCATCACTGATGCCGCCATGATGGCCGAGGAGCTGAAGAAGGAGC 5331
                ********************* ************************************

MyH1_Cavia      AGTGACAGCAGCGCCCACCTGGGAGCGCATGAAGAAGAACCTGGAGCAGACGGTCAAGGA 5385
MyH2_Cavia      AG-GACACCAGCGCCCACCTGG-AGCGCATGAAGAAGAACATGGAGCAGACGGTCAAGGA 5393
MyH4_Cavia      AG-GACACCAGCGCCCACCTGG-AGCGCATGAAGAAGAACCTGGAGCAGACGGTCAAGGA 5389
                ** **** ************** ***************** ******************

MyH1_Cavia      CCTGCAGCACCGGCCTGGACGAGGCCGAGCAGCTGGCGCTGAAGGGCGGCAAGAAGCAGA 5445
MyH2_Cavia      CCTGCAGCTCCG-TTTGGACGAGGCCGAGCAGCTGGCGCTGAAGGGCGGCAAGAAGCAGA 5452
MyH4_Cavia      CCTGCAGCACCG-GCTGGACGAGGCCGAGCAGCTGGCGCTGAAGGGCGGCAAGAAGCAGA 5448
                ******** ***   ******************************************

MyH1_Cavia      TCCAGAAGCTGGAGGCCAGG----GTACGTGAACTTGAAGGGGAAGTGGAAAGCGAACAG 5501
MyH2_Cavia      TCCAGAAGCTGGAGGCCAGG----GTGCGTGAGCTGGAAGGCGAGGTAGAGAGTGAGCAA 5508
MyH4_Cavia      TCCAGAAGCTGGAGGCCAGGCCAGGTGAGGGAACTTGAAAACGAAGTTGAAAATGAGCAG 5508
                ********************    **  * ** ** ***   ** ** ** *  ** **
```

FIGURE 4.4 – Guinea pig cDNA coding sequence alignment of theoretical guinea pig MHC isoforms MyH1, 2, and 4 derived from the guinea gDNA sequence as located by multiple sequence alignment (**FIGURE 4.3**). Asterisks indicate nucleotides which are conserved across all sequences. Oligonucleotide primers indicated are RevGSP (blue box), RevNestedGSP (blue underline), ForGSP (grey box), and ForNestedGSP (grey underline).

4.3.4.1 – Rapid amplification of cDNA ends (RACE)

For 5’ and 3’ RACE reactions, total RNA from soleus, extensor digitorum longus and quadriceps specimens was modified by adding a region of known sequence at the 5’ terminus in accordance with (**CHAPTER 4.2.4**). First-strand complimentary DNA was generated using a modified Oligo dT primer, thus adding a region of known sequence at the 3’ terminus (**FIGURE 4.5A**). 5’ RACE reactions were performed initially using primers GeneRacer 5’ and RevGSP to generate approximately 300bp of coding sequence plus the novel 5’ UTR, whilst 3’ RACE reactions were performed using primers GeneRacer 3’ and ForGSP to generate 400bp of coding sequence plus the novel 3’ UTR (**FIGURE 4.5B**).

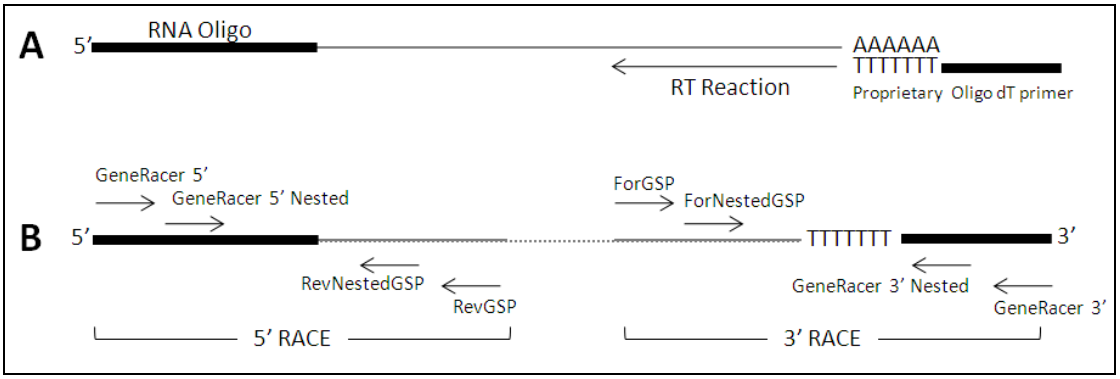

FIGURE 4.5 – Schematic representation of 5’ and 3’ RNA modifications (A), and priming locations for guinea pig 5’ and 3’ RACE protocols (B).

For maximum amplicon specificity, high fidelity *Taq* polymerase was utilised (Invitrogen) and a touchdown PCR approach taken. The cycling parameters were 94^{o}C for 2m; (94^{o}C for 30s, 72^{o}C for 2m) x5; (94^{o}C for 30s, 70^{o}C for 2m) x5; (94^{o}C for 30s, 65^{o}C for 30s, 68^{o}C for 2m) x 25 followed by a final elongation phase at 68^{o}C for 10m. Both 5' and 3' RACE protocols resulted in the formation of numerous RACE amplicons, of varying size (**FIGURE 4.6**).

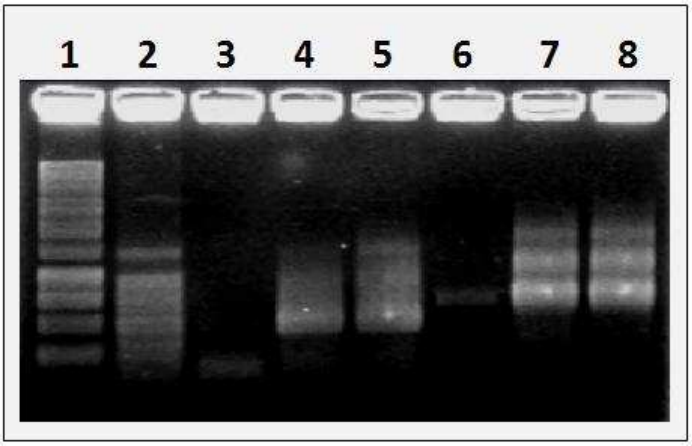

FIGURE 4.6 – Initial 5' and 3' RACE protocol using primers GeneRacer 5' and RevGSP for 5' RACE and GeneRacer 3' and ForGSP for 3' RACE on guinea pig derived cDNA. Lane 1: 1 Kb ladder, Lane 2: 100 bp ladder, Lanes 3 – 5: 5' RACE on soleus, EDL and quadriceps cDNA respectively, Lanes 6 – 6: 3' RACE on soleus, EDL and quadriceps cDNA respectively.

To increase the abundance of the intended RACE transcripts, the resulting PCR products from the first round of the RACE protocol (**FIGURE 4.6**) were column purified (Sigma GenElute) (**METHOD 2.2.1**) and used as template in a series of nested reactions using primers GeneRacer 5' Nested and RevNestedGSP for 5' RACE and primers GeneRacer 3' Nested and ForNestedGSP for 3' RACE (**FIGURE 4.5B**). Although the reactions still resulted in the amplification of multiple products, the nested

protocol enhanced the abundance of the intended transcript over and above that of the competing non-specific products (**FIGURE 4.7**).

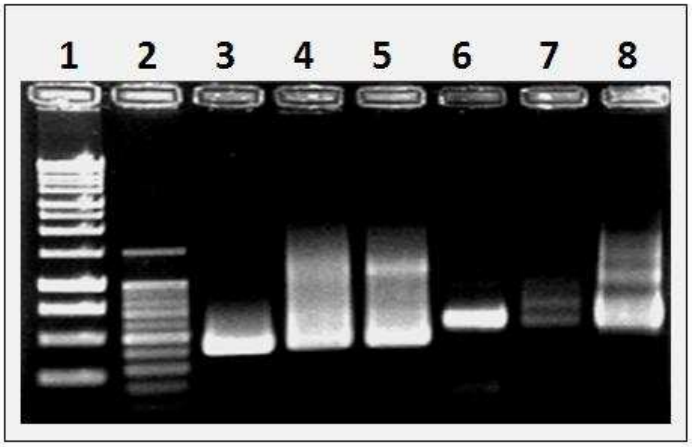

FIGURE 4.7 – Nested 5' and 3' RACE protocol utilising primers GeneRacer 5' Nested and RevNestedGSP for 5' RACE and GeneRacer 3' Nested and ForNestedGSP for 3' RACE and the amplicons from the first round of RACE as template. Lane 1: 1 Kb ladder, Lane 2: 100 bp ladder, Lanes 3 – 5: 5' RACE on soleus, EDL and quadriceps cDNA respectively, Lanes 6 – 6: 3' RACE on soleus, EDL and quadriceps cDNA respectively.

4.3.4.2 – Cloning and EcoR1 digest of 5' and 3' RACE products

The resulting nested RACE products from the second round of RACE (**FIGURE 4.7**) were cloned into the TOPO TA vector system (Invitrogen) (**METHOD 2.2.3)**. Following standard overnight culture on LB plates containing 100µg/ml ampicilin for the selection of insert containing resistant colonies, 10 colonies from each reaction were added to LB media containing 100µg/ml ampicilin and cultured for a further 18 hours (**METHOD 2.2.3**). To assess whether the plasmids from overnight culture contained RACE products, all 10 cultures from each RACE reaction were mini-prepped (**METHOD 2.2.4**), and subjected to the restriction endonuclease EcoR1 (**METHOD**

2.2.5), known to cut at two sites flanking the multiple cloning site (**FIGURE 4.8**) and thereby liberate any insert.

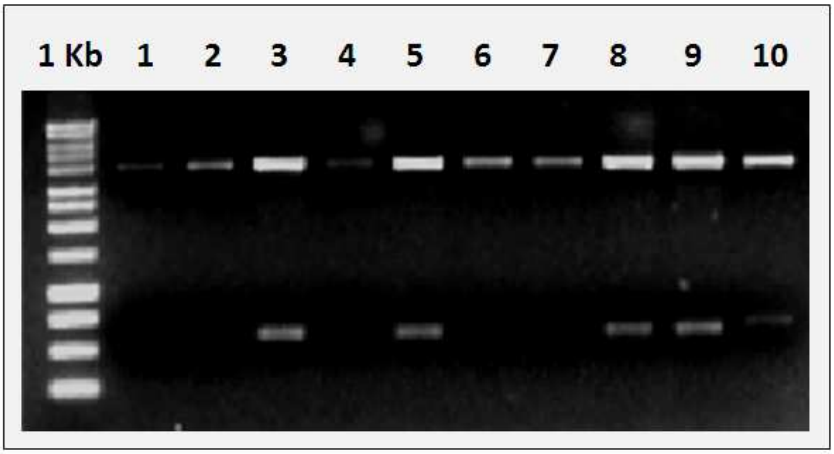

FIGURE 4.8 – Representative *EcoR1* digested MyH 5' and 3' RACE products from guinea pig quadriceps cDNA. Lane 1: 1 Kb ladder, Lanes 2 – 10: EcoR1 digested 3' RACE products. Positive insert containing colonies are present in lanes 3, 5, 8, 9 and 10 (faint).

4.3.4.3 – Sequencing of positive RACE colonies

5 positive colonies from each RACE reaction and muscle (30 clones in total) were selected for one-way sequencing using M13 primers to target a sequence within the vector. Following sequencing, the length of coding sequence amplified with each novel UTR was used to determine which MyH isoform the clone related to by using BLAT to compare each RACE product against the partially annotated guinea pig gDNA database.

For each MyH transcript, 5' RACE sequences encoded approximately 300bp of coding sequence accompanying the 5' UTR, whilst 3' RACE sequences encoded approximately 400bp of coding sequence followed by the 3' UTR. For all three MyH

derived RACE products assessed, the resulting novel 5' UTRs encoded three distinct exons, the first two of which fell within a 100-200bp region, the third was located more distantly and encoded the signal to instigate translation (ATG in this instance). The novel 3' UTRs encoded a single exon starting immediately downstream of the stop codon (**TAA** in MyH1 and MyH4, and **TGA** in MyH2) **FIGURE 4.9**.

All novel 3' and 5' sequences were deposited in GenBank and are included in **FIGURES 4.10A-B** along with their accompanying accession numbers.

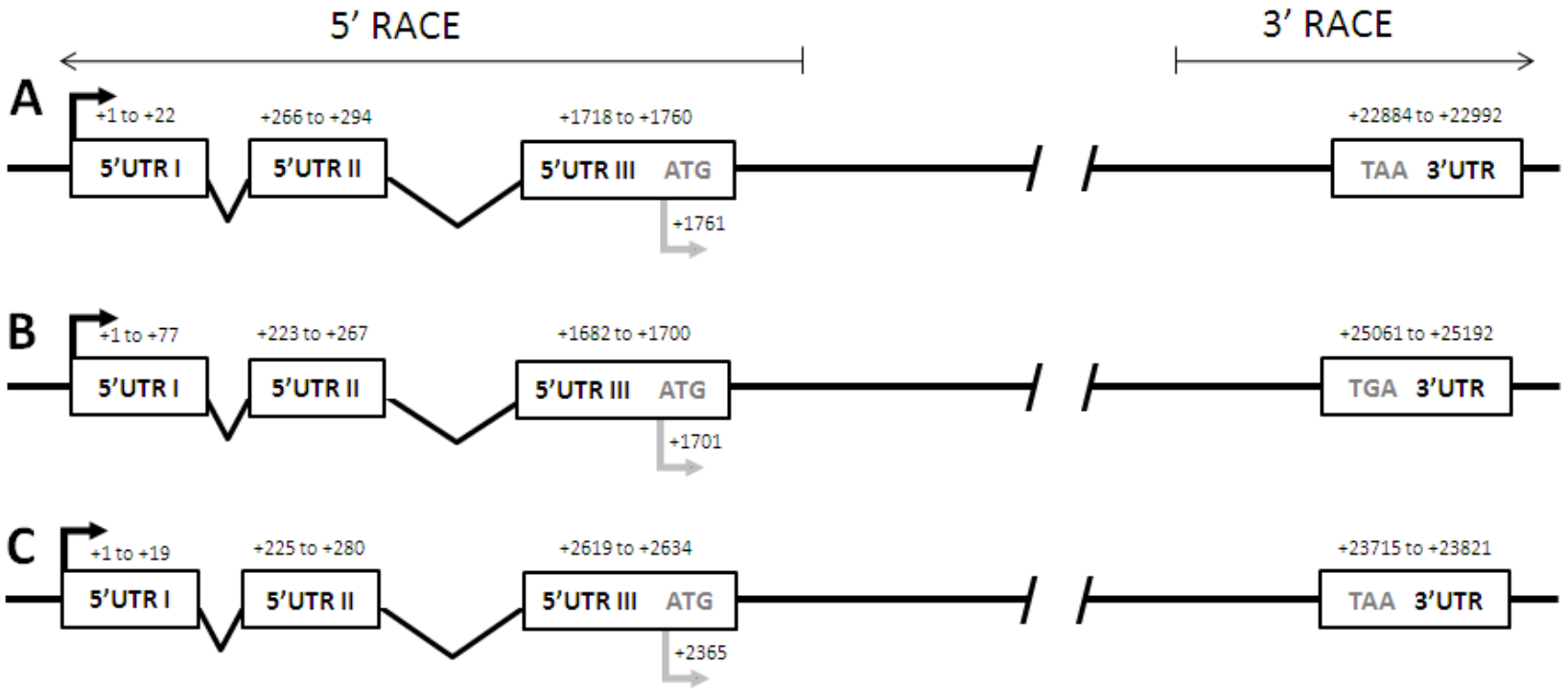

FIGURE 4.9 – Illustration of the relative 5' and 3' genomic structure of guinea pig MyH 1 (A), 2 (B) and 4 (C) derived from 5' and 3' RACE products indicating the transcription start site and exon positions. Open boxes – individual exons; Thick black arrow – transcription start site; Thick grey arrow – translation start site; Numbers indicate the position relative to the transcription start site in the respective gene.

MyH1 5’UTR and CDS (**GenBank: GU288593**)
TCTTTCCTCATAAAGCTTCAAGTTCTGACCCACTTCAAGGTTTCATCCCTACAGGCAAGGTCCTTAGCC
GGGCTGCCATCAATAACCTGCAGCCATGAGTTCCGACTCTGAGATGGCCATTTTTGGGGAGGCTGCT
CCTTACCTCCGAAAGTCTGAAAAGGAGCGAATCGAAGCTCAGAACAAGCCTTTTGATGCCAAGTCCT
CTGTCTTTGTGGTGGACGCCAAAGAGTCCTTTGTGAAGGCGACCGTACAGAGCAGGGAAGGGGGGA
AGGTGACAGCCAAGACAGAAGGCGGAGCTACTGTAACAGTGAAGGATGACCAGGTGTTCCCCATGA
ACCCTCCCAAATACGACAAGATCGAGGACATGGCCATGATGACCCACCTGCACGAG

MyH2 5’UTR and CDS (**GenBank: GU288594**)
ACGGGCCTTTGAAGAGCGACACTGGCCGCGGCCACGCTGCCTCGGCGGCTGCTGCTGCTGCTGCTGC
TGCTGGTTCTGAACCGTCTGACGTCCAGGCTACATCTTCTTGCTTGCTAACAAGGACCTCTGAGTACA
ACAGCCATGAGTGGCGCCGACTCAGAAATGGCTGTCTTTGGGGAGGCTGCCCCTTACCTCCGAAAGT
CTGAGAAAGAGCGCATTGAAGCCCAGAATAGGCCCTTTGATGCCAAGACATCTGTCTTTGTGGCGGA
GCCCAAGGAGTCCTTTGTCAAAGGGACGATTCAGAGCAGAGAAGCAGGAAAAGTAACTGTGAAAAC
CGAAGCGGGAGCGACCTTGACAGTGAAGGATGACCAGGTGTTCCCCATGAACCCTCCCAAATTTGAC
AAGATCGAGGACATGGCCATGATGACCCACCTGCACGAG

MyH4 5’UTR and CDS (**GenBank: GU288595**)
GTCCTTCCTCAAAATTCTTACAGTAATTGCCTGCTTTGAGCCTGCCACCTGCTTCATCTGGTCACATAA
GAGGTACACCTAACCTGCAGCCATGAGTTCCGACTCTGAGATGGCCGTTTTTGGGGAGGCTGCTCCT
TACCTCCGAAAGTCTGAAAAGGAGCGAATCGAAGCTCAGAACAAGCCTTTTGATGCCAAGTCCTCTG
TCTTTGTGGTGGACGCCAAAGAGTCCTACGTGAAGGCGACCGTACAGAGCAGGGAAGGGGGGAAG
GTGACAGCCAAGACAGAAGGCGGAGCTACTGTCACAGTTAAGGAAGACCAAGTCTTTTCCATGAACC
CTCCCAAATATGACAAGATCGAGGACATGGCCATGATGACCCACCTGCACGAG

FIGURE 4.10A – Novel 5’ sequences relating to MyH 1, 2 and 4 as determined by the accompanying 300bp of coding sequence. Diagram includes Novel UTR (underline), Coding sequence (CDS – standard text), translation start site (grey shading) and RevNestedGSP primer location (open box).

MyH1 CDS and 3’ UTR (**GenBank: GU288596**)

AAGGGCGGCAAGAAGCAGATCCAGAAGCTGGAGGCCAGGGTACGTGAACTTGAAGGGGAAGTGG
AAAGCGAACAGAAGCGCAATGTTGAAGCCGTCAAGGGCCTGCGGAAACACGAGAGAAGAGTGAAA
GAACTCACCTACCAAACCGAGGAGGACCGCAAGAATGTTCTCCGGCTCCAGGACCTTGTGGACAAAC
TGCAAGCCAAGGTGAAGGCGTACAAGAGACAAGCAGAGGAAGCGGAGGAACAATCCAATGTCAAC
CTCTCCAAGTTCCGCAAGATCCAGCACGAGCTGGAGGAAGCTGAGGAACGGGCTGACATCGCTGAG
TCCCAGGTCAACAAACTCCGGGTGAAGAGCCGGGAGGTTCACACGAAAATCATCAGCGAAGAGTAA
TTCATCCAAATGCAGGAAAGTGACCAAAGACATACACAAAATGTGAAAATCTTTGTCACTGTTTTGTA
TTTATGACTTTTGGAGATAAAGAATTTATCTACCAAGAAAAAAAAAAAAAAAAAAAAAAA

MyH2 CDS and 3’ UTR (**GenBank: GU288597**)

AAGGGCGGCAAGAAGCAGATCCAGAAGCTGGAGGCCAGGGTGCGTGAGCTGGAAGGCGAGGTAG
AGAGTGAGCAAAAGCGTAACGCGGAGGCCGTCAAAGGTCTGCGCAAACACGAGAGGCGAGTGAAG
GAACTCACCTACCAGACGGAAGAAGGTCGGAAAAATATCCTCAGGCTCCAGGATCTGGTCGATAAAC
TTCAGGCAAAAGTAAAATCTTACAAGAGGCAAGCGGAGGAGGCTGAGGAACAATCCAACACGAATC
TATCCAAGTTCCGCAAGCTCCAGCACGAGCTGGAGGAAGCCGAGGAACGGGCTGACATCGCTGAGT
CCCAGGTCAACAAACTCCGGGTGAAGAGCCGTGAGGTTCACACAAAAATCATCAGCGAAGAGTGATT
CAAGCCCTGAGGCTGTGGAATGACCAGAGCAAGACACACAATGTGAAGTCTCTGGTCATTTCTCTTT
GTGTTTTGTCTGTCCTACCCTATTGCAAAGGAAATAAAGAGCAGAGGGTTCTTTGCAAATAAAAAAAA
AAAAAAAAAAAAAAAAAA

MyH4 CDS and 3’ UTR (**GenBank: GU288598**)

AAGGGCGGCAAGAAGCAGATCCAGAAGCTGGAGGCCAGGGTGAGGGAACTTGAAAACGAAGTTG
AAAATGAGCAGAAGCGCAATGTGGAGGCCGTCAAAGGTCTTCGTAAGCATGAGAGAAGAGTGAAG
GAACTCACTTACCAGACTGAGGAGGACCGCAAGAATGTTCTCAGGCTGCAGGACTTGGTGGACAAAT
TACAGAGCAAAGTGAAAGCTTACAAGAGACAGGCTGAAGAGGCCGAGGAACAATCCAATGTCAACC
TTGCCAAGTTCCGCAAGATCCAGCACGAGCTGGAGGAAGCCGAGGAGCGGGCCGACATCGCTGAGT
CCCAGGTCAACAAACTCCGGGTGAAGAGCCGGGAGGTTCACACGAAAGTCGTCAGCGAGGAGTAAC
TCCATCTACTGCTGCAACGTGACCAAAGAAATGCACAAAATGTGACGTTCTTTGTCACTGTCCTGTAT
ATCAAGGAAATAAAATCTGCAGAGTTTTGCAATCAAAAAAAAAAAAAAAAAAAAAA

FIGURE 4.10B – Novel 3’ UTR sequences relating to MyH 1, 2 and 4 as determined by the accompanying 400bp of coding sequence. Diagram includes Novel UTR (underline), Coding sequence (CDS – standard text), stop codon (grey shading) and ForNestedGSP primer location (open box).

4.3.5 – Designing MHC transcript isoform specific oligonucleotide primers for quantitative PCR

In order to assess whether the novel untranslated region sequence was any less conserved across the three isoforms than the respective coding sequence, and therefore the potential to design isoform specific primers, 5' and 3' UTRs were aligned using ClustalW2 (**FIGURES 4.11A-B**). As hypothesised, there was a distinct reduction in sequence identity in both 5 and 3' UTRs, most likely due to reduced selective pressure. Although both the 5 and 3' UTRs of each MHC isoform mRNA were sufficiently distinct as to permit the design of isoform specific primers, the 3' UTR was selected based on the larger number of bases available.

All MHC isoform specific primers were designed from the novel 3' UTR sequence data using Primer3 software (Koressaar and Remm 2007) and are included in (**FIGURE 4.11B**). The primer pairs were named MyH13'UTR, MyH23'UTR and MyH43'UTR and amplified MyH1, 2 and 4 respectively. To allow complete MHC isoform analysis of skeletal muscles, a primer pair to MyH7 (slow type MHC) were designed towards the 3' termini of a full length cDNA sequence available through Ensemble (ENSCPOG00000004208, Release 56).

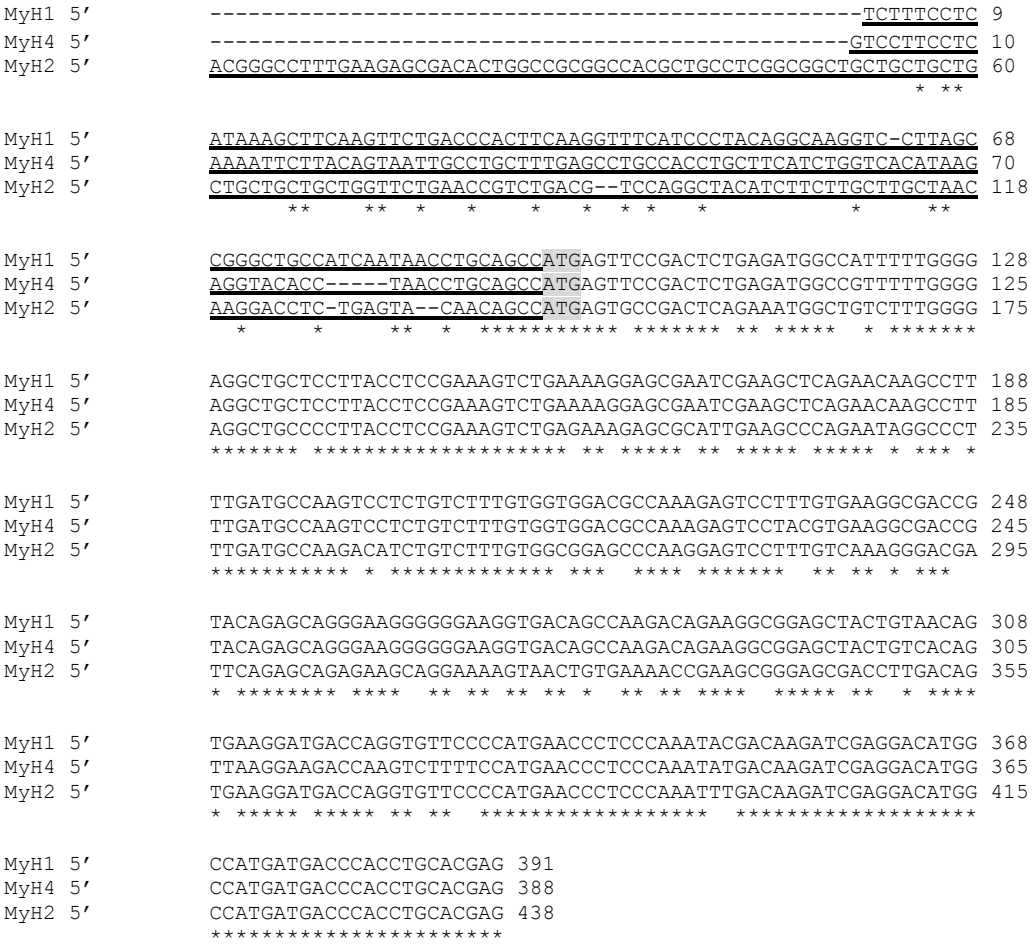

FIGURE 4.11A – Sequence alignment of novel 5'UTRs of MyH cDNAs (underline) and accompanying partial coding sequence. Transcription start codon is identified in grey. Asterisks indicate nucleotides which are conserved across all sequences.

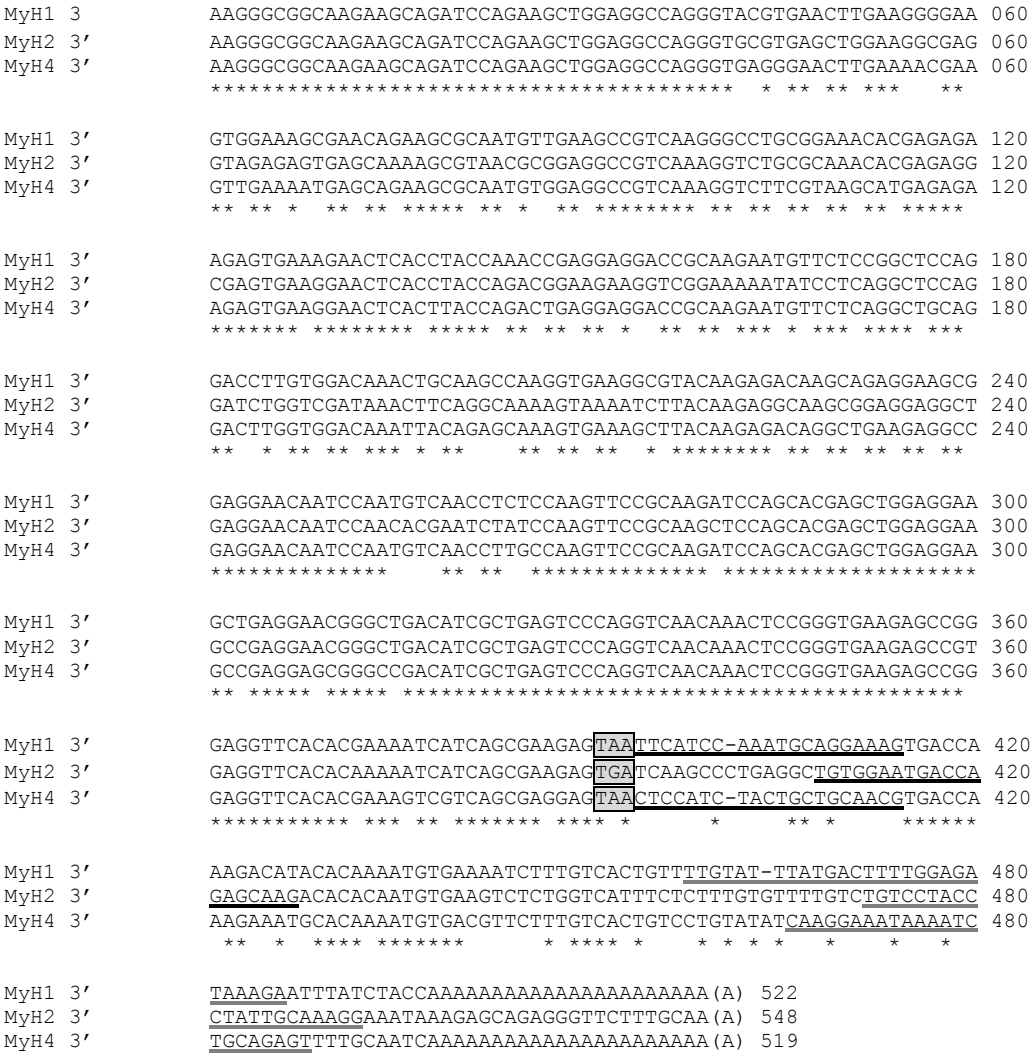

FIGURE 4.11B – Sequence alignment of novel 3'UTRs (from stop-codon) and accompanying partial coding sequence. Translation stop codon is identified in grey. Isoform specific primers are denoted in black (forward) and grey (reverse) underline. Asterisks indicate nucleotides which are conserved across all sequences.

4.3.6 – Testing the specificity of guinea pig MHC transcript isoform specific primers

Due to the high degree of homology between MHC isoforms MyH1, 2 and 4, the respective primer pairs were subjected to an experimental assessment of specificity. Vectors containing the 3' UTRs of MyH1, 2 and 4 were linearised by *Bgl*1 endonuclease digestion (NEB) known to cut once within the vector sequence (**METHOD 2.2.5**). The resulting linearised vectors contained the respective 3' UTR sequences (**FIGURE 4.10B**) flanked by vector sequence (**FIGURE 4.12**).

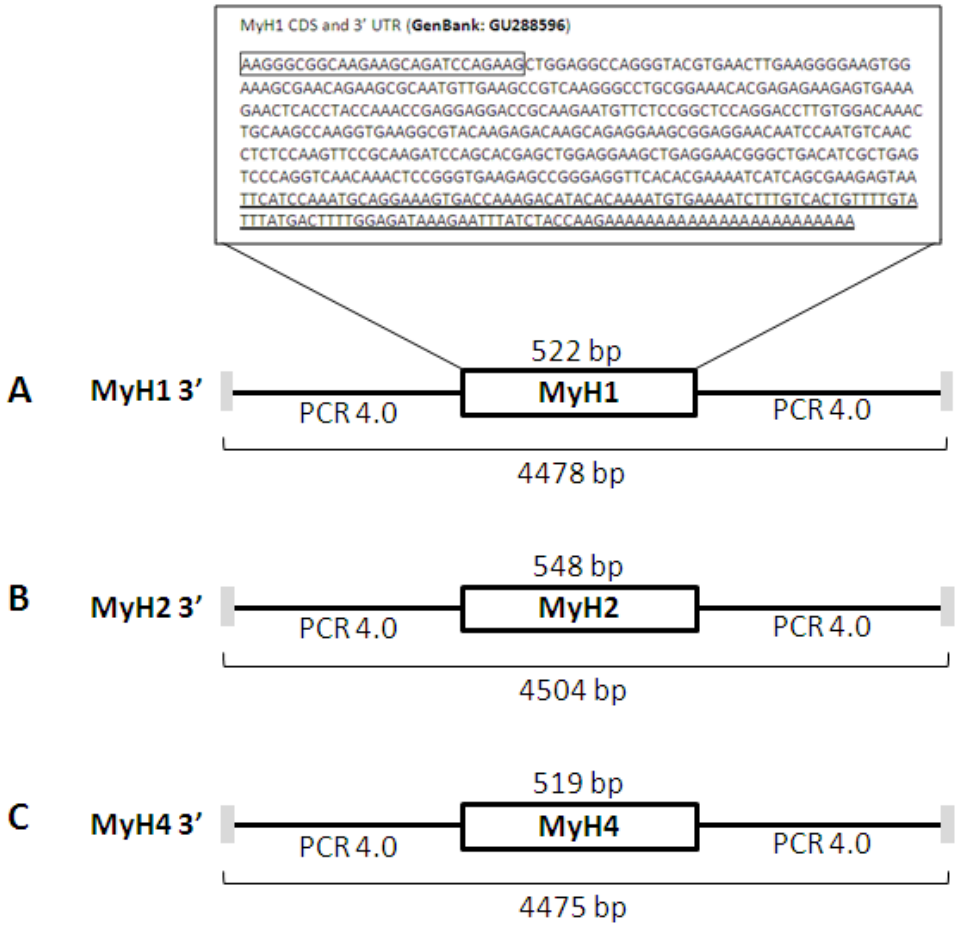

FIGURE 4.12 – Linearised vector maps (Bgl1) of clones MyH1 (A), MyH2 (B) and MyH4 (C). Diagram shows MyH inserts (black box) with respective size (above box). The complete insert size, inclusive of the included region of PCR 4.0 vector sequence, is indicated under the bracket. An exemplar sequence is inset above part (A); please refer to figure 4.10B for details of each MyH insert.

Each vector (**FIGURE 4.12**) was adjusted to 2ng/µl and serially diluted 5-fold to produce a 7-point standard curve. Five-fold serial dilutions were then mixed 1:1 (v/v) with molecular biology grade water (control) or a combination of the two competing vectors at a concentration of 0.4ng/µl. For example primer pair MyH13'UTR were used to amplify vector MyH1 3' (control) and then used to amplify a combination of vectors MyH1 3', MyH2 3' and MyH4 3' (competitors added). Quantitative PCR was carried out using SYBR green quantification technology (Roche) (**METHOD 2.1.7.2**). **FIGURE 4.13** shows the respective reactions for MyH1 (A), MyH2 (B) and MyH4 (C) with the concentration of product plotted against the crossing point (Cp). No cross reaction was observed between any of the primer pairs and the competing vectors as amplification of the target vector was unaffected in the presence of any completing vector, confirming the specificity of the primers for their intended target.

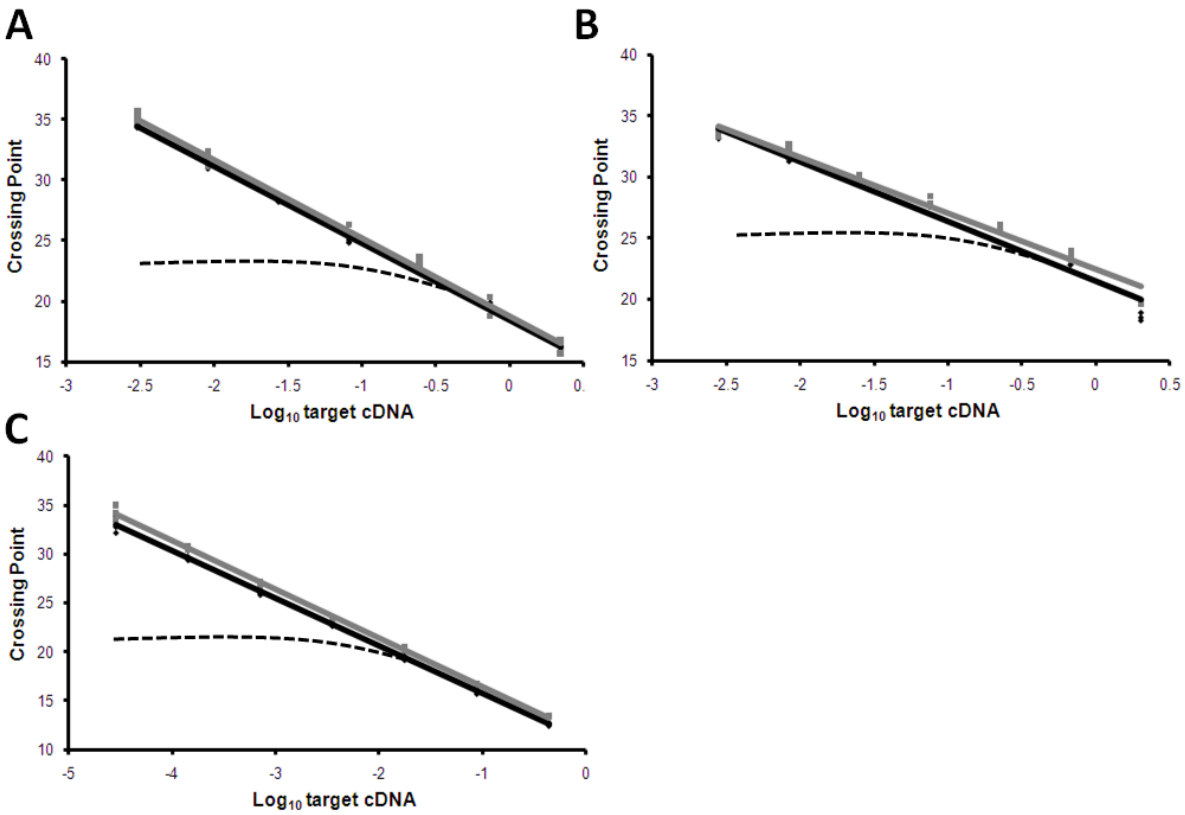

FIGURE 4.13 - Specificity of quantitative PCR reactions for each target MHC gene transcript (A) MyH1, (B) MyH2 (C) MyH4. Black line – control reaction; Grey line – reaction with competitor vectors added; Dashed line – predicted observation should cross-reaction occur.

4.3.7 – MHC transcript expression in three distinct guinea pig skeletal muscles

In order to validate further the utility of the oligonucleotide primers designed, three distinct guinea pig muscles were analysed in terms of their MHC mRNA expression. Based on studies in other laboratory rodents, the soleus is known to be a slow, postural muscle with a predominance of MyH7 and MyH2 mRNA variants. In contrast, extensor digitorum longus has a faster contractile phenotype and a predominance of MyH1 and MyH4 mRNA. Finally, quadriceps femoris is known to express all variants of MHC mRNA. Quantitative PCR analysis of guinea samples from the above muscles revealed expression patterns as expected. MyH7 and MyH2 were

most abundantly detected in the slow-twitch, postural Soleus. MyH1 and MyH4 were detected most abundantly in the fast twitch Extensor digitalis longus, whilst all four transcripts were detected at intermediate levels in the quadriceps muscle (**FIGURE 4.14**).

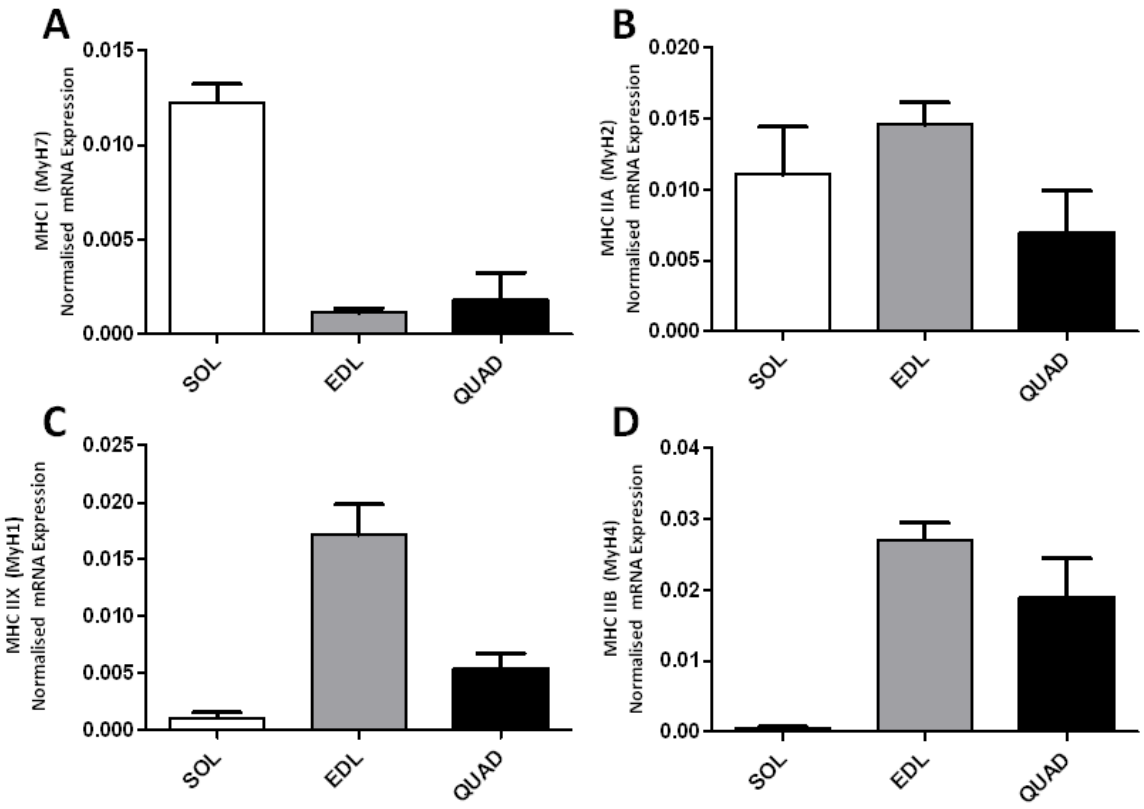

FIGURE 4.14 - Expression of transcripts MyH7 (A), MyH2 (B), MyH1 (C) and MyH4 (D) respectively in three distinct skeletal muscles as determined by quantitative PCR reactions in triplicate. SOL – Soleus; QUAD – Quadriceps; EDL - Extensor digitorum longus. Error bars indicate mean mRNA expression normalised to first strand cDNA concentration + S.E.M; n=6.

4.3.8 – Multi-species MyH UTR and coding sequence comparisons

Guinea pig-specific 5' UTRs and attached coding sequence pertaining to MyH1, 2, and 4 (FIGURE 4.10A) were compared with respective rat, mouse and human cDNA sequences retrieved via Ensemble (Ensemble release 56) (**TABLE 4.1**) using ClustalW2 (Larkin, Blackshields et al. 2007).

Sequence conservation was expressed as a percentage identity using ClustalW2 and revealed a high level of conservation between guinea pig, rat, mouse and human sequence data within a single MyH gene. Interestingly, guinea pig MyH1 and MyH4 displayed the strongest sequence identity with the respective human sequences (87 and 86% respectively). Sequence conservation between guinea pig and human MyH2 was lower (56%), however guinea pig MyH2 showed a high level of consensus sequence with both rat and mouse MyH2 (81 and 72% respectively) (**FIGURES 4.15 – 4.17**).

```
Cavia_MyH1      --TCTTTCCTCATAAAGCTTCAAGTTCTGACCCACT-TCAAGGTTTCATCCCTACAGGCA
Homo_MyH1       TGTCTCTCCTCATAAAGCTTCAAGTTCTGATCCACT-TTAAGGTCGCATCTCTAC-GCCA
Rattus_MyH1     --TCTTTCCTCATAAAGCTTCAAGTTCAGACCCACGGTCGAAGTTGCATCCCTAAAGGCA
Mus_MyH1        -------------AAAGCTTCAAGTTTGGACCCACGGTCGAAGTTGCATCCCTAAAGGCA
                             *************  ** ****  *  * **  **** ***  * **

Cavia_MyH1      AGGTCCTTAGCCGGGCTGCCATCAATAACCTGCAGCCATGAGTTCCGACTCTGAGATGGC
Homo_MyH1       GGGTCCTTAACTGGGCTACCATCAATAACCTGCAGCCATGAGTTCCGACTCTGAGATGGC
Rattus_MyH1     GACTCTCCCACTGGGCTGCCCCCAATAGCCCGCAGCCATGAGTTCCGACGCCGAGATGGC
Mus_MyH1        GGCTCTCTCACTGGGCTGCAACCAATAGCCCGCAGCCATGAGTTCCGACGCCGAGATGGC
                   **     * ***** *   ***** ** ****************** * ********

Cavia_MyH1      CATTTTTGGGGAGGCTGCTCCTTACCTCCGAAAGTCTGAAAAGGAGCGAATCGAAGCTCA
Homo_MyH1       CATTTTTGGGGAGGCTGCTCCTTTCCTCCGAAAGTCTGAAAGGGAGCGAATTGAAGCCCA
Rattus_MyH1     CGTTTTCGGGGAGGCTGCTCCTTACCTCCGGAAGTCTGAAAAGGAGCGAATCGAGGCTCA
Mus_MyH1        CGTTTTCGGGGAGGCTGCTCCTTACCTCCGGAAGTCTGAAAAGGAGCGAATCGAGGCTCA
                * **** ***************** ****** ********** ********* ** ** **

Cavia_MyH1      GAACAAGCCTTTTGATGCCAAGTCCTCTGTCTTTGTGGTGGACGCCAAAGAGTCCTTTGT
Homo_MyH1       GAACAAGCCTTTTGATGCCAAGACATCAGTCTTTGTGGTGGACCCTAAGGAGTCCTTTGT
Rattus_MyH1     GAACAAGCCTTTTGATGCCAAGTCATCCGTGTTTGTGGTGGATGCTAAGGAGTCTTTTGT
Mus_MyH1        GAACAAGCCTTTTGACGCCAAGTCATCGGTGTTTGTGGTGGATGCTAAGGAGTCTTTTGT
                *************** ****** * ** ** ***********  * ** ***** *****

Cavia_MyH1      GAAGGCGACCGTACAGAGCAGGGAAGGGGGGAAGGTGACAGCCAAGACAGAAGGCGGAGC
Homo_MyH1       GAAAGCAACAGTGCAGAGCAGGGAAGGGGGGAAGGTGACAGCTAAGACCGAAGCTGGAGC
Rattus_MyH1     AAAAGCAACGGTGCAGAGCAGGGAAGGGGGGAAGGTGACAGCCAAGACCGAAGGTGGCGC
Mus_MyH1        AAAAGCAACGGTGCAGAGCAGGGAAGGGGGGAAGGTGACAGCCAAGACCGAAGGCGGAAC
                 ** ** ** ** ****************************** ***** ****  **  *

Cavia_MyH1      TACTGTAACAGTGAAGGATGACCAGGTGTTCCCCATGAACCCTCCCAAATACGACAAGAT
Homo_MyH1       TACTGTAACAGTGAAAGATGACCAAGTCTTCCCCATGAACCCTCCCAAATATGACAAGAT
Rattus_MyH1     TACTGTAACAGTAAAAGATGATCAAGTCTTCCCCATGAACCCTCCCAAGTACGACAAGAT
Mus_MyH1        TACTGTAACAGTAAAAGATGATCAGGTCTACCCCATGAACCCTCCCAAGTACGACAAGAT
                ************ ** ***** ** ** * ****************** ** ********

Cavia_MyH1      CGAGGACATGGCCATGATGACCCACCTGCACGAG
Homo_MyH1       CGAGGACATGGCCATGATGACTCATCTACACGAG
Rattus_MyH1     CGAGGACATGGCCATGATGACCCACCTCCACGAG
Mus_MyH1        CGAGGACATGGCCATGATGACCCACCTGCATGAG
                ********************* ** ** ** ***
```

FIGURE 4.15 – Multi-species alignment comparison of guinea pig (Cavia), human (Homo), rat (Rattus) and mouse (Mus) MyH1 5’ UTR and partial coding sequence. Asterisks denote nucleotides conserved across all four species; black box denotes translation start site.

```
Cavia_MyH2      ACGGGCCTTTGAAGAGCGACACTGGCCGCGGCCACGCTGCCTCGG--CGGCTGCTGCTGC
Rattus_MyH2     ------------------------------------------------------------
Mus_MyH2        ------------------TAGCTAGCCATATAAAAGAGTCCCGAA--CGAGGCTGACTCG
Homo_MyH2       ------------------ATAGCTATCCATATAAAAGAGCCCTTGGAATGAGGCTGACTCG


Cavia_MyH2      TGCTGCTGCTGCTGGTTCTGA--ACCGTCTGACGTCCAGGCTACATCTTCTTGCTTGCTA
Rattus_MyH2     TCCTGCTTTAAAAAGCTCCAAGGACCCTCTTACTTCCCAGCTGCACCTTCTCATTTGCCA
Mus_MyH2        TCCTGCTTTAAAAAGCTCCAAGGACCCTCTTATTTCCCAGCTGCACCTTCTCGTTTGCCA
Homo_MyH2       TCCTGCTTTAAAAAGCTCCAAGAACTGTCTCACTCCCAGGCTACATCTTCTCACTTGCTA
                * *****       * **  *  **  *** *   **  *** ** *****   **** *


Cavia_MyH2      ACAAGGACCTCTGAGTACAACAGCCATGAGTGGCGCCGACTCAGAAATGGCTGTCTTTGG
Rattus_MyH2     ATAAGGGTCTGTGAGTTCAGCAGCCATGAG---TTCCGACTCTGAGATGGCCGTTTTCGG
Mus_MyH2        GTAAGGGTCTGTGAGTTCAGCAGTCATGAG---CTCCGACGCCGAGATGGCCGTTTTCGG
Homo_MyH2       ACAAGGACCTCTGAGTTCAGCAGCCATGAG---TTCAGACTCAGAATTGGCTGTTTTTGG
                  ****  ** ***** ** *** ******     * *** * **  **** ** ** **


Cavia_MyH2      GGAGGCTGCCCCTTACCTCCGAAAGTCTGAGAAAGAGCGCATTGAAGCCCAGAATAGGCC
Rattus_MyH2     GGAGGCTGCTCCTTACCTCCGGAAGTCTGAAAAGGAGCGAATCGAGGCCCAGAATAGGCC
Mus_MyH2        GGAGGCTGCCCCTTACCTCCGGAAGTCCGAAAAGGAGCGAATCGAGGCCCAGAATAGGCC
Homo_MyH2       GGAGGCTGCTCCTTTCCTCCGAAAGTCTGAAAGGGAGCGCATTGAGGCCCAGAATAGGCC
                ********* **** ****** ***** ** *  ***** ** ** **************


Cavia_MyH2      CTTTGATGCCAAGACATCTGTCTTTGTGGCGGAGCCCAAGGAGTCCTTTGTCAAAGGGAC
Rattus_MyH2     TTTTGATGCCAAAACATCTGTCTTTGTGGCGGAGCCCAAGGAGTCCTTTGTCAAAGGAAC
Mus_MyH2        TTTTGATGCCAAAACATCTGTCTTTGTGGCGGAGCCCAAGGAATCCTTTGTCAAAGGAAC
Homo_MyH2       CTTTGATGCCAAAACATCTGTCTTTGTGGCGGAGCCCAAAGAATCCTTTGTCAAAGGGAC
                 *********** ************************** ** ************** **


Cavia_MyH2      GATTCAGAGCAGAGAAGCAGGAAAAGTAACTGTGAAAACCGAAGCGGGAGCGACCTTGAC
Rattus_MyH2     CATTCAGAGCAAAGACGCAGGGAAAGTGACTGTGAAAACTGAAGCAGGAGCGACCCTGAC
Mus_MyH2        CATTCAGAGCAAAGATGCAGGGAAAGTGACTGTGAAAACAGAAGCAGGAGCGACCCTGAC
Homo_MyH2       CATCCAGAGCAGAGAAGGAGGAAAAGTGACGGTGAAGACTGAGGGAGGAGCGA--TGAGT
                 ** ******* *** * *** ***** ** ***** ** ** *  *******


Cavia_MyH2      AGTGAAGGATGACCAGGTGTTCCCCATGAACCCTCCCAAATTTGACAAGATCGAGGACAT
Rattus_MyH2     GGTGAAAGAAGACCAGATCTTCCCCATGAACCCTCCCAAGTACGACAAGATCGAGGACAT
Mus_MyH2        CGTGAAAGAAGACCAGATCTTCCCCATGAACCCTCCCAAGTACGACAAGATCGAGGACAT
Homo_MyH2       TCAGACTCAGAATTGGCTGTTTTTGGGGAGGCTGCTCCTTTCCTCCGAAAGTCTGAAAGG
                   **   *  *   * * **      **  *  * *   *    * * *    * *


Cavia_MyH2      GGCCATGATGACCCACCTGCACGAG
Rattus_MyH2     GGCCATGATGACCCACCTCCACGAG
Mus_MyH2        GGCCATGATGACCCACCTGCACGAG
Homo_MyH2       GAGCGCATTGAGGC-CCAGAATAGG
                *  *    ***  * **   *   *
```

FIGURE 4.16 – Multi-species alignment comparison of guinea pig (Cavia), human (Homo), rat (Rattus) and mouse (Mus) MyH2 5' UTR and partial coding sequence. Asterisks denote nucleotides conserved across all four species; black box denotes translation start site.

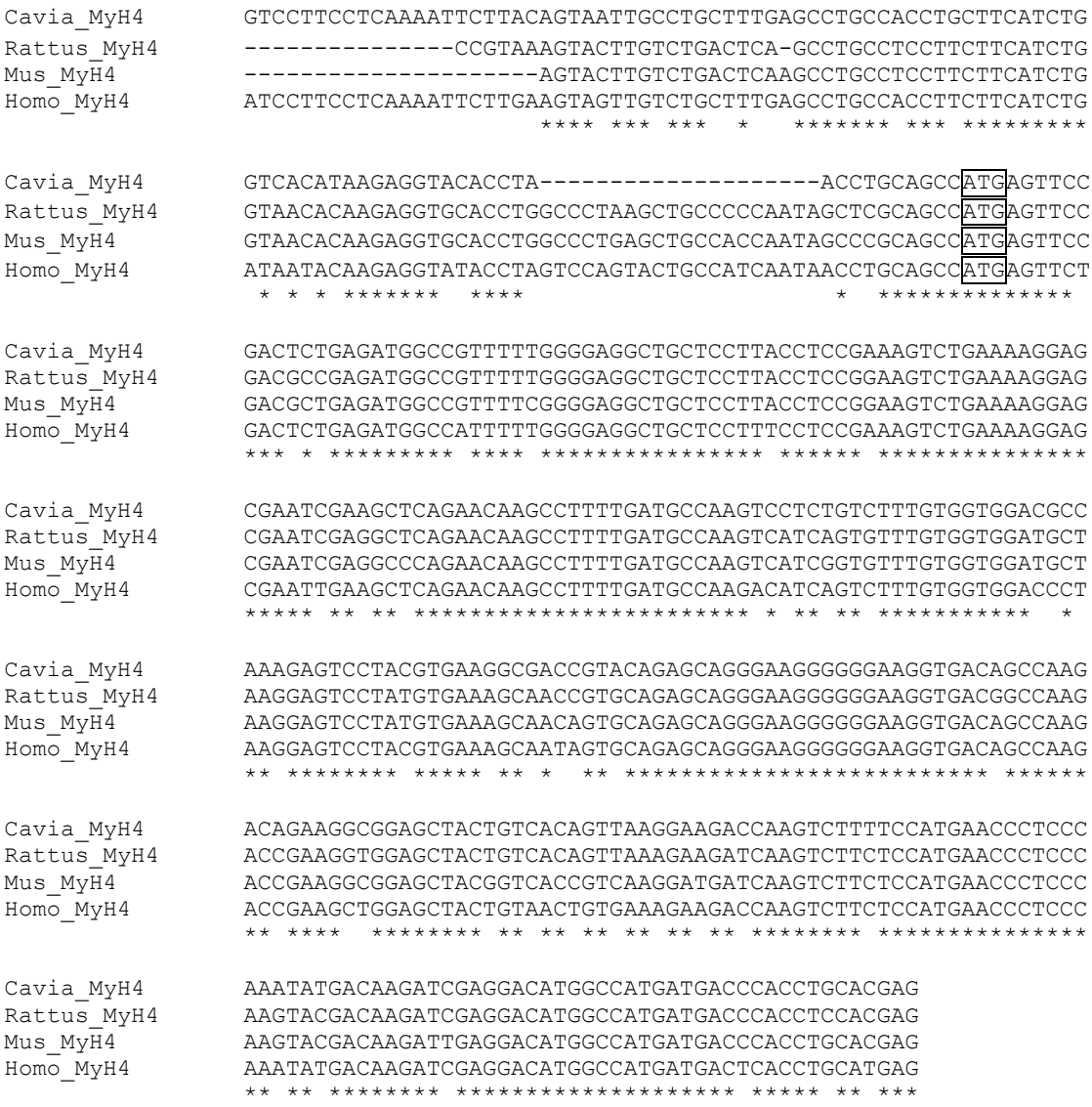

FIGURE 4.17 – Multi-species alignment comparison of guinea pig (Cavia), human (Homo), rat (Rattus) and mouse (Mus) MyH4 5' UTR and partial coding sequence. Asterisks denote nucleotides conserved across all four species; black box denotes translation start site.

4.3.9 – Analysis of promoter elements

Using the cDNA sequences described in **TABLE 4.1**, genomic DNA sequences pertaining to MyH1, 2 and 4 for guinea pig, human, rat and mouse were retrieved from Ensemble (Ensemble release 56). For the analysis of likely proximal promoter elements, -600 to +200bp of the transcription start site (UTR exon 1) of each genomic DNA sequence was aligned using ClustalW2 (Larkin, Blackshields et al. 2007).

Previously identified myosin heavy chain promoter elements (identified in the mouse MyH4 promoter) including a conserved CAP motif, TATA-box, proximal motif (PROX), NF-1, serum response factor (SRF), two AT-rich regions (AT-1/2), myocyte enhancer factor-2 (MEF-2) and Oct-1 (Takeda 1992; Allen, Weber et al. 2005) were identified and are highlighted on **FIGURES 4.18**, **4.19** and **4.20** for MyH isoforms 1, 2 and 4 respectively.

4.3.9.1 – Sequence conservation across species within each MyH gene

Both AT-2 and NF-1/SRF/NF-1 (CArG) elements were well-conserved across the four species within myosin heavy chain genes MyH1, MyH2 and MyH4 respectively. Whilst AT-2 regions were 100% conserved across species within each MyH isoform, CArG elements were more divergent **(FIGURES 4.18 – 4.20)**.

Multiple alignments of the promoter sequences (-600 to +200bp TSS) were used to construct phylogenetic trees and therefore assess how closely related the promoter elements of rat, mouse, guinea pig and human were. For all MyH isoforms assessed, two distinct pathways were present, one of which included the mouse and rat, the other comprising human and guinea pig **(FIGURE 4.21 A-C)**.

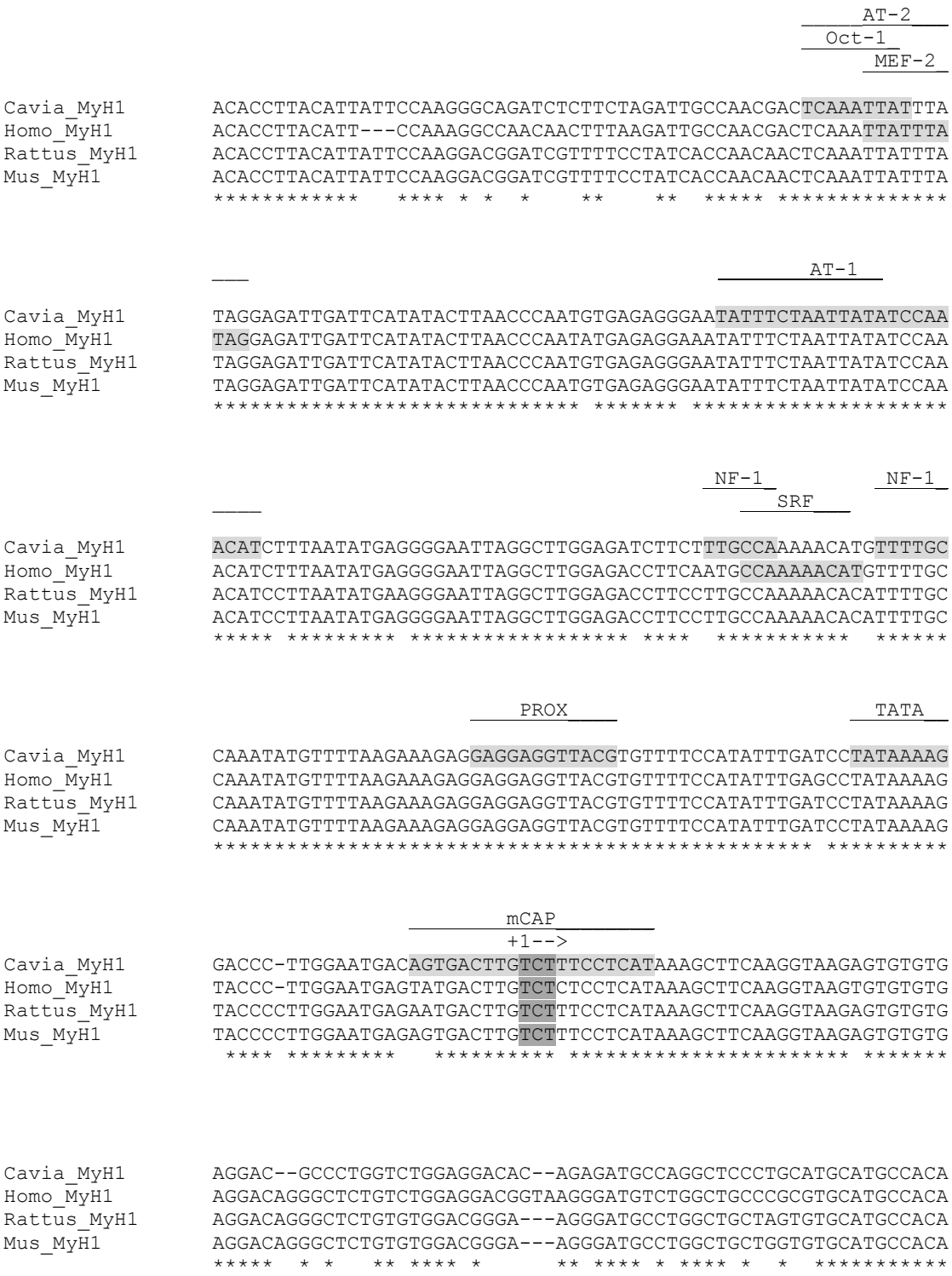

FIGURE 4.18 – Multi-species alignment comparison of guinea pig (Cavia), human (Homo), rat (Rattus) and mouse (Mus) MyH1 genomic DNA sequence located -265 to +95bp of the transcription start site. Asterisks denote nucleotides conserved across all four species; +1 denotes the transcription start site.

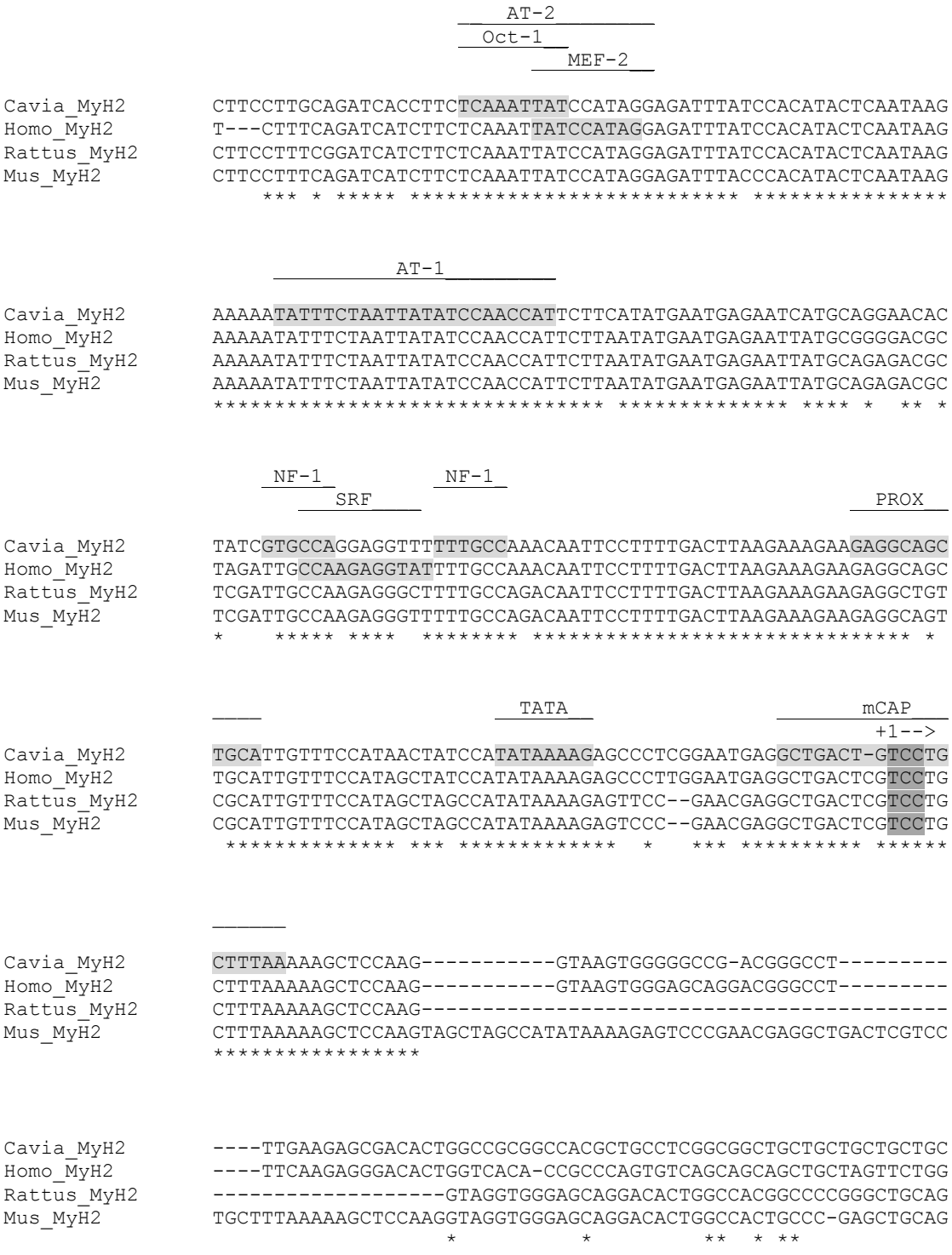

FIGURE 4.19 – Multi-species alignment comparison of guinea pig (Cavia), human (Homo), rat (Rattus) and mouse (Mus) MyH2 genomic DNA sequence located -235 to +104bp of the transcription start site. Asterisks denote nucleotides conserved across all four species; +1 denotes the transcription start site.

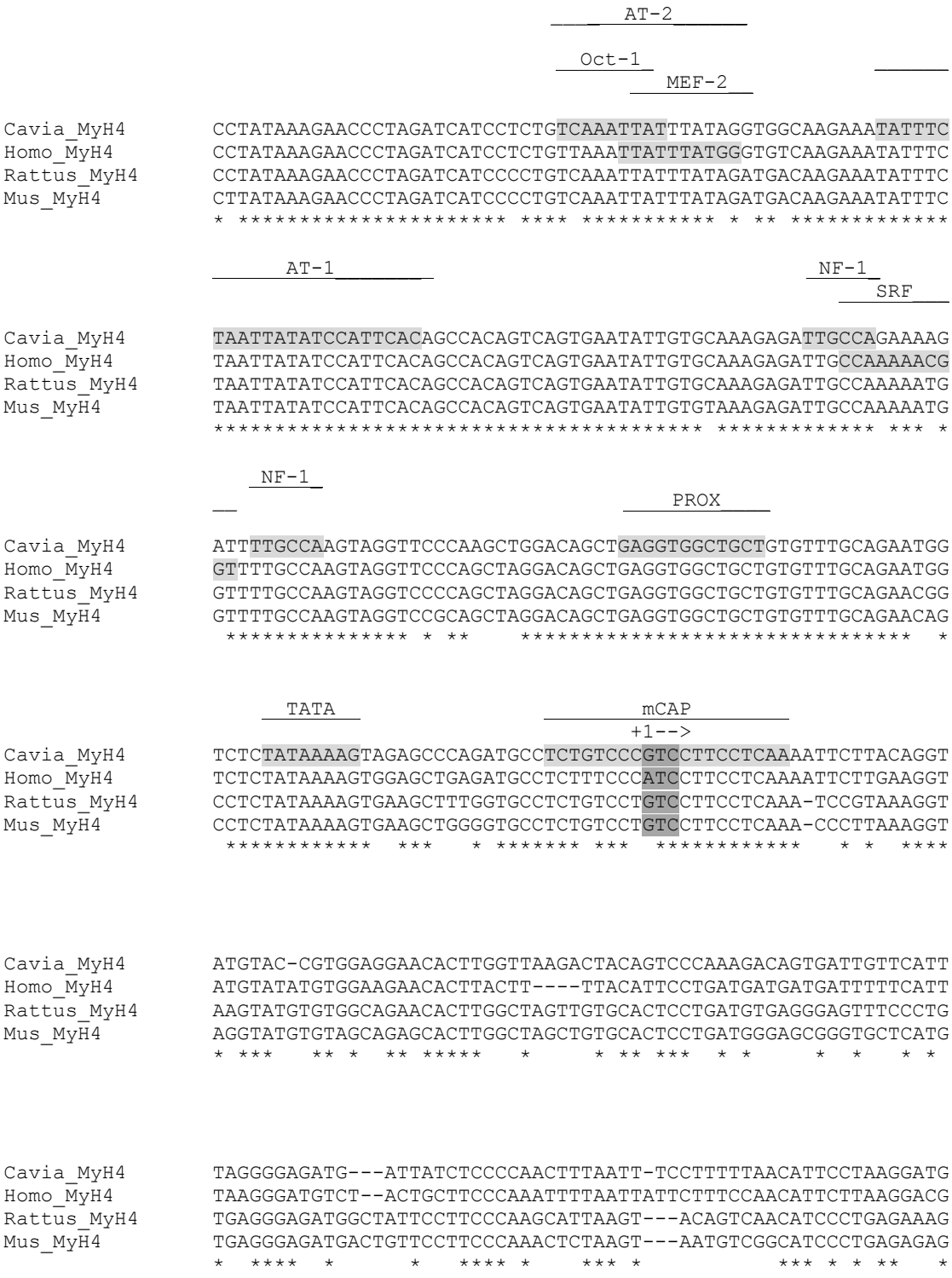

FIGURE 4.20 – Multi-species alignment comparison of guinea pig (Cavia), human (Homo), rat (Rattus) and mouse (Mus) MyH4 genomic DNA sequence located -215 to +145bp of the transcription start site. Asterisks denote nucleotides conserved across all four species; +1 denotes the transcription start site.

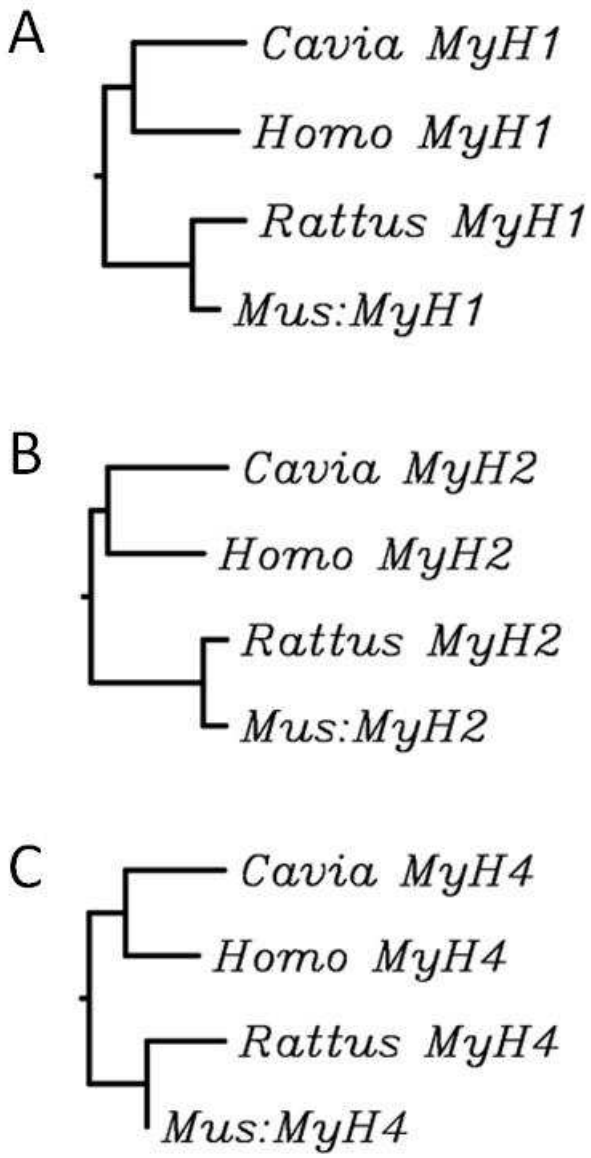

FIGURE 4.21 – Phylogenetic trees representing the relationship of MyH1 (A), MyH2 (B) and MyH4 (C) promoter sequence between the guinea pig (*Cavia*), human (*Homo*), rat (*Rattus*) and mouse (*Mus*) produced using ClustalW.

Sequence homology was calculated as a percentage of the total number of bases included within each alignment. (A) *Cavia* MyH1 shared 82% sequence homology with *Homo*. (B) *Cavia* MyH2 shared 65% sequence homology with *Homo*. (C) *Cavia* MyH4 shared 84% sequence homology with *Homo*.

4.3.9.2 – Sequence conservation between myosin heavy chain genes MyH1, 2 and 4

Previous work has reported that divergent changes exist in the promoter elements of MyH1 and MyH2 when compared to the functional mouse MyH4 promoter in which they were initially described (Allen, Weber et al. 2005). Moreover, it has been reported that the AT-2 (Oct-1/MEF-2) and CArG regions (NF-1/SRF/NF-1) may regulate MyH4 promoter activity and therefore the expression of distinct MyH4 transcripts and MHC IIB protein (Allen, Weber et al. 2005).

Previously identified AT-2 and CArG regions from guinea pig, human, rat and mouse (**FIGURES 4.17-4.20**), were aligned within each species to assess the conservation between promoter elements of the three fast myosin heavy chain genes. The mouse MyH4 promoter AT-2 and CArG elements, previously reported to be functional, were also included within each alignment (**FIGURES 4.22-4.23**) for comparison.

Guinea pig MyH1, 2 and 4 promoters had functional Oct-1 binding sites however displayed divergent changes to the myocyte enhancer factor-2 (MEF-2) binding site. Moreover, whilst both NF-1 binding sites appeared functional in comparison to the verified mouse MyH4 CArG element, several point mutations were noted in the core of the serum response factor (SRF) binding site.

Human MyH1 and MyH2 promoters had functional Oct-1 binding sites however MyH4 encoded a single base change (T/G) in comparison to the verified mouse MyH4 binding site. Human MyH1, 2 and 4 MEF-2 binding sites displayed similar divergent changes to those noted in the guinea pig. Both NF-1 binding sites appeared functional in comparison to the verified mouse MyH4 CArG element; however several point mutations were noted in the core of the SRF binding site as noted in the three guinea pig promoters assessed.

Both AT-2 and CArG binding sites in the rat MyH4 promoter displayed complete sequence identity with the verified mouse sequence. Rat MyH1 and MyH2 promoters

displayed similar divergence from the mouse MyH4 promoter sequence as noted in the guinea pig and human sequence. Mouse MyH1 and MyH2 again displayed a similar level of sequence divergence located within the MEF-2 and SRF binding site and presented with conserved NF-1 and Oct-1 motifs.

```
                      Oct-1
                             MEF-2
Cavia_MyH1_AT2        TCAAATTATTTATAGG 16
Cavia_MyH2_AT2        TCAAATTATCCATAGG 16
Cavia_MyH4_AT2        TCAAATTATTTATAGG 16
Functional            TCAAATTATTTATAGA 16
                      *********  ****

                      Oct-1
                             MEF-2
Homo_MyH1_AT2         TCAAATTATTTATAGG 16
Homo_MyH2_AT2         TCAAATTATCCATAGG 16
Homo_MyH4_AT2         TTAAATTATTTATGGG 16
Functional            TCAAATTATTTATAGA 16
                      * *******  ** *

                      Oct-1
                             MEF-2
Rattus_MyH1_AT2       TCAAATTATTTATAGG 16
Rattus_MyH2_AT2       TCAAATTATCCATAGG 16
Rattus_MyH4_AT2       TCAAATTATTTATAGA 16
Functional            TCAAATTATTTATAGA 16
                      *********  ****

                      Oct-1
                             MEF-2
Mus_MyH1_AT2          TCAAATTATTTATAGG 16
Mus_MyH2_AT2          TCAAATTATCCATAGG 16
Mus_MyH4_AT2          TCAAATTATTTATAGA 16
Functional            TCAAATTATTTATAGA 16
                      *********  ****
```

FIGURE 4.22 – Comparison of AT-2 element sequence across the three fast isoforms of guinea pig, human, rat and mouse in comparison to the functional sequence derived from mouse MyH4 (Allen, Weber et al. 2005). Nucleotides that differ from the mouse MyH4 sequence appear in red.

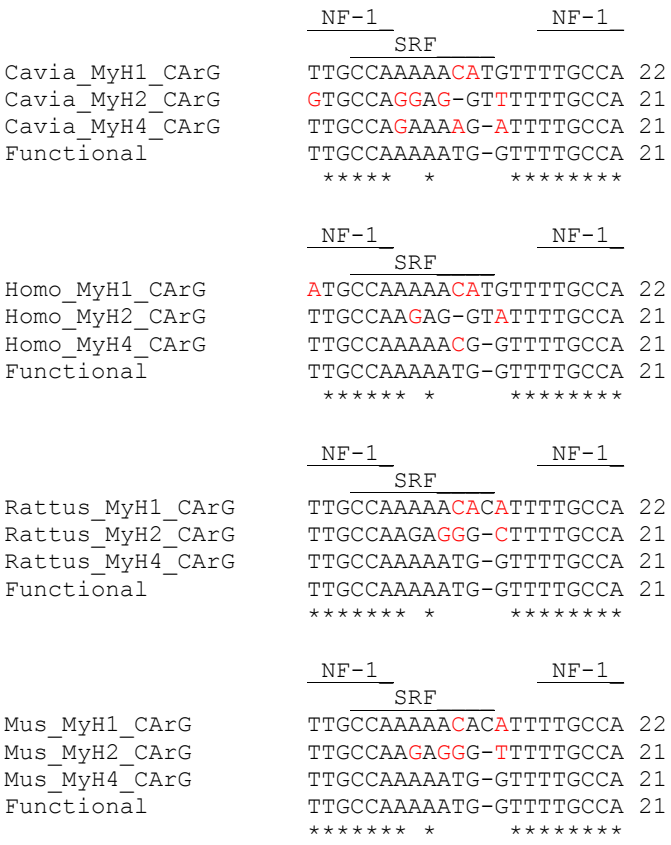

FIGURE 4.23 – Comparison of CArG element sequence across the three fast isoforms of guinea pig, human, rat and mouse in comparison to the functional sequence derived from mouse MyH4 (Allen, Weber et al. 2005). Nucleotides that differ from the mouse MyH4 sequence appear in red.

4.4 – Discussion

In this study, the structure of the MHC multi-gene family in the common guinea pig (*Cavia porcellus*) was characterised. Using 5' and 3' RACE methodology, novel UTR and coding sequence for each of the "fast" MHC mRNAs was elucidated, and the boundaries of each gene demarcated. The MHC genes were found to be located in a head-to-tail fashion in the order MyH3/ MyH2, MyH1/, MyH4 and MyH8/ MyH13, in a 5' to 3' direction. Although the exact chromosomal locations are still unknown due to restricted genomic annotation, the MyH7β gene was found to be located in a distinct area of contiguous sequencing data. Numerous studies have previously reported that the MHC gene family is found in a highly conserved head-to-tail fashion in several species (Weiss and Leinwand 1996; Rinaldi, Haddad et al. 2008). Moreover, previous publications also report that the MyH7β gene (encoding MHC I) is consistently found on a separate chromosome from other members of the multi-gene family (Weiss and Leinwand 1996). These previous findings are consistent with the results obtained in this study.

Specific oligonucleotide primers for MyH7β, MyH2, MyH1 and MyH4 mRNA variants were designed and validated, and for the first time, the adult skeletal muscle associated MHC variants were successfully differentiated and quantified in the guinea pig by quantitative PCR analysis. The use of PCR to quantify MHC mRNA in relation the skeletal muscle fibre type has been highly cited within the relevant literature. Furthermore, MHC mRNA has been shown to correlate highly with both MHC protein levels (Marx, Kraemer et al. 2002), and other measures of skeletal muscle fibre type including mATPase staining, MHC histochemistry and measures of metabolic profile (Quiroz-Rothe and Rivero 2004). To date, the resolution of MHC protein from guinea pig skeletal muscle has not been achieved.

Sequence analysis was performed to compare the guinea pig 5' UTR and partial coding sequences derived in this study with those of human, rat and mouse. Multiple species comparison revealed that guinea pig MyH1 and MyH4, coding for myosin heavy chain isoforms IIX and IIB, were most comparable to the human sequence data whereas guinea pig MyH2 was most comparable to the rat. Numerous muscle pathologies are associated with the atrophy of type II muscle fibres (Lexell, Taylor et al. 1988; Baracos, Devivo et al. 1995; Lecker, Jagoe et al. 2004), encoded by myosin heavy chain genes MyH1 and MyH4 (Weiss and Leinwand 1996). Given that the coding sequence of these two genes appeared highly conserved between the guinea pig and the human, and that humans do not generally express MHC IIB muscle fibres (encoded by MyH4) (Harridge 2007), it was of interest with respect to the use of the guinea pig as an *in vivo* model of human pathology, as to whether the regulatory elements of both genes were similar and moreover, whether guinea pig skeletal muscle expresses MHC IIB protein.

With a view to assessing the control of MyH4 mRNA in the guinea pig, promoter analysis was performed on the proximal 600bp to the transcription start site in comparison to promoter sequence derived from rat and mouse which are known to express MHC IIB and human which has the capacity to express MyH4 mRNA (Horton, Brandon et al. 2001) but does not routinely express MHC IIB protein (Harridge 2007). Previously reported myosin heavy chain promoter elements (identified in the mouse MyH4 promoter) including a conserved CAP motif, TATA-box, proximal motif (PROX), NF-1, serum response factor (SRF), two AT-rich regions (AT-1/2), myocyte enhancer factor-2 (MEF-2) and Oct-1 (Takeda 1992; Allen, Weber et al. 2005) were identified. SRF and myocyte enhancer factor-2 have been previously shown to contribute to the expression of muscle-specific genes either independently, or via their interaction with other ubiquitously expressed proteins including NF-1, Sp-1 and Oct-1 (Allen, Weber et al. 2005).

Examination of the AT-2 region across the three fast MHC isoforms revealed that whilst functional AT-2 regions were present in the MyH4 promoters of the rat and mouse, these sites were mutated in the MyH 1 and 2 promoters assessed across all four species. Analysis of the AT-2 region of the guinea pig and human MyH4 promoters revealed mutations in the MEF-2 binding site in the AT-2 region that were consistent with those mutations in the rat and mouse MyH1 promoters, and that have been previously shown to affect Oct-1 and MEF-2 binding (Allen, Weber et al. 2005). Allen and colleagues, 2005 have previously reported mutations in the AT-2 region of mouse MyH1 and MyH2 promoters in comparison with the MyH4 promoter. Electrophoretic mobility shift-assays (EMSA) have demonstrated that the mutations in the MyH2 promoter were sufficient to completely prevent the binding of Oct-1 and MEF-2, and mutations in the MyH1 promoter sufficient to significantly reduce the binding of these transcription factors (Allen, Weber et al. 2005) and subsequently decrease promoter activation. It is therefore suggested that Oct-1 and MEF-2 induced activation of the MyH4 promoter (MHC IIB) in the guinea pig and human may be restricted to a level similar to MyH1 promoter activation in the mouse or rat.

Examination of the CArG region (comprising two NF-1 sites and a single SRF core) across the three fast MHC isoforms revealed that whilst functional SRF binding elements were present in the MyH4 promoters of the rat and mouse, these sites were mutated in the MyH1 and 2 promoters assessed across all four species. Analysis of the CArG region of guinea pig and human MyH4 promoters revealed mutations in the site reported to bind SRF, a potent transcriptional activator (Joseph 2003). The CArG region binds NF-1 and SRF (Joseph 2003), and has been previously reported as a further activator (in addition to the AT-2 regions) of the MyH4 promoter (MHC IIB) (Allen, Weber et al. 2005). Allen and colleagues have reported that mutations in the mouse MyH1 and MyH2 promoters were sufficient to dramatically decrease promoter activity and it is therefore inferred that mutation of the SRF binding site in

the human and guinea pig MyH4 may have similar negative effects on promoter activity.

Analysis of the two promoter elements shown to regulate MyH4 promoter activity (Takeda 1992; Allen, Weber et al. 2005) suggests that the human and guinea pig MyH4 promoter is less able to bind SRF, MEF-2 and Oct-1 and therefore activation of the MyH4 promoter via this system is likely to be reduced in these species. Despite these findings, MyH4 mRNA was detected in the EDL and quadriceps muscles of the guinea pig in this study (**FIGURE 4.14**) and has previously been detected in human quadriceps samples (Horton, Brandon et al. 2001). It is therefore possible that alternative regulatory mechanisms exist for the activation of MyH4 promoters in these species, the identity of which are not apparent at this time.

In considering the apparent discrepancy between the ability of the guinea pig and human MyH4 promoters to bind their well-characterised transcriptional activators and the abundant expression of MyH4 mRNA, it is necessary to consider that the regulation of MHC gene expression is likely to occur at several levels. Such control mechanisms are likely to include potential promoter activation or inhibition (Lakich, Diagana et al. 1998) (as described in this study), differing mRNA stability, translational control of the various mRNAs and protein stability (Takeda 1992).

At the level of transcriptional control, it appears that only the TATA box, located at -30bp from the TSS, is required for the transcription of MyH4 (Swoap 1998). Despite this, the transcription of MyH4 mRNA in constructs lacking the AT-2 and CArG regions was much lower than that observed in guinea pig skeletal muscle (**FIGURE 4.14**). Given that the expression of MyH4 mRNA in the guinea pig was higher than that previously noted in constructs lacking AT-2 and CArG regions, and that MyH1 promoters have been shown to bind SRF, MEF-2 and Oct-1 but with reduced avidity (Allen, Weber et al. 2005), it is one possibility is that the activation of MyH4 promoters in these species is under similar control mechanisms to the MyH1 (MHC

IIX) promoter in the rat and mouse. To date, little is known about which factors specifically activate the MyH1 promoter, and recent attempts to characterise specific binding factors via gene transfer protocols have been unsuccessful (Pandorf, Haddad et al. 2007).

4.4.1 – Closing Remarks

The methods developed here enable the rapid and accurate quantification of changes in the MHC expression of guinea pig skeletal muscle. Moving forward, the tools developed here will be utilised to quantify acute changes in the MHC expression of the guinea pig quadriceps skeletal muscle in response to developing and progressing knee-OA.

CHAPTER 5 - CHARACTERISATION OF THE DEVELOPMENT OF SPONTANEOUS OSTEOARTHRITIS, AND ASSOCIATED QUADRICPES CHANGES, IN THE DUNKIN HARTLEY GUINEA PIG

5.1 – Introduction and Rationale

In **CHAPTER 3**, the role of quadriceps muscle dysfunction in the rat meniscectomy-induced model of OA was reported. The MNX model permitted the assessment of muscle dysfunction coincident with OA as well as the opportunity to modulate muscle function with various hypertrophic agents at defined time points prior to disease induction. Data derived from **CHAPTER 3** confirmed that the MNX procedure resulted in OA-like lesions that were morphologically similar to those of the human condition and that clenbuterol administration was indeed able to induce marked muscle hypertrophy prior to OA induction. Despite these positive findings, the initial data suggested that increased quadriceps mass had no effect on disease severity in the MNX induced model. It was considered that the rate at which OA develops in the MNX model may have precluded any beneficial effects of increased muscle mass that would have otherwise be evident in the human population. Therefore a spontaneous model of OA was considered. Following successful molecular tool development as reported in **CHAPTER 4**, it was possible to study molecular changes in the quadriceps muscle following the development of spontaneous OA in the Dunkin Hartley guinea pig, which has similar disease progression rates to that of the human condition.

The spontaneous development of knee OA in the Dunkin Hartley guinea pig is considered to be an improvement on surgically induced disease models in terms of comparative pathology and translational research; however the converse is that lesion development takes place over a period of months as opposed to days in the previously utilised rat model. OA occurs spontaneously in the Dunkin Hartley strain guinea pig in both males and females (Jimenez and Glasson 1997). Due to their larger body mass, males tend to develop more rapid and consistent pathologies than females making them more amenable to scientific research. Evidenced by previous studies, lesion development was found to be initially restricted to the medial compartment of the knee, the earliest changes being evident in 50% of animals around 3 months of age or 700g (Tokuda 1997). At 6 months of age, or 900g in

bodyweight, over 90% of animals are found to present with minimal to moderate lesions of the medial tibial plateau. 9 month old animals presented with mild to moderate medial tibial lesions, with mild femoral involvement (Bendele 2001) however it was not until animals reached one year of age that the first clinical signs of gait abnormality and or knee extension difficulties are noted (Bendele 2001).

The Dunkin Hartley model of OA has demonstrated clear parallels with the human condition during both initiation and disease progression (Jimenez and Glasson 1997). Numerous studies have reported that OA develops predominantly on the medial aspect of the tibial condyle, with involvement of the medial femoral condyle only in response to disease progression (Bendele and White 1987; Bendele and Hulman 1988; Bendele, White et al. 1989; Bendele and Hulman 1991; Jimenez and Glasson 1997; Bendele 2001; Bendele 2002). This finding replicates the human situation where approximately 75% of the load is passed through the medial aspect of the knee (Bendele, et al., 2001). The development of OA in the Dunkin Hartley strain has also been strongly associated with increased age and body mass (Tessier, Bowyer et al. 2003) as with the human condition (Arden and Nevitt 2006). Further similarities between the Dunkin Hartley model and human OA have been described at the molecular level. The development of human knee OA has been associated with the expression of collagenase 1 and collagenase 3, also known as matrix matelloproteinases 1 and 13 respectively, at the site of OA development (Mitchell, Magna et al. 1996; Reboul, Pelletier et al. 1996). Both collagenases are found to be highly expressed in the Dunkin Hartley model but are absent from rodent and murine systems (Huebner, Otterness et al. 1998).

Extensive literature characterises the development of OA in the Dunkin Hartley guinea pig at the level of the cartilage and subchondral bone (Bendele and White 1987; Bendele and Hulman 1988; Bendele, White et al. 1989; Bendele and Hulman 1991; Bendele, Sennello et al. 1997) however no literature exists regarding the effects of OA development on skeletal muscle function. The aim of this study was

therefore to investigate the contribution of muscle dysfunction to disease progression, and furthermore, begin to elucidate the likely mechanisms instigating muscle dysfunction if present.

5.1.1 – Hypotheses and aims

Bilateral knee OA will present in the Dunkin Hartley guinea pig from around 3 months of age. Consistent with other literature, it is expected that the severity of OA will increase with advancing age and increasing body mass. Functional changes to the quadriceps muscle will occur coincident with the development of knee OA, and animals may present with changes to contractile (MHC) or metabolic muscle parameters.

The following specific aims will be addressed;

- Characterise the development of knee OA at 2, 3, 5 and 7 months of age
- Characterise coincident changes, indicative of functional changes, to the quadriceps muscle group
- Elucidate the likely mechanisms driving muscle changes (if present)

5.2 - Experimental Protocol

5.2.1 - Animals and housing

Male Dunkin Hartley guinea pigs (N=24) were sourced from Charles Rivers, UK at 6 weeks of age. Animals were group housed in a single large pen (4m x 8m) with free access to standard guinea pig chow (Purina, UK) and water. Animals were weighed twice per week to ensure all animals were gaining weight over the course of the study. At 2, 3, 5 and 7 months of age, 6 animals were selected based on their proximity to the median weight of the cohort. Time and finances permitting, the experimental time course would have been increased to 18 months, at which point previous studies have shown marked osteoarthritic changes in all animals (Bendele and Hulman 1988). All animal procedures were carried out at the Bioresource Unit, Sutton Bonington. Given that the guinea pigs were simply allowed to age to pre-defined time points and subsequently euthanised by a schedule I procedure, this study did not fall within the remit of the Home Office Animals (Scientific Procedures) Act 1986 however animals were maintained under such guidelines nevertheless.

5.2.2 – Termination and histopathology

Animals were euthanised by intra-peritoneal injection of Pentobarbital Sodium, and death confirmed by cervical dislocation in accordance with Home Office Schedule I. Knee joints were obtained for histopathological analysis by making a full thickness cut 2 cm above and below the patella. The joints were formalin fixed and decalcified in 10% formic acid prior to processing by routine vacuum assisted wax infiltration (**METHOD 2.4**). Toluidine blue stained step-coronal sections were prepared at 300µm intervals and evaluated using a validated, guinea pig-specific scoring system (Huebner 2006) as show in **TABLE 5.1**. The observer was blinded to both the animal number and age in all cases. Pathological features at each condyle were combined to calculate a femoral, tibial and combined OA score.

5.2.3 – Biospecimens

Whole bilateral quadriceps muscle samples, inclusive of the rectus femoris, were dissected, weighed and immediately snap frozen in isopentane cooled with liquid nitrogen. Care was taken to avoid inclusion of any adipose tissue or additional muscle, most importantly the tensor fasciae latae and sartorius which are located within the dissected area (Tonge, Jones et al.). Whole blood was drawn via cardiac puncture into clot-activator tubes (Sarstedt) and serum obtained by centrifugation. All serum was kept at -80^{o}C prior to analysis.

TABLE 5.1 – Semi-quantitative grading scheme for guinea pig knee joints re-drawn from (Huebner 2006)

Parameter (grade)	Description
Articular Cartilage Structure	
0	Normal, smooth, uninterrupted
1	Mild surface irregularities, no clefts
2	Irregular surface, 1-3 superficial clefts
3	>3 clefts and/or loss of superficial zone
4	1-3 clefts extending into the middle zone
5	>3 clefts and/or loss of the middle zone
6	1-3 clefts extending into the deep zone
7	>3 clefts and/or loss of cartilage into the deep zone
8	Clefts extending to the zone of calcified cartilage
Toluidine Blue Staining	
0	Uniform staining throughout the articular cartilage
1	Loss in the superficial zone, < ½ surface
2	Loss in the superficial zone ≥ ½ surface
3	Loss in the superficial and middle zones < ½ surface
4	Loss in the superficial and middle zones ≥ ½ surface
5	Loss in all 3 zones < ½ surface
6	Loss in all 3 zones ≥ ½ surface
Osteophytosis	
0	No osteophytes present
1	Small osteophytes
2	Medium-sized osteophytes
3	Large osteophytes

5.2.4 – Collagen Turnover

Disruption to the structural integrity of articular cartilage is the major histological finding in osteoarthritis and rheumatoid arthritis. Type II collagen is the major organic constituent of articular cartilage (Pieper 2002) and degradation products which include the terminal telopeptide of type II collagen (CTX II) are released into the circulatory system following cartilage degradation (Nielsen and Stoop 2008). Non-pathogenic cartilage turnover (also presenting with increased serum CTX II) occurs at the growth plate during normal skeletal development, however serum levels decrease with age and stabilise following skeletal maturity (Hoegh-Andersen and Tanko 2004). For the study of spontaneous OA, it is therefore imperative to characterise the change in serum CTX II concentration with advancing age, and to select appropriately aged animals to minimise growth plate contribution to serum CTX II concentration.

Serum CTX II concentration was determined by a validated enzyme linked immunosorbent assay with a monoclonal antibody specific for the neo-epitope formed when collagen type II is degraded to form CTX II (Serum Cartilaps, IDS, USA). The assay was run according to the manufacturer's instructions using 25µl of guinea pig serum against standards produced from rat CTX II of known concentration (0 - 247.6pg/ml). At the end of the procedure, absorbance was read at 450nm within 5 minutes. The absorbance at 650nm was also taken to correct for optical imperfections on the supplied 96-well plate.

The concentration of CTX II was determined by subtracting the absorbance at 650nm from the 450nm value, and delineating from a standard curve of A450-650nm against known CTX II concentration (pg/ml). All samples were analysed in duplicate and a coefficient of variation < 5% deemed acceptable.

5.2.5 – Haematology

Osteoarthritis has been previously correlated with elevated serum cholesterol (Sturmer, Sun et al. 1998) and triglyceride (Cheras, Whitaker et al. 1997) concentration, as described in **CHAPTER 1.1.4.1**. As such, analysis of serum cholesterol and triglyceride was carried out by Mrs Laura Tonge, University of Nottingham. Serum cholesterol was determined from 30µl serum using the Infinity cholesterol determination kit (Sigma) according to the supplied instructions. Serum triglyceride concentration was determined from 30µl serum using a specific triglyceride determination kit (TR0100, Sigma) according to the supplied instructions. Cholesterol and triglyceride standards (7.76mM and 2.26mM respectively, Thermo Scientific) were included with each sample set to assess the accuracy of all determinations. All samples were run in triplicate and a coefficient of variation (CV) < 5% deemed acceptable.

5.2.6 – Luminex analysis

The involvement of cytokines and inflammation in the pathogenesis and progression of rheumatoid arthritis is well established; however, the role of such intracellular messengers in osteoarthritis is less well defined. Moreover, it is well-established that some cytokines elicit changes in skeletal muscle mass (Lang, Frost et al. 2007) including Interleukin 6 (IL-6) and tumour necrosis factor alpha (TNFα). Therefore, serum cytokines were quantified with respect to their association with developing OA, and in terms of their potential muscle modulating effects.

Given the problems associated with obtaining specific antibodies that cross-react with guinea pig proteins, a *novel* protein array system (Bio-Plex Protein Array System Bio-Rad, Hercules, CA) targeting conserved peptide sequences was tested with regards its cross-reaction with guinea pig serum (School of Biology, University of Nottingham). The protein array contained 23 cytokines and chemokines including IL-1α, IL-1β, IL-2, IL-3, IL-4, IL-5, IL-6, KC (a murine IL-8 homologue), IL-9, IL-10, IL-12p40, IL-12p70, IL-13, IL-17, granulocyte macrophage colony-stimulating factor (GM-CSF),

granulocyte colony-stimulating factor (G-CSF), interferon gamma (IFN-γ), macrophage inflammation protein 1 alpha (MIP-1α), MIP-1β, RANTES (regulated upon activation, normal T-cell expressed and secreted), tumour necrosis factor alpha (TNF-α), MCP-1 and Eotaxin. Serum samples from all guinea pigs were analysed as recommended by the manufacturer (complete instructions available from Bio-Rad) against a range of rat cytokine standards (0 - 3200 pg/ml) and a sample dilution of 1:3, utilising a total of 30 µl of sera.

All samples were analysed (Bio-Plex 200) in triplicate, with a coefficient of variation < 5% deemed acceptable.

5.2.7 – Expression analysis by quantitative PCR

Quantitative PCR analysis was carried out on quadriceps muscle samples as described in (**METHOD 2.1.7**) using the standard curve method of data acquisition. To advance on previous methods of data normalisation (GeNorm), the expression data from this study was normalised to cDNA concentration using OliGreen (Invitrogen), shown to specifically bind with single stranded DNA molecules (Rhinn, Marchand-Leroux et al. 2008; Rhinn, Scherman et al. 2008). Following reverse transcription as described in (**METHOD 2.1.5**), 3µl of the resulting cDNA was mixed with an equal volume of OliGreen reagent. Following incubation at room temperature for 5 minutes, fluorescence was read at 522nm at 80^{o}C using the LightCycler (Roche, LC480). Reactions were read at 80^{o}C as this temperature has been shown to increase specificity by reducing the contribution of fluorescence given off by the binding of OliGreen to RNA (Rhinn, Marchand-Leroux et al. 2008), to the cDNA signal. Normalising data in this manner not only accounts for variation in sample loading, but also controls for total reverse transcription reaction efficiency.

5.2.8 – Oligonucleotide primer design

Targets were selected to assess changes in factors associated with skeletal protein degradation and muscle atrophy, the apoptotic response, muscle fibre composition and those factors involved in metabolite signalling.

5.2.8.1 – Quadriceps muscle fibre-type composition

Skeletal muscle fibre characterisation was determined by the expression of myosin heavy chain mRNAs using methodology developed in (**CHAPTER 4**).

5.2.8.2 – Skeletal protein degradation and atrophy

To determine changes in skeletal protein degradative potential, key components of the proteosome and calpain system were assessed. The mRNAs of downstream E3 ligases muscle RING finger protein 1 (MuRF1) and muscle atrophy F-box (MAFBx) which in combination with ubiquitin conjugating enzymes, target proteins for degradation by the proteosome via ubiquitination (Ardley and Robinson 2005) were assessed. Skeletal muscle fibres express both ubiquitous calpain I and II and skeletal muscle specific calpain III (p94) isoforms (Murphy and Lamb 2008). Calpain activation is associated with the initiation of proteosome dependent skeletal muscle protein degradation (Smith and Dodd 2007) and as such the mRNAs of calpain isoforms I – III were also determined.

5.2.8.3 – Apoptotic potential

The apoptotic response potential of quadriceps skeletal muscle was assessed by quantifying the mRNAs of pro-apoptotic Bax and anti-apoptotic Bcl2 which are key components of the mitochondrial-mediated apoptotic pathway (Otter, Conus et al. 1998) using specific oligonucleotide primers for PCR.

5.2.8.4 – Metabolite signalling and muscle fibre-type changes

Factors involved in metabolite signalling, potentially related to metabolic changes in skeletal muscle were assessed. Oligonucleotide primers were designed to PGC1α, PGC1β, PPARα and PPARδ, the functions of which are described in (**CHAPTER 3**). Oligonucleotide primers were also designed to Six-1 and Eya-1, two novel transcription factors reported to induce slow-twitch to fast-twitch muscle fibre changes with an accompanied increase in glycolytic metabolic potential (Grifone, Laclef et al. 2004).

Due to the limited availability of annotated guinea pig cDNA sequence data, rat and mouse cDNA sequences were compared to the partially annotated *Cavia porcellus* database using the BLAT utility (Kent 2002) available from Ensemble Release 56 (Ensemble) in order to locate the corresponding guinea pig cDNA.

TABLE 5.2 – Oligonucleotide primer sequences for quantitative PCR reactions

Gene Name	Accession Number	Forward Primer (5' - 3')	Reverse Primer (5' - 3')	Amplicon (bp)
MyH1 (MHC IIX)	GU288596	TTCATCCAAATGCAGGAAAG	TCTTTATCTCAAAAGTCATAAATACAA	129
MyH2 (MHC IIA)	GU288597	TGTGGAATGACCAGAGCAAG	CCTTTGCAATAGGGTAGGACA	90
MyH4 (MHC IIB)	GU288598	TCCATCTACTGCTGCAACG	ACTCTGCAGATTTTATTTCCTTG	85
MyH7 (MHC I)	ENSCPOG00000004208	AAGTATCGCAAGGCTCAA	CCTTTCCTTAATTCCAAGC	93
Bax	ENSCPOG00000011196	GGGTTGTCGCCCTTTTCTAT	CCCATGTTCTTCCAGATGGT	250
Bcl2	ENSCPOT00000019808	GAGTGTCAACCGGGAGATGT	AAACAGAGGCCGTACACTGG	151
MuRF1	ENSCPOT00000027054	GGAGCAGGAAGAGAAGCTGA	TGCTTTGGATGAGTTGCTTG	158
MAFBx	ENSCPOT00000010062	GGCTGCTGTGGAAGAATCTC	CCAGGAGAGAATGTGGCAAT	188
Calpain I	ENSCPOT0000004006	GGTGAAAGGCCATGCATACT	CTCCCCATCTTCCATCTTCA	196
Calpain II	ENSCPOT00000024361	TGCAAGATCATGGTGGACAT	TCAATGTTGAGCTCGTCGTC	245
Calpain III	ENSCPOT00000024237	GACAGCTGGAAGGACTGGAG	CATTCACCGACACTGTCCAC	193
PPAR Alpha	ENSCPOT0000001502	GATGCCGAGGTCTGAGAAAG	GGCCTTGACCTTGTTCATGT	151
PPAR Delta	ENSCPOT00000011491	TGTGCACGAGGCTATCTTTG	TCACTGTCGTCGAGTTCCAG	186
PGC1 Alpha	ENSCPOT0000001538	CCAAAGCTGAAGTCCTCCTG	GGGCCGCTTAGTCTTTCTCT	189
PGC1 Beta	ENSCPOT0000001980	GTCCGGAGAACTCTGAGACG	ACGGTGTGTCTCCTTCATCC	177
Six-1	ENSCPOT00000015700	AACTCCTCCTCCAACAAGCA	TTCTGAGCTGGACATGATCG	72
Eya-1	ENSCPOT0000000719	TGCATATGGGCAAACACAGT	AATTCCATACGGCTGTCCTG	88

5.2.9- Statistical Analysis

All data are reported as means + standard error of the mean (S.E.M). Comparisons were performed by analysis of variance (ANOVA) between multiple groups. Where statistical significance of the ANOVA permitted, the Bonferroni test was used to test for significance, with significance accepted as $P < 0.05$. All statistical analyses were performed using SPSS 17.0. Symbols used to indicate statistical significance were; * $P < 0.05$; ** $P < 0.01$; *** $P < 0.001$. # $P = < 0.1$ was regarded as a trend (Tominaga, Ndu et al. 2006; Jung, Reichstein et al. 2010).

5.3 – Results

5.3.1 - Animal weight parameters

All animals were in good general health throughout the study and all 24 were included in the following analyses. During the course of the study, both body mass (g) and quadriceps mass (g) were significantly increased with advancing age at all time points (P = <0.001). Animal weights progressed from a mean body mass of 510.60 + 3.27g at 2 months to 1160.78 + 48.72g at 7 months of age, whilst mean quadriceps mass increased from 4.68 + 0.28g at 2 months to 13.40 + 1.24g at 7 months of age. The quadriceps to body mass ratio, calculated by body mass (g) over quadriceps mass (g), remained constant at all ages (P = 1.000) (**FIGURE 5.1**).

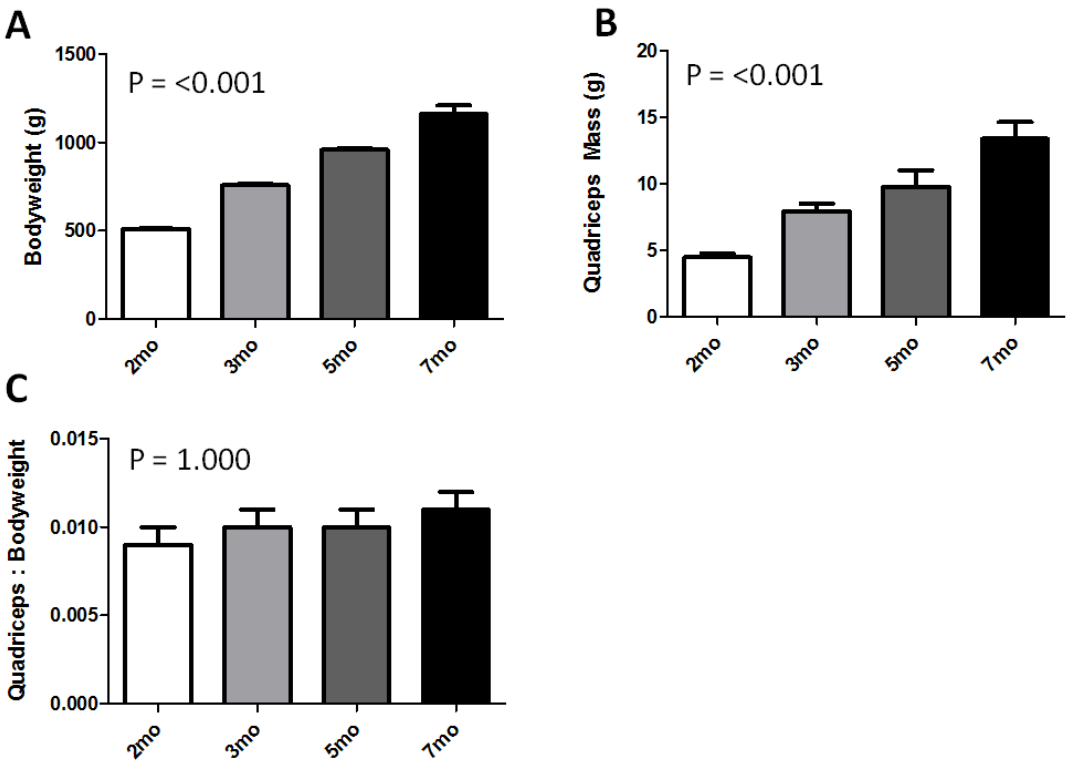

FIGURE 5.1 – The effects of advancing age on bodyweight (A), quadriceps mass (B) and quadriceps mass to bodyweight ratio (C). Data are mean + S.E.M; n = 6.

5.3.2 – Tibiofemoral pathology

Histological examination of tibiofemoral joints was performed at all ages as per (**METHOD 5.2.2**). At 2 months of age, animals were generally free from OA, with the exception of one animal which presented with mild proteoglycan loss in the superficial zone. At 3 and 5 months of age, animals presented with proteoglycan loss extending as deep as the mid-zone and mild cartilage surface irregularities. At 7 months of age, proteoglycan loss and cartilage surface irregularities were more pronounced than at previous ages, although no animals exhibited osteophytosis at any of the joint margins studied. Significant differences in the combined OA score were apparent between the ages of 2 and 3 months (P = 0.002) and 5 and 7 months (P = 0.093; trend). OA severity between the ages of 3 and 5 months remained unchanged (P = 0.394) (**FIGURE 5.2**).

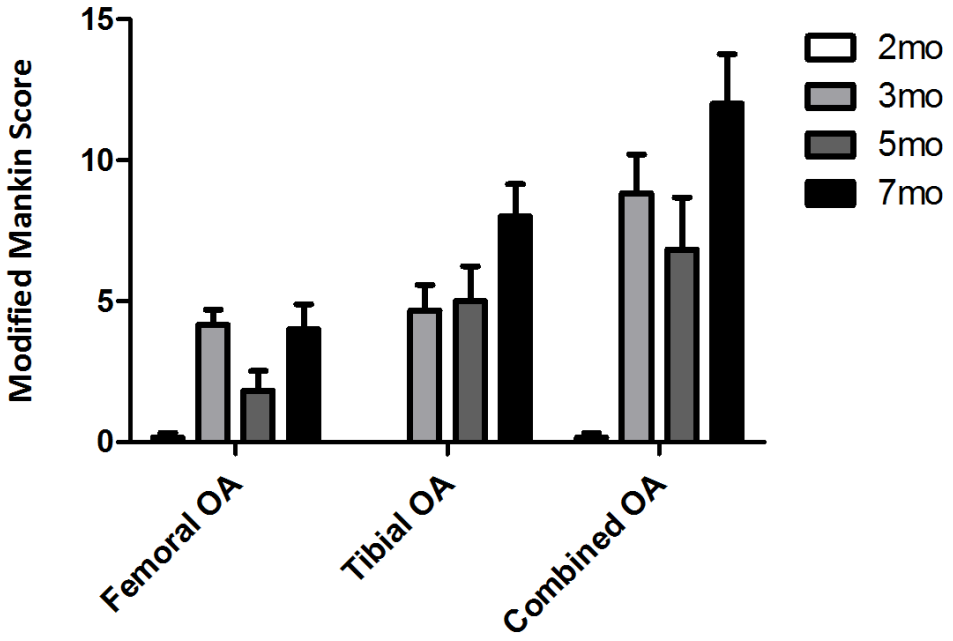

FIGURE 5.2 – The association of advancing age and tibiofemoral pathology. Data are mean modified Mankin scores + S.E.M; n = 6.

TABLE 5.3 – Individual modified Mankin scores for guinea pig joints.

Animal	Age (mo)	Toluidine Blue Staining				Articular Cartilage Structure				Osteophytosis			
		Med FEM	Med TIB	Lat FEM	Lat TIB	Med FEM	Med TIB	Lat FEM	Lat TIB	Med FEM	Med TIB	Lat FEM	Lat TIB
K	2	0	0	0	0	0	0	0	0	0	0	0	0
M	2	0	0	0	0	0	0	0	0	0	0	0	0
T	2	0	0	0	0	0	0	0	0	0	0	0	0
U	2	0	0	0	0	0	0	0	0	0	0	0	0
X	2	0	0	0	0	0	0	0	0	0	0	0	0
Z	2	0	1	0	0	0	0	0	0	0	0	0	0
B	3	2	1	2	3	1	0	0	0	0	0	0	0
G	3	3	3	3	4	0	2	0	0	0	0	0	0
H	3	0	1	4	2	0	0	0	0	0	0	0	0
J	3	0	2	2	1	0	0	0	0	0	0	0	0
L	3	2	2	2	2	0	0	0	0	0	0	0	0
P	3	2	2	2	2	0	1	0	0	0	0	0	0
D	5	1	2	2	2	0	0	0	0	0	0	0	0
F	5	0	1	0	1	0	0	0	1	0	0	0	0
N	5	2	3	1	3	0	0	0	3	0	0	0	0
V	5	2	2	1	3	0	0	1	3	0	0	0	0
W	5	0	1	0	0	0	0	0	0	0	0	0	0
Y	5	1	1	0	1	0	2	0	1	0	0	0	0
A	7	0	1	1	2	0	0	0	0	0	0	0	0
C	7	2	5	2	4	1	1	0	1	0	0	0	0
E	7	2	3	2	3	0	1	0	1	0	0	0	0
I	7	1	3	2	3	1	3	1	1	0	0	0	0
R	7	1	3	1	2	0	3	0	1	0	0	0	0
S	7	2	3	3	2	2	1	0	1	0	0	0	0

5.3.3 – Collagen type II degradation

Serum CTX II telopeptide was measured using a quantitative ELISA (Cartilaps) as described previously (**METHOD 5.2.4**). At 2 months of age, when cartilage turnover was most active, mean CTX II was 462.340 + 7.316 pg/ml. Following growth plate closure around the age of 3-4 months, serum CTX II levels dropped significantly (P = <0.001) until 7 months of age when levels were detected at just 33.632 + 3.169 pg/ml.

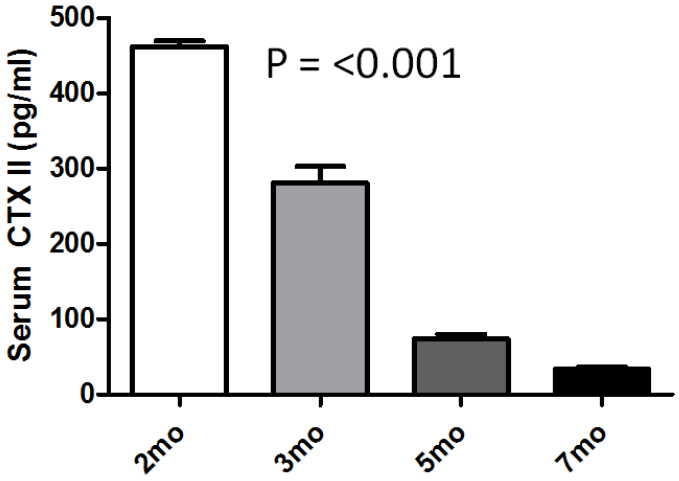

FIGURE 5.3 – The effects of advancing age on serum CTX II concentration. Data are mean + S.E.M; n = 6. P value refers to one-way analysis of variance.

5.3.4 - Serum cholesterol and triglyceride

Serum cholesterol and triglyceride concentrations were determined by specific ELISA. Serum cholesterol concentration was lowest at 2 months of age, and appeared elevated at 3 months (P = 0.099). Serum triglyceride concentration was unaffected by age (**FIGURE 5.4**).

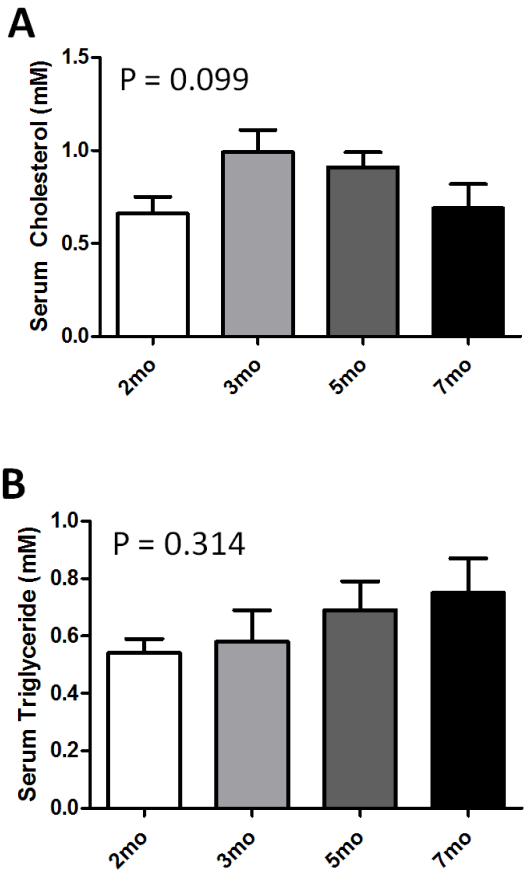

FIGURE 5.4 – The effects of advancing age on serum cholesterol (A) and triglyceride (B) concentration. Data are mean + S.E.M; n = 6. P value refers to one-way analysis of variance.

5.3.5 - Serum cytokines and chemokines

Serum cytokines and chemokines were determined quantitatively by Luminex™ analysis. In general, serum cytokine and chemokine levels remained static with advancing age with the exception of RANTES which was significantly affected by age (P = 0.034). Post-hoc analysis revealed a significant difference between the ages of 2 months and 3 months (P = 0.033) (**FIGURE 5.5**). A full serum analysis by Luminex™ quantification is included in (**TABLE 5.4**).

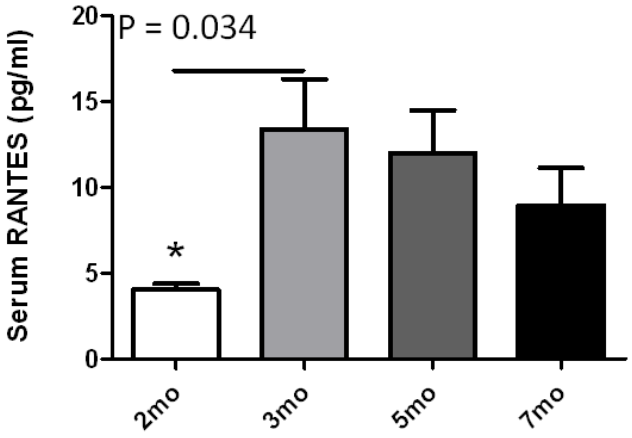

FIGURE 5.5 – The effects of advancing age on serum RANTES concentration. Data are mean + S.E.M; n = 6. P value refers to one-way analysis of variance.

TABLE 5.4 - Mean serum cytokine / chemokine concentration (pg/ml) ± S.E.M; n = 6

Parameter	2mo	S.E.M	3mo	S.E.M	5mo	S.E.M	7mo	S.E.M	P =
IL-4 (39)	2.410	0.043	2.403	0.057	2.390	0.043	2.426	0.061	0.969
IL-12(p70) (78)	77.360	17.177	67.119	11.414	76.704	10.052	76.713	16.242	0.946
IL-1a (53)	5.585	0.446	6.354	0.572	5.968	0.501	6.097	0.578	0.776
IL-1b (19)	51.139	3.655	54.865	4.227	49.284	2.429	52.148	3.366	0.722
IL-2 (36)	6.239	0.144	6.213	0.123	6.132	0.131	6.505	0.190	0.344
IL-3 (18)	2.803	0.065	2.697	0.118	2.536	0.090	2.749	0.097	0.246
IL-5 (52)	4.202	0.202	4.227	0.272	4.213	0.185	4.418	0.254	0.944
IL-6 (38)	1.898	0.428	1.839	0.223	2.099	0.339	1.878	0.343	0.950
IL-9 (33)	71.479	2.160	72.722	4.190	71.739	2.159	75.254	3.677	0.829
IL-10 (56)	25.784	2.533	23.746	2.141	23.688	1.816	26.580	2.837	0.824
IL-12(p40) (76)	16.420	1.837	15.374	1.576	17.698	1.079	16.870	1.316	0.735
IL-13 (37)	378.062	32.213	378.478	26.888	353.667	23.634	356.592	27.135	0.871
IL-17 (72)	5.208	0.084	5.278	0.170	5.176	0.111	5.518	0.120	0.237
Eotaxin (74)	1176.138	57.942	1198.557	57.804	1238.376	84.429	1215.193	80.605	0.937
G-CSF (54)	5.724	0.276	5.615	0.218	5.768	0.216	5.883	0.338	0.914
GM-CSF (73)	21.629	4.463	24.969	3.808	25.498	3.231	27.336	4.527	0.792
IFN-g (34)	16.218	2.056	15.661	1.592	14.318	0.790	16.263	1.499	0.844
KC (57)	2.042	0.182	2.011	0.195	1.918	0.102	1.923	0.163	0.945
MCP-1 (51)	94.265	6.402	86.629	4.545	90.825	3.398	92.004	3.513	0.682
MIP-1a (77)	142.137	31.764	163.923	18.540	161.734	33.596	198.083	28.391	0.353
MIP-1b (75)	16.673	1.267	15.791	1.672	14.906	1.049	15.688	0.764	0.794
RANTES (55)	4.017	0.369	13.416	2.907	12.014	2.497	8.937	2.209	**0.034**
TNF-a (21)	38.155	4.374	34.993	3.688	33.216	2.395	39.588	3.379	0.576

5.3.6 - Quadriceps femoris contractile and metabolic associated parameters

Quadriceps muscles were characterised with respect to their contractile and metabolic characteristics. Contractile properties of the quadriceps muscle were assessed by the expression of MHC specific mRNAs at all ages. MHC I mRNA expression was subject to considerable inter-animal variation at the ages of 3 and 5 months. MHC IIA mRNA was stable with increasing age (P = 0.623). Similar stability was noted with regards MHC IIB mRNA (P = 0.423), the expression of which remained constant irrespective of age. MHC IIX mRNA levels demonstrated a trend increase between the ages of 2 and 3 months (P = 0.087) followed by a reduction to baseline at 5 and 7 months of age.

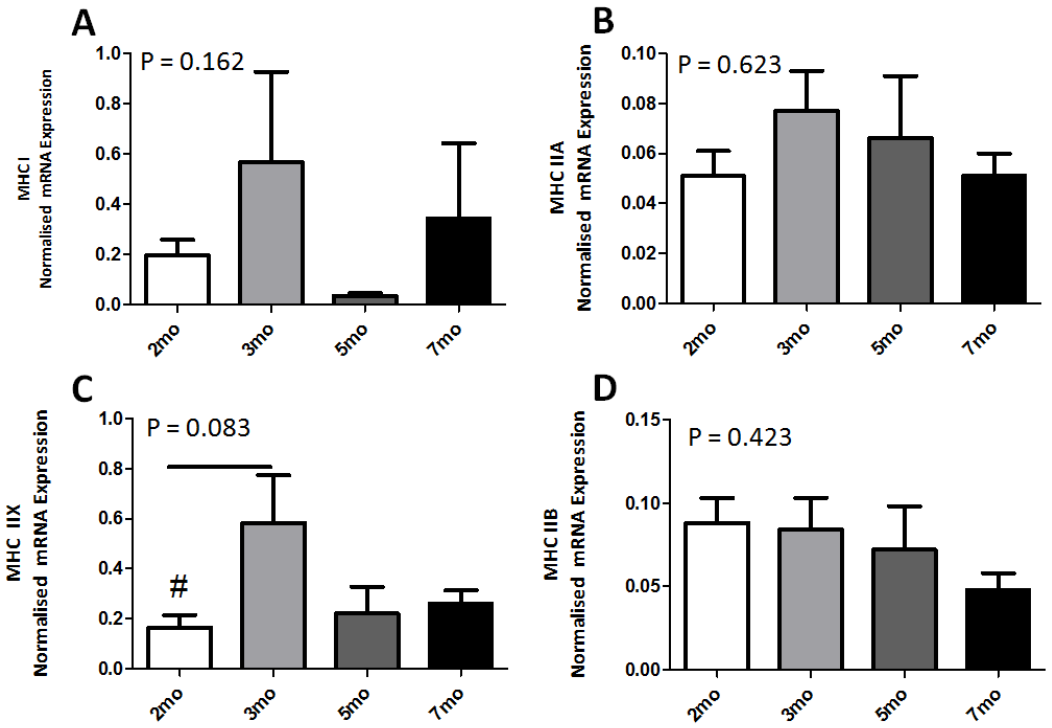

FIGURE 5.6 – The effects of advancing age on the myosin heavy chain isoform specific mRNAs of MHC I (A), MHC IIA (B), MHC IIX (C) and MHC IIB (D). Data are mean expression units + S.E.M normalised to total first strand cDNA concentration; n = 6. P values refer to one-way analysis of variance.

Isocitrate dehydrogenase (ICDH) enzyme activity, associated with slow-twitch muscle fibres, was determined in quadriceps tissue homogenates as an index of metabolic capacity. Similarly, lactate dehydrogenase (LDH) activity, associated with faster-twitch fibres was determined as an indicator of glycolytic metabolic capacity. Enzyme activities were normalised to total extractable protein concentration and expressed as mOD/min/µg total protein. ICDH activity appeared to be modulated by age (P = 0.096) and demonstrated a trend increase between the ages of 2 and 7 months (P = 0.071). The increase in ICDH activity was also noted between the ages of 5 and 7 months (non-significant). Glycolytic metabolic capacity remained static irrespective of age (**FIGURE 5.6**).

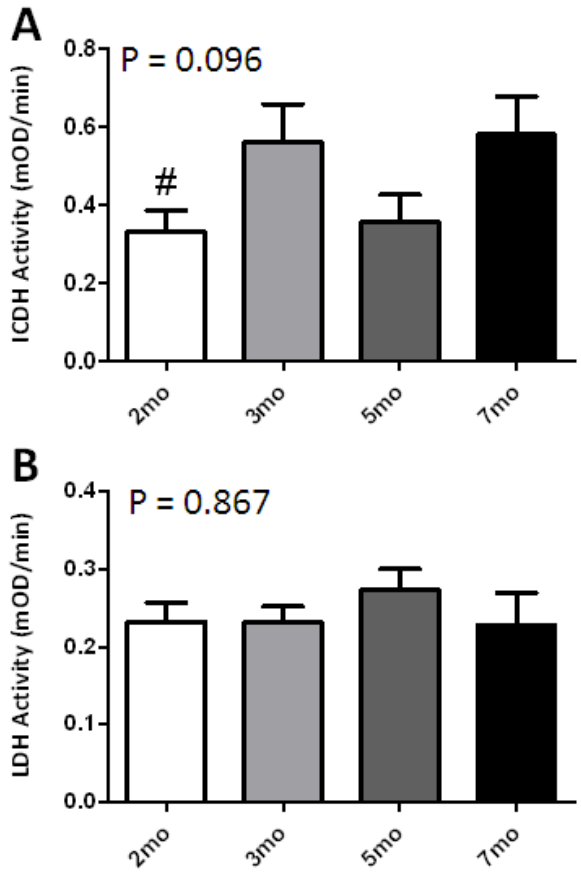

FIGURE 5.7 – The effects of advancing age on ICDH and LDH activity in whole quadriceps homogenates. Data are mean mOD/min normalised to total extractable protein + S.E.M; n = 6. P values refer to one-way analysis of variance.

5.3.7 – Protein synthetic potential

As an index of protein synthetic potential, phosphorylated and total 4EBP1 protein was quantified by western blot. 4EBP1 is an elongation factor 4E (eIF4E) associated protein that controls mRNA translation by regulating the formation of the cap-initiation complex. When 4EBP1 is hyperphosphorylated by mTOR (mammalian target of rapamycin), its inhibitory binding to eIF4E is prevented thereby enhancing protein synthesis (Connolly, Braunstein et al. 2006). No changes to the phosphorylation status (ratio) of 4EBP1 were noted with respect to advancing age.

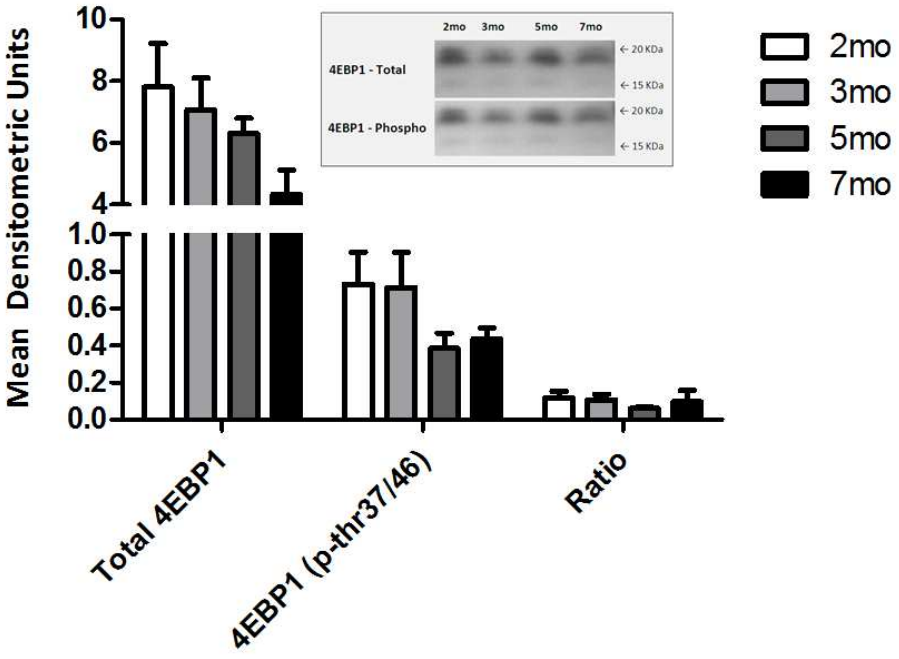

FIGURE 5.8 – The effects of advancing age with the ratio of phosphorylated to total 4EBP1 protein. Data are mean densitometric units, normalised to total protein load + S.E.M; n = 6. Inset – representative blot showing 4EBP1 immuno-reactivity of animals aged 2, 3, 5 and 7 months from 75µg protein.

The gene expression profiles of known modulators of muscle function were assessed by quantitative PCR. Due to difficulties in obtaining annotated cDNA sequences specific to guinea pig, all cDNAs were derived by comparison with rat and mouse sequence data as previously described (**METHOD 5.2.8**). A description of the specific pathways targeted can be found within (**CHAPTER 1.3.6**).

5.3.8 – Skeletal protein degradation

To gain an indication of changes in skeletal protein degradation, factors involved in proteosomal degradation and proteolysis via the calpain system were assessed. MuRF and MAFBx are involved in the targeting of proteins for degradation via the proteosome. Whilst MAFBx mRNA remained unaltered irrespective of age (P = 0.637), MuRF mRNA was dramatically reduced at 7 months of age compared with all other age points studies, however this effect failed to reach the level of a statistical trend (P = 0.102).

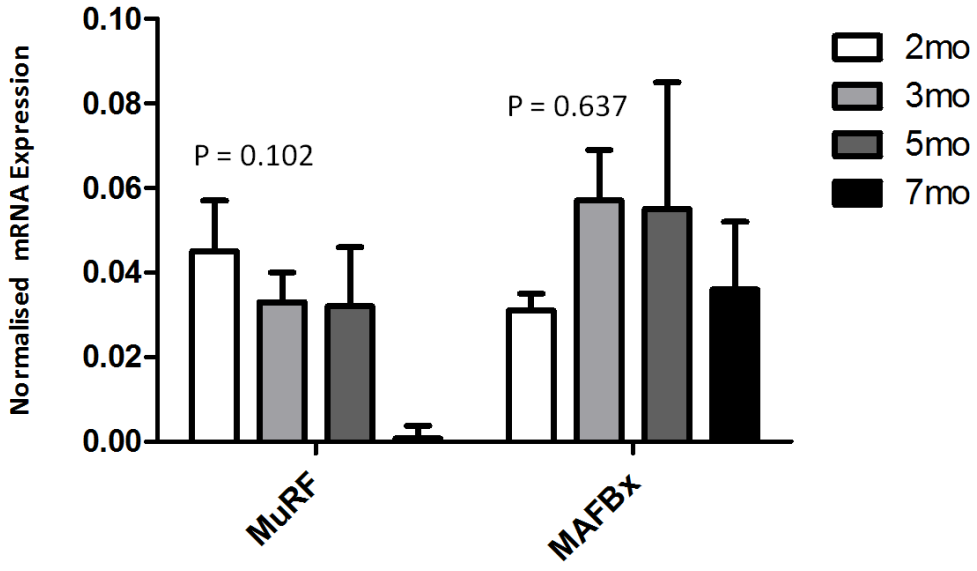

FIGURE 5.9 – The effects of age with the mRNA expression of the E3 ligases MuRF and MAFBx. Data are mean normalised expression units + S.E.M; n = 6

Assessment of calpain family members I, II and III revealed little modulation with respect to age. Calpain I, II and calpain III showed no response to age (P = 0.208, 0.103 and 0.407 respectively).

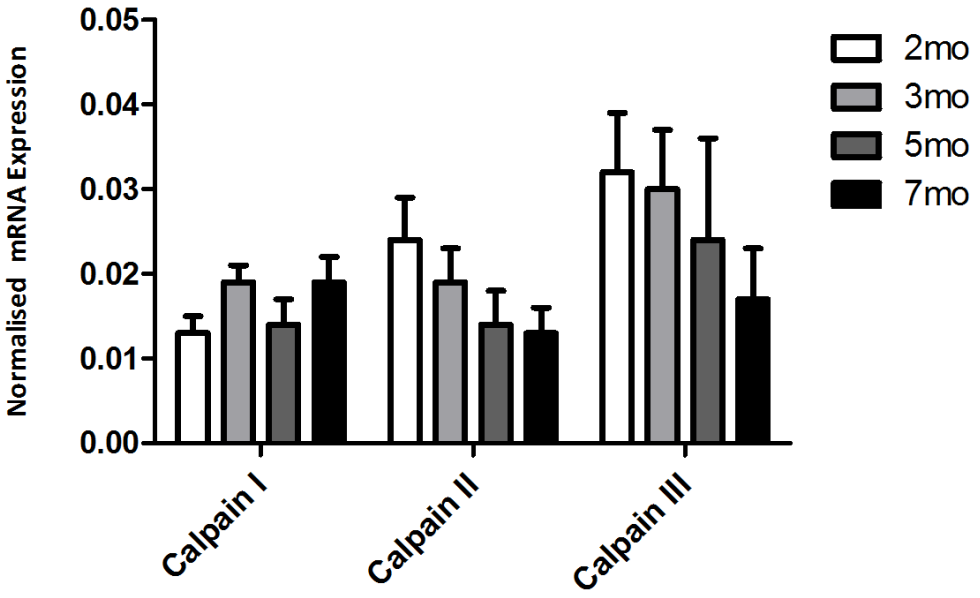

FIGURE 5.10 – The effects of age with the mRNA expression of calpain I, II and III. Data are mean normalised expression units + S.E.M; n = 6.

5.3.9 – Apoptotic potential

The apoptotic response potential of the quadriceps skeletal muscle was assessed by quantifying the mRNAs of pro-apoptotic Bax and anti-apoptotic Bcl2 (Otter, Conus et al. 1998). Whilst Bcl2 mRNA was relatively stable with respect to age, Bax mRNA decreased dramatically after 3 months of age (P = 0.004) suggesting a reduced apoptotic potential.

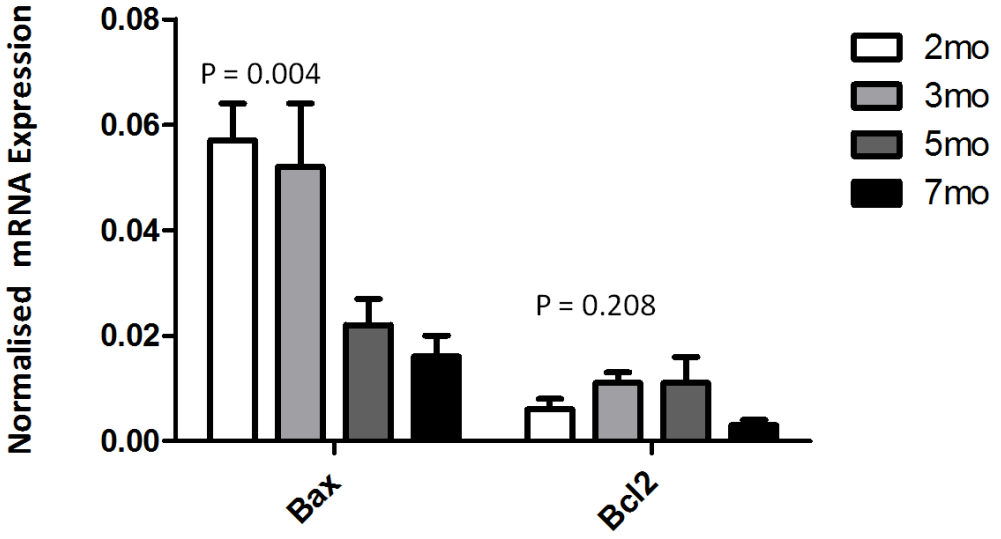

FIGURE 5.11 – The effects of age on mRNA expression of Bax and Bcl2. Data are mean normalised expression units + S.E.M; n = 6. P values refer to one-way analysis of variance.

5.3.10 – Metabolite signalling

To detect potential changes in metabolite signalling, members from the PGC1 and PPAR families were assessed with respect to age. PGC1α, PGC1β and PPARα displayed similar expression profiles but were statistically unaffected by age (P = 0.513, 0.241, 0.305 respectively). PPARδ mRNA however, was most abundantly expressed at 2 months of age and reduced thereafter (P = 0.042).

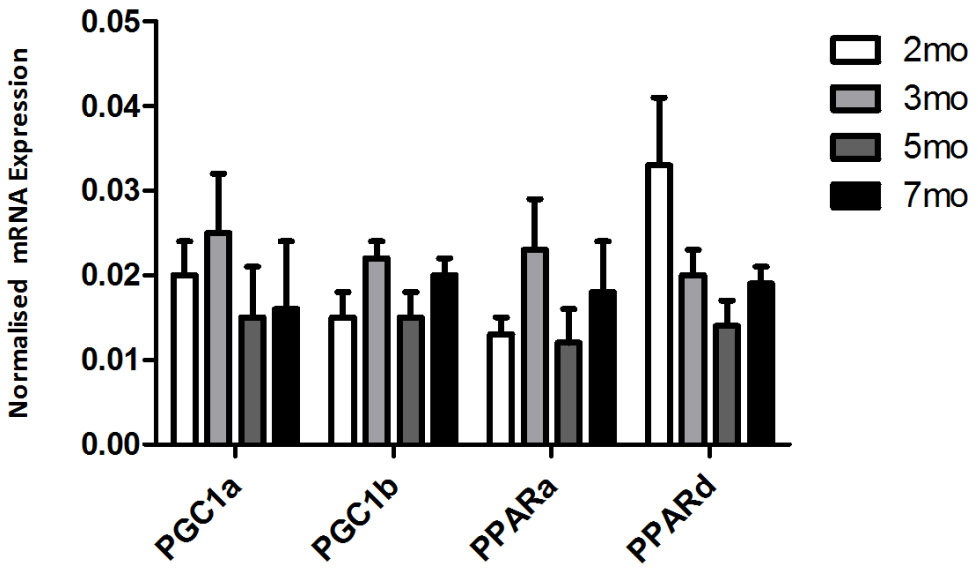

FIGURE 5.12 – The association of age with the mRNA expression of factors involved in metabolite signalling. Data are mean normalised expression units + S.E.M; n = 6

The mRNA of Six-1 and Eya-1, two novel transcription factors reported to induce slow-twitch to fast-twitch muscle fibre changes with an accompanied increase in glycolytic metabolic potential (Grifone, Laclef et al. 2004) were also quantified in quadriceps skeletal muscle samples. Whilst the expression profiles of both genes appeared similar, the expression of Six-1 was increased between the ages of 2 and 3 months and similarly 5 or 7 months (0.065) whereas Eya-1 expression remained unaltered by age.

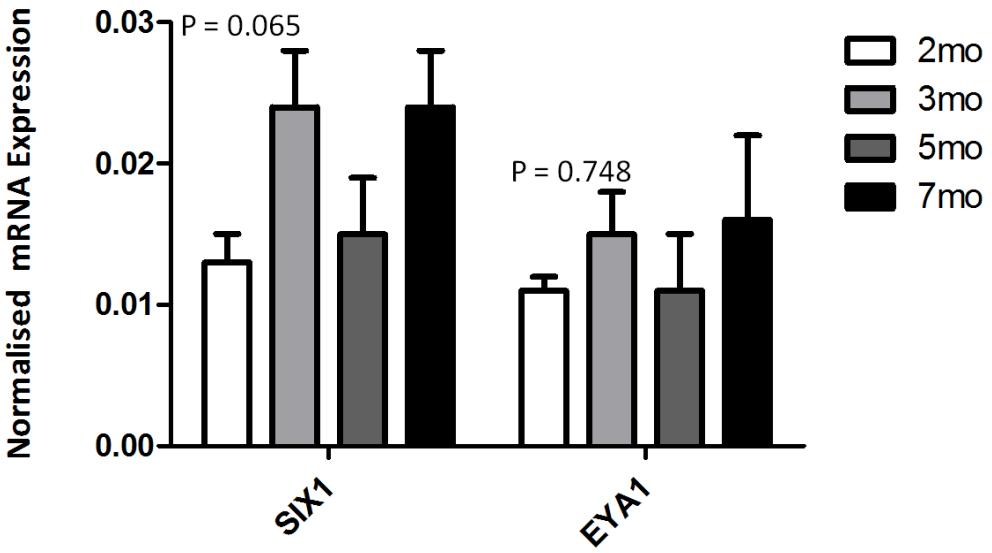

FIGURE 5.13 – The association of age with the mRNA expression Six-1 and Eya-1. Data are mean normalised expression units + S.E.M; n = 6. P values refer to one-way analysis of variance.

5.3.11 – Correlation of muscle parameters with OA severity

Pearson's product moment calculation (PPMC) was used to elucidate correlation between OA severity and the parameters of quadriceps function assessed at each age. Both body mass and age displayed a strong positive correlation with OA severity (r^2 = 0.671, P = <0.001; r^2 = 0.642, P = 0.001 respectively). In order to elucidate more subtle relationships, partial correlation was performed controlling for body mass in

all animals. The fast-twitch muscle fibre associated MHC IIX isoform was found to positively correlate with OA severity (r^2 = 0.527, P = 0.012) suggesting that those animals with more abundant MHC IIX mRNA had more severe osteoarthritic lesions. Both E3 ligases MuRF and MAFBx, and the skeletal muscle associated cysteine protease Calpain III, were negatively correlated with OA severity suggesting that OA was not linked with proteolytic activity in this study (**TABLE 5.5**).

TABLE 5.5 – Correlation between combined OA score and various quadriceps parameters (controlled for body mass)

Parameter	Association with OA score (r^2)	P =
MHC IIX mRNA	0.527	**0.012**
MuRF mRNA	-0.545	**0.007**
MAFBx mRNA	-0.446	**0.033**
Calpain III mRNA	-0.532	**0.009**

5.3.12 – Correlation of serum cytokines with OA severity

Serum cytokine and chemokine concentrations (pg/ml) were assessed with respect to their relationship with OA severity at all ages. Interestingly, none of the factors assessed demonstrated any significant relationship with the severity of knee OA noted (**TABLE 5.6**).

TABLE 5.6 – Correlation between serum cytokines and OA severity (controlled for body mass)

Parameter	Association with OA score (r^2)	P =
IL-4 (39)	0.106	*0.630*
IL-12(p70) (78)	-0.055	*0.802*
IL-1a (53)	0.153	*0.487*
IL-1b (19)	0.224	*0.303*
IL-2 (36)	0.245	*0.259*
IL-3 (18)	-0.036	*0.869*
IL-5 (52)	0.060	*0.786*
IL-6 (38)	0.045	*0.839*
IL-9 (33)	0.177	*0.418*
IL-10 (56)	0.113	*0.607*
IL-12(p40) (76)	-0.132	*0.547*
IL-13 (37)	0.064	*0.771*
IL-17 (72)	0.166	*0.448*
Eotaxin (74)	0.095	*0.667*
G-CSF (54)	-0.057	*0.797*
GM-CSF (73)	0.052	*0.812*
IFN-g (34)	-0.005	*0.983*
KC (57)	-0.041	*0.853*
MCP-1 (51)	-0.097	*0.659*
MIP-1a (77)	0.249	*0.252*
MIP-1b (75)	0.181	*0.408*
RANTES (55)	0.110	*0.618*
TNF-a (21)	-0.067	*0.761*
IL-4 (39)	0.106	*0.630*

5.4 – Discussion

This is the first study to report age-related changes to contractile and metabolic parameters of the quadriceps femoris skeletal muscle group in the Dunkin Hartley guinea pig, and furthermore endeavour to link these to the severity of knee osteoarthritis which commonly affects this strain. As the initial development of osteoarthritis occurs in the DH guinea pig during the longitudinal growth phase, it was anticipated that body mass would be significantly elevated all time points studied. As such, an ontogeny-based approach was taken by initially comparing the effects of age on both osteoarthritis and muscle function, and then subsequently correlating these findings to disease severity.

5.4.1 – Development of OA-like lesions and cartilage turnover

As anticipated, advancing age was associated with increased body mass and quadriceps mass. The quadriceps to body mass ratio, indicative of quadriceps hypertrophy / atrophy in relation to body mass remained unaltered as age increased, suggesting that overt quadriceps atrophy was not present in any of the animals assessed. CTX II telopeptide was measured in serum as an index of growth plate maturity using an assay that detects degradation products of C-terminal type II collagen. Levels fell significantly as age increased and the growth-plate closed at approximately 3-4 months of age. CTX II concentrations were concurrent with other published reports in the same strain which have also reported growth plate-closure at approximately 3-4 months of age (Watson, Hall et al. 1996; Huebner, Deberg et al. 2007).

Assessment of toluidine blue stained step coronal sections revealed evidence of osteoarthritic-like lesions from as early as 3 months of age. OA-like lesions tended to be more severe on the tibial condyles than on the respective femoral condyles, with tibias presenting with higher OA scores than femurs at all ages assessed. OA-like lesions did not predominantly affect any particular aspect of the knee, with medial

and lateral aspects of both condyles presenting with similar OA scores. Pathology was associated with reduced proteoglycan staining at the joint margin and changes to articular cartilage structure as detailed in **TABLE 5.1**, however no osteophytosis was noted at any site in any of the animals assessed. In general, OA scores progressed concurrent with age through until 7 months of age when the final analyses were performed. With reference to the existing literature available for the assessment of OA in the Dunkin Hartley strain, total histological scores were concurrent with those of other published studies, utilising the same strain and joint scoring system (Huebner 2006). In this study, tibial condyles exhibited more pronounced osteoarthritic changes than the respective femurs, an observation reported by several other studies (Bendele and Hulman 1991; Bendele 2001; Bendele 2002; Tessier, Bowyer et al. 2003). Given that guinea pigs transfer around 75% of load through the medial aspects of their joints (Bendele 2001), it may perhaps be expected that the medial portion of the tibial condyle would be predominantly affected by OA-like lesions. Medial predominance to OA was not noted in this study, however previous studies have not routinely separated medial and lateral pathology scores, and therefore it is unclear whether the increased medial joint load translates to increased medial OA severity in practice.

5.4.2 – Changes in biomarkers of skeletal muscle function

Examination of factors indicative of contractile and metabolic properties of the quadriceps skeletal muscle revealed age-related effects on specific muscle fibre-types. Slow-twitch associated MHC I mRNA demonstrated marked inter-animal variation, and increased mean expression around the time of OA initiation. Although this observation failed to reach statistical significance in isolation ($P = 0.162$); ICDH activity, associated with slow-type muscle fibres and indicative of oxidative potential (Brandstetter, Picard et al. 1997), also displayed a similar expression pattern, adding evidence towards an effect of age on MHC I mRNA. MHC I is associated with type I, fatigue resistant muscle fibres (Bamford, Putman et al. 2005) most commonly found in postural, stabilising skeletal muscles (Adams, Haddad et al. 1994). It is one

possibility that the changes in MHC I expression noted may indicate altered joint stability around the time of OA initiation, although joint biomechanics were not assessed in this study.

When considering faster-twitch muscle fibres, MHC IIX was elevated at 3 months of age compared to all other ages (P = 0.083). The mRNA of Six-1 , a novel factor associated with fast-twitch muscle fibres was also increased at 3 months (Grifone, Laclef et al. 2004), however the anticipated increase in glycolytic activity did not concur with no apparent effect of age on quadriceps LDH activity. Although LDH activity remained unchanged, studies reporting strong correlations between LDH activity and fibre type have generally been carried out on untreated subjects and therefore assessed basal muscle fibre type (Briand, Talmant et al. 1981). Moreover, studies inducing changes in muscle fibre type have previously reported a disparity between fibre type and LDH activity (Mounier, Cavalié et al. 2007), suggesting that different mechanisms are responsible for the control of MHC fibre type and metabolic potential. In this study, other measures of glycolytic potential such as the measurement of phosphofructokinase, the rate limiting glycolytic enzyme (Trivedi and Danforth 1966), may have provided a further indication of glycolytic potential, however the possibility still exists that MHC changes were present without the expected change in metabolic potential. The relative transcript abundance of MHC IIA and MHC IIB mRNAs were unaffected by age. MHC IIX is associated with the expression of fast glycolytic muscle fibres. MHC IIX is the second fastest MHC isoform in many laboratory species including the mouse and rat (Weiss and Leinwand 1996), however it is the fastest MHC isoform in the human (Harridge 2007). The elevated expression of MHC IIX, indicative of fast glycolytic muscle fibre expression, occurred around the time of OA induction, as with the change in MHC I expression. This finding may add further weight to the possibility of altered joint biomechanics around the time of OA induction.

5.4.3 – Assessment of quadriceps transcriptome

Quadriceps gene expression of known modulators of muscle function was determined by quantitative PCR. Assessment of factors involved in proteosomal degradation and proteolysis via the calpain system revealed no changes at the level of mRNA expression in response to advancing age.

Pro-apoptotic Bax mRNA was however, significantly decreased with advancing age in all animals studied. Previous studies on aged rats have demonstrated age-related *increases* in Bax expression with concomitant decreases in Bcl-2 expression (Chung and Ng 2006). In the same context, Song and colleagues have shown increased Bax and decreased Bcl-2 in old sedentary rats with age-related sarcopenia (Song, Kwak et al. 2006). Interestingly, the latter study demonstrated that the pro-apoptotic state could be altered by 12 weeks of exercise training (Song, Kwak et al. 2006). Although such studies are unable to explain the decrease in Bax expression noted in this study, taken together with the unaltered quadriceps to body mass ratio, they further confirm that age-related sarcopenia / atrophy was not present and therefore unlikely to be the cause of OA in this strain.

5.4.4 – Serum analytes

In this study, serum cholesterol concentration was found to be highest at 3 months of age, when the first histological evidence of osteoarthritis was found. Levels fell thereafter and by 7 months of age, were comparable to 2 month old animals. Osteoarthritis has been previously associated with elevated serum cholesterol concentration (Sturmer, Sun et al. 1998) which has been reported to be an independent risk factor for OA (Sturmer, Sun et al. 1998). In this study, it would appear that cholesterol concentration was more closely involved with the initiation of OA rather than its progression. Conversely, serum triglyceride levels were statistically unaffected by age in this study, however numerically levels increased with age. Previous clinical studies in human patients have positively associated elevated triglyceride levels with the incidence of OA (Cheras, Whitaker et al. 1997)

however this study was carried out in patients with degenerative hip OA. Although elevated serum cholesterol and triglyceride levels were not correlated with OA severity in this study, it must be noted that all animals presented with mild osteoarthritic lesions which have previously been shown to continue to progress until 18 months of age (Bendele 2001). It is therefore possible that a potential relationship between serum cholesterol / triglyceride and OA may become apparent as disease progresses.

Serum cytokine analysis was performed by Luminex™ analysis as described in **CHAPTER 5.2.6**. Cytokine determination revealed that although the majority of cytokines and chemokines remained static with advancing age, regulated upon activation, normal T-cell expressed and secreted (RANTES) concentration was significantly elevated around the time of OA initiation (3 months), and decreased with age thereafter. RANTES has been implicated in articular cartilage degradation by the enhancement of matrix metalloproteinase - 3 (MMP-3) production and suppression of proteoglycan in osteoarthritic chondrocytes (Yuan, Masuko-Hongo et al. 2001). Moreover, elevated serum RANTES concentrations have been specifically associated with active osteoarthritic disease when compared with healthy controls and people with established, non-active disease (Toncheva, Remichkova et al. 2009) suggesting that RANTES expression may play a role in the initial development of osteoarthritic disease.

It is noteworthy that other articular joints have yet to be assessed with respect to osteoarthritis in the Dunkin Hartley strain guinea pig. It must therefore be retained that elevated RANTES could, for example, be attributed to disease in a distant articular joint.

5.4.5 – Correlation between OA severity and biomarkers of skeletal muscle function

Correlation between the severity of knee OA in the 24 subjects analysed, and the various measures of weight and muscle function revealed that OA severity was

correlated principally with bodyweight, however a strong positive correlation between OA severity and MHC IIX mRNA abundance was also statistically significant. MHC IIX mRNA expression was markedly elevated around the time of OA initiation (3 months), adding further weight towards an association between muscle fibre-type and OA severity. Numerous studies have correlated OA with body mass both in the human population (Arden and Nevitt 2006; Grotle, Hagen et al. 2008) and in the Dunkin Hartley strain as utilised here (Bendele and Hulman 1991; Bendele 2001; Hyttinen, Arokoski et al. 2001). Furthermore, dietary restriction resulting in decreased bodyweight has been shown to reduce OA lesion severity in the Dunkin Hartley strain (Bendele and Hulman 1991). Increased MHC IIX mRNA expression may be indicative of increased expression of fast glycolytic muscle fibres. Although fibre type was not directly assessed in this study, if fast glycolytic fibres were expressed at the expense of slow, stabilising muscle fibres, it is therefore possible that altered joint biomechanics may be implicated in the development and progression of osteoarthritis in this strain.

OA was significantly negatively correlated with quadriceps skeletal muscle expression of MuRF, MAFBx and calpain III at the mRNA level. These findings suggest that the severity of osteoarthritis was not associated with skeletal muscle proteolysis routinely reported in muscle atrophy conditions (Lecker, Jagoe et al. 2004). Considered in association with the lack of quadriceps to body mass ratio perturbations noted previously, and the age-related decreased in pro-apoptotic Bax mRNA expression, these changes suggest that skeletal muscle atrophy is not associated with OA severity in the Dunkin Hartley guinea pig.

Furthermore, correlation analysis between serum cytokine and chemokine levels and OA severity revealed no significant association with any of the factors assessed, suggesting that OA severity differed irrespective of inflammatory status. Only one study directly assessing cytokine and chemokine levels in the Dunkin Hartley strain has been conducted to date. The authors reported that the histological grade of

osteoarthritis was significantly associated with serum interleukin-6 (IL-6) and granulocyte colony-stimulating factor (G-CSF) concentration (Huebner, Seifer et al. 2007). Although the data obtained in this study does not concur with the observations of Huebner and colleagues, 2007, several differences in the study design exist which may preclude the direct comparison of results. Firstly, the oldest animals assessed within this thesis were 7 months of age whereas Huebner and colleagues were able to obtain animals up to 18 months of age when osteoarthritic changes are more pronounced. Secondly, Huebner and colleagues had access to control animals (Strain 13), which have become subsequently unavailable due to out-breeding, which permitted them to control for strain differences prior to correlating cytokine concentrations with histological evidence of OA.

When considering further studies utilising the Dunkin Hartley strain guinea pig, the natural progression would be to perform an intervention study assessing the effects of clenbuterol induced hypertrophy on disease progression. This experimental design (treated verses control) would also circumvent the problems associated with obtaining a suitable control strain, as the untreated Dunkin Hartley guinea pigs would suffice for this purpose.

5.4.6 – Summary

In summation, this study confirmed that the spontaneous development of knee OA in the Dunkin Hartley strain was indeed associated with altered quadriceps muscle properties. Data suggest that the development of OA in the Dunkin Hartley guinea pig was associated with changes in MHC expression, indicative of altered quadriceps muscle fibre type. Conversely, assessment of quadriceps mass and the expression of proteolytic signalling factors suggested that overt skeletal muscle atrophy did not develop coincident with OA in this strain. Taken together, these findings suggest that altered quadriceps function was more likely a product of altered MHC expression, and by inference altered muscle function, than of altered skeletal muscle mass *per se*.

CHAPTER 6 - THE EFFECTS OF OSTEOARTHRITIS ASSOCIATED CYTOKINES ON MARKERS OF MUSCLE DYSFUNCTION IN VITRO

6.1 – Introduction

Although traditionally osteoarthritis has been considered a non-inflammatory disease, the role of inflammatory cytokines such as TNFα and IL1β in the pathogenesis of OA has gained extensive interest due to their involvement during disease initiation and progression, and the potential benefits of anti-cytokine therapeutics (Goldring 1999). Although there is still some disagreement within the current literature, it is generally accepted that IL1β is involved in the early and late stages of OA whilst TNFα is involved almost exclusively in the initiation of osteoarthritic changes (Goldring 1999), and considered a principal pro-inflammatory cytokine. Both TNFα and IL1β are thought to be produced locally, by the inflamed synovium and chondrocytes (Chen, Lin et al. 2008) and are thought to contribute to the development and progression of OA via their ability to inhibit proteoglycan synthesis in chondrocytes (Fernandes, Martel-Pelletier et al. 2002). Moreover, extensive cell culture studies using chondrocytes or cartilage fragments have demonstrated that TNFα, in combination with IL1β was able in induce degradation of the cartilage matrix (Westacott and Sharif 1996; Goldring 1999).

Although neither cytokine was found to be significantly elevated in association with the early stages of developing OA in the guinea pig model of disease (**CHAPTER 5**), extensive evidence reports their involvement in the human condition (Westacott 1990; Westacott and Sharif 1996; Fernandes, Martel-Pelletier et al. 2002) and it is therefore noteworthy as to whether these factors are able to induce changes in skeletal muscle phenotype and therefore ascertain whether they could, potentially be responsible for the skeletal muscle changes associated with OA of the knee.

In order to assess the direct effects of cytokine treatment on skeletal muscle phenotype in the absence of other confounding factors, an *in vitro* model utilising rat-derived L6.G8.C5 myotubes was proposed. The myogenic L6.G8.C5 cell line was originally developed by Yaffe, 1968 (Yaffe 1968) and exhibits many myogenic

characteristics including the formation of myoneural junctions, contractility and the expression of creatine kinase (Elsner, Quistorff et al. 1998). Despite many publications spanning almost 50 years, little information is available with regards the myosin heavy chain (MHC) expression profile of this cell line. Whilst some publications suggest that the L6 cell lines express embryonic, neonatal and adult MHC IIB mRNAs (Arcangelis, Coletti et al. 2005), others suggest that the cells are committed to producing MHC IIX fibres only (Pin and Merrifield 1997). It was therefore necessary to characterise the basal MHC expression profile of the L6.G8.C5 cell line prior to embarking on the cytokine treatment study.

6.1.1 – Hypotheses and aims

Rat-derived myotubes (L6.G8.C5) will express a range of MHC isoforms, indicative of the presence of multiple fibre types, and thus model the *in vivo* situation. Osteoarthritis has been associated with both elevated serum TNFα concentration and type II muscle fibre atrophy. It is therefore hypothesised that the administration of recombinant rat TNFα to rat-derived myotubes will result in changes to their MHC composition, indicative of fibre type shifts. More specifically, it is hypothesised that TNFα will induce a reduction in the abundance of fast-type II fibre specific mRNAs (MHC IIX, MHC IIB), providing these fibre-types are in fact expressed by the L6.G8.C5 cell line.

The following specific aims will be addressed;

- Characterise the L6.G8.C5 cell line with respect to MHC expression
- Collect preliminary data regarding the effects of TNFα on MHC expression

6.2 – Experimental Protocol

6.3.1 – Characterisation study

L6.G8.C5 rat derived myoblasts were obtained from ECACC (92121114). Cells were seeded at a density of 60,000 cells / ml media onto 6-well plates (Nunc) and cultured in Glutamax-1™ media (Gibco, Invitrogen) supplemented with 10% (v/v) foetal calf serum (FCS), 100 units penicillin and 100µg streptomycin / ml media (Gibco). The anti-mycotic fungizone, commonly included within commercially available anti-biotic / anti-mycotic preparations for cell culture, was not included within the media as previous studies have reported altered cell morphology and differentiation following its administration (Ilarraza-Lomeli, Cisneros-Vega et al. 2007). At approximately 80% confluence, total RNA was extracted from three random wells. The remaining cells were differentiated into myotubes by culture in serum restricted Glutamax-1™ media containing 2% horse serum (HS), 100 units penicillin and 100µg streptomycin / ml for 4, 6 and 8 days respectively. At each time point, total RNA was extracted from three random wells.

6.3.2 – Cytokine treatment studies

L6.G8.C5 cells were cultured as above until 4 days post differentiation. Cells were treated with varying concentrations of recombinant rat TNFα (between 100 and 10,000pg / ml media) (Fisher) for 48 hours in triplicate. Following cytokine treatment, total RNA was extracted and stored at -80^{o}C.

6.3.3 – RNA extraction, DNase digestion and reverse transcription

Total RNA was extracted in accordance with (**METHOD 2.1.1**) with the exception that 1ml TRIzol was added directly to the 6-well plate, and the cells scraped from the surface and passed through a 23-gauge needle 10-times rather than homogenising with a Polytron probe to reduce sample loss. Contaminating genomic DNA was removed in accordance with (**METHOD 2.1.2**), and complementary DNA (cDNA) generated as in (**METHOD 2.1.5**) using random primers (Promega).

6.3.4 – Quantitative RT PCR

The expression of myosin heavy chain (MHC) isoforms I, IIA, IIX and IIB were determined by quantitative PCR as described in (**METHOD 2.1.7.2**) using oligonucleotide primers published previously by Jaschinski et al, 1998 (Jaschinski, Schuler et al. 1998). The embryonic isoform of MHC (MHC-Emb) was also determined based upon L6.G8.C5 cells being essentially of neonatal origin. Finally, myogenin mRNA was determined as an index of myoblast differentiation, using primers directed against rat cDNA sequence accession number ENSRNOG00000030743 (Ensemble Release 56). Oligonucleotide primer sequences are included within (**TABLE 6.1**). Expression data was determined using the comparative CP / dCT method (**CHAPTER 3.2.7**) and all quantitative PCR reactions were normalised to the concentration of first strand cDNA (OliGreen, Invitrogen) (**METHOD 5.2.7**).

6.3.5 – Statistical analysis

All data are reported as means + standard error of the mean (S.E.M). Comparisons were performed using analysis of variance (ANOVA) between multiple groups. The Dunnett's post-hoc test was used to test for significance relative to control. Symbols used to indicate statistical significance were; * $P < 0.05$; ** $P < 0.01$; *** $P < 0.001$. # $P = < 0.1$ was regarded as a trend (Tominaga, Ndu et al. 2006; Jung, Reichstein et al. 2010).

TABLE 6.1 – Oligonucleotide primer sequences for quantitative PCR reactions

Gene Name	Forward Primer (5' - 3')	Reverse Primer (5' - 3')	Amplicon (bp)
MHC I	ACAGAGGAAGACAGGAAGAACCTAC	GGGCTTCACAGGCATCCTTAG	81
MHC IIA	TATCCTCAGGCTTCAAGATTTG	TAAAATAGAATCACATGGGGACA	265
MHC IIX	CGCGAGGTTCACACCAAA	TCCCAAAGTCGTAAGTACAAAATGG	178
MHC IIB	CTGAGGAACAATCCAACGTC	TTGTGTGATTTCTTCTGTCACCT	129
MHC - Emb	AGCAGAGGAGGCTGAGGAACAATC	GGCCTCCTCAAGATGCGTTTACTC	181
Myogenin	AGTGAATGCAACTCCCACAGC	GTGGCGTCTGACACCAACTCA	254

6.3 – Results

6.3.1 – Characterisation of L6.G8.C5 rat derived myoblasts

6.3.1.1 – Cell morphology

Seeded myoblasts reached 80% confluence 2 days post seeding. Following serum restriction, cells began to elongate and form multinuclear complexes as shown in (**FIGURE 6.1**), with myotubes becoming increasingly large up until 8 days post differentiation. At 8 days post differentiation, cells were still firmly adhered to the 6 well plates in which they were grown, suggesting that culture for longer than 8 days was possible.

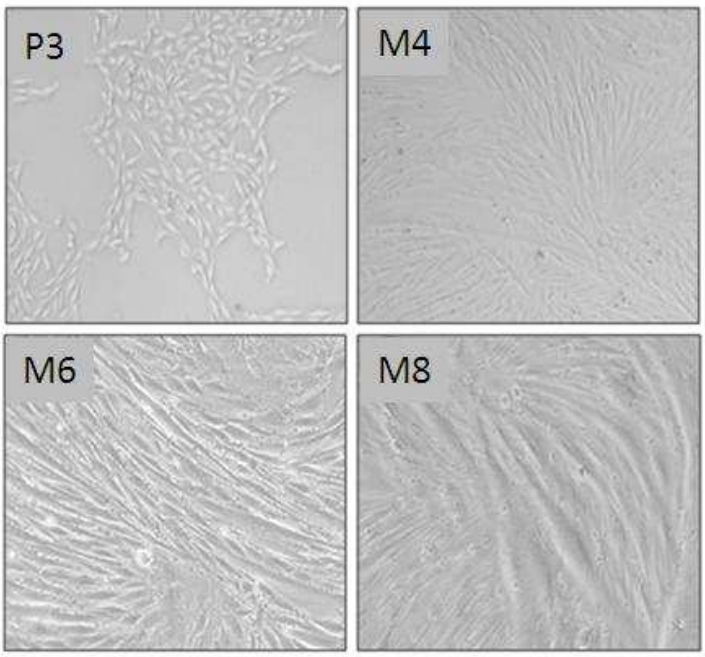

FIGURE 6.1 – Photomicrographs of L6.G8.C5 cells (P3) myoblasts, and 4, 6, and 8 days post differentiation (M4, M6, and M8 respectively) x 20 magnification. Photomicrograph P3 shows proliferating single nuclear fibroblastic cells. M4 to M8 show cells fusing to form multinucleated myotubes of increasing maturation.

6.3.1.2 – mRNA expression

Myogenin mRNA was quantified as an index of myoblast differentiation. Myogenin is one of many myogenic regulatory factors (Witzemann and Sakmann 1991) involved in muscle differentiation (Buckingham 2001). Myogenin mRNA was barely detectable in proliferating myoblasts cultured in FCS-containing growth media at 80% confluence. Following differentiation, abundant myogenin mRNA was detected in all samples. Myogenin mRNA levels remained elevated until eight days post differentiation when the final samples were taken for analysis.

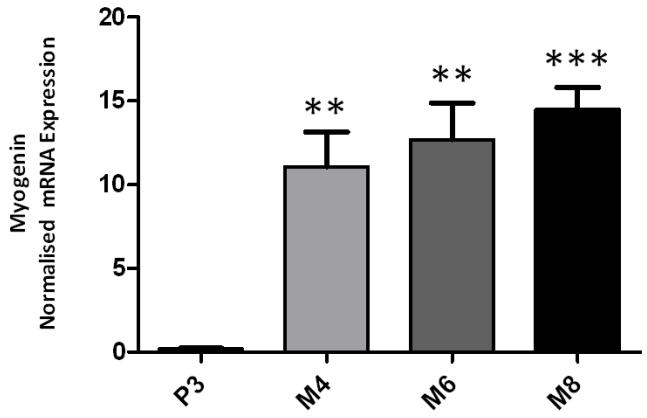

FIGURE 6.2 – Myogenin mRNA expression in proliferating (P3), and differentiating (M4, M6, M8) muscle cells. Data are mean normalised expression units + S.E.M; n = 3; significant differences expressed relative to P3.

Isoform-specific MHC mRNA was quantified as an index of muscle fibre type variation to assess the suitability of the L6.G8.C5 cell line as an *in vitro* model of skeletal muscle *in vivo*. Embryonic MHC (MHC-Emb) mRNA was barely detectable in proliferating myoblasts cultured in FCS-containing growth media at 80% confluence. Following differentiation, abundant MHC-Emb was detected in all samples, the abundance of which increased until eight days post differentiation. MHC I, IIX and IIB mRNAs were detected in both proliferating myoblasts and differentiated myotubes. In general, transcript abundance increased with the number of days post

differentiation. MHC IIA mRNA was not detected within the L6.G8.C5 cell line at any developmental stage (data not shown).

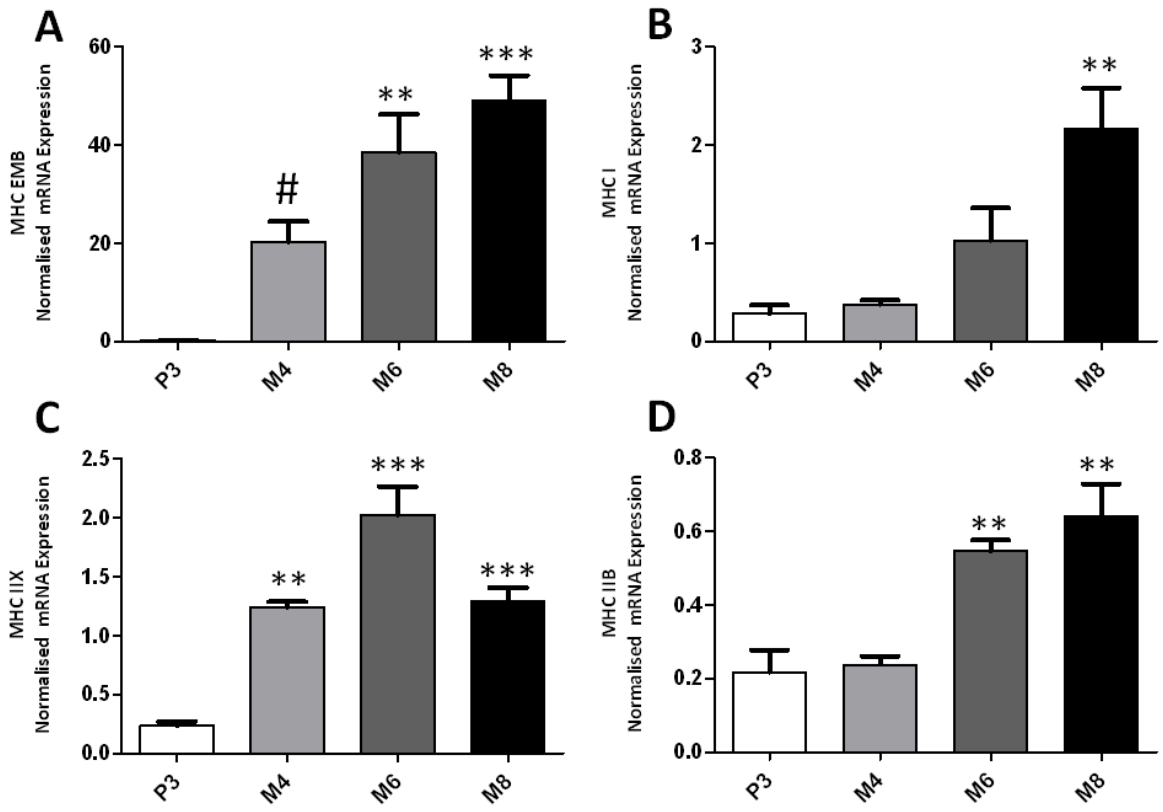

FIGURE 6.3 – MHC embryonic (A), I (B), IIX (C), IIB (D) mRNA expression in proliferating (P3), and differentiating (M4, M6, M8) muscle cells. Data are mean normalised expression units + S.E.M; n = 3; significant differences expressed relative to P3.

6.3.2 – The effects of TNF Alpha on the expression of MHC

Myotubes cultured until four days post differentiation were treated with rat recombinant TNFα at concentrations between 100 and 10,000pg / ml media for 48 hours (**METHOD 6.3.2**). Following treatment, total RNA extraction and reverse transcription were carried out as previously described (**METHOD 6.3.3**). Myogenin mRNA was quantified as an index of myotube differentiation. Treatment with

concentrations of TNFα ranging from 100 – 10000pg/ml had no effect on myogenin mRNA expression (P = 0.298) (**FIGURE 6.4**).

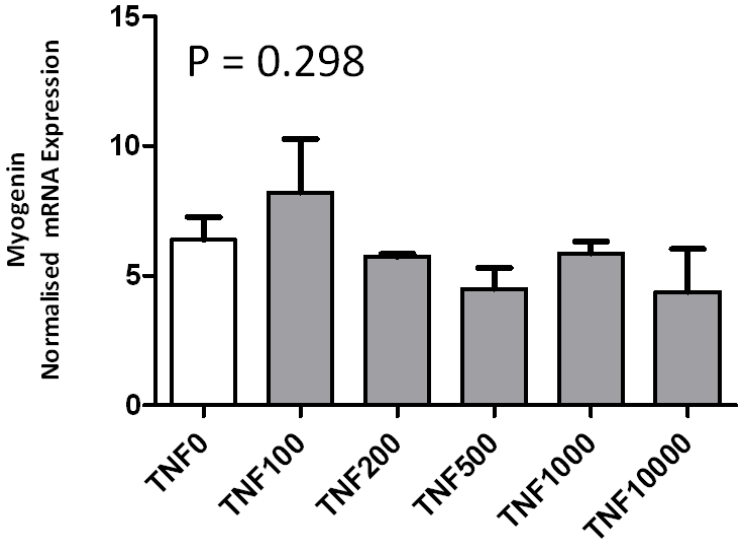

FIGURE 6.4 – Myogenin mRNA expression of differentiated (M4) myotubes treated with rat recombinant TNFα for 48 hours. Data are mean normalised expression units + S.E.M; n = 3; P value refers to one-way analysis of variance

Isoform-specific MHC mRNA was quantified as an index of muscle fibre type variation. Treatment with concentrations of TNFα ranging from 100 – 10000pg/ml had no effect on the mRNA expression of embryonic MHC or slow-twitch associated MHC I (P = 0.352 and 0.608 respectively). Treatment with rat recombinant TNFα did however significantly reduce MHC IIX mRNA although this effect was only evident when cells were treated with the two highest concentrations (1000 and 10000pg/ml respectively) (**FIGURE 6.5**).

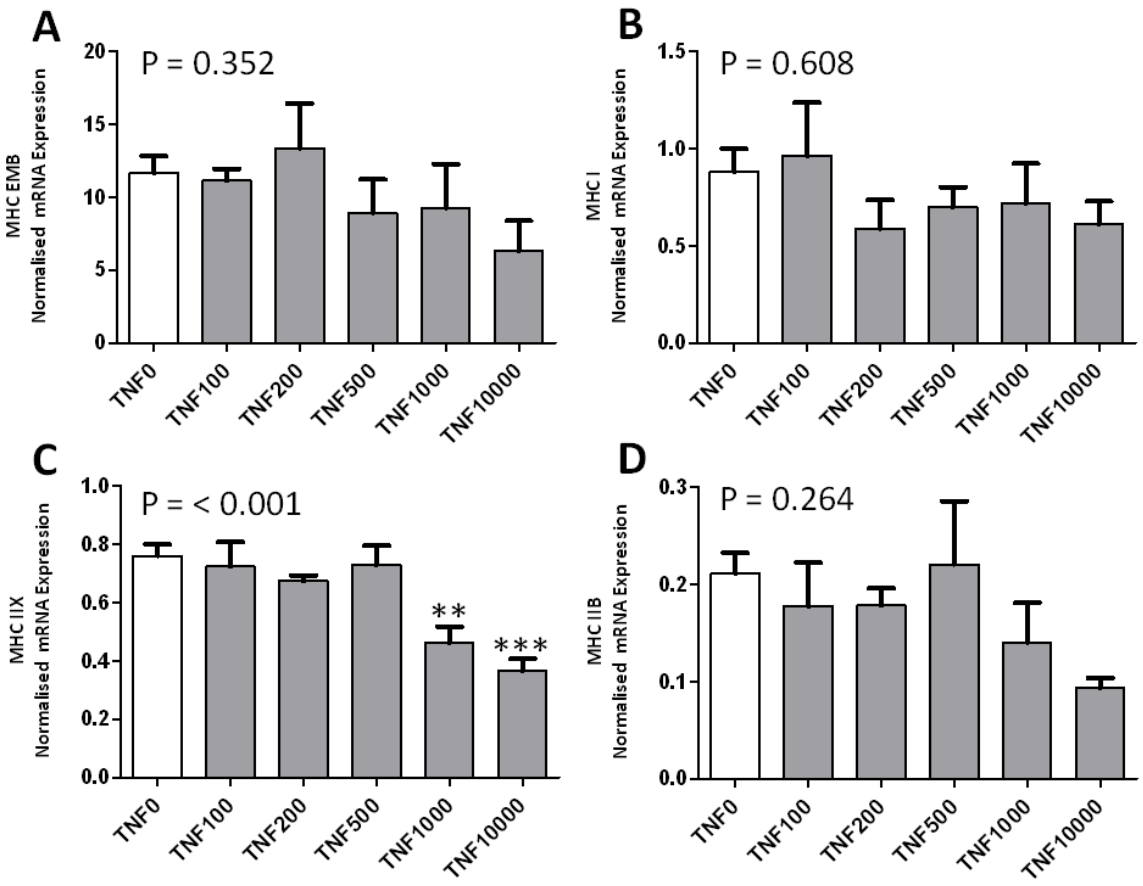

FIGURE 6.5 – MHC embryonic (A), I (B), IIX (C), IIB (D) mRNA expression of differentiated (M4) myotubes treated with rat recombinant TNFα for 48 hours. Data are mean normalised expression units + S.E.M; n = 3; P values refer to one-way analysis of variance; Stars designate a significant difference from the control group.

6.4 – Discussion

The initial aim of this study was to characterise the L6.G8.C5 rat derived muscle cell line with respect to differentiation, and MHC mRNA expression profile. Following suitable characterisation, the effects of the osteoarthritis associated cytokine TNFα, on the MHC mRNA expression were assessed *in vitro*.

L6.G8.C5 cells reached confluence in 6-well plates 48 hours post seeding, and reliably differentiated to form myotubes approximately 4 days after serum restriction. Although cells were harvested 8 days following differentiation, microscopically, they appeared viable and still firmly adhered to the 6-well plates in which they were cultured suggesting they would be amenable to more prolonged culture. Indeed, other studies utilising L6 myotubes have reported prolonged culture times as long as 20 days (Graber and Woodworth 1986).

Myogenin mRNA was determined as a marker of myoblast differentiation as reported previously (Park, Kim et al. 2002). Myogenin mRNA was barely detectable in proliferating myoblasts (n = 3). Following serum restriction, a marked increase in myogenin mRNA was noted with all samples showing strong expression. Expression persisted until 8 days post differentiation when the last samples were taken. These results were consistent with other studies utilising myogenin as a marker of differentiation on similar cell lines (Park, Kim et al. 2002). Myogenic differentiation involves the expression of a family of regulatory factors including Myf5, MyoD, MRF4 and myogenin which belong to the basic helix-loop-helix transcription factor family (Edmondson and Olson 1993). Whereas skeletal muscle differentiation has been shown to proceed in the absence of Myf5 (Braun, Rudnicki et al. 1992) or MyoD (Rudnicki, Braun et al. 1992), the targeted disruption of myogenin has been reported to induce severe skeletal muscle deficiency and lethality (Hasty, Bradley et al. 1993; Nabeshima, Hanaoka et al. 1993).

As an index of the likely muscle fibre types expressed by the L6.G8.C5 cell line, MHC mRNA was determined. Proliferating myoblasts expressed slow-twitch MHC I, faster-twitch MHC IIX and fast-twitch MHC IIB at the mRNA level. No embryonic MHC mRNA was detected in any of the samples of proliferating myoblasts. Following differentiation, the expression of MHC I, IIX and IIB increased with the number of days post differentiation. Embryonic MHC was also detected from 4 days post differentiation onwards and displayed a similar increase in expression as the cells became more differentiated. Interestingly, the expression of MHC IIA, linked with oxidative glycolytic muscle fibre types was not detected at any developmental stage suggesting the absence of this fibre type. When considering these results in light of previous publications, it is clear that much variation exists within the literature. Whilst Arcangelis and colleagues, 2005 found that the L6 cell line expressed embryonic, neonatal and adult MHC IIB mRNAs (Arcangelis, Coletti et al. 2005), Pin and colleagues, 1997 (Pin and Merrifield 1997) found the L6 cell line to be committed to the production of MHC IIX fibres only. These discrepancies may be due in part to the vast array of different cell lines termed “L6”, which appear have subtle differences in their MHC profile (Pin and Merrifield 1997; Arcangelis, Coletti et al. 2005) or the methods used to assess MHC composition.

MHC determination was performed at the mRNA level in this study and not by the electrophoretic separation of MHC protein. This was purely due to insufficient material being available from cells grown in 6-well plates to permit both mRNA and protein extraction. The characterisation of MHC expression at the protein level would further enhance the utility of this study as it is the expression of MHC isoform specific proteins that essentially contribute towards muscle contractility.

With reference to osteoarthritis, L6.G8.C5 cells were treated with recombinant rat TNFα, a cardinal pro-inflammatory cytokine implicated in the pathogenesis of osteoarthritis, for 48 hours. The dosage range of TNFα was selected to encompass pathological values in both osteoarthritis (mean 500pg/ml synovial fluid) and

rheumatoid arthritis (mean 390pg/ml synovial fluid) (Westacott 1990; Westacott and Sharif 1996), and include treatment at supra-pathological levels. TNFα treatment had no discernable effects on differentiation as determined by myogenin mRNA, or the expression of embryonic MHC or MHC I. TNFα treatment did however modulate the expression of MHC IIX by significantly reducing MHC IIX mRNA abundance. MHC IIX perturbations are noted in several pathologies with a component of skeletal muscle dysfunction. Although specific muscle fibre involvement in osteoarthritis has not been consistently described, the consensus is that fast-type muscle fibres atrophy preferentially to slow muscle fibres. Contrary to many laboratory species which express three fast fibre types (Weiss and Leinwand 1996), MHC IIX fibres are the fastest isoform expressed in the human (Harridge 2007). It is therefore possible that MHC IIX fibres are responsible for the reduction in quadriceps mass noted in osteoarthritic patients. Furthermore, a distinct reduction in MHC IIX mRNA is noted in age related sarcopenia (Chow and Nair 2005; Boirie 2009) and a trend association in chronic obstructive pulmonary disease (Wijnhoven, Janssen et al. 2006). Interestingly all of the above conditions are associated with increased TNFα production (Phillips and Leeuwenburgh 2005; Matera, Calzetta et al.) and reduced MHC IIX fibre expression. MHC IIX mRNA was found to be elevated in the Dunkin Hartley model of knee-OA as reported in **CHAPTER 5.3.6**. Although the increase in MHC IIX mRNA is suggestive of increased MHC IIX containing muscle fibre abundance, it could also be a reparative response to reduced MHC IIX protein and certainly warrants further assessment at the protein level.

The effects of TNFα are elicited by its binding to specific receptors (TNFR1, TNFR2), present on the cell surface of most cell types (Baud and Karin 2001). TNFα has been reported to stimulate a large array of signalling events including the induction of apoptosis, activation of the NFκβ pathway (Naggar, Kanda et al. 2004) and activation of the PI3K pathway (Kim, Lee et al. 1999). It is one possibility that TNFα may be responsible for the induction of specific muscle fibre atrophy noted in numerous conditions associated with skeletal muscle dysfunction. Indeed, Naggar and

colleagues have previously reported that TNFα decreased the expression of myofibrillar proteins in L6 cells (Naggar, Kanda et al. 2004). With reference to the specific effects of TNFα on MHC IIX noted in this study, Plomgaard and colleagues have reported that TNFα expression was localised in type II fast muscle fibres, with no evidence of TNFα expression in slow type I fibres (Plomgaard, Penkowa et al. 2005). Furthermore, it is possible that TNFα receptor abundance may vary by muscle fibre type and therefore represent another plausible way by which fibre-specific effects may be induced. However, TNFα receptor abundance in different muscle fibres has not been studied to date.

Although other pathologies associated with both increased TNFα production and reduced MHC IIX may provide some confirmatory evidence for the *in vitro* results obtained here, it must be noted that MHC IIX mRNA was reduced only at the two highest TNFα concentrations (1000 and 10000pg/ml respectively), both in excess of the concentrations reported in the synovial fluid of osteoarthritic joints (500pg/ml). Furthermore, the lack of MHC IIA mRNA expression is an important consideration when evaluating the L6.G8.C5 cell line as an *in vitro* model of skeletal muscle development or pathology. When considering the reduction in MHC IIX mRNA noted in response to TNFα administration, the absence of MHC IIA (as determined during the characterisation studies) may preclude any observations given that MHC IIA and MHC IIX are encoded by iteratively located genes (Weiss and Leinwand 1996), and some evidence suggests that they are co-regulated (Pandorf, Haddad et al. 2006). It is therefore possible that the absence of MHC IIA expression will likely influence basal levels of MHC IIX prior to any experimental procedures, making the extrapolation of *in vitro* data to the *in vivo* situation more tentative.

Finally, it is necessary to consider the relationship between *in vitro* findings and the *in vivo* setting in which they may be inferred. The L6 cell lines has been utilised in skeletal muscle research since its development in 1968. The L6 line displays many myogenic characteristics including the formation of myoneural junctions,

contractility and the expression of creatine kinase (Elsner, Quistorff et al. 1998). Moreover, the cell line has also been shown to respond to various treatments including dexamethasone induced atrophy (Sultan, Henkel et al. 2006) and IGF-1 induced hypertrophy (Li, Hasselgren et al. 2004) as would be expected in skeletal muscle. A disadvantage of myotube culture is that cells are not routinely maintained under stretch, which has been previously shown to regulate skeletal muscle mass and fibre type (Wang, Kawano et al. 2006; Giger, Bodell et al. 2009), and may therefore limit the extrapolation of results from the *in vitro* to *in vivo* setting. More recent advances in cell culture techniques have described the development of cell culture plates, able to maintain myotubes under stretch and or electrical stimulation during experimentation, which may enhance the translational value of *in vitro* results in the *in vivo* setting (Ebihara, Hussain et al. 2002).

In conclusion, the data presented here report that the L6.G8.C5 cell line is readily differentiated into myotubes using standard cell culture techniques, and that the resulting myotubes express all the adult isoforms of MHC with the exception of MHC IIA. TNFα treatment resulted in a reduction in MHC IIX mRNA however the concentration of TNFα required to elicit this change was within the supra-pathological range. Given the lack of MHC IIA mRNA expression, the L6.G8.C5 cell line should be used with caution when attempting to model skeletal muscle development or pathology, in particular those conditions resulting in type II fibre muscle dysfunction.

CHAPTER 7 – GENERAL DISCUSSION

7.1 – Introduction and overall aims

It is established that patients with knee osteoarthritis (OA) exhibit marked muscle weakness, one of the most frequent and earliest reported symptoms associated with knee OA. Weakness primarily affects the quadriceps muscle with little evidence of hamstring involvement. Traditionally, muscle weakness has been considered a secondary effect in knee OA, resulting from disuse of the affected joint due to the presence of pain and/or inflammation, and therefore has received little attention with regards to its involvement in the initiation or progression of OA. However, there is clinical evidence which suggests that quadriceps weakness may precede the onset of radiographic evidence of OA and subsequent pain, and therefore may be directly involved in its pathogenesis. Furthermore, targeted exercise regimes aimed at improving quadriceps function indicate therapeutic benefits with regards to both the initiation and progression of knee OA.

Quadriceps muscle dysfunction in knee OA is currently poorly understood and represents a great and unmet clinical need. Unlike other atrophy associated conditions which have well-established effects on specific muscle fibre-types, it is unclear as to whether atrophy in OA is fibre-type specific. Whilst the majority of evidence suggests that type II fibres are preferentially affected (Nakamura and Suzuki 1992), others report that up to one third of patients present with type I atrophy (Fink, Egl et al. 2007).

In attempting to better understand the involvement of skeletal muscle in the initiation and progression of OA, the aims of this work were to characterise changes in the quadriceps skeletal muscle in two independent animal models of OA; the rat meniscectomy induced model, and the spontaneous development of OA in the Dunkin Hartley strain guinea pig. MHC isoform composition was used to detect subtle changes in skeletal muscle contractile phenotype whilst lactate dehydrogenase (LDH) and isocitrate dehydrogenase (ICDH) activity were determined

as an assessment of quadriceps metabolic potential. Throughout this work, evidence of skeletal muscle proteolysis, associated with atrophy, was determined by the assessment of several known atrophy associated factors (reviewed in **CHAPTER 1.3.6**).

Moreover, in attempting to assess the disease modulating potential of increased quadriceps skeletal muscle mass and increased type II fibre content prior to the development of OA, the effects of β2-agonist administration on disease severity were assessed. Finally the effects of TNFα on skeletal muscle cells were determined to investigate whether OA-associated cytokines were able induce the muscle fibre atrophy so commonly noted in the human condition.

7.2 – Summary of Findings

7.2.1 - The effects of osteoarthritis on markers of muscle function

It was hypothesised that the development of OA would be associated with quadriceps muscle atrophy, predominantly affecting type II muscle fibres, presenting as a reduction in quadriceps mass and in MHC isoforms IIX and IIB. Whilst rat meniscal tear induced disease was associated with marginal quadriceps atrophy (as evidenced by reduced quadriceps mass relative to body mass), OA in the guinea pig was not associated with any gross changes to quadriceps mass. The induction of OA in the rat meniscal tear model was associated with the induction of MHC I, indicative of an increase in type I muscle fibres. Considerable inter-animal variation in MHC I mRNA was also noted in guinea pigs developing spontaneous knee arthritis (**CHAPTER 5.3.6**) around the time of disease initiation however this observation was not statistically significant given the small number of animals utilised. The two models differed with respect to their expression of MHC IIX, related to fast-twitch type II muscle fibres, which was increased in the guinea pig spontaneous model of OA, but remained unaltered in the rat. Indeed, MHC IIX expression was significantly correlated with disease severity in the guinea pig. Notably, neither of the two models assessed showed evidence of reduced type II muscle fibre-associated MHC isoforms.

MHC I expression is associated with slow, postural anti-gravity muscles such as the soleus (Adams, Haddad et al. 1994). Although the induction of MHC I expression in the rat surgical model of OA could have perhaps been considered a response to joint destabilisation following transection of the collateral ligament (**CHAPTER 3.2.3**), the induction of inter-animal variation in the guinea pig suggests that this is more likely to be associated with the development of OA. The isolated effect of induced MHC IIX expression in the guinea pig is perhaps more difficult to reason. Whilst increased MHC IIX expression has not been previously associated with OA, it has been reported following the development of disuse atrophy in rodents (Caiozzo, Haddad et al. 1996; Adams, Haddad et al. 2000). This would not however explain why MHC IIX expression

was induced only around the time of disease initiation and not thereafter and warrants further investigation. There is a large body of evidence from human studies reporting reduced type II fibre number or cross-sectional area in response to developing OA when assessed by histochemical techniques. However, data derived from this study of MNX-induced and spontaneous OA suggest that altered skeletal muscle function may result preferentially from increased type I fibre-associated MHC isoforms rather than from reduced type II fibres or muscle mass *per se.* In considering the difference in the muscle fibre-type data presented here and in other histochemical studies, it is possible that increased type I fibre number or cross-sectional area may artificially reduce the apparent abundance of other muscle fibre types when assessed by traditional histochemical techniques. It is therefore considered that the use of MHC protein electrophoretic techniques, as reported here, gives a more accurate overview, indicative of muscle fibre-type properties.

7.2.2 - The effects of osteoarthritis on markers of atrophy

As reviewed in **CHAPTER 1**, numerous atrophy conditions are associated with the induction of a similar set of genes which include the E3 ligases, the calpain system and apoptotic-associated factors Bax and Bcl2 (Lecker, Jagoe et al. 2004). The mRNAs of these systems were quantified by quantitative PCR in both *in vivo* models of disease. It was subsequently hypothesised that the same proteolytic systems implicated in the pathogenesis of numerous other atrophy associated conditions, would be noted in response to developing OA.

The expression of E3 ligases MuRF and MAFBx was unaffected by the development of OA in both experimental models, suggesting that degradation via the proteasome system was not associated with the development of osteoarthritis. Although E3 ligase activity has received little attention with reference to human OA, this result is of interest given that these factors are consistently elevated in numerous atrophy conditions (Dehoux, van Beneden et al. 2003; Lecker, Jagoe et al. 2004; Glass 2005) and that human knee-OA is associated with marked muscle atrophy (reviewed in

CHAPTER 1.3.8). Similar results were obtained for calpains I – III, which were also unmodified in both disease models. Apoptotic potential of the quadriceps skeletal muscle was determined by quantification of mRNAs encoding pro-apoptotic Bax and anti-apoptotic Bcl2. The development of OA in the rat was not associated with expression changes in Bax mRNA; however Bax was reduced with advancing age in the guinea pig. Bcl2 mRNA remained unaltered by disease in both animal models of OA. The assessment of factors involved in muscle atrophy signalling, interpreted in context with quadriceps mass data and muscle fibre type assessment suggest that the muscle dysfunction noted in response to developing OA was most strongly associated with changes in muscle function rather than mass *per se*.

7.2.3 – The effects of clenbuterol pre-treatment on OA severity

The effects of clenbuterol-induced quadriceps hypertrophy prior to the development of OA were investigated in the rat model of OA. It was hypothesised that clenbuterol would induce skeletal muscle hypertrophy, and increase expression of fast-twitch muscle fibres detected as increased MHC IIX and IIB expression. Furthermore, it was hypothesised that increased quadriceps mass, with a faster contractile phenotype, would reduce disease severity following the induction of OA.

Preliminary data demonstrated that clenbuterol administration induced marked quadriceps hypertrophy. Clenbuterol did not modulate the MHC composition of the quadriceps skeletal muscle following 14 days of administration although this was likely due to the high baseline complement of fast muscle fibres (**CHAPTER 3, FIGURE 3.2**). The study design permitted the marked induction of skeletal muscle hypertrophy specifically prior to the induction of OA which enabled the assessment of whether a larger quadriceps was protective of OA severity following disease development. The quadriceps mass of the treated subjects was significantly larger at the time of OA induction, however the increased muscle mass was lost by the study end point. Clenbuterol administration was able to ablate the OA associated increase in MHC I protein noted in saline treated animals, however disease severity remained

unaltered. A full discussion of the effects of clenbuterol pre-treatment is included in **CHAPTER 3**.

7.2.4 – Characterisation of the guinea pig sarcomeric myosin heavy chain family

The characterisation of the sarcomeric myosin heavy chain family in the guinea pig (**CHAPTER 4**) elucidated partial cDNA sequence data for MyH 1, 2 and 4 (MHC IIX, IIA, IIB). Furthermore, this study reported and validated a set of specific oligonucleotide primers for the differential determination of MHC isoforms I, IIA, IIX and IIB. Perhaps most striking is the observation that guinea pig MHC isoform-specific cDNAs and their promoter sequences appeared to be more closely related to the human than to other small mammals. This data is of considerable use to the numerous research groups who utilise the guinea pig in translational research, and also furthers our limited knowledge of this species.

7.2.5 – The effects of OA-associated cytokines on markers of muscle function

The L6.G8.C5 cell line was found to readily differentiate into myotubes using standard cell culture techniques. The resulting myotubes were found express all of the adult isoforms of MHC with the exception of MHC IIA. TNFα treatment resulted in a reduction in MHC IIX mRNA however the concentration of TNFα required to elicit this change was within the supra-pathological range. The finding that the L6.G8.C5 cell line lacks the expression of MHC IIA is considered to have important implications in the *in vitro* modelling of disease. In particular, caution should be exercised when modelling diseases known to result in perturbations in type II muscle fibres in this cell line.

7.3 – Limitations

As with all scientific studies, it is necessary to consider possible limitations, in particular when utilising *in vivo* models of pathology. Many animal models of OA have been developed as tools to study the pathogenesis and progression of the disease. Some models serve to elucidate new mechanisms and pathways, whilst others are employed in the pharmacological testing of new anti-arthritic drugs and analgesics. Due to the rapid time-course over which OA develops in some of the induced models, and fundamental inter-species variations, it is appreciated that no single experimental model is without its disadvantages. The rat meniscectomy model is characterised by the rapid onset of well defined osteoarthritis-like lesions on both tibial and femoral condyles – although a predisposition to increased tibial severity was noted in this study. Due to the regimented and consistent onset of disease, this model is particularly useful for targeting specific phases of its pathogenesis. For intervention studies, previous research recommends pre-treating animals with the experimental compound to a steady serum concentration prior to surgery (Bendele 2001), as in this study. In terms of comparative pathogenesis, lesions in this model are morphologically similar to those of human OA (Bendele 2001), but occur at a significantly enhanced rate. It is considered that lesions progress as such due to the apparent lack of perception of the animal that it should discontinue use of the unstable joint, a key difference with respect to the human condition. Technically, this offers a restricted opportunity in which to elicit physiological changes prior to disease initiation as noted previously (Bendele 2001). It is therefore possible that potential improvements in OA that may be evident in the human population are precluded by the rapid onset and progression of disease in this rodent model.

The spontaneous development of knee OA in the Dunkin Hartley guinea pig (as utilised in **CHAPTER 5**) is considered to be an improvement on surgically induced disease models in terms of its comparative pathology and translational research value (reviewed in **CHAPTER 5.1**). Despite this, the development of OA in the Dunkin

Hartley stain coincided with the longitudinal growth phase in this study. Due to the lack of a suitable control strain, separating the effects of osteoarthritis from those of normal growth was therefore more complex and restricted the assessment of muscle dysfunction and OA to the level of a correlation as reported in **CHAPTER 5.3**. The use of an intervention based protocol, and therefore the opportunity to compare treated and control subjects, would ensure more robust data was derived from subsequent studies.

A further possible limitation of this collection of studies is the methodology utilised for the determination of skeletal muscle fibre characteristics. Due to the lack of reliable methodology by which to resolve the four MHC proteins in the guinea pig, an mRNA quantification technique was developed (**CHAPTER 4**) and utilised for the determination of MHC expression in the guinea pig quadriceps. Conversely, high-resolution MHC protein electrophoresis was used to determine the MHC expression profile in the rat skeletal muscle samples. Although MHC profile in the two models was therefore quantified by different techniques, both MHC mRNA and protein measurements have been previously shown to correlate strongly (Marx, Kraemer et al. 2002) in addition to correlating well with other measures of fibre-type including mATPase staining, MHC immunohistochemistry and metabolic profile (Quiroz-Rothe and Rivero 2004). Despite this, it is likely that the quantification of specific MHC mRNAs enabled the detection of earlier changes indicative of muscle fibre-type transitions, given that a change in mRNA abundance is usually required to elicit a change in each respective MHC protein.

7.4 – Overview

Considering only changes found to be concordant between both *in vivo* models of knee OA, the most striking observation was that the modulation of quadriceps parameters, indicative of contractile and metabolic function, coincided with the development of OA in both model species utilised. The quadriceps changes were

characterised by the induction of MHC I expression noted at the protein level in the rat and mRNA level in the guinea pig. Moreover, the expression of MHC IIX appeared to be correlated with disease severity in the guinea pig, although this correlation was derived from small animal numbers (n = 6). Equally striking is that neither model presented with overt quadriceps muscle atrophy or increased atrophy signalling. It thus appears that altered quadriceps function in OA may result from altered contractile and metabolic properties rather than reduced mass which may have important implications for treatment and rehabilitation regimes.

7.5 – Main Implications and Future Work

It is considered that the data presented within this thesis raise important issues with respect to our understanding of muscle dysfunction and OA, and therefore have potential implications in the design of pharmaceuticals and rehabilitation regimes for the treatment of OA. Although further human clinical studies are required to confirm the observations reported here, the apparent induction of MHC I as opposed to the anticipated reduction in fast-twitch fibre-associated MHC may highlight new targets with which to develop novel pharmaceuticals and therefore warrants further investigation as outlined below.

Given the numerous beneficial findings obtained from this series of studies, it is felt that further scientific work is warranted. Firstly, it is suggested that any further study should include a physiological assessment of quadriceps function and thus draw comparison between the MHC isoform composition as determined by electrophoresis and functional aspects of the quadriceps muscle. Fish and colleagues have previously described an electrophysiological method for the determination of maximal twitch, maximal rate of rise of twitch tension, maximal time to peak tension and fatigue (Fish, McKee et al. 1989). It is felt that such measurements would complement existing MHC determination. In terms of MHC determination, it is

suggested that further studies should directly measure muscle fibre cross sectional area in addition to MHC electrophoresis, given that it is this parameter that essentially defines atrophy. A comparison of the two techniques could subsequently determine whether increased type I fibre abundance or cross-sectional area is in fact able to artificially reduce the apparent number of type II fibres when assessed by histochemical techniques. Numerous studies have described the existence of MHC isoform-specific antibodies which could be optimised for use with frozen sections of skeletal muscle. Such methodology would enable the determination of both MHC complement, and the cross-sectional area of each specific fibre-type. With regards metabolic enzyme determination, it is suggested that further markers of glycolysis are utilised in addition to LDH. Whilst LDH has been determined in numerous studies, it is not a rate-limiting enzyme in the glycolytic pathway, which may explain the lack of modulation noted in these studies. It is suggested that the inclusion of PFK and enolase activity measurements would give a more sensitive index of glycolytic potential.

The promoter analysis reported in (**CHAPTER 4**), yielded some particularly interesting novel data which appear to show the differential regulation of guinea pig and human MyH4, encoding MHC IIB, in comparison to the mouse and rat. To follow-up on this initial work, it is suggested that electrophoretic mobility shift assays (EMSAs) are performed to determine whether the mutations noted in the promoter regions of the guinea pig and human MyH4 gene do in fact prevent the binding of their respective regulatory and enhancer factors. This further work will enhance our limited knowledge of fibre-type control and may have important implications in the targeted hypertrophy of specific fibre-types.

Given the differences in quadriceps involvement in the two animal models of OA when compared with the human disease noted here, it is important to further confirm these changes in alternative models of pathology. A further assessment into the differential effects of altered fibre-type and quadriceps mass would require an

animal model in which disease results exclusively as a result of muscle atrophy. Longino and colleagues have described such a model in which quadriceps weakness results from the administration of botulinum toxin, a potent neurotoxin (Longino, Frank et al. 2005; Longino, Frank et al. 2005). The proposed system would enable dissection of the independent effects of altered fibre type, quadriceps mass or both on the development of OA. Further advantages of this system would include the opportunity to modulate the extent and anatomical location of muscle weakness both by varying the administration of botulinum toxin or the addition of hypertrophy inducing agents such as β2-agonists. Prior to any intervention studies, it would be necessary to perform a short pilot study to ensure that quadriceps weakness does in fact lead to the development of osteoarthritis in this species.

The ideal design for any study of disease pathogenesis is to utilise tissue from the species in question. Whilst several large scale population-based osteoarthritis studies have been conducted over the years (Felson, Naimark et al. 1987; Wilson, Michet Jr et al. 1990; Oliveria, Felson et al. 1995; Cooper, Snow et al. 2000), none have included the collection of quadriceps muscle tissue as part of their protocols. Although several studies have reported the collection and analysis of muscle biopsy material (Nakamura and Suzuki 1992; Fink, Egl et al. 2007), these were from patients selected specifically due to their end stage disease (Fink, Egl et al. 2007) or conducted only on female participants (Nakamura and Suzuki 1992) and fibre-type determination was limited to muscle histochemical techniques. The ideal follow-up study would be population based, and characterise the incidence of quadriceps muscle changes at the individual fibre level within the human population in comparison to radiographic data. Although quadriceps biopsy material could be obtained from end-stage OA patients during knee-replacement surgery, it is envisaged that the collection of such biopsy material from early disease patients would be more problematic. Suggested endpoint measurements would include MHC immunohistochemistry, MHC electrophoresis, metabolic enzyme activities (ICDH, PFK, and enolase) and electrophysiological determination of quadriceps function.

7.6 – Closing Remarks

To date, there are no disease modifying drugs available for the treatment of knee-OA, which still represents a great and unmet clinical need. Data reported in this thesis support the theory that OA is a whole-joint disease, affecting cartilage, bone and the surrounding musculature. Taking into account the numerous reports suggesting quadriceps involvement in the initiation and progression of knee-OA, and the data reported here, it is proposed that the standard care of knee-OA patients should include consideration of quadriceps skeletal muscle function and the prescription of appropriate strengthening exercises where indicated.

REFERENCES

Acharyya, S., K. J. Ladner, et al. (2004). "Cancer cachexia is regulated by selective targeting of skeletal muscle gene products." The Journal of Clinical Investigation **114**(3): 370-378.

Adams, G., F. Haddad, et al. (1994). "Interaction of chronic creatine depletion and muscle unloading - effects on postural and locomotor muscles." Journal of Applied Physiology **77**(3): 1198-1205.

Adams, G. R., F. Haddad, et al. (2000). "Effects of spaceflight and thyroid deficiency on rat hindlimb development. II. Expression of MHC isoforms." J Appl Physiol **88**(3): 904-916.

Adams, G. R., B. M. Hather, et al. (1993). "Skeletal muscle myosin heavy chain composition and resistance training." J Appl Physiol **74**(2): 911-915.

Allen, D. L., C. A. Sartorius, et al. (2001). "Different pathways regulate expression of the skeletal myosin heavy chain genes." Journal of Biological Chemistry **276**(47): 43524-43533.

Allen, D. L., J. N. Weber, et al. (2005). "Myocyte Enhancer Factor-2 and Serum Response Factor Binding Elements Regulate Fast Myosin Heavy Chain Transcription in Vivo." Journal of Biological Chemistry **280**(17): 17126-17134.

Altman, R., G. Alarcon, et al. (1991). "The American College of Rheumatology criteria for the classification and reporting of osteoarthritis of the hip." Arthritis & Rheumatism **34**(5): 505-514.

Amin, S., K. Baker, et al. (2009). "Quadriceps Strength and the Risk of Cartilage Loss and Symptom Progression in Knee Osteoarthritis." Arthritis & Rheumatism **60**(1): 189-198.

Amthor, H., A. Otto, et al. (2009). "Muscle hypertrophy driven by myostatin blockade does not require stem/precursor-cell activity." Proceedings of the National Academy of Sciences **106**(18): 7479-7484.

Arcangelis, V. D., D. Coletti, et al. (2005). "Hypertrophy and transcriptional regulation induced in myogenic cell line L6-C5 by an increase of extracellular calcium." Journal of Cellular Physiology **202**(3): 787-795.

Arden, N. and M. Nevitt (2006). "Osteoarthritis: Epidemiology." Best Practice & Research in Clinical Rheumatology **20**(1): 3-25.

Ardley, H. and P. Robinson (2005). "E3 ubiquitin ligases." Essays in Biochemistry **041**(1): 15-30.

Baker, K. R., M. E. Nelson, et al. (2001). "The efficacy of home based progressive strength training in older adults with knee osteoarthritis: A randomized controlled trial." Journal of Rheumatology **28**(7): 1655-1665.

Bamford, J. A., C. T. Putman, et al. (2005). "Intraspinal microstimulation preferentially recruits fatigue-resistant muscle fibres and generates gradual force in rat." The Journal of Physiology **569**(3): 873-884.

Bamman, M. M., J. R. Shipp, et al. (2001). "Mechanical load increases muscle IGF-I and androgen receptor mRNA concentrations in humans." Am J Physiol Endocrinol Metab **280**(3): E383-390.

Baracos, V. E., C. Devivo, et al. (1995). "Activation of the ATP-Ubiquitin-Proteasome pathway in skeletal muscle of cachectic rats bearing a hepatoma." American Journal of Physiology-Endocrinology and Metabolism **268**(5): E996-E1006.

Baud, V. and M. Karin (2001). "Signal transduction by tumor necrosis factor and its relatives." Trends in Cell Biology **11**: 372-377.

Becker, R., A. Berth, et al. (2004). "Neuromuscular quadriceps dysfunction prior to osteoarthritis of the knee." Journal of Orthopaedic Research **22**(4): 768-773.

Beehler, B. C., P. G. Sleph, et al. (2006). "Reduction of Skeletal Muscle Atrophy by a Proteasome Inhibitor in a Rat Model of Denervation." Exp. Biol. Med. **231**(3): 335-341.

Bendele, A. (2001). "Animal models of Osteoarthritis." J Musculoskel Neuron Interact **1**: 363-376.

Bendele, A. (2002). "Animal models of osteoarthritis in an era of molecular biology." J Musculoskel Neuron Interact **2**: 501-503.

Bendele, A. and J. Hulman (1988). "Spontaneous cartilage degeneration in guinea-pigs." Arthritis & Rheumatism **31**(4): 561-565.

Bendele, A. and J. Hulman (1991). "Effects of body-weight restriction on the development and progression of spontaneous osteoarthritis in guinea-pigs." Arthritis & Rheumatism **34**(9): 1180-1184.

Bendele, A., G. Sennello, et al. (1997). "Effects of interleukin-1 receptor antagonist alone and in combination with methotrexate in adjuvant arthritic rats." Arthritis & Rheumatism **40**(9): 899-899.

Bendele, A. and S. White (1987). "Early histopathologic and ultrastructural alteration in femorotibial joints of partial medial meniscectomized guinea-pigs." Veterinary Pathology **24**(5): 436-443.

Bendele, A., S. White, et al. (1989). "Osteoarthrosis in guinea-pigs - histopathologic and scanning electron-microscopic features." Laboratory animal science **39**(2): 115-121.

Bendjaballah, M. Z., A. Shirazi-Adl, et al. (1995). "Biomechanics of the human knee joint in compression: reconstruction, mesh generation and finite element analysis." The Knee **2**(2): 69-79.

Bezalel, T., E. Carmeli, et al. (2010). "The effect of a group education programme on pain and function through knowledge acquisition and home-based exercise among patients with knee osteoarthritis: A parallel randomised single-blind clinical trial." Physiotherapy **96**(2): 137-143.

Bhasin, S., O. M. Calof, et al. (2006). "Drug Insight: testosterone and selective androgen receptor modulators as anabolic therapies for chronic illness and aging." Nat Clin Pract End Met **2**(3): 146-159.

Bishop, D., D. Jenkins, et al. (1999). "The effects of strength training on endurance performance and muscle characteristics." Medicine & Science in Sports & Exercise **31**(6): 886-891.

Block, S. M. (1996). "Fifty Ways to Love Your Lever: Myosin Motors." Cell **87**(2): 151-157.

Bodine, S., E. Latres, et al. (2001). "Identification of ubiquitin ligases required for skeletal muscle atrophy." Science **294**(5547): 1704-1708.

Bodine, S. C., T. N. Stitt, et al. (2001). "Akt/mTOR pathway is a crucial regulator of skeletal muscle hypertrophy and can prevent muscle atrophy in vivo." Nat Cell Biol **3**(11): 1014-1019.

Boirie, Y. (2009). "Physiopathological mechanism of sarcopenia." The Journal of Nutrition, Health and Aging **13**(8): 717-723.

Boncompagni, S., H. Kern, et al. (2007). "Structural differentiation of skeletal muscle fibers in the absence of innervation in humans." Proceedings of the National Academy of Sciences **104**(49): 19339-19344.

Bradford, M. M. (1976). "Rapid and Sensitive method for quantification of microgram quantities of protein utilizing principle of protein-dye binding." Analytical Biochemistry **72**(1-2): 248-254.

Brandstetter, A., B. Picard, et al. (1997). "Regional variations of muscle fibre characteristics in m. semitendinosus of growing cattle." Journal of Muscle Research and Cell Motility **18**(1): 57-62.

Brandstetter, A. M., B. Picard, et al. (1998). "Muscle fibre characteristics in four muscles of growing male cattle II. Effect of castration and feeding level." Livestock Production Science **53**(1): 25-36.

Brandt, K., D. Heilman, et al. (1999). "Quadriceps strength in women with radiographically progressive osteoarthritis of the knee and those with stable radiographic changes." Journal of Rheumatology **26**(11): 2431-2437.

Brandt, K., D. Heilman, et al. (2000). "A comparison of lower extremity muscle strength, obesity, and depression scores in elderly subjects with knee pain with and without radiographic evidence of knee osteoarthritis." Journal of Rheumatology **27**(8): 1937-1946.

Braun, T., M. A. Rudnicki, et al. (1992). "Targeted inactivation of the muscle regulatory gene Myf-5 results in abnormal rib development and perinatal death." Cell **71**(3): 369-382.

Briand, M., A. Talmant, et al. (1981). "Metabolic types of muscle in the sheep: II. Lactate dehydrogenase activity and LDH isoenzyme distribution." European Journal of Applied Physiology and Occupational Physiology **46**(4): 359-365.

Brooke, M. and K. Kaiser (1970). "3 myosin adenosine triphosphatase systems - nature of their pH lability and sulfhydryl dependence." Journal of HIstochemistry & Cytochemistry **18**(9): 670-&.

Bua, E. A., S. H. McKiernan, et al. (2002). "Mitochondrial abnormalities are more frequent in muscles undergoing sarcopenia." J Appl Physiol **92**(6): 2617-2624.

Buckingham, M. (2001). "Skeletal muscle formation in vertebrates." Current Opinion in Genetics & Development **11**(4): 440-448.

Buller, A. J., J. C. Eccles, et al. (1960). "Differentiation of fast and slow muscles in the cat hind limb." The Journal of Physiology **150**(2): 399-416.

Busquets, S., M. T. Figueras, et al. (2004). "Anticachectic Effects of Formoterol: A Drug for Potential Treatment of Muscle Wasting." Cancer Res **64**(18): 6725-6731.

Cai, D., J. D. Frantz, et al. (2004). "IKK[beta]/NF-[kappa]B Activation Causes Severe Muscle Wasting in Mice." Cell **119**(2): 285-298.

Caiozzo, V. J., F. Haddad, et al. (1996). "Microgravity-induced transformations of myosin isoforms and contractile properties of skeletal muscle." Journal of Applied Physiology **81**(1): 123-132.

Carbó, N., J. López-Soriano, et al. (1997). "Comparative effects of [beta]2-adrenergic agonists on muscle waste associated with tumour growth." Cancer Letters **115**(1): 113-118.

Carman, W. J., M. Sowers, et al. (1994). "Obesity as a risk factor for osteoarthritis of the hand and wrist: A prospective study." American Journal of Epidemiology **139**(2): 119-129.

Chang, K. C. (2007). "Key signalling factors and pathways in the molecular determination of skeletal muscle phenotype." animal **1**(05): 681-698.

Chen, L. X., L. Lin, et al. (2008). "Suppression of early experimental osteoarthritis by in vivo delivery of the adenoviral vector-medated NF-kappa Bp65-specific siRNA." Osteoarthritis and Cartilage **16**(2): 174-184.

Chen, S.-E., B. Jin, et al. (2007). "TNF-{alpha} regulates myogenesis and muscle regeneration by activating p38 MAPK." Am J Physiol Cell Physiol **292**(5): C1660-1671.

Cheras, P. A., A. N. Whitaker, et al. (1997). "Hypercoagulability and Hypofibrinolysis in Primary Osteoarthritis." Clinical Orthopaedics and Related Research **334**: 57-67.

Chow, L. S. and K. S. Nair (2005). "Sarcopenia of Male Aging." Endocrinology & Metabolism Clinics of North America **34**(4): 833-852.

Chung, L. and Y. C. Ng (2006). "Age-related alterations in expression of apoptosis regulatory proteins and heat shock proteins in rat skeletal muscle." Biochimica et Biophysica Acta - Molecular Basis of Disease **1762**(1): 103-109.

Connolly, E., S. Braunstein, et al. (2006). "Hypoxia Inhibits Protein Synthesis through a 4E-BP1 and Elongation Factor 2 Kinase Pathway Controlled by mTOR and Uncoupled in Breast Cancer Cells." Mol. Cell. Biol. **26**(10): 3955-3965.

Cooper, C., S. Snow, et al. (2000). "Risk factors for the incidence and progression of radiographic knee osteoarthritis." Arthritis & Rheumatism **43**(5): 995-1000.

Costelli, P., C. GarcÃ-a-MartÃ-nez, et al. (1995). "Muscle protein waste in tumor-bearing rats is effectively antagonized by a beta 2-adrenergic agonist (clenbuterol). Role of the ATP-ubiquitin-dependent proteolytic pathway." The Journal of Clinical Investigation **95**(5): 2367-2372.

d'Albis, A., F. Goubel, et al. (1994). "The effect of denervation on myosin isoform synthesis in rabbit slow-type and fast-type muscles during terminal differentiation." European Journal of Biochemistry **223**(1): 249-258.

Davis, M. A., W. H. Ettinger, et al. (1989). "The association of knee injury and obesity with unilateral and bilateral osteoarthritis of the knee." Am. J. Epidemiol. **130**(2): 278-288.

Dehoux, M. J. M., R. P. van Beneden, et al. (2003). "Induction of MafBx and Murf ubiquitin ligase mRNAs in rat skeletal muscle after LPS injection." FEBS Letters **544**(1-3): 214-217.

Dieppe, P. A., Ed. (1995). The classification and diagnosis of osteoarthritis. Osteoarthritic Disorders. Rosemont, IL, American Academy of Orthopedic Surgeons.

Diracoglu, D., R. Aydin, et al. (2005). "Effects of kinesthesia and balance exercises in knee osteoarthritis." JCR-Journal of Clinical Rheumatology **11**(6): 303-310.

Dogra, C., H. Changotra, et al. (2006). "Tumor Necrosis Factor-like Weak Inducer of Apoptosis Inhibits Skeletal Myogenesis through Sustained Activation of Nuclear Factor-κB and Degradation of MyoD Protein." Journal of Biological Chemistry **281**(15): 10327-10336.

Dubowitz, V. (2007). Muscle biopsy: a practical approach, Elservier.

Dubowitz, V. and A. G. E. Pearse (1960). "A comparative histochemical study of oxidative enzyme and phosphorylase activity in skeletal muscle." Histochemie **2**(2): 105-117.

Ebihara, S., S. N. A. Hussain, et al. (2002). "Mechanical Ventilation Protects against Diaphragm Injury in Sepsis . Interaction of Oxidative and Mechanical Stresses." Am. J. Respir. Crit. Care Med. **165**(2): 221-228.

Eccles, J. C., R. M. Eccles, et al. (1958). "The action potentials of the alpha motoneurones supplying fast and slow muscles." The Journal of Physiology **142**(2): 275-291.

Edmondson, D. G. and E. N. Olson (1993). "Helix-loop-helix proteins as regulators of muscle-specific transcription." Journal of Biological Chemistry **268**(2): 755-758.

Elsner, P., B. Quistorff, et al. (1998). "Regulation of glycogen accumulation in L6 myotubes cultured under optimized differentiation conditions." AJP - Endocrinology and Metabolism **275**(6): E925-933.

Engel, W. K. (1963). "Adenosine Triphosphatase of Sarcoplasmic Reticulum Triads and Sarcolemma identified histochemically." Nature **200**(4906): 588-589.

Ericsson, Y., E. Roos, et al. (2006). "Muscle strength, functional performance, and self-reported outcomes four years after arthroscopic partial meniscectomy in middle-aged patients." Arthritis & Rheumatism **55**(6): 946-952.

Evans, W. and W. Campbell (1993). "Sarcopenia and age-related changes in body composition and functional capacity." J Nutr **123**: 465-468.

Evans, W. J. (2010). "Skeletal muscle loss: cachexia, sarcopenia, and inactivity." Am J Clin Nutr **91**(4): 1123S-1127.

Evans, W. J., J. E. Morley, et al. (2008). "Cachexia: A new definition." Clinical Nutrition **27**(6): 793-799.

Eyigor, S. (2004). "A comparison of muscle training methods in patients with knee osteoarthritis." Clinical Rheumatology **23**(2): 109-115.

Falduto, M. T., S. M. Czerwinski, et al. (1990). "Glucocorticoid-induced muscle atrophy prevention by exercise in fast-twitch fibers." J Appl Physiol **69**(3): 1058-1062.

Felson, D., A. Naimark, et al. (1987). "The prevalence of knee osteoarthritis in the elderly - the Framingham osteoarthritis study." Arthritis & Rheumatism **30**(8): 914-918.

Felson, D. T. (1990). "The epidemiology of knee osteoarthritis: Results from the framingham osteoarthritis study." Seminars in Arthritis and Rheumatism **20**(3, Supplement 1): 42-50.

Fernandes, J., J. Martel-Pelletier, et al. (2002). "The role of cytokines in osteoarthritis pathophysiology." Biorheology **39**(1-2): 237-246.

Fink, B., M. Egl, et al. (2007). "Morphologic changes. in the vastus medialis muscle in patients with osteoarthritis of the knee." Arthritis & Rheumatism **56**(11): 3626-3633.

Fish, J. S., N. H. McKee, et al. (1989). "Isometric contractile function recovery following tourniquet ischemia." Journal of Surgical Research **47**(4): 365-370.

Flannery, C. (2010). "Novel Therapies in OA." Current Drug Targets **11**: 614-619.

Fluck, M. (2006). "Functional, structural and molecular plasticity of mammalian skeletal muscle in response to exercise stimuli." J Exp Biol **209**(12): 2239-2248.

Forsberg, N. E., M. A. Ilian, et al. (1989). "Effects of Cimaterol on Rabbit Growth and Myofibrillar Protein Degradation and on Calcium-Dependent Proteinase and Calpastatin Activities in Skeletal Muscle." J. Anim Sci. **67**(12): 3313-3321.

Franklin, C. C. and A. S. Kraft (1997). "Conditional Expression of the Mitogen-activated Protein Kinase (MAPK) Phosphatase MKP-1 Preferentially Inhibits p38 MAPK and Stress-activated Protein Kinase in U937 Cells." Journal of Biological Chemistry **272**(27): 16917-16923.

Gardiner, P., M. Favron, et al. (1992). "Histochemical and contractile responses of rat medial gastrocnemius to 2 weeks of complete disuse." Canadian journal of physiology and pharmacology **70**(8): 1075-1081.

Giger, J. M., P. W. Bodell, et al. (2009). "Rapid muscle atrophy response to unloading: pretranslational processes involving MHC and actin." J Appl Physiol **107**(4): 1204-1212.

Glass, D. J. (2003). "Signalling pathways that mediate skeletal muscle hypertrophy and atrophy." Nat Cell Biol **5**(2): 87-90.

Glass, D. J. (2005). "Skeletal muscle hypertrophy and atrophy signaling pathways." The International Journal of Biochemistry & Cell Biology **37**(10): 1974-1984.

Goldring, M. B. (1999). "The Role of Cytokines as Inflammatory Mediators in Osteoarthritis: Lessons from Animal Models." Connective Tissue Research **40**(1): 1-11.

Gorza, L. (1990). "Identification of a novel type 2 fiber population in mammalian skeletal muscle by combined use of histochemical myosin ATPase and anti-myosin monoclonal antibodies." J. Histochem. Cytochem. **38**(2): 257-265.

Gosker, H. R., M. P. Engelen, et al. (2002). "Muscle fiber type IIX atrophy is involved in the loss of fat-free mass in chronic obstructive pulmonary disease." Am J Clin Nutr **76**(1): 113-119.

Graber, S. G. and R. C. Woodworth (1986). "Myoglobin expression in L6 muscle cells. Role of differentiation and heme." Journal of Biological Chemistry **261**(20): 9150-9154.

Grifone, R., C. Laclef, et al. (2004). "Six1 and Eya1 Expression Can Reprogram Adult Muscle from the Slow-Twitch Phenotype into the Fast-Twitch Phenotype." Mol. Cell. Biol. **24**(14): 6253-6267.

Grotle, M., K. B. Hagen, et al. (2008). "Obesity and osteoarthritis in knee, hip and/or hand: An epidemiological study in the general population with 10 years follow-up." Bmc Musculoskeletal Disorders **9**.

Grounds, M. (2002). "Reasons for the degeneration of ageing skeletal muscle: a central role for IGF-1 signalling." Biogerontology **3**(1): 19-24.

Guth, L. and F. J. Samaha (1969). "Qualitative differences between actomyosin ATPase of slow and fast mammalian muscle." Experimental Neurology **25**(1): 138-152.

Hafer-Macko, C. E., S. Yu, et al. (2005). "Elevated Tumor Necrosis Factor-{alpha} in Skeletal Muscle After Stroke." Stroke **36**(9): 2021-2023.

Hansen, M. J., R. C. Gualano, et al. (2006). "Therapeutic prospects to treat skeletal muscle wasting in COPD (chronic obstructive lung disease)." Pharmacology & Therapeutics **109**(1-2): 162-172.

Harridge, S. D. R. (2007). "Plasticity of human skeletal muscle: gene expression to in vivo function." Experimental Physiology **92**(5): 783-797.

Hart, D. J., C. Cronin, et al. (2002). "The relationship of bone density and fracture to incident and progressive radiographic osteoarthritis of the knee: The Chingford study." Arthritis & Rheumatism **46**(1): 92-99.

Hasty, P., A. Bradley, et al. (1993). "Muscle deficiency and neonatal death in mice with a targeted mutation in the myogenin gene." Nature **364**(6437): 501-506.

Hayes, K., J. Song, et al. (2002). "The quadriceps/hamstring ratio and protection against pateliofemoral osteoarthritis progression." Arthritis & Rheumatism **46**(9): S142-S142.

Henriksson, J. (1992). "Effects of physical training on the metabolism of skeletal muscle." Diabetes Care **15**(11): 1701-1711.

Herrera, N. M., A. N. Zimmerman, et al. (2001). "Clenbuterol in the prevention of muscle atrophy: A study of hindlimb-unweighted rats." Archives of Physical Medicine and Rehabilitation **82**(7): 930-934.

Herrero-Beaumont, G., J. A. Roman-Blas, et al. (2009). "Primary Osteoarthritis No Longer Primary: Three Subsets with Distinct Etiological, Clinical, and Therapeutic Characteristics." Seminars in arthritis and rheumatism **39**(2): 71-80.

Higgins, J. A., Y. V. Lasslett, et al. (1988). "The relation between dietary restriction or clenbuterol (a selective ?2 agonist) treatment on muscle growth and calpain proteinase (EC 3.4.22.17) and calpastatin activities in lambs." British Journal of Nutrition **60**(03): 645-652.

Hochberg, M., M. Lethbridgecejku, et al. (1995). "The association of body-weight, body fatness and body-fat distribution with osteoarthritis of the knee - data

from the Baltimore longitudinal study of aging." Journal of Rheumatology **22**(3): 488-493.

Hoegh-Andersen, P. L. and Tanko (2004). "Ovariectomized rats as a model of postmenopausal osteoarthritis: validation and application." Arthritis Research & Therapy **6**(2): 169-180.

Hortobagyi, T., L. Westerkamp, et al. (2005). "Altered hamstring-quadriceps muscle balance in patients with knee osteoarthritis." Clinical Biomechanics **20**(1): 97-104.

Horton, M. J., C. Brandon, et al. (2001). "Abundant expression of myosin heavy-chain IIB RNA in a subset of human masseter muscle fibres." Archives of oral biology **46**(11): 1039-1050.

Huebner, J. (2006). "Assessment of the utility of biomarkers of osteoarthritis in the guinea pig." Osteoarthritis and Cartilage **14**: 923-930.

Huebner, J. L., M. Deberg, et al. (2007). "111 COLL2-1 AND COLL2-1 NO2: Markers of early disease in the Hartley guinea pig model of spontaneous OA." Osteoarthritis and Cartilage **15**(Supplement 3): C70-C70.

Huebner, J. L., I. G. Otterness, et al. (1998). "Collagenase 1 and collagenase 3 expression in a guinea pig model of osteoarthritis." Arthritis & Rheumatism **41**(5): 877-890.

Huebner, J. L., D. R. Seifer, et al. (2007). "A longitudinal analysis of serum cytokines in the Hartley guinea pig model of osteoarthritis." Osteoarthritis and Cartilage **15**(3): 354-356.

Huey, K. A. and S. C. Bodine (1998). "Changes in myosin mRNA and protein expression in denervated rat soleus and tibialis anterior." European Journal of Biochemistry **256**(1): 45-50.

Hurley, M. (1999). "The role of muscle weakness in the pathogenesis of osteoarthritis." Rheumatic disease clinics of North America **25**(2): 283-+.

Hyttinen, M. M., J. P. A. Arokoski, et al. (2001). "Age matters: collagen birefringence of superficial articular cartilage is increased in young guinea-pigs but decreased in older animals after identical physiological type of joint loading." Osteoarthritis and Cartilage **9**(8): 694-701.

Ikeda, S., H. Tsumura, et al. (2005). "Age-related quadriceps-dominant muscle atrophy and incident radiographic knee osteoarthritis." Journal of Orthopaedic Research **10**(2): 121-126.

Ilarraza-Lomeli, R., B. Cisneros-Vega, et al. (2007). "Dp71, utrophin and [beta]-dystroglycan expression and distribution in PC12/L6 cell cocultures." NeuroReport **18**(16): 1657-1661 1610.1097/WNR.1650b1013e3282f1650e1642d.

Ivanavicius, S., A. Ball, et al. (2007). "Structural pathology in a rodent model of osteoarthritis is associated with neuropathic pain: Increased expression of ATF-3 and pharmacological characterisation." Pain **128**(3): 272-282.

Jackman, R. W. and S. C. Kandarian (2004). "The molecular basis of skeletal muscle atrophy." Am J Physiol Cell Physiol **287**(4): C834-843.

Jagoe, R. T. and A. L. Goldberg (2001). "What do we really know about the ubiquitin-proteasome pathway in muscle atrophy? [Article]." Current Opinion in Clinical Nutrition & Metabolic Care **4**(3): 183-190.

Jan, M., J. Lin, et al. (2008). "Investigation of clinical effects of high- and low-resistance training for patients with knee osteoarthritis: A randomized control-led trial." Physical Therapy **88**(4): 427-436.

Jaschinski, F., M. Schuler, et al. (1998). "Changes in myosin heavy chain mRNA and protein isoforms of rat muscle during forced contractile activity." American Journal of Physiology-Cell Physiology **43**(2): C365-C370.

Jimenez, P. A. and S. S. Glasson (1997). "Spontaneous osteoarthritis in Dunkin Hartley guinea pigs: histologic, radiologic, and biochemical changes.
." Laboratory Animal Science **47**(6): 598.

Jobin, J. P., F. M. D. Maltais, et al. (1998). "Chronic Obstructive Pulmonary Disease: Capillarity and Fiber-Type Characteristics of Skeletal Muscle." Journal of Cardiopulmonary Rehabilitation November/December **18**(6): 432-437.

Johnston, I. A. (2006). "Environment and plasticity of myogenesis in teleost fish." J Exp Biol **209**(12): 2249-2264.

Jones, S. W., R. J. Hill, et al. (2004). "Disuse atrophy and exercise rehabilitation in humans profoundly affects the expression of genes associated with the regulation of skeletal muscle mass." Faseb J: 03-1228fje.

Joseph, M. M. (2003). "Serum response factor: toggling between disparate programs of gene expression." Journal of molecular and cellular cardiology **35**(6): 577-593.

Jung, M., M. Reichstein, et al. (2010). "Recent decline in the global land evapotranspiration trend due to limited moisture supply." Nature **advance online publication**.

Kadi, F. (2000). "Adaptation of human skeletal muscle to training and anabolic steroids." Acta Physiol Scand(646): 1-52.

Kadi, F., N. Charifi, et al. (2005). "The behaviour of satellite cells in response to exercise: what have we learned from human studies?" Pflügers Archiv European Journal of Physiology **451**(2): 319-327.

Kadi, F., A. Eriksson, et al. (1999). "Effects of anabolic steroids on the muscle cells of strength-trained athletes." Medicine & Science in Sports & Exercise **31**(11): 1528.

Kadi, F., P. Schjerling, et al. (2004). "The effects of heavy resistance training and detraining on satellite cells in human skeletal muscles." The Journal of Physiology **558**(3): 1005-1012.

Kalichman, L., Y. Zhang, et al. (2007). "The association between patellar alignment on magnetic resonance imaging and radiographic manifestations of knee osteoarthritis." Arthritis Research & Therapy **9**(2): -.

Keefe, F., J. Blumenthal, et al. (2004). "Effects of spouse-assisted coping skills training and exercise training in patients with osteoarthritic knee pain: a randomized controlled study." Pain **110**(3): 539-549.

Kellgren, J. H. and J. S. Lawrence (1957). "Radiological assessment of osteo-arthrosis." Annals of Rheumatic Diseases **16**(4): 494-502.

Kent, W. J. (2002). "BLAT - The BLAST-Like Alignment Tool." Genome Research **12**(4): 656-664.

Kim, B.-C., M.-N. Lee, et al. (1999). "Roles of Phosphatidylinositol 3-Kinase and Rac in the Nuclear Signaling by Tumor Necrosis Factor-Î± in Rat-2 Fibroblasts." Journal of Biological Chemistry **274**(34): 24372-24377.

Kirkwood, T. B. L. (1997). "3 What is the relationship between osteoarthritis and ageing?" Baillière's Clinical Rheumatology **11**(4): 683-694.

Kline, W. O., F. J. Panaro, et al. (2007). "Rapamycin inhibits the growth and muscle-sparing effects of clenbuterol." J Appl Physiol **102**(2): 740-747.

Koressaar, T. and M. Remm (2007). "Enhancements and modifications of primer design program Primer3." Bioinformatics **23**(10): 1289-1291.

Kovacheva, E. L., A. P. Sinha Hikim, et al. "Testosterone Supplementation Reverses Sarcopenia in Aging through Regulation of Myostatin, c-Jun NH2-Terminal Kinase, Notch, and Akt Signaling Pathways." Endocrinology **151**(2): 628-638.

Krämer, D. K., M. Ahlsén, et al. (2006). "Human skeletal muscle fibre type variations correlate with PPARα, PPARδ and PGC-1α mRNA." Acta Physiologica **188**(3-4): 207-216.

Kramerova, I., E. Kudryashova, et al. (2005). "Calpain 3 participates in sarcomere remodeling by acting upstream of the ubiquitin-proteasome pathway." Hum. Mol. Genet. **14**(15): 2125-2134.

Kurosaka, M. and H. Naito (2009). "Effects of voluntary wheel running on satellite cells in the rat plantaris muscle." Journal of Sports Science and Medicine **8**: 51-57.

Kutscher, E. C., B. C. Lund, et al. (2002). "Anabolic Steroids: A Review for the Clinician." Sports Medicine **32**: 285-296.

Laemmli, U. K. (1970). "Cleavage of Structural Proteins during the Assembly of the Head of Bacteriophage T4." Nature **227**(5259): 680-685.

Lakich, M. M., T. T. Diagana, et al. (1998). "MEF-2 and Oct-1 Bind to Two Homologous Promoter Sequence Elements and Participate in the Expression of a Skeletal Muscle-specific Gene." Journal of Biological Chemistry **273**(24): 15217-15226.

Lang, C. H., R. A. Frost, et al. (2007). "Skeletal muscle protein synthesis and degradation exhibit sexual dimorphism after chronic alcohol consumption but not acute intoxication." Am J Physiol Endocrinol Metab **292**(6): E1497-1506.

Larkin, M. A., G. Blackshields, et al. (2007). "Clustal W and Clustal X version 2.0." Bioinformatics **23**(21): 2947-2948.

Lecker, S. H., R. T. Jagoe, et al. (2004). "Multiple types of skeletal muscle atrophy involve a common program of changes in gene expression." Faseb J **18**(1): 39-51.

Lexell, J., C. C. Taylor, et al. (1988). "What is the cause of the ageing atrophy?: Total number, size and proportion of different fiber types studied in whole vastus lateralis muscle from 15- to 83-year-old men." Journal of the Neurological Sciences **84**(2-3): 275-294.

Li, B.-G., P.-O. Hasselgren, et al. (2004). "Insulin-Like Growth Factor-I Blocks Dexamethasone-Induced Protein Degradation in Cultured Myotubes by Inhibiting Multiple Proteolytic Pathways: 2002 ABA Paper." Journal of Burn Care & Research **25**(1): 112-118.

Li, Y.-P., Y. Chen, et al. (2005). "TNF-{alpha} acts via p38 MAPK to stimulate expression of the ubiquitin ligase atrogin1/MAFbx in skeletal muscle." Faseb J **19**(3): 362-370.

Li, Y.-P. and M. B. Reid (2000). "NF-kappa B mediates the protein loss induced by TNF-alpha in differentiated skeletal muscle myotubes." Am J Physiol Regul Integr Comp Physiol **279**(4): R1165-1170.

Lohmander, L., P. Englund, et al. (2007). "The long-term consequence of anterior cruciate ligament and meniscus injuries - Osteoarthritis." American Journal of Sports Medicine **35**(10): 1756-1769.

Longino, D., C. Frank, et al. (2005). "Acute botulinum toxin-induced muscle weakness in the anterior cruciate ligament-deficient rabbit." Journal Orthopaedic Research **23**(6): 1404-1410.

Longino, D., C. Frank, et al. (2005). "Proposed model of botulinum toxin-induced muscle weakness in the rabbit." Journal of Orthopaedic Research **23**(6): 1411-1418.

Lynch, G. and J. Ryall (2008). "Role of beta-adrenoceptor signaling in skeletal muscle: Implications for muscle wasting and disease." Physiological Reviews **88**(2): 729-767.

Lynch, G., J. Schertzer, et al. (2008). "Anabolic agents for improving muscle regeneration and function after injury." Clinical and Experimental Pharmacology and Physiology **35**(7): 852-858.

Mahadeva, H., G. Brooks, et al. (2002). "ms1, a novel stress-responsive, muscle-specific gene that is up-regulated in the early stages of pressure overload-induced left ventricular hypertrophy." FEBS Letters **521**(1-3): 100-104.

Maltin, C. A., S. M. Hay, et al. (1989). "The action of the beta-agonist clenbuterol on protein-metabolism in innervated and denervated phasic muscles." Biochemical Journal **261**(3): 965-971.

Marks, R., S. Kumar, et al. (1994). "Quadriceps femoris activation in healthy women with genu-varum and women with osteoarthrosis and genu-varum
" Journal of Electromyography and Kinesiology **4**(3): 153-160.

Marx, J. O., W. J. Kraemer, et al. (2002). "Effects of Aging on Human Skeletal Muscle Myosin Heavy-Chain mRNA Content and Protein Isoform Expression." The Journals of Gerontology Series A: Biological Sciences and Medical Sciences **57**(6): B232-B238.

Matera, M. G., L. Calzetta, et al. (2009). "TNF-[alpha] inhibitors in asthma and COPD: We must not throw the baby out with the bath water." Pulmonary Pharmacology & Therapeutics **23**(2): 121-128.

McAlindon, T. E., P. Jacques, et al. (1996). "Do antioxidant micronutrients protect against the development and progression of knee osteoarthritis?" Arthritis & Rheumatism **39**(4): 648-656.

McKoy, G., W. Ashley, et al. (1999). "Expression of insulin growth factor-1 splice variants and structural genes in rabbit skeletal muscle induced by stretch and stimulation." The Journal of Physiology **516**(2): 583-592.

McNally, E. M., K. A. Lapidos, et al. (2006). Skeletal Muscle Structure and Function. Principles of Molecular Medicine**:** 674-681.

Mikesky, A., S. Mazzuca, et al. (2006). "Effects of strength training on the incidence and progression of knee osteoarthritis." Arthritis & Rheumatism **55**(5): 690-699.

Miller, J. B., E. A. Everitt, et al. (1993). "Cellular and molecular diversity in skeletal muscle development: News from in vitro and in vivo." BioEssays **15**(3): 191-196.

Mills, P., Y. Wang, et al. (2008). "Tibio-femoral cartilage defects 3-5 years following arthroscopic partial medial meniscectomy." Osteoarthritis and Cartilage **16**(12): 1526-1531.

Mitchell, P. G., H. A. Magna, et al. (1996). "Cloning, expression, and type II collagenolytic activity of matrix metalloproteinase-13 from human osteoarthritic cartilage." The Journal of Clinical Investigation **97**(3): 761-768.

Mizunoya, W., J. Wakamatsu, et al. (2008). "Protocol for high-resolution separation of rodent myosin heavy chain isoforms in a mini-gel electrophoresis system." Analytical Biochemistry **377**(1): 111-113.

Mohammadi, F., S. Taghizadeh, et al. (2008). "Proprioception, dynamic balance and maximal quadriceps strength in females with knee osteoarthritis and normal control subjects." International Journal of Rheumatic Diseases **11**(1): 39-44.

Mounier, R., H. Cavalié, et al. (2007). "Molecular impact of clenbuterol and isometric strength training on rat EDL muscles." Pflügers Archiv European Journal of Physiology **453**(4): 497-507.

Murphy, R. M. and G. D. Lamb (2008). "Calpains and skeletal muscle function." Australian Physiological Society **38**.

Musaro, A., K. McCullagh, et al. (2001). "Localized Igf-1 transgene expression sustains hypertrophy and regeneration in senescent skeletal muscle." Nat Genet **27**(2): 195-200.

Nabeshima, Y., K. Hanaoka, et al. (1993). "Myogenin gene disruption results in perinatal lethality because of severe muscle defect." Nature **364**(6437): 532-535.

Naggar, E. A. e., F. Kanda, et al. (2004). "Direct effects of Tumor Necrosis Factor Alpha(TNF-a) on L6 Myotubes." Kobe J Med Sci **50**(2): 39-46.

Nakamura, T. and K. Suzuki (1992). "Muscular changes in osteoarthritis of the hip and knee." Nippon Seikeigeka Gakkai Zasshi **66**(5): 467-475.

NICE (2008) "National institute for health and clinical excellence - the care and management of osteoarthritis in adults."

Nielsen, R. H. and R. Stoop (2008). "Evaluation of cartilage damage by measuring collagen degradation products in joint extracts in a traumatic model of osteoarthritis." Biomarkers **13**(1): 79-87.

Nishimura, A., M. Hasegawa, et al. (2010). "Risk factors for the incidence and progression of radiographic osteoarthritis of the knee among Japanese." International Orthopaedics.

O'Reilly, S. C., K. R. Muir, et al. (1999). "Effectiveness of home exercise on pain and disability from osteoarthritis of the knee: a randomised controlled trial." Annals of Rheumatic Diseases **58**(1): 15-19.

Ohira, Y., T. Yoshinaga, et al. (1999). "Myonuclear domain and myosin phenotype in human soleus after bed rest with or without loading." J Appl Physiol **87**(5): 1776-1785.

Oishi, Y., K. Imoto, et al. (2002). "Clenbuterol induces expression of multiple myosin heavy chain isoforms in rat soleus fibres." Acta Physiologica Scandinavica **176**(4): 311-318.

Oliveria, S. A., D. T. Felson, et al. (1995). "Incidence of symptomatic hand, hip, and knee osteoarthritis among patients in a health maintenance organization." Arthritis & Rheumatism **38**(8): 1134-1141.

Ono, Y., L. Boldrin, et al. (2010). "Muscle satellite cells are a functionally heterogeneous population in both somite-derived and branchiomeric muscles." Developmental Biology **337**(1): 29-41.

Orlowski, R. and E. C. Dees (2003). "The role of the ubiquitination-proteasome pathway in breast cancer: Applying drugs that affect the ubiquitin-proteasome pathway to the therapy of breast cancer." Breast Cancer Res **5**(1): 1 - 7.

Ottenheijm, C., L. Heunks, et al. (2008). "Diaphragm adaptations in patients with COPD." Respiratory Research **9**(1): 12.

Otter, I., S. Conus, et al. (1998). "The Binding Properties and Biological Activities of Bcl-2 and Bax in Cells Exposed to Apoptotic Stimuli." Journal of Biological Chemistry **273**(11): 6110-6120.

Pandorf, C. E., F. Haddad, et al. (2007). "IIx myosin heavy chain promoter regulation cannot be characterized in vivo by direct gene transfer." Am J Physiol Cell Physiol **293**(4): C1338-1346.

Pandorf, C. E., F. Haddad, et al. (2006). "Dynamics of Myosin Heavy Chain Gene Regulation in Slow Skeletal Muscle." Journal of Biological Chemistry **281**(50): 38330-38342.

Pap, G., A. Machner, et al. (2004). "Strength and voluntary activation of the quadriceps femoris muscle at different severities of osteoarthritic knee joint damage." Journal of Orthopaedic Research **22**(1): 96-103.

Pap, M. and G. M. Cooper (2002). "Role of translation initiation factor 2B in control of cell survival by the phosphatidylinositol 3-kinase/Akt/glycogen synthase kinase 3B signaling pathway." Molecular and Cellular Biology **22**(2): 578-586.

Park, K. C., J. H. Kim, et al. (2002). "Antagonistic regulation of myogenesis by two deubiquitinating enzymes, UBP45 and UBP69." Proceedings of the National Academy of Sciences of the United States of America **99**(15): 9733-9738.

PARR, T., R. G. BARDSLEY, et al. (1992). "Changes in calpain and calpastatin mRNA induced by β-adrenergic stimulation of bovine skeletal muscle." European Journal of Biochemistry **208**(2): 333-339.

Peat, G., R. McCarney, et al. (2001). "Knee pain and osteoarthritis in older adults: a review of community burden and current use of primary health care." Annals of Rheumatic Diseases **60**(2): 91-97.

Pellegrino, M. A., G. D'Antona, et al. (2004). "Clenbuterol antagonizes glucocorticoid-induced atrophy and fibre type transformation in mice." Experimental Physiology **89**(1): 89-100.

Perez-Ruiz, A., Y. Ono, et al. (2008). "{beta}-catenin promotes self-renewal of skeletal-muscle satellite cells." J Cell Sci **121**(9): 1373-1382.

Peter, J. (1972). "Metabolic profiles of three fiber types of skeletal muscle in guinea pigs and rabbits
" Biochemistry **11**: 2627-2633.

Pette, D., M. E. Smith, et al. (1973). "Effects of long-term electrical stimulation on some contractile and metabolic characteristics of fast rabbit muscles." Pflügers Archiv European Journal of Physiology **338**(3): 257-272.

Pette, D. and R. S. Staron (2001). "Transitions of muscle fiber phenotypic profiles." Histochemistry and Cell Biology **115**(5): 359-372.

Phillips, T. and C. Leeuwenburgh (2005). "Muscle fiber-specific apoptosis and TNF-alpha; signaling in sarcopenia are attenuated by life-long calorie restriction." Faseb J **1-33**.

Pieper, J. S. (2002). "Crosslinked type II collagen matrices:preparation, characterization, and potential for cartilage engineering." Biomaterials **23**(15): 3183-3192.

Pin, C. L. and P. A. Merrifield (1997). "Developmental Potential of Rat L6 Myoblastsin VivoFollowing Injection into Regenerating Muscles." Developmental Biology **188**(1): 147-166.

Plomgaard, P., M. Penkowa, et al. (2005). "Fiber type specific expression of TNF-alpha, IL-6 and IL-18 in human skeletal
muscles." Exerc Immunol Rev **11**: 53-63.

Quiroz-Rothe, E. and J.-L. L. Rivero (2004). "Coordinated expression of myosin heavy chains, metabolic enzymes, and morphological features of porcine skeletal muscle fiber types." Microscopy Research and Technique **65**(1-2): 43-61.

Rayment, I., H. Holden, et al. (1993). "Structure of the actin-myosin complex and its implications for muscle contraction." Science **261**(5117): 58-65.

Reardon, K. A., J. Davis, et al. (2001). "Myostatin, insulin-like growth factor-1, and leukemia inhibitory factor mRNAs are upregulated in chronic human disuse muscle atrophy." Muscle & Nerve **24**(7): 893-899.

Reboul, P., J. P. Pelletier, et al. (1996). "The new collagenase, collagenase-3, is expressed and synthesized by human chondrocytes but not by synoviocytes. A role in osteoarthritis." The Journal of Clinical Investigation **97**(9): 2011-2019.

Rehfeldt, C., I. Fiedler, et al. (2000). "Myogenesis and postnatal skeletal muscle cell growth as influenced by selection." Livestock Production Science **66**(2): 177-188.

Rhinn, H., C. Marchand-Leroux, et al. (2008). "Housekeeping while brain's storming Validation of normalizing factors for gene expression studies in a murine model of traumatic brain injury." BMC Molecular Biology **9**(1): 62.

Rhinn, H., D. Scherman, et al. (2008). "One-step quantification of single-stranded DNA in the presence of RNA using Oligreen in a real-time polymerase chain reaction thermocycler." Anal Biochem **372**: 116 - 118.

Ricart-Firinga, C., L. Stevens, et al. (2000). "Effects of beta(2)-agonist clenbuterol on biochemical and contractile properties of unloaded soleus fibers of rat." American Journal of Physiology-Cell Physiology **278**(3): C582-C588.

Rinaldi, C., F. Haddad, et al. (2008). "Intergenic bidirectional promoter and cooperative regulation of the IIx and IIb MHC genes in fast skeletal muscle." American Journal of Physiology-Regulatory integrative and comparative physiology **295**(1): R208-R218.

Rommel, C., S. C. Bodine, et al. (2001). "Mediation of IGF-1-induced skeletal myotube hypertrophy by PI(3)K/Akt/mTOR and PI(3)K/Akt/GSK3 pathways." Nat Cell Biol **3**(11): 1009-1013.

Rosemffet, M., E. Schneeberger, et al. (2004). "Effects of functional electrostimulation on pain, muscular strength, and functional capacity in patients with osteoarthritis of the knee." JCR-Journal of clinical rheumatology **10**(5): 246-249.

Rothwell, N. and M. Stock (1987). "Effect of a selective beta-2-adrenergic agonist (clenbuterol) on energy-balance and body-composition in normal and protein-deficient rats." Bioscience Reports **7**(12): 933-940.

Rudnicki, M. A., T. Braun, et al. (1992). "Inactivation of MyoD in mice leads to up-regulation of the myogenic HLH gene Myf-5 and results in apparently normal muscle development." Cell **71**(3): 383-390.

Russell, A. P. (2009). "Molecular regulation of skeletal muscle mass." Clinical and Experimental Pharmacology and Physiology **37**: 378-384.

Ryall, J. and G. Lynch (2008). "The potential and the pitfalls of beta-adrenoceptor agonists for the management of skeletal muscle wasting." Pharmacology & Therapeutics **120**(3): 219-232.

Samanta, A., A. Jones, et al. (1993). "Is osteoarthritis in women affected by hormonal changes or smoking?" Rheumatology **32**(5): 366-370.

Sato, T., H. Akatsuka, et al. (1984). "Age changes in size and number of muscle fibers in human minor pectoral muscle." Mechanisms of Ageing and Development **28**(1): 99-109.

Schmittgen, T. D. and K. J. Livak (2008). "Analyzing real-time PCR data by the comparative CT method." Nat. Protocols **3**(6): 1101-1108.

Schroeder, E., M. Terk, et al. (2003). "Androgen therapy improves muscle mass and strength but not muscle quality: results from two studies." American Journal of Physiology-Endocrinology and Metabolism **285**(1): E16-E24.

Segal, N. A., N. A. Glass, et al. (2010). "Quadriceps weakness predicts risk for knee joint space narrowing in women in the MOST cohort." Osteoarthritis and Cartilage **18**(6): 769-775.

Segal, N. A., J. C. Torner, et al. (2009). "Effect of thigh strength on incident radiographic and symptomatic knee osteoarthritis in a longitudinal cohort." Arthritis Care & Research **61**(9): 1210-1217.

Sharma, L., D. D. Dunlop, et al. (2003). "Quadriceps strength and osteoarthritis progression in maligned and lax knees." Annals of Internal Medicine **138**(8): 613-619.

Sheffield-Moore, M. (2000). "Androgens and the control of skeletal muscle protein synthesis." Annals of Medicine **32**(3): 181-186.

Sinha-Hikim, I., J. Artaza, et al. (2002). "Testosterone-induced increase in muscle size in healthy young men is associated with muscle fiber hypertrophy." Am J Physiol Endocrinol Metab **283**(1): E154-164.

Sinha-Hikim, I., S. M. Roth, et al. (2003). "Testosterone-induced muscle hypertrophy is associated with an increase in satellite cell number in healthy, young men." Am J Physiol Endocrinol Metab **285**(1): E197-205.

Slemenda, C., K. Brandt, et al. (1997). "Quadriceps weakness and osteoarthritis of the knee." Annals of Internal Medicine **127**(2): 97-&.

Slemenda, C., D. Heilman, et al. (1998). "Reduced quadriceps strength relative to body weight - A risk factor for knee osteoarthritis in women?" Arthritis & Rheumatism **41**(11): 1951-1959.

Smith, I. J. and S. L. Dodd (2007). "Calpain activation causes a proteasome-dependent increase in protein degradation and inhibits the Akt signalling pathway in rat diaphragm muscle." Experimental Physiology **92**(3): 561-573.

Song, W., H. B. Kwak, et al. (2006). "Exercise training attenuates age-induced changes in apoptotic signaling in rat skeletal muscle." Antioxidants and Redox Signaling **8**(3-4): 517-528.

Spangenburg, E. E. and F. W. Booth (2003). "Molecular regulation of individual skeletal muscle fibre types." Acta Physiologica Scandinavica **178**(4): 413-424.

Spector, T., D. Hart, et al. (1994). "Incidence and progression of osteoarthritis in women with unilateral knee disease in the general-population - the effect of obesity." Annals of Rheumatic Diseases **53**(9): 565-568.

Spector, T., D. Nandra, et al. (1997). "Is hormone replacement therapy protective for hand and knee osteoarthritis in women? The Chingford study." Annals of the Rheumatic Diseases **56**(7): 432-434.

Spector, T. D. and A. J. MacGregor (2004). "Risk factors for osteoarthritis: genetics." Osteoarthritis and Cartilage **12**(Supplement 1): 39-44.

Spencer, M. J., J. R. Guyon, et al. (2002). "Stable expression of calpain 3 from a muscle transgene in vivo: Immature muscle in transgenic mice suggests a role for calpain 3 in muscle maturation." Proceedings of the National Academy of Sciences of the United States of America **99**(13): 8874-8879.

Staron, R., E. Malicky, et al. (1990). "Muscle hypertrophy and fast fiber type conversions in heavy resistance-trained women." European Journal of Applied Physiology and Occupational Physiology **60**(1): 71-79.

Stevens, L., C. Firinga, et al. (2000). "Effects of unweighting and clenbuterol on myosin light and heavy chains in fast and slow muscles of rat." American journal of physiology-cell physiology
279(5): C1558-C1563.

Stevens, L., B. Gohlsch, et al. (1999). "Changes in myosin heavy chain mRNA and protein isoforms in single fibers of unloaded rat soleus muscle." FEBS Letters **463**(1-2): 15-18.

Stitt, T. N., D. Drujan, et al. (2004). "The IGF-1/PI3K/Akt Pathway Prevents Expression of Muscle Atrophy-Induced Ubiquitin Ligases by Inhibiting FOXO Transcription Factors." Molecular Cell **14**(3): 395-403.

Sturmer, T., Y. Sun, et al. (1998). "Serum cholesterol and osteoarthritis. The baseline examination of the Ulm osteoarthritis study." Journal of Rheumatology **25**(9): 1827-1832.

Sultan, K. R., B. Henkel, et al. (2006). "Quantification of hormone-induced atrophy of large myotubes from C2C12 and L6 cells: atrophy-inducible and atrophy-resistant C2C12 myotubes." Am J Physiol Cell Physiol **290**(2): C650-659.

Swoap, S. J. (1998). "In vivo analysis of the myosin heavy chain IIB promoter region." Am J Physiol Cell Physiol **274**(3): C681-687.

Takeda, D. (1992). "A possible regulatory role for conserved promoter motifs in an adult-specific muscle myosin gene from mouse." Journal of Biological Chemistry **267**: 16957 - 16967.

Talmadge, R. J. and R. R. Roy (1993). "Electrophoretic separation of rat skeletal-muscle myosin heavy-chain isoforms." Journal of Applied Physiology **75**(5): 2337-2340.

Tessier, J. J., J. Bowyer, et al. (2003). "Characterisation of the guinea pig model of osteoarthritis by in vivo three-dimensional magnetic resonance imaging." Osteoarthritis and Cartilage **11**(12): 845-853.

Thomas, K. S., K. R. Muir, et al. (2002). "Home based exercise programme for knee pain and knee osteoarthritis: randomised controlled trial." British Medical Journal **325**(7367): 752-755.

Thorstensson, C., I. Petersson, et al. (2004). "Reduced functional performance in the lower extremity predicted radiographic knee osteoarthritis five years later." Annals of Rheumatic Diseases **63**(4): 402-407.

Tokuda, M. (1997). "Histological study of spontaneous osteoarthritis in the knee joint of guinea pigs." Journal of Orthopaedic Research **2**(4): 248-258.

Tominaga, Y., A. Ndu, et al. (2006). "Neck ligament strength is decreased following whiplash trauma." BMC Musculoskeletal Disorders **7**(1): 103.

Toncheva, A., M. Remichkova, et al. (2009). "Inflammatory response in patients with active and inactive osteoarthritis." Rheumatology International **29**(10): 1197-1203.

Tonge, D. P., S. W. Jones, et al. (2009). "β2-Adrenergic agonist-induced hypertrophy of the quadriceps skeletal muscle does not modulate disease severity in the rodent meniscectomy model of osteoarthritis." Osteoarthritis and Cartilage **18**(4): 555-562.

Trivedi, B. and W. H. Danforth (1966). "Effect of pH on the Kinetics of Frog Muscle Phosphofructokinase." Journal of Biological Chemistry **241**(17): 4110-4114.

Tsika, G. L., J. L. Wiedenman, et al. (1996). "Induction of beta-MHC transgene in overloaded skeletal muscle is not eliminated by mutation of conserved elements." Am J Physiol Cell Physiol **271**(2): C690-699.

Vandesompele, J., K. De Preter, et al. (2002). "Accurate normalization of real-time quantitative RT-PCR data by geometric averaging of multiple internal control genes." Genome Biology **3**(7): research0034.0031 - research0034.0011.

Wang, X. D., F. Kawano, et al. (2006). "Mechanical load-dependent regulation of satellite cell and fiber size in rat soleus muscle." Am J Physiol Cell Physiol **290**(4): C981-989.

Wang, Y.-X., C.-L. Zhang, et al. (2004). "Regulation of Muscle Fiber Type and Running Endurance by PPARδ." PLoS Biol **2**(10): e294.

Watson, P. J., L. D. Hall, et al. (1996). "Degenerative joint disease in the guinea pig: Use of magnetic resonance imaging to monitor progression of bone pathology." Arthritis & Rheumatism **39**(8): 1327-1337.

Weiss, A. and L. A. Leinwand (1996). "The mammalian myosin heavy chain gene family." Annual Review of Cell and Developmental Biology **12**: 417-439.

Westacott, C. (1990). "Synovial fluid concentration of five different cytokines in rheumatic diseases." BMJ **49**(676-681).

Westacott, C. and M. Sharif (1996). "Cytokines in osteoarthritis: Mediators or markers of joint destruction?" Seminars in Arthritis and Rheumatism **25**(4): 254-272.

Whittom, F., J. Jobin, et al. (1998). "Histochemical and morphological characteristics of the vastus lateralis muscle in patients with chronic obstructive pulmonary disease." Medicine & Science in Sports & Exercise **30**(10): 1467-1474.

Wijnhoven, J. H., A. J. M. Janssen, et al. (2006). "Metabolic capacity of the diaphragm in patients with COPD." Respiratory Medicine **100**(6): 1064-1071.

Wilder, F. V., B. J. Hall, et al. (2002). "History of acute knee injury and osteoarthritis of the knee: a prospective epidemiological assessment: The Clearwater Osteoarthritis Study." Osteoarthritis and Cartilage **10**(8): 611-616.

Wilson, M. G., C. J. Michet Jr, et al. (1990). "Idiopathic symptomatic osteoarthritis of the hip and knee: A population-based incidence study." Mayo Clinic Proceedings **65**(9): 1214-1221.

Witzemann, V. and B. Sakmann (1991). "Differential regulation of MyoD and myogenin mRNA levels by nerve induced muscle activity." FEBS Letters **282**(2): 259-264.

Wluka, A., S. Davis, et al. (2001). "Users of oestrogen replacement therapy have more knee cartilage than non-users." Annals of Rheumatic Diseases **60**(4): 332-336.

Xu, Q. and Z. Wu (2000). "The Insulin-like Growth Factor-Phosphatidylinositol 3-Kinase-Akt Signaling Pathway Regulates Myogenin Expression in Normal Myogenic Cells but Not in Rhabdomyosarcoma-derived RD Cells." Journal of Biological Chemistry **275**(47): 36750-36757.

Yaffe, D. (1968). "Retention of differentiation potentialities during prolonged cultivation of myogenic cells." Proceedings of the National Academy of Sciences of the United States of America **61**(2): 477-483.

Yang, X., J. Chen, et al. (2007). "Muscle type-specific responses of myoD and calpain 3 expression to recombinant porcine growth hormone in the pig." animal **1**(07): 989-996.

Yuan, G.-H., K. Masuko-Hongo, et al. (2001). "The role of C-C chemokines and their receptors in osteoarthritis." Arthritis & Rheumatism **44**(5): 1056-1070.

APPENDICES

Appendix A – Standard Buffers

2 x SDS PAGE loading buffer – 2mL glycerol, 1.25mL 1M Tris-HCl pH 6.8, 4mL 10% w/v sodium dodecyl sulphate (SDS), 1mL 1M DTT and 2.5mg of bromophenol blue made up to 10mL with distilled water –stored at -20^{o}C.

1 x SDS PAGE loading buffer – Prepared by diluting 2 x SDS loading buffer (above) in distilled water - stored at -20^{o}C.

LB Agar – Luria broth agar comprising 2% w/v tryptone, 1% w/v yeast extract, 2% w/v NaCl and 3% w/v Bacto-Agar (Oxoid) prepared in distilled water and autoclaved prior to use.

LB Media - 2% w/v tryptone (Oxoid), 1% w/v yeast extract (Oxoid) and 2% w/v NaCl prepared in distilled water and autoclaved prior to use.

Ponceau S Stain – 0.5% (w/v) Ponceau S (BDH), 5% (w/v) trichloroacetic acid prepared in distilled water.

Protein extraction buffer - 150mM NaCl, 50mM Hepes, 2.5mM EDTA, 1mM Na_3VO_3, 10mM NaF, 10% v/v glycerol and 1% v/v triton X prepared in distilled water and stored at 4^{o}C.

SDS PAGE running buffer - 0.25M Tris-base, 1.92M glycine, and 1% (w/v) – sourced as a 10 X stock solution from National diagnostics and diluted 10-fold in distilled water prior to use.

SOC Media - 2% w/v tryptone, 0.5% w/v yeast, 10mM NaCl, 2.5mM KCl, 10mM $MgCl_2$, 10mM $MgSO_4$, 20mM glucose prepared in distilled water and autoclaved prior to use.

TAE - Tris-acetate-ethylenediamine tetraacetic acid buffer comprising a final concentration of 40mM Tris-HCl, 1mM EDTA (pH 8.0) and 1.142mL glacial acetic acid per litre of distilled water.

TBS-T Buffer – Tris buffered saline buffer comprising 20mM Tris-HCl pH7.5, 0.9% (w/v) NaCl and 0.1% (v/v) Tween 20 prepared in distilled water.